JWES-AE-9607

Report on International Workshop on the Integrity of Nuclear Components

May8, 1996

TAEJON, KOREA

1 9 9 6 年 8 月

社団法人　日本溶接協会

原 子 力 研 究 委 員 会

Workshopの会場にて（中央が矢川教授、その右がKim教授）

挨拶するDr.Yoon（KINS副所長）

挨拶する矢川教授

挨拶するKim教授

鹿島委員の講演

KINSの入口で

月城発電所入口で

使用済み燃料の乾式貯蔵施設とその説明図

序

世界のエネルギー事情は大きく変わりつつある。特に、アジア地域では２０１０年の需要見直しが、１９９２年の２倍にも達するという急カーブを描く。この需要激増に対して、この地域での原子力発電が、新しい供給源となることは間違いない。

これまで、我が国の原子力開発は欧米との協力のもとで行われることが主であったが、原子力発電の安全確保などの問題については、地理的つながりの強い地域内での共通課題として問題を共有し、かつ協力していくことが重要である。

我が国は、これまで長年にわたって原子力発電の良好な発電実績を有し、またその安全技術について国際的に高い評価を受けてきた。この優れた安全運転の実績は、改めて言うまでもなく、高信頼性の材料・機器設計のハードウエア面と、高度な運転管理技術・保守技術・検査技術・教育訓練などのソフトウエア面の両者がベースとなっている。このような背景のもと、今後、アジア地区での原子力開発がますます活発化するにあたって、我が国からの原子力発電機器・材料の輸出も盛んになっていくことが予想される。

このような状況にあって、原子力機器・材料に関わっている研究者・技術者の交流も極めて重要度を増しつつある。今回のワークショップの目的はまさにこの点にあり、原子力発電の安全確保の最重要事項の１つである機器コンポーネントの健全性に関する討議を、我が国と韓国の研究者・技術者を一同に会して行うことにした。

本報告書は、このワークショップ、さらには付随して得られた情報をまとめたものである。

ワークショップ開催にあたっては日韓両国の関係者の献身的御努力があった。この場を借りて厚く御礼申し上げたい。（矢川）

Wednesday, May 8

9:00 Registration

9:20 Opening Ceremony
Welcoming Address
Dr. Young.S Eun(Vice-President, KINS)
Prof. Y.J.Kim(Professor, SungKyunKwan Univ.)
Prof. G. Yagawa(Professor, Univ. of Tokyo)

Session A [Meeting Room #208] [Chairman, Prof. Y.J.Kim]

---

1 10:00 Application of Leak-Before-Break Using Piping Evaluation Diagram (PED)
Y.J.Yu*, K.S. Yoon, S.H.Park, K.B. Park(KAERI), Y.J.Kim(SungKyunKwan Univ.)

2 10:25 A Research Program for Dynamic Fracture Evaluation of Japanese Carbon Steel Pipes
K.Kashima*(CRIEPI)

3 10:50 Effects of Dynamic Strain Aging on the Leak-Before-Break Analysis in SA 106 Gr.C Piping Steel
I.S.Kim*, J.W.Kim(KAIST)

4 11:15 Probabilistic Fracture Mechanics Analyses of Nuclear Pressure Vessels Under PTS Events
G.Yagawa*(Univ. of Tokyo), S. Yoshimura(CRIEPI), M. Hirano(JAERI)

5 11:40 Improved Toughness of the SA 508 Class 3 Steel for Nuclear Pressure Vessel Through the Steel-Making and Heat Treatment
J.T.Kim*, H.K.Kwon, H.S.Chang(HANJUNG)

12:05 Lunch

Session B [Meeting Room #208] [Chairman, Prof. G.Yagawa]

---

6 13:30 Crack Shape Evolution of Surface Flaws under Fatigue Loading of Austenitic Pipes
I.S. Hwang*, J.H.Kim(Seoul National Univ.)

7 13:55 Study on the Effect of the Crack Length on the J_{IC} Value
M.Kikuchi*(Science Univ. of Tokyo)

8 14:20 Development of New Z-factors for the Evaluation of the Circumferencial Surface Crack in Nuclear Pipings
Y.H.Choi*, Y.K.Chung, Y.W.Park, J.B.Lee(KINS),
G.Wilkowski(Battelle Memorial Institute)

9 14:45 Requirements for Pressure Boundary Integrity of Operation Nuclear Plant-Japanese Standards
H.Kobayashi*(Tokyo Institute of Technology)

10 15:10 The Development Status of Mechanical Component Code for Nuclear Power Application in Korea
N.H.Kim*, J.S.Nah(KOPEC)

15:35 Coffee Break

Session C [Meeting Room #208] [Chairman, Dr. Y.W.Park]

---

11 15:50 Progress of Component Aging and Structural Integrity Research Program at JAERI
K.Shibata*(JAERI)

12 16:15 Development of Expert System for Nuclear Piping Integrity
Y.J.Kim*, M.W. Suh, C.S. Seok, H.K. Jun(SungKyunKwan Univ.)
Y.W.Park, Y.H.Choi, J.B.Lee(KINS)

13 16:40 Recent Progress in Korean Nuclear PLIM Program
T.E. Jin*, H.J. Choi(KOPEC), I.S.Jeong, S.Y. Hong(KEPCO)

17:05 General Discussion on the Presented Topics

17:30 Discussion on Future Activities of Workshop and Conclusion

18:00 Dinner hosted by Japanese Participants at KINS' Restaurant

目　　次

1　計画の経緯と概要

日韓の原子力技術の交流の計画が具体化したのは、平成７年６月に韓国原子力研究所の若い研究者 Dr.H.Y. Lee が訪日したのがきっかけとなった。

川崎重工業（株）の国松委員の紹介により菊池が Dr.Lee と合い、日本側の要望の伝達を依頼した。その二週間後、同研究所の主任研究員である B.Yoo 氏が来日し、東大の矢川教授室にて具体的な協議を行う運びとなった。

Yoo 氏は帰国後、韓国機械学会内の原子力研究部門にて日本側の要望を検討し、積極的に進める事を決定した。韓国側の担当は成均館大学の Kim 教授とＫＩＮＳ（韓国原子力安全研究院）の Dr.Park に決定した。

日本側もこうした事態の進展を受けて、平成７年１１月の原子力研究委員会において正式に開催を決定し、国際研究連絡小委員会を母胎として、矢川委員長と菊池委員とが折衝に当たる事となった。

開催の時期は日本の連休明けの５月第二週とし、講演依頼、講演要旨の募集、原稿執筆依頼、と準備は順調に進展し、予定通り５月８日に開催の運びとなった。

韓国では、ＫＩＮＳが主催する「原子力施設・機器の安全性に関するシンポジウム」が1993 年以来すでに二度開催され、毎回７０～８０名近い参加者を得て活発に行われてきた。

今回の企画は第３回目のシンポジウムと合同で企画されたものである。韓国国内のシンポジウムは前日の７日に同じ会場で開催された。７日の夕食会に招待された我々日本側は、予期しなかった多数の参加者に会って驚かされた。

翌８日９時３０分から Workshop は開始した。出席者は約７０名であった。

冒頭にＫＩＮＳ副所長の K.S.Yoon 博士より「韓国国内で原子力施設の安全性研究の重要性が高まっている事からこの Workshop の成果に期待している事、またこのような技術交流の場が将来はアジア地域の共同の場となることを望んでいる」との挨拶があった。

続いて成均館大学の Kim 教授の挨拶では Open Minded Discussion を行おうとの呼びかけがあり、日本側を代表して矢川教授からはアジアでの原子力大国としての日－韓－台の将来の協力が重要になるとの指摘がなされた。

講演会では日本側から５件、韓国側から８件の論文が発表され、双方から活発な質疑・応答が行われた。以下にそれらの要約を、参加者の感想を含めて記す。また参加者の構成と発表テーマを韓国側でまとめているので、参考までにそれらを図１，２に示す。ただしこれは前日行われた韓国の国内シンポジウムも含めた結果である。

講演会終了後、今後の活動方針が Dr.Park より発表された。その詳細は後に記す。

その後、日本側の主催により夕食会を開催した。手配は韓国側にお願いしたが、蟹や肉

などの韓国料理とともにお寿司や赤飯、刺身がならび、大変なごちそうであった。

ＫＩＮＳのある大田市は日本のつくば市のような科学技術都市であり、多くの韓国側の出席者は車で来ているとの事で、あまりお酒が進まなかったのは少々残念であったが、たっぷりと懇親の時を持つ事ができたのは有意義であった。さらにＫＩＮＳの若手の研究者数名は、夕食後に我々のホテルを訪ねてくれて、深夜まで楽しく歓談を続けた。（菊池）

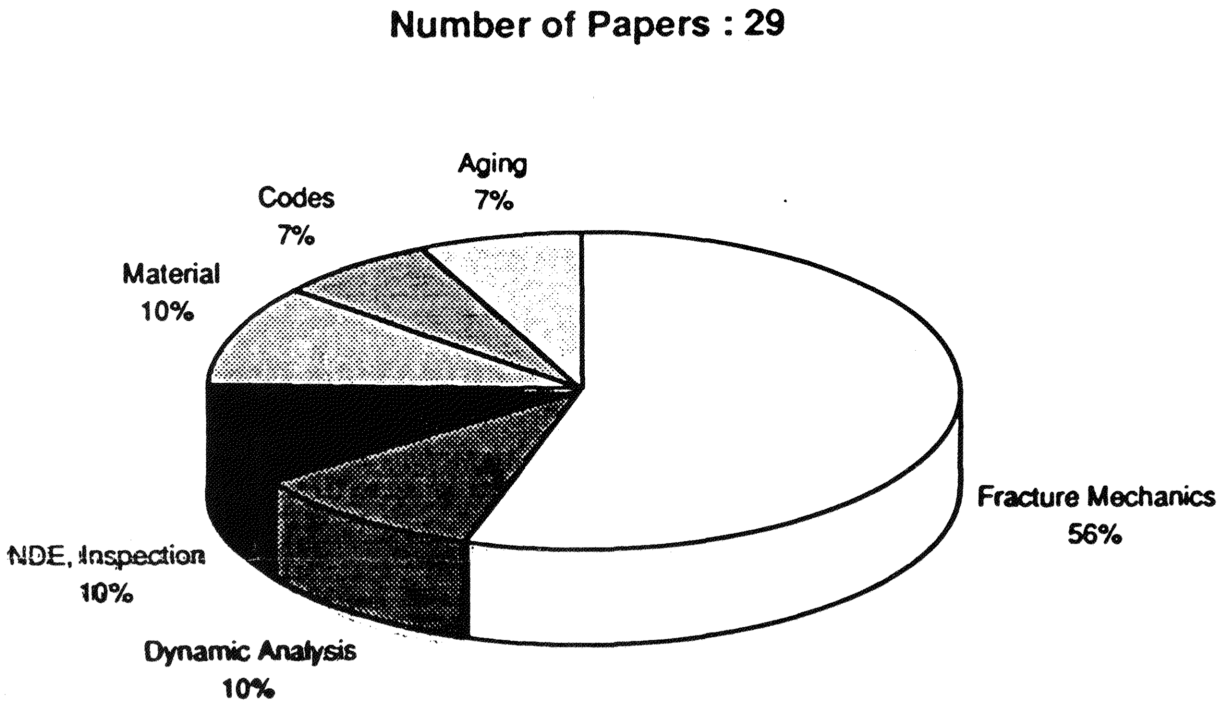

図１　研究分野

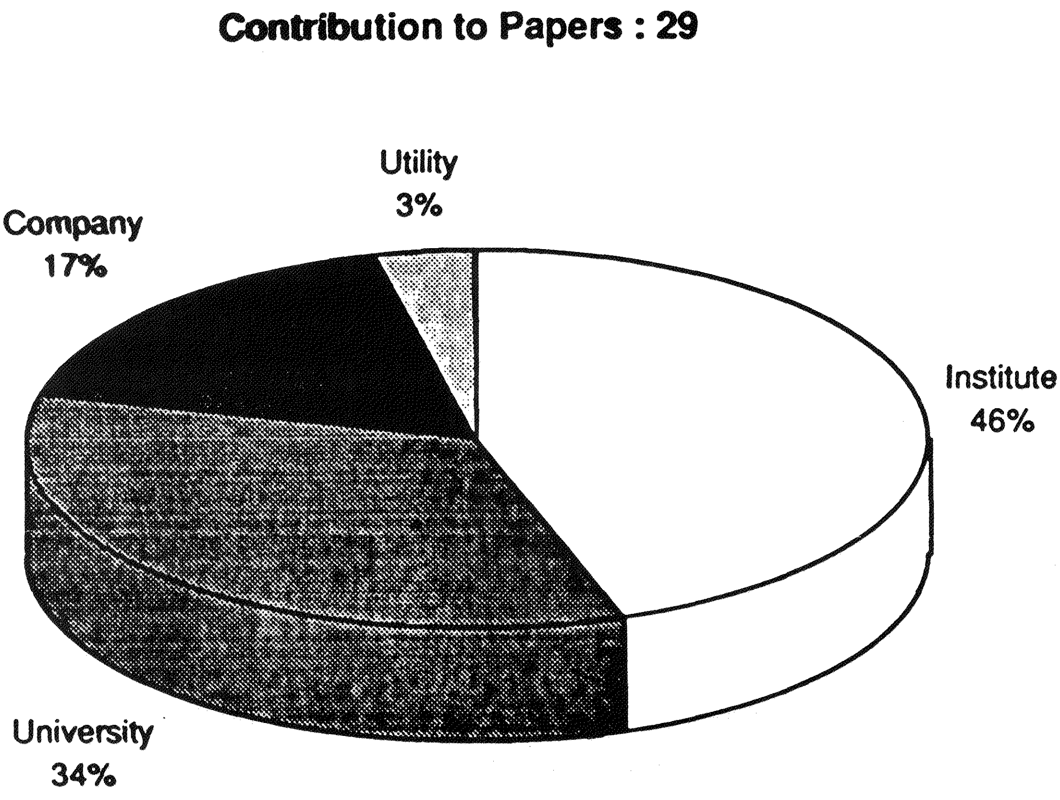

図２　発表者の所属

2　日韓ワークショップ概要

2.1　セッションA

セッションAでは、５件の論文（日本側３件、韓国側２件）が発表された。内訳は、配管のＬＢＢ関係が３件、圧力容器関係が２件である。以下に各論文の発表要旨を示す。

１）"Application of Leak-Before-Break Using Piping Evaluation Diagram", by Y.J.Yu, K.S.Yoon, S.H.Park, K.B.Park (KAERI), Y.J.Kim (Sung Kyun Kwan 大学)

韓国原子力研究所Ｙｕ氏より、配管評価線図（ＰＥＤ）を用いたＬＢＢ適用性の評価に関する発表があった。配管システムにＬＢＢを適用するためには、配管形状、材料特性、配管の荷重など、プラント固有のデータが必要である。従って、配管設計とその手順が既知でないと、ＬＢＢの評価は不可能である。本論文では、ＰＥＤと呼ばれる配管評価線図(通常運転荷重とＳＳＥ荷重との関係をき裂長さをパラメータとして示した線図) をＬＢＢ適用箇所（例えば、配管ーノズル接合部）に対して作成し、設計段階でもＬＢＢ適用性を評価できる手法を示した。本手法は、韓国次世代炉のＬＢＢ設計に活用される予定である。

２）"A Research Program for Dynamic Fracture Evaluation of Japanese Carbon Steel Pipes" by K.Kashima (CRIEPI)

電力中央研究所の鹿島より、日本の炭素鋼配管に関する研究計画について発表があった。本研究は、日本のＳＴＳ４１０炭素鋼配管の破壊に及ぼす動的荷重の効果に関するものであり、材料試験、配管試験、解析評価からなる。材料試験では、流動応力は歪み速度にあまり依存していないこと、配管試験では、破壊荷重は準静的荷重、動的荷重両者に対しほぼ正味応力基準（塑性崩壊基準）で予測出来ることが示され、顕著な動的効果は認められないとの報告があった。さらに、繰り返し荷重下でのき裂進展からその後の不安定破壊に至る一連の挙動を予測する破壊力学評価手法を開発し、実測結果との良好な一致を示した。

３）"Effect of Dynamic Strain Aging on the Leak-Before-Break Analysis in SA106 Gr.C Piping Steel" by I.S.Kim and J.W.Kim (KAIST)

韓国科学技術院のＫｉｍ教授より、ＳＡ１０６鋼Ｇｒ．Ｃ配管材のＬＢＢ評価における動的歪み時効（ＤＳＡ）の効果に関して発表があった。各種温度、荷重条件下で得られる

引張り試験データ、Ｊ－Ｒ試験データをもとに、漏洩検知可能なき裂寸法、不安定破壊時のき裂寸法に及ぼすＤＳＡの効果を評価して、結果を"LBB Allowable Load Window"としてまとめた。不安定破壊荷重は、プラントの運転温度域で荷重速度に依存する。このため、ＬＢＢの成立範囲は、２５０～３００℃付近では室温に比べて約３０％減少し、また、高荷重速度下でも減少することが認められた。

４）"Probabilistic Fracture Mechaniucs Analyses of Nuclear Pressure Vessels under PTS Events" by G.Yagawa, S.Yoshimura (Univesity of Tokyo), N.Soneda (CRIEPI), M.Hirano (JAERI)

東京大学矢川教授より、圧力容器の確率論的破壊力学解析に関する発表がなされた。論文では、日本機械学会のＲＣ１１１委員会で行われた圧力容器の破壊力学解析、特に加圧熱衝撃下における圧力容器の破損確率に対する評価手順の開発に関する研究活動が紹介された。米国ではＥＰＲＩ、ＮＲＣにおいてＰＴＳのベンチマーク研究が行われており、これに対し、日米で開発された４種類の解析コードを用い、破損確率に及ぼすデータの不確実性に関する各種の感度解析を実施した。

５）"Improved Toughness of the SA508 Class 3 Steel for Nuclear Pressure Vessel through the Steel-Making and Heat Treatment" by J.T. Kim, H.K. Kwon, H.S. Chang (HANJUNG)

韓国技術研究院の Kim 氏から、圧力容器鋼 SA508 Cl3 の製造、熱処理における靭性改善について発表があった。真空炭素脱酸法（ＶＣＤ）では、靭性値は基準を満たすものの低い値であり、改良ＶＣＤとして、最小冷却速度（１５Ｃ／ｍｉｎ）を用いることが推奨された。さらに、アルミニウムとシリコンキルド鋼を加えることにより、十分な靭性（ＫＩＣ）を確保できることを示した。これは組織の細粒化によるものであり、粒の寸法は、ＶＣＤで５０ミクロンであったものが、改良ＶＣＤでは２０ミクロンの値となることが報告された。

(所感)　セッションＡの韓国側の発表では、配管のＬＢＢ関連の成果がいくつか報告された。韓国におけるＬＢＢ研究は比較的最近開始されたものであるが、諸外国の研究成果を急速に取り入れて国内プラントの評価を実施し、一部プラントにはＬＢＢを適用済みとのことであり、韓国側の関心の高さがうかがわれた。ＬＢＢに対する基本的な考え方、アプローチは、ＮＲＣなど米国の基準に忠実に従っているが、動的歪み時効など米国配管材

における問題点を同様に抱えている点で、国産材料をベースとした我が国とは相違がある。基本的な材料試験、解析評価等においては十分な力をつけているが、大型構造試験、実証試験についてはデータがまだ十分ではないとの印象を受けた。(鹿島)

2.2　セッション　B

6）"Crack Shape Evolution of Surface Flaws under Fatigue loading of Austenitic Pipes" I.S.Hwang, J.H.Kim(Seoul National Univ.)

ソウル大学原子核工学科 黄　一淳助教授が Ni-Fe 基超合金（インコロイ 908）の疲労き裂進展に伴う表面き裂形状の変化について講演した。インコロイ 908 は国際熱核融合実験炉 ITER（International Thermonuclear Experimental Reactor）の中央ソレノイド導管の主候補材料で、ITER の中央ソレノイドマグネットの寿命予測が研究の目的である。予測に際して、Paris 則を以下で表示する。

深さ方向：$da/dN = CA \Delta Km$

表面方向：$dc/dN = CB \Delta Km$

表面き裂平板の実験結果から CA と CB を決定し、アスペクト比 a/c の変化と寿命を予測し、予測の精度を確認した。さらに、中央ソレノイド導管について、初期アスペクト比を a/c=0.1 として、概念設計案（CDA）と工学設計案（EDA）に基づき、寿命予測を行い、アスペクト比の変化を考慮しないと寿命を過小評価すること、EDA の寿命は要求プラズマパルスサイクル（5,000 回×安全係数 2）を十分に上回ることを示した。

主な討論は以下のとおりである。(菊池教授）形状変化はビーチマークで検出できる。(黄助教授）ビーチマークはオーステナイト鋼に適用できない。(KAIST 李 順福助教授）き裂閉口を考慮すべきである。(黄助教授）応力比 R=0 なので、き裂閉口の考慮は必要ない。(矢川教授）ITER の設計に際しては、電磁力の動的効果を考慮する必要はないのか。(黄助教授）ひずみ速度は遅く、動的効果はない。

本研究は黄助教授の米国 NBS（R.L.Tobler 博士）留学中の仕事の延長のようである（韓国は ITER に参加していない)。

7）"Study on the Effect of the Crack Length on the JIc Value" M.Kikuchi (Science Univ. of Tokyo)

東京理科大学　菊池正紀教授が A533B 鋼とアルミニウム合金の CT 試験片、3 点曲げ試験片および CCT 試験片の弾塑性破壊靱性 JIc に及ぼす初期き裂長さ比 a/W の影響につい

て講演した。

見掛けのJIcはき裂先端の拘束（３軸応力）の減少に伴い増大し、き裂先端応力場の第２パラメータであるQ係数(HRR解からの偏差）とよい相関を示す。　主な討論は以下の通りである。（ソウル大学　黄 一淳助教授）JIcに及ぼす拘束の影響はASTMの試験方法やASMEの基準で検討されているか。（菊池教授）検討されていないけれど、検討されるべきである。（小林教授）拘束の効果はJIcの試験方法に考慮する必要はない。構造部材の破壊評価には考慮すべきであり、ASME Sec.XI規格委員会では破壊靭性に及ぼす拘束の影響を検討している。

８）"Development of New Z-factors for the Evaluation of the Circumferencial Surface Crack in Nuclear Pipings" Y.H.Choi, Y.K.Chung, Y.W.Rark, J.B.Lee(KINS), G.Wilkowski (Battelle Memorial Institute)

韓国原子力安全技術院（KINS）の崔栄煥博士が配管の周方向表面き裂の評価に使用する新しいZ係数の開発について講演した。GE/EPRIの方法に基づき提案されたSC.TNP方法（薄肉管の表面き裂の解析方法）によってJ積分を解析し、J-R曲線を用いてモーメントー回転角関係を数値解析し、最大荷重を決定する。この方法によって、従来のASME規格の４つのZ係数（フェライト母材、フェライト溶接部、オーステナイト母材、オーステナイト溶接部）に対して、新しいZ係数を開発し、48の配管破壊試験結果と比較してよく一致することを示し、ASME規格のZ係数の過大な裕度を削減できるとしている。

主な討論は以下の通りである。（小林教授）ASME規格のZ係数はRm/tの関数Aと管外径ODの積の一次式であるが、新しいZ係数はこれにAとODの二乗の積の二次項を加えている。多項式にすれば、実験結果とよく一致するのは当然で、さらに三次項、四次項が要求され、きりがない。日本の維持基準のZ係数のODの項は対数表示である。比較して欲しい（コメント）。（小林教授）破壊評価線図を用いてZ係数を決定する方が、簡単ではないか（コメント）。

本研究は崔博士の米国バッテル研究所（G.Wilkowski博士）留学中の仕事の延長のようである。

９）"New Maintenance Code for Operating Nuclear Power Plants in Japan" (Draft) K.Iida (JPEIC), H.Kobayashi (TIT), Y.Imamura (MHI), K.Hasegawa (Hitachi)

東京工業大学　小林英男教授が発電設備技術検査協会で作成された日本の維持基準原案の概要について講演した。維持基準の構成は、（1）非破壊検査（NDE）基準、（2）欠陥評価基準、（3）補修／取替え基準であり、特に（1）と（2）についてASME規格、Sec.XI、Div.1の相違点が強調された。

主な討論は以下のとおりである。（KINS 崔栄煥博士）維持基準における材料劣化の扱いを説明して欲しい。（小林教授）日本の維持基準では材料劣化として圧力容器フェライト鋼の中性子照射脆化とステンレス鋳鋼の時効を取上げている。それ以外の材料劣化は日本の鋼ではない。中性子照射脆化の予測式は、米国R.G.1.99 Rev.2と特に溶接部に対して異なる。ステンレス鋳鋼の時効脆化は破壊評価線図を用いて評価するが、破壊評価線図は準備中である。（崔博士）維持基準のPDI(Performance Demonstration Initiative)への対応を説明して欲しい。（小林教授）日本の維持基準では、ASME規格Sec.XI Appendix V（企）とそこで要求される超音波探傷試験の資格試験に対応するプログラム（PDI）は採用していない。しかし、将来的には採用する見通しであり、発電設備技術検査協会に「UTによる欠陥検出性およびサイジング精度に関する確証試験」委員会が組織され、PDIへの対応を議論している。（質問者不明）維持基準におけるエロージョン／コロージョン（E/C）の扱いを説明して欲しい。（小林教授）現状の維持基準では、評価基準の中身は欠陥評価のみである。将来的には、疲労評価、E/C評価、破壊靭性評価、その他を含める予定で、現在、これらについて検討中である。

１０）"The Development Status of Mechanical Component Code for Nuclear Power Application in Korea" N.H.Kim, J.S.Nah (KOPEC)

韓国電力技術株式会社の金 南河技術士が韓国電力工業規格（KEPIC）のうちの機械的機器（Mechanical Component）規格の現状と今後の展開について講演した。韓国は従来、原子力プラントの設計／製造規格はなく、外国規格を準用してきたが、種々の不都合が生じた。1995年11月に、機械、電気、構造、防火、品質保証の分野のKEPICが制定、出版された。KEPIC-機械はレベルIとレベルIIがあり、レベルIは原子力機器でASME規格Sec.III Div.1に相当し、レベルIIは非原子力機器と機器への共通要求（材料仕様書、非破壊試験、溶接認定）である。ASME規格を参照して、整備と拡大が継続されている。

主な討論は以下のとおりである。（柴田勝之博士）配管防御規格はあるか。（金技術士）ない。（小林）

2.3　セッションC

１１）"Progress of Component Aging and Structural Integrity Research Program at JAERI" by K. Shibata (JAERI)

日本原子力研究所機器信頼性研究室の柴田室長より、原研における機器の経年化対策研究の現状に関する総括的な紹介があった。主な項目は、(a) パイプの信頼性実証のための疲労試験とＬＢＢ試験、(b) 経年化ＬＷＲ機器の信頼性実証試験、であり、(b) の項目については、経年化の機構と予測手法の開発、経年化評価手法、安全性評価手法の各項目について現在進行中の研究テーマが説明された。また質問に答えて、研究の一部は USNRC と共同で実施していることが報告された。

１２）"Developing of Expert System for Nuclear Piping Integrity" by Y.J.Kim, M.W.Suh, C.S.Seok, H.K.Jun (Sung Kyu Kwan Univ.), Y.W.Park, Y.H.Choi, J.B.Lee (KINS)

成均館大学の Kim 教授が発表した。構造信頼性評価には多くの知識と経験が必要であることから、その補助のためにエキスパートシステム"NPiES"を作製した。このシステムにはデータベースが蓄えられているが、古い材料のデータが不充分な場合、それを現在入手可能なデータから推論することができる。たとえば応力ーひずみ関係のデータがない場合、これを降伏応力と引張り強さのデータから精度よく推論できる。今後はＬＢＢ評価へこのシステムを拡張したい。これに対し矢川教授から推論機構としてニューラルネットワークを利用することを推奨する意見が出された。

１３）"Recent Progress in Korean Nuclear PLIM Program " by T.E.Jin, H.J.Choi, (KOPEC), I.S.Jeong, S.Y.Hong (KEPCO)

韓国電力会社の Jin 氏より発表があった。現在韓国では１０基の原子炉が稼働中で、６基が建設中、さらに７基が計画中であり、PLIM(Plant Life Management) の必要性が大きくなっている。PLIM Program は三期に分けて実施予定であり、現在は 1993 年から 1996 年までの Phase I として Feasibility Study を実施中である。これは韓国の最初の商業炉である Kori Unit 1 を主な対象としている。今後詳細な評価を行う Phase II (1997-2001), 補修・交換を行う Phase III(2001-2008) と、順次実施する予定である。

個人的な感想としては、Dr. Park の言っていた、「半導体や車の分野では日韓は競争関係にあるが、原子力施設の安全性確保という分野では両者は協力関係にある」という言葉

が印象的であった。また Kim 教授の"Open Minded Discussion"の呼びかけなど、韓国側の率直な姿勢に感銘を受けた。（菊池）

3　サイト見学報告

ワークショップの一環として5月9日（木）、月城(Walsong)原子力発電所の見学を行った。参加者と面会者は下記の通りである。

参加者：矢川（東大），小林（東工大），菊池（理科大），鹿島（電中研），柴田（原研），馬郡（事務局）

面会者：機械部課長、ベイ（Bae Young-Song)氏，機械部長，リー(Lee MyungBok)氏

ワークショップの翌日早朝，KINSが差回したマイクロバスで大田市を出発、見学先の月城(Walsong)原子力発電所に向かった。

天気は快晴で最高の見学日和であった。KINSのチャン（Chung Yeon-Ki)氏が付添いとして同行した。

韓国には、古里(Kori)，月城　(Walsong)，ウルチン（Ulchin)，霊光（Yonggwang)の4か所に原子力発電所があり、すべて韓国電力公社(KEPCO)が所有している。

月城発電所はその一つである。前日ワークショップが開催された大田市から約200km南東の慶州市にあり、日本海に面している。大田市から約4時間の行程である。途中、慶州市内で昼食を取った後、さらに市内から1時間東に位置するサイトに向い、午後1時に到着した。

到着後、機械部課長のベイ（Bae Young-Song)氏の案内を受けた。

最初に展示館を案内され、その後1～4号機を外部から見学し、さらに機械部を訪問し部長のリー(Lee Myung-Bok)氏と面談した。最後に、丘の上にある使用済み燃料の乾式貯蔵施設を見学した。

このサイトの従業員は約6,000人である。

月城のサイトでは、1号機が1983年から稼働している。現在、2,3,4号機が建設中である。1～4号機ともAECL（カナダ）製のキャンドウ6型炉を採用していることが特徴である。電気出力は、1号機が68万kW，2,3,4号機が70万kWで，仕様もほとんど同じになっている。1号基は2ループタイプで、各ループには蒸気発生器が2基設置されている。周知のように、キャンドウ炉は重水減速、重水冷却炉で，横型のカランドリア構造が特徴である。稼働中でも燃料交換できる特長がある。燃料交換は自動，半自動，手動等の方法で行われる等について燃料交換機器の説明を受けた。燃料交換は常時行われており、平均16バンドル/1日程度（20バンドル／チャンネル）である。

カランドリアを貫通するカランドリア管の数は380本である。カランドリア管の内側には、軽水炉の圧力容器に相当するZr合金製の圧力管が挿入されている。圧力管のISIはサンプリングで実施しており、超音波探傷と渦流探傷の他、肉厚測定も行われる。超音波探

傷と渦流探傷の結果、インディケーションがある場合には次の年にも検査を実施することになっているそうである。定検期間は30～40日程度でかなり効率的に行われているようである。

1号機以外については、2号機は今年の10月に燃料装荷が始まり、来年6月から営業運転を開始する予定。3号機は1998年、4号機は1999年と1年毎に運転開始する予定になっている。4号機は、5月にカランドリアが原子炉建屋内に搬入される予定になっている。当初3号機と4号機は計画されていなかったが立地が困難なため、3,4号機もこのサイトに建設されることになったそうである。これまで、運転員はAECLに派遣して教育訓練していたが、現在キャンドウ6型炉のシミュレータを建設しており、5月に完成するので、それ以後はサイト内での訓練が可能となる。

さらに、我が国と同様に韓国でも立地問題が深刻で、将来このサイトに5～8号機の建設も検討しているとのことである。　最後に、乾式使用済み燃料貯蔵施設を見学した。乾式貯蔵施設は、サイトの裏山を整地した小高い場所に設置されている。この場所からサイト全体とその後ろに日本海が見渡せる。左から1～4号機が整然と設置されていた。

貯蔵施設には、直径3m ×高さ5.5m のサイロが5体X12列の合計60体設置されている。1体のサイロで、60個X9段の使用済み燃料バスケットが保管できる。外側のコンクリート容器の中に本体のステンレス鋼製容器が入る構造になっている。崩壊熱は、自然放熱により冷却され、ステンレス容器の設計温度は150℃である。

各ユニットにある使用済み燃料プールは10年分の貯蔵能力があるが、いずれ不足するので乾式貯蔵することにしたとのことである。6年間燃料プールで冷却後、この場所で乾式貯蔵されることになっている。乾式貯蔵を、いつまで続けるのかとの問いに対して、まだ見通しがなく永久保管の可能性もあるとのことであった。

日本では見られない、キャンドウ炉および乾式貯蔵施設を見学でき見聞を広めることができた。なお、時間の制限により原子炉の内部に立入れなかったのは残念であった。

韓国では現在、11基の原子力プラントが稼働し、その他7基が建設中、計画中が2基である。炉型はPWRとPHWR（加圧重水炉）であるが、輸入相手国は、米国，カナダ，フランスで製造会社もWH，CE，フラマトム，AECLと多様であり、これは国策として進められているようである。発電設備容量は、現在、950万kWとスエーデンについで世界第10位で、2002年までに建設中の7基が稼働するので、近い将来第9位となる。また、1995年の実績では原子力発電で電力全体の約50％を賄っており原子力への依存度はフランスについで世界第2位で、我が国の30％を遥かに上回っている。すでに原子力発電大国になっている。

原子力発電の原価は、石油が38ウオン/kWh，原子力が20ウオン/kWhとのことで、我

が国の約 1/3 程度である。電力は国策会社の韓国電力公社 (KEPCO:Korea Electric PowerCorporation) が一社独占で供給しており、KAERI,KINS 等の機関を含め、官民一体で原子力開発が進められているようである。我が国と同様に資源に乏しい韓国としては、コストの低い原子力発電への期待が極めて高いことが以上からうかがえる。

霊光発電所は黄海に面しているが、その他はすべて日本海側に位置している。霊光発電所を含め山陰・北九州地区からわずか 200～300km 程の範囲に、我が国のプラント以外に建設中も含めると 18 基のプラントが在ることになる。原子力発電の安全性の観点からは、我が国だけでなく韓国の発電所発も含めて検討していく必要があることを強く感じた。

最後に、この見学の手配をして頂いた、KINS と KEPKO の関係者に御礼申しあげます。(柴田)

4　成果と今後の課題

SMiRT 会議などで日韓両国の機器や材料の健全性の研究者・技術者が顔を合わせることはこれまでにも数回あったが、今回のワークショップのような形で深く話し合ったり情報交換を行うといった機会はほとんどなかったものと思われる。韓国の技術レベルはかなり高く、両国の発表に対する討論も十分にかみ合った。このような意味で今回のワークショップは大成功であったと思われる。後で韓国側の代表者の一人に今回の感想をたずねたが、韓国側の印象としても今回のワークショップの意義は極めて高かったと評価していた。

今回は日韓の２国間のみでの会合であったが次回は台湾も含めてより強化した形での開催が予定されている。

参加者については今回は我が国からは中立研究者のみであったが次回は我が国で開催予定であり産業界、官界からの参加も期待したい。

このような試みは必ずしも短期的視点ではすぐに果実が得られるものではかもしれないが、長期的観点から育てていくことが重要であると思われる。（矢川）

5　今後の計画

韓国側から Dr.Park と Kim 教授、日本側から矢川教授と菊池が出席して、今後の活動方針に付いて協議し、以下の案を作成した。

5.1　今後の研究交流について

今後の研究交流のための機関として"Eastern Association for Integrity of Nucl ear Components"（仮題）を結成する。当面は日本と韓国の二国からの代表で構成し将来的には台湾を初めとしてアジアの原子力発電所所有国に対象を広げる。各国は代表委員一名、幹事一名、委員若干名を選ぶ。

Workshop を 2 年に一度開催する。またその際適当な施設の見学会も行う。次回は 1 998 年に日本で開催する。そのときは台湾にも参加を呼びかける。

5.2　講演論文の公表について

"Nuclear Enginering design (NED) "の Special Volume として印刷する方向で検討する。今回の Workshop の論文については日本、韓国それぞれで集めて、 NED の方式にしたがって校閲を行う。出版予定は 1997 年 4 月を目指す。

以上の案を Workshop 終了後参加者全員に図り賛同を得た。

6　あとがき

今回のワークショップは、まさにアジア地区の関連研究者・技術者の対話のスタートであり、２１世紀に向かってこの輪が大きく拡がっていくことが期待される。内外の関係諸機関ならびに各位の御理解と御援助を賜れれば幸いである。（矢川）

7　付録

これらはＫＩＮＳから提供された資料である。韓国における基準作りの現状、ＣＡＮＤＵ型原子炉の詳細など、興味深いと思われるので全文を付録として本報告集に掲載する事とした。

원전 기기의 건전성 평가 기술
WORKSHOP

Part II: International Workshop on the Integrity of Nuclear Components

한 국 원 자 력 안 전 기 술 원

CONTENTS

Session A

Session B

Session C

SESSION A

1 Application of Leak-Before-Break Using Piping Evaluation Diagram (PED)

Y.J. Yu*, K.S. Yoon, S.H. Park, K.B. Park (KAERI),
Y.J. Kim (SungKyunKwan Univ.)

Application of Leak-Before-Break Using Piping Evaluation Diagram(PED)

Y.J.Yu*, K.S.Yoon, S.H.Park, K.B.Park
(Korea Atomic Energy Research Institute)

Y.J.Kim
(SungKyunKwan University)

ABSTRACT

Plant specific data, such as pipe geometry, material properties and pipe loads, are required to apply LBB to a piping system. Thus, LBB evaluation can not be done until piping design and routing is completed. A simple method for evaluating LBB for piping systems during design process is presented in this paper. This method produces a piping evaluation diagram, called PED, for intermediate pipe locations and pipe-nozzle interface locations which defines the LBB requirements to the piping designer for use during the design process and is independent of pipe routing. This methodology will be used for the LBB evaluation of a new plant design such as KNGR(Korean Next Generation Reactor).

INTRODUCTION

It was previously required that structures, systems, and components important to safety be appropriately protected against the dynamic effects of missiles, pipe whip, and discharging fluids that may result from a postulated pipe break. Although the assumption of an instantaneous double ended pipe break in large high energy lines provided a convenient way to envelope the loads that might result from pipe rupture, it provided little or no relationship to the way which such pipes actually behave. This approach led to the need for substantial protective measures to guard against the consequence of such postulated breaks. These protective measures are expensive to build and maintain, and lead to a potential degradation of plant safety. The placement of pipe whip restraints degrades plant safety if thermal expansion is restricted and when the accessibility for and effectiveness of inservice inspection is reduced.

The research of the last decade on elastic-plastic fracture mechanics has led to a means to justify a more reasonable alternative: Leak-Before-Break(LBB). The fundamental premise of LBB is that the materials used in nuclear power plant piping are sufficiently tough that even a large throughwall crack, which could result in coolant leak rates well in excess of those detectable by present leak detection systems, would remain stable and would not result in a double-ended guillotine break under maximum loading conditions. Thus the dynamic effects of postulated ruptures in the piping system are eliminated from the design basis when the piping system is shown to meet all the criteria for the application of leak before break presented in NUREG 1061, Volume 3[1] and Standard Review Plan 3.6.3[2].

Since the mid-1980's, the LBB technology has been applied extensively to a high energy piping system[3] in existing plants. However, there are differences between the application of LBB to an existing plant and a new plant design. In this paper a simple approach is introduced which is intended to use for application of LBB to a new plant design such as KNGR. This approach is based on LBB PED developed by Fabi[4] and extended to the pipe-nozzle interface location in this paper.

CURRENT REGULATORY CRITERIA

NUREG-1061 sets forth stringent criteria to be applied to each piping system to determine if LBB is a viable alternative to postulating a DEGB (Double-Ended Guillotine Break). "The LBB approach should not be considered applicable to high energy fluid system piping, or portions thereof, that operating experience has indicated particular susceptibility to failure from the effects of corrosion(e.g., intergranular stress corrosion cracking), water hammer or low and high cycle (i.e., thermal, mechanical) fatigue". To the extent that fatigue may exist in a particular piping system, it must be considered when performing a LBB evaluation. For those piping systems to which LBB is applied, the following criteria must be met:

(1) A leak detection system is required that is capable of detecting a leakage rate (less than 1.0 gallon per minute for the primary system as a requirement of Regulatory Guide 1.45), to which NUREG-1061 applies a margin of 10.
(2) Throughwall cracks which are large enough to leak 10 times the detection capability (i.e. 10 gallon per minute for primary system piping) must be stable for $\sqrt{2}$ times the sum of the normal operation and safe shutdown earthquake(SSE) loads.
(3) Throughwall cracks twice as long as a crack which leaks 10 times the detection capability must be stable under the sum of normal operation and SSE loads.

In developing PED, the appropriate margins required in the current regulatory criteria are included.

REQUIRED INPUT FOR ANALYSIS

PED defines the LBB requirement to the piping designer for use during the design process. In order to define the LBB requirements, several sets of LBB analyses are performed for each different pipe size and material considered in the LBB application. The following are the input for the analyses to develop the PED.

Material Properties

Previous work[5] by ABB-CE has shown that a conservative bounding analysis results when the material stress-strain properties of the base metal (lower yield) and the fracture properties of the weld metal (lower toughness) are used for the entire structure. Industry data [6,7,8] are reviewed to establish the lower bound stress-strain and J-R curves for each material. For both the final design and as-built configurations, the actual material properties used for piping systems subject to LBB shall be reviewed to confirm the application of LBB.

Applied Loading

There are two aspects to the loading for Leak-Before-Break. First, the normal operating (NOP) load is used in determining the detectable leakage crack length. The NOP loading includes the system pressure and the thermal expansion piping moment. The NOP load is generally small enough so there is no concern for stability with this loading alone. Two NOP loads which cover the entire range of possible loading for the line under consideration is assumed. The second aspect of the loading is the LBB loadings, which is the NOP plus additional loading(s) such as safe shutdown earthquake(SSE) loading and stratified flow(SF) loading. The LBB loading provides an additional piping design requirement which has to be met.

Leak Detection Capability

The basic premise of the Leak-Before-Break concept in piping is that a flaw will be detected via loss of fluid prior to the failure of the pipe. This requires a detectable leak rate in conjunction with stress-strain curve for pipe material. It is assumed that the plant is capable of detecting a leakage of one gallon per minute with an hour based on the requirements of Regulatory Guide 1.45[9].

LBB ANALYSIS FOR PED

Crack stability evaluation

The methodology to evaluate the stability of through-wall cracks requires knowledge of the applied loads, a leakage crack size, and the material properties. Finite element models of three different crack lengths were developed for the leakage crack and twice the leakage crack to consider the crack extension. One set of model having crack sizes of a, $a-\delta$ and $a+\delta$ at normal operation loads was used to demonstrate safety margin on the loads. "a" is the detectable leakage crack length, and "δ" is a small increase or decrease in "a". Another set of models, having crack lengths $2a$, $2a+\delta$, $2a-\delta$ were used to demonstrate the margins on crack size. The crack lengths are input to the detailed stability analysis of the through wall cracks in piping systems. The FEA is carried out for the estimated leakage crack size and twice that length.

Two planes of symmetry are used for pipe model to minimize the size of FE models. Therefore, each model represents one quarter of the pipe as shown in Figure 1. The model for location near the nozzle is shown in Figure 2. Here one plane of symmetry is used to minimize the model size, meaning that one half of the pipe-nozzle is modeled.

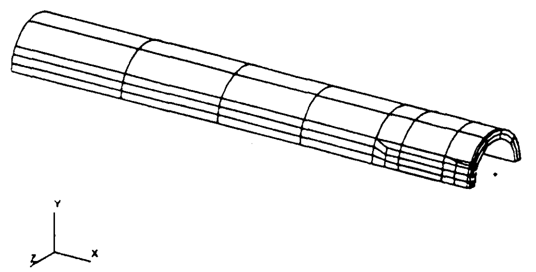

Figure 1. Finite Element Mesh for Pipe Model

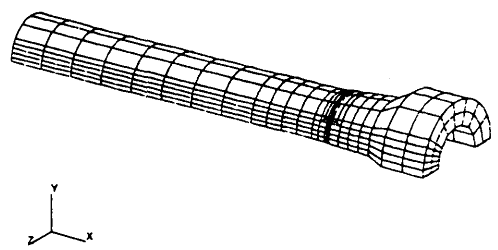

Figure 2. Finite Element Mesh for Pipe-Nozzle Model

J-Integral

To evaluate the intensity of the stress field near a crack tip for the elastic-plastic problem, the J-integral parameter is used. The J-integral parameter is related to the energy release rate at the crack tip. The method used to evaluate the J-integral is virtual crack extension method, where; $J=(1/t)(dE/da)$ and dE is the change in the strain energy release rate for a virtual crack extension, da. To calculate dE , small virtual displacements of the nodes in elements near the

crack tip are applied in the direction of the crack extension.
The J-integral is determined by FEA for pressure, normal operation, and SSE loading for three different crack length for each geometric model. To evaluate the margin on crack length, J-integral is evaluated for the applied loads for 2 times the detectable leakage crack size. For the margin on loads evaluation the J-integral is also evaluated $\sqrt{2}$ times the applied loads for the detectable leakage crack size.

Stability Evaluation

The stability of the cracked pipe is assessed by comparing the J-integral value due to the applied loads on the pipe to the material crack resistance. The stability criteria employed for ductile crack extension is:

Crack Stability is assured if:

$$J_{applied} < J_{material} \qquad (1)$$

and

$$\frac{dJ_{applied}}{da} < \frac{dJ_{material}}{da} \qquad (2)$$

The slope of the J-integral vs. a curve for each location is obtained by fitting a polynomial curve through the J-integral values. By plotting J-integral vs. dJ/da which is called a J-T diagram, both parts of the stability criterion above can be evaluated simultaneously.

Development of J-T diagram

The J-integral vs. dJ/da curve is called a J-T diagram. The J-T diagram is developed for both crack length a and $2a$. This is done as follows;

1. The J-T diagram due to applied load:

   a. From FEA, determine applied J for cracks a, $a+\delta$ and $a-\delta$ as well as $2a$, $2a+\delta$, and $2a-\delta$ for defined loading.
   b. This gives J as a function of crack length a. Thus dJ/da in the vicinity of a and $2a$ can be determined.
   c. Polynomial is fit to J where:

$$J(a) = c_1 a^2 + c_2 a + c_3 \qquad (3)$$

thus

$$\frac{dJ}{da} = 2c_1 a + c_2 \qquad (4)$$

2. The J-T diagram due to material properties

   a. Material J-R curve defines J for different crack lengths
   b. Power law curve is fit to J-R data curve

$$J = C_1(\Delta a)^{C_2} \qquad (5)$$

thus,

$$\frac{dJ}{da} = C_1 C_2 (\Delta a)^{C_2 - 1} \qquad (6)$$

This process is outlined in Figure 3. Once the J-T diagram is developed, the load that causes instability is defined, for each of the highest stressed location in the pipe. At the point of intersection of the loading curve and material curve, the following holds true:

$$J_{applied} = J_{material} \qquad (7)$$

and

$$\frac{dJ_{applied}}{da} = \frac{dJ_{material}}{da} \qquad (8)$$

This is the point above which unstable crack growth will occur for the given load. This instability load is compared to the actual applied load at that point. If the LBB applied load is less than the instability load, then the point passes the LBB criteria. If LBB applied load is greater than the instability load then the point fails the LBB criteria.

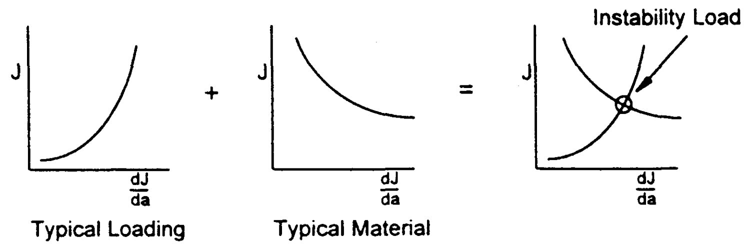

Figure 3. Stability Evaluation

CONSTRUCTING A PED

PED for intermediate location

The procedure for constructing a PED for Intermediate pipe location was developed by Fabi [4]. The procedure is as follows;

For detectable leakage length, the LBB procedure requires a margin on loads. Thus the maximum load equals to NOP+SSE.

$$M_{\max(i)} = \sqrt{2}\,(M_{SSE(i)} + M_{NOP(i)}) \qquad (9)$$

This can be solved for the allowable SSE loading ;

$$M_{SSE(i)} = M_{\max(i)} / \sqrt{2} - M_{NOP(i)} \qquad (10)$$

where, i = each NOP condition for analysis of leakage crack length 'a'

For twice the detectable leakage length, the LBB procedure requires an additional margin on crack length. Again setting the maximum load equals NOP+SSE.

$$M_{\max(i)} = M_{SSE(i)} + M_{NOP(i)} \qquad (11)$$

Solving for the allowable SSE loading ;

$$M_{SSE(i)} = M_{\max(i)} - M_{NOP(i)} \qquad (12)$$

where, i = each NOP condition for analysis of twice leakage crack length '$2a$'

A typical PED for a GTAW weld in a SA312 Type 347 stainless steel 12 inch schedule 160 class 1 pipe is shown in Figure 4.

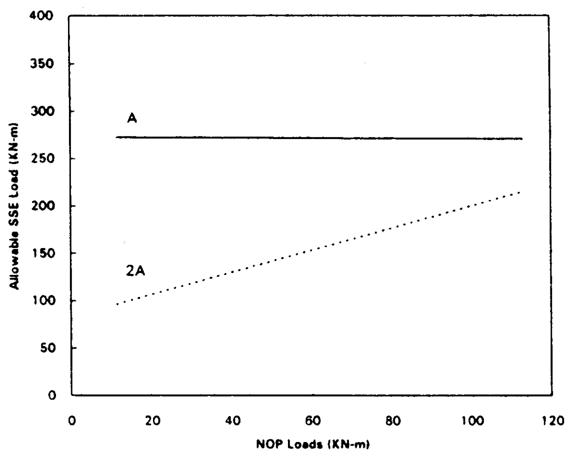

Figure 4. PED for 304 mm diameter stainless steel pipe (SA312 Type 347)

PED for pipe-nozzle interface location(terminal ends)

Typical LBB (Leak-Before-Break) analysis is performed for the highest stress location for each different type of material in the high energy pipe line. In most cases, the highest stress occurs at the nozzle and pipe interface location at the terminal end. The standard finite element analysis approaches to calculate J-integral values at the crack tip utilizes symmetry conditions when modeling near the nozzle as well as away from the nozzle region to minimize the model size and simplify the calculation of J-integral values at the crack tip. A factor of two is typically applied to the J-integral value to account for symmetric conditions. The stiffness of the residual piping system and non-symmetries of geometry along with different material for the nozzle, safe end and pipe are usually omitted in current LBB methodology. A study, done by Yu et.al [11], shows that this simplified analysis can lead to conservative results especially for small diameter pipes where the asymmetry of the pipe-nozzle interface is ignored.

In this paper, a PED for pipe-nozzle interface location is developed to consider the effects of non-symmetries due to geometry and material at the pipe-nozzle interface. The procedure to construct the PED for the pipe-nozzle interface location is basically the same as that for an intermediate pipe location. However, the calculation of a detectable crack length for the pipe-nozzle interface location is somewhat different with that for the intermediate pipe location. Consideration of the nozzle requires an iterative procedure to find an appropriate crack length which leaks at 10 gpm and employs both the finite element model used for the crack stability analysis and the PICEP code[10]. Since the stiffness of the nozzle is included in the stability analysis it must also be included in the leakage calculation. The procedure uses the PICEP program as a flow calculator for a given assumed crack length and calculated area from the pipe-nozzle finite element model. This procedure is as follows[11]:

Step 1: Assume a flaw length in FE model.
Step 2: Apply normal operating load to the FE model and calculate the crack opening area.
Step 3: Using PICEP with the same length flaw vary the applied moment until the area is the same area as calculated with the FE model.
Step 4: If the PICEP flow is greater than 10 gpm the crack length is decreased - go to step 1.
If the PICEP flow is less than 10 gpm the crack length is increased - go to step 1.
If PICEP flow is 10 gpm - STOP.

The final step establishes the pipe-nozzle interface crack length which leaks at the detectability limit(with margin) of 10 gpm.
Figure 5 presents a PED for the nozzle-pipe interface location and the intermediate pipe location where "A" and "2A" are the detectable leakage crack length and twice the leakage crack length, respectively.

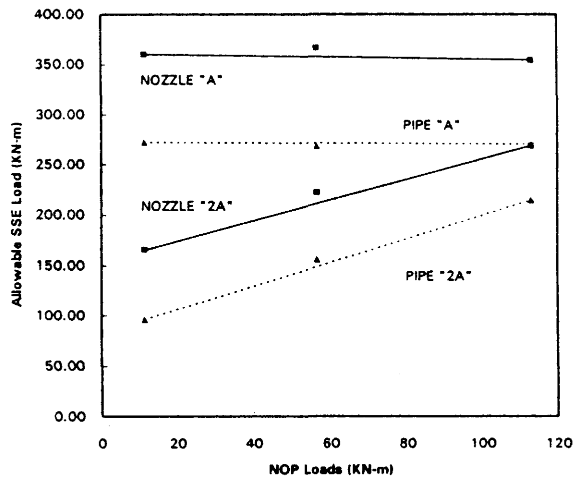

Figure 5. Comparison of pipe and nozzle-pipe PED

LBB EVALUATION USING PED

For the highest stressed location for each different type of material in the line, the NOP and SSE loading are plotted on Figure 6. If this point falls below both curves in Figure 6 (loading represented by point P), the line passed LBB with appropriate safety margin already included in the plot. If the highest stressed points fall above either curve in Figure 6(loading represented by points X,Y and Z), the line fails LBB. Then the piping designer can modify the piping design in order to pass LBB.

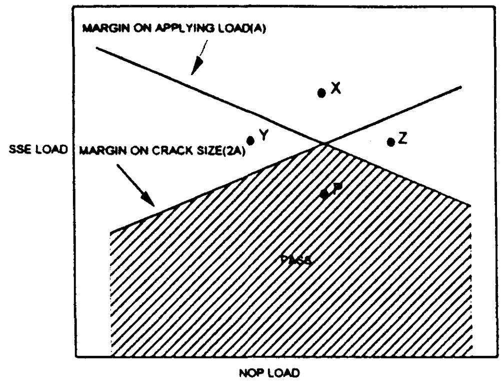

Figure 6. Typical piping evaluation diagram (PED)

DISCUSSIONS AND CONCLUSIONS

An approach is presented which is suitable for application of LBB for a new plant design such as KNGR. The advantage of this approach is that the piping designer can quickly iterate to a design which satisfies both the ASME code and LBB requirement.
However, LBB evaluation using PED can be very conservative for some cases because PED uses industrial lower bound material data and loads calculated from a elastic analysis based on the piping system being uncracked. A modified PED which can consider the effects of applying load at the cracked pipe section due to the residual compliance of the piping system are now under developing at KAERI and SungKyunKwan University.

REFERENCES

[1] NUREG-1061,Vol.3., "Evaluation of Potential for Pipe Break."
[2] USNRC Draft Standard Review Plan 3.6.3, "Leak-Before-Break Evaluation Procedure," March, 1987.
[3] K. Wichman, J.Tsao, M. Mayfield, 1996, "LBB Application in the U.S.A. Operating and Advanced Reactors," NEA/CSNI/R(95)18, Volume 1, pp13~19.
[4] R.J. Fabi, D.A. Peck, 1994, "Leak Before Break Piping Evaluation Diagram, " Presented at The1994 PVP Conference, PVP-Vol.283, pp. 111~115.
[5] EPRI Report NP-5057, "Analysis of Cracked Pipe Weldments", February 1987.
[6] A.L.Hiser and G.M.Callahan, "A User's Guide to the NRC's Piping Fracture Mechanics Data Base (PIFRAC)", NUREG/CR-4894 (MEA-2210), Materials Engineering Associates, Inc., Lanham, MD, May 1987.
[7] Y.J.Kim et. al, 1993, " Fracture Properties Evaluation of BOP Piping Systems for the Yonggwang 3/4 Nuclear Generating Station," Trans. of the 12th SMiRT Conference, Vol. G, pp. 435~440.
[8] SungKyunKwan Univ.,1995, "LBB Test Evaluation of Primary Piping Weld Materials for Ulchin 3/4 Nuclear Power Plants(RCL/PZR Surge Line Field Fabrication)," SKKU/SAL-9502.
[9] USNRC Regulatory Guide 1.45, "Reactor Coolant Boundary Leakage Detection Systems", May 1973.
[10] EPRI Report NP-3596-SR Rev.1, "PICEP: Pipe Crack Evaluation Computer Program", Electric Power Research Institute, July 1987
[11] Y.J.Yu, S.H.Park, G.H.Sohn, Y.J.Kim and W. Urko, 1995, " Application of LBB to a Nozzle-Pipe Interface", NEA/CSNI/R(95)18, Volume 1, pp83~91.

2 A Research Program for Dynamic Fracture Evaluation of Japanese Carbon Steel Pipes

K. Kashima* (CRIEPI)

Presented at International Workshop on the Integrity of Nuclear Components
May 8, 1996, KINS, Korea

A Research Program for Dynamic Fracture Evaluation of Japanese Carbon Steel Pipes

K.Kashima, N.Miura
Central Research Institute of Electric Power Industry (CRIEPI), Tokyo, Japan
S.Kanno, K.Miyazaki, M.Ishiwata and N.Gotoh
Hitachi Ltd., Ibaraki, Japan

Abstract

The research program was developed to investigate the dynamic load effect on Japanese carbon steel STS410 pipe. The program comprises material tests, pipe fracture tests and development of estimation scheme.

Material property tests showed that the flow stress was nearly constant or slightly increased with strain rate. Pipe tests showed that fracture load was nearly predicted by the net-section collapse criterion for quasi-static and dynamic loading. A significant dynamic effect was not observed for STS410 carbon steel piping. Crack growth was well formulated by using J-integral parameter for low cycle fatigue. Combining the crack growth behavior and unstable fracture criterion, an estimation scheme was newly developed and validated for constant cyclic loading conditions.

1. Introduction

Leak-before-break (LBB) is one of the potential concepts to evaluate the piping integrity for light water reactors. Many LBB researches in the government, research institutes, utilities and manufacturers have been conducted to demonstrate the validity of this concept and apply it to the piping designs in nuclear power plants.

In Japan, the LBB research programs were initiated at NUPEC (Nuclear Power Engineering Corporation) for stainless steel piping in 1977 and carbon steel piping in 1985 under the sponsorship of MITI [1,2]. In these programs, fundamental material tests, full-scale pipe fracture tests and LBB assessment were conducted. Many researchers joined the programs and CRIEPI was responsible to evaluate unstable pipe fracture using fracture mechanics approach. JAERI also developed another LBB program including the evaluations of fatigue crack growth, unstable pipe fracture and pipe whip restraints [3]. In 1987, USNRC organized an international research program group, "IPIRG" under the funding from 9 countries including USA (USNRC, EPRI), UK (Nuclear Electric), France (CEA), Italy (ENEA), Sweden (SPI), Switzerland (HSK), Canada (AECB), Taiwan (TPC), Japan (CRIEPI). The main objective of the IPIRG program was to study the effect of seismic (dynamic/cyclic) loading on pipe fracture. The program has been in Phase-2 since 1992 and will be terminated in April, 1996.

The IPIRG results showed the dynamic and cyclic loading effects on pipe fracture for some materials. This trend was significantly observed in A106 Grade B, typical carbon steel in USA. In 1991, CRIEPI and Hitachi initiated a collaborative research program to investigate the effects of dynamic and cyclic loading on the fracture of Japanese carbon steel piping [4-6]. This paper presents the summary of this program and the major findings.

2. Program Milestones

The 6-years research program was started in 1991 as the joint study of CRIEPI with Hitachi and will be terminated in 1996. The program includes the following milestones:

(1) Conduct material tests under quasi-static and dynamic loading conditions,
(2) Conduct pipe fracture tests under monotonic and cyclic loading conditions,
(3) Develop an effective evaluation scheme for highly low cycle fatigue crack growth and
(4) Evaluate the dynamic and cyclic loading effects on Japanese carbon steel piping.

The schedule of these milestones is shown in Table 1.

3. Material Property Tests

Material tests were conducted to obtain the tensile properties for base metal and submerged-arc weld metal of STS410, one of the typical carbon steels used in Japanese nuclear piping. The chemical compositions of the materials are tabulated in Table 2. Tensile tests were conducted at room temperature and high temperature (288C or 300C) under quasi-static strain rate (10^{-4} /sec) to dynamic strain rates (10^{1} /sec). Test specimens were taken from the pipe in the axial direction. Figure 1 shows the geometry and dimensions of the round-bar specimens.

Figures 2 (a) and (b) show the results of tensile tests for base metal and weld metal. For both materials, yield stress (0.2% proof stress) and ultimate stress increased with the increase of strain rate at room temperature. At high temperature, yield stress increased with strain rate and ultimate stress decreased with strain rate. These results clearly showed the dependency of the tensile properties on strain rate. However, it should be noted that the flow stress, a major dominating parameter for plastic collapse of ductile material, did not show a significant dynamic effect on strain rate at high temperature because it was nearly constant or slightly increased with strain rate when it was defined as the mean value of yield stress and ultimate stress.

4. Pipe Fracture Tests

Specimens for pipe fracture tests were circumferentially through-wall or surface-cracked pipes of STS410 base metal and welded joint with 6-inch diameter. Figure 3 shows the geometry and dimensions of the specimen. Initial notch with the total angle of 30 or 60 degree was introduced by electrical discharge machining after mechanical machining. Figure 4 illustrates the apparatus used for the pipe fracture tests at room temperature and high temperatures. In high temperature tests, the specimens were heated up to 265C to 285C by forced circulation of hot air.

The pipe specimens were subjected to four-point bending under the following loading types:

Type (1): Monotonic loading tests

Type (2): Constant amplitude cyclic loading tests
Type (3): Incremental amplitude cyclic loading tests
Type (4): Random cyclic loading tests

Figure 5 illustrates these loading types. Strain rates were quasi-static except for Type (1), where both quasi-static (0.05 mm/sec) and dynamic (5 mm/sec) displacement rate were applied. The effect of loading rate on monotonic pipe fracture was investigated in Type (1) test. In Type (2) tests, the loading wave was an alternating triangle of the constant load amplitude with the frequency of 0.1 Hz. The numbers of cycles at pipe failure were measured for pipe specimens subjected to the constant load amplitudes equal to 50-90% of the plastic collapse load. Type (3) and (4) deal with the complex loading types of increasing load amplitude and random load.

More than 40 pipe tests were conducted in Type(1) to (4). Figure 6 shows the results of Type (1) tests as the relationship between normalized maximum load and displacement rate. The normalized maximum load was defined as the ratio of the measured maximum load to net-section collapse load and the displacement rate was measured at the loading point on pipe specimen. These results indicates that the normalized maximum load is nearly constant or slightly increasing with strain rate. They mean that fracture load is nearly predicted by the net-section collapse criterion for quasi-static and dynamic loading and STS410 does not show the significant dynamic effect as was observed for A106 carbon steel [7].

5. Estimation Scheme to Predict Failure Life

An estimation scheme was developed to evaluate a series of fracture behavior from the cyclic crack growth to unstable fracture for circumferentially cracked pipe subjected to constant amplitude cyclic bending.

For crack growth under very low cycle fatigue condition, the elastic-plastic stress conditions near the crack tip should be taken into account. Therefore, the elastic-plastic fracture mechanics parameter, ΔJ, was introduced to the crack growth rate equation, instead of the prevailing elastic parameter, ΔK. A new equation was developed to calculate ΔJ for circumferential crack using the Jmax (monotonic J-integral) and crack length [4]. Jmax can be easily calculated using the GE-EPRI handbook [8]. The calculation steps are as follows:

(1) Calculate Jmax for initial crack length (a_0) in the first loading cycle.
(2) Translate Jmax into Δ J.
(3) Calculate cyclic crack growth rate (da/dN) from "(da/dN)- Δ J" relation.
(4) Update the crack length (a) by adding the crack growth (da).
(5) Decide whether pipe will fracture or not by net-section collapse criterion.
(6) If no fracture will result, repeat the above steps (1) to (5) in the next loading cycle.

Figure 7 shows the comparison of the experimental and predicted relationship between the crack extension and number of cycles for 6 cases at room temperature and high temperature. The predicted behavior is in good agreement with the test results.

6. Conclusions

The research program was developed to investigate the effect of dynamic and cyclic load on Japanese carbon steel STS410 pipe. The program comprises material tests, pipe fracture tests and development of estimation scheme.

1) Material property tests showed that tensile stress and yield stress were dependent on strain rate but the flow stress was nearly constant or slightly increased with strain rate.
2) Pipe tests showed that fracture load was nearly predicted by the net-section collapse criterion for both quasi-static and dynamic loading. A significant dynamic effect was not observed for STS410 carbon steel.
3) Cyclic crack growth was formulated by introducing J-integral parameter, Δ J. Combining the cyclic crack growth equation and unstable fracture criterion, a new estimation scheme was developed and validated for constant cyclic loading conditions.

References

[1] NUPEC, "Proving Test on Stress Corrosion Cracking in BWR",NUPEC,(1984).
[2] NUPEC, "Proving Test on the Integrity of Carbon Steel Piping in LWRs", NUPEC, (1989).
[3] K.Shibata, et al., "Results of Reliability Test Program on Light Water Reactor Piping", Nuclear Engineering and Design, 153, (1994), 71.

[4] N.Miura, et al., "Low Cycle Fatigue and Ductile Fracture for Japanese Carbon Steel Piping under Dynamic Loading", Nuclear Engineering and Design, 153, (1994), 57.
[5] N.Miura, et al., "Low Cycle Fatigue Crack Growth and Ductile Fracture under Dynamic/Cyclic Loading for Japanese Carbon Steel Piping ,Part-2:Analytical Study", ASME PVP 266,(1983),175.
[6] N.Miura, et al., "Application of Cyclic J-integral to Low Cycle Fatigue Crack Growth of Japanese Carbon Steel Pipe", Proceedings of LBB95, Lyon, France, October,1995.
[7] R.A.Schmidt, G.M.Wilkowski, "The International Piping Integrity Research Group (IPIRG) Program: An Overview", SMIRT-11, Tokyo, Vol.G, (1991), 177.
[8] V.Kumar, et al., "Further Developments in Elastic-Plastic Analysis", EPRI NP-5596, (1988).

Table 1 Program milestones

ITEM	1991	1992	1993	1994	1995	1996
(1) Material Tests	●Base (RT)	●Base (HT)	●Weld (RT/HT)			
(2) Pipe Tests	●Base (RT)	●Base (HT)	●Weld (RT)	●Weld (HT)		
(3) Estimation Scheme	●Base (RT)	●Base (RT)	●Base (HT)	●Weld (RT)	●Weld (HT)	
(4) Evaluation of Dynamic Cyclic Effect for STS410						●

Table 2 Chemical compositions of materials

(wt%)

			C	Si	Mn	P	S
STS410 Carbon Steel	Base	*Specified*	*< 0.30*	*0.10 - 0.35*	*0.30 - 1.40*	*< 0.035*	*< 0.035*
		Measured	0.14	0.30	1.20	0.009	0.001
	Weld	*Specified*	*< 0.19*	*0.30 - 0.60*	*1.30 - 1.60*	*< 0.020*	*< 0.020*
		Measured	0.06	0.49	1.40	0.008	0.004

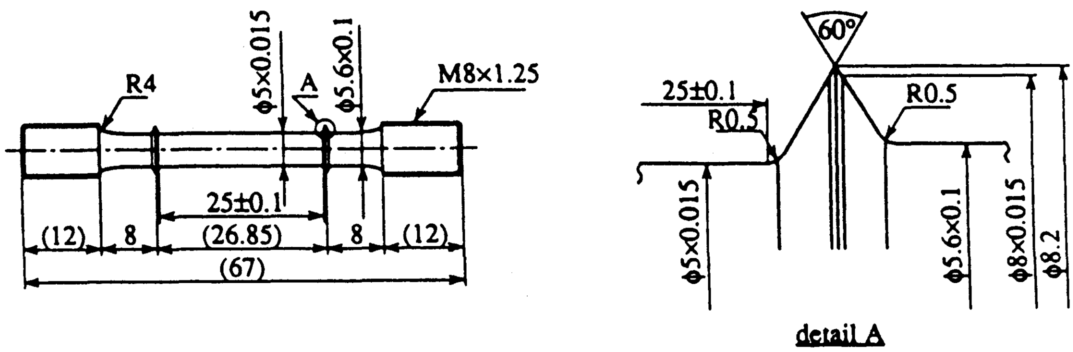

Figure 1 Geometry and dimensions of tensile specimen

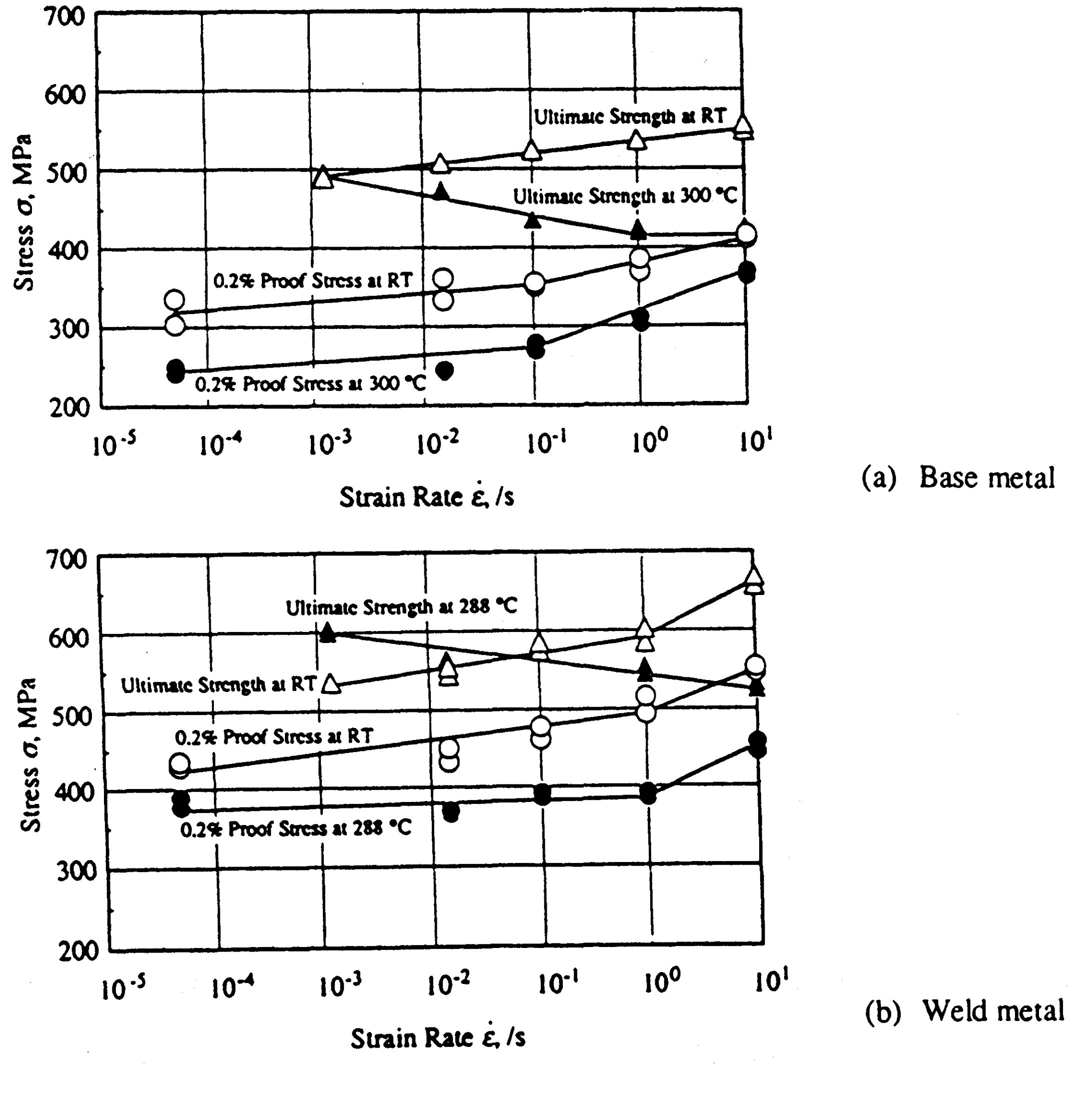

Figure 2 Results of tensile tests for various strain rates

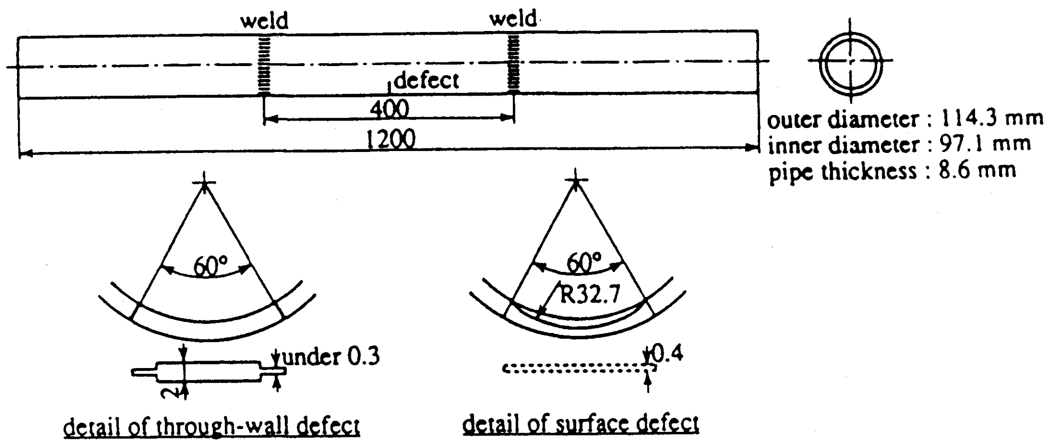

Figure 3 Geometry and dimensions of notched pipe specimen

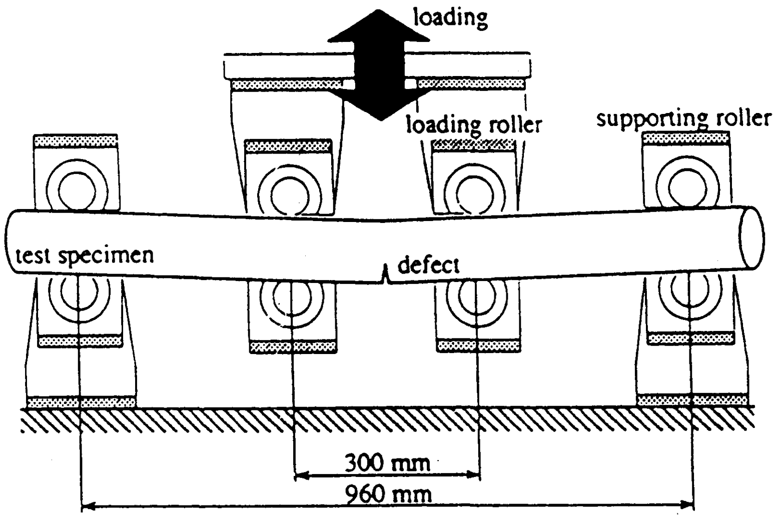

Figure 4 Schematic view of pipe fracture tests apparatus

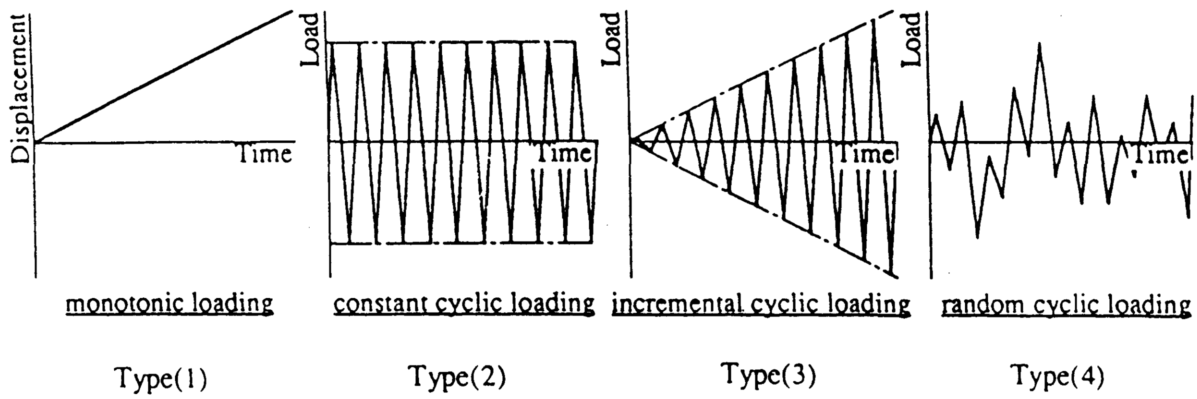

Figure 5 Loading types for pipe fracture tests

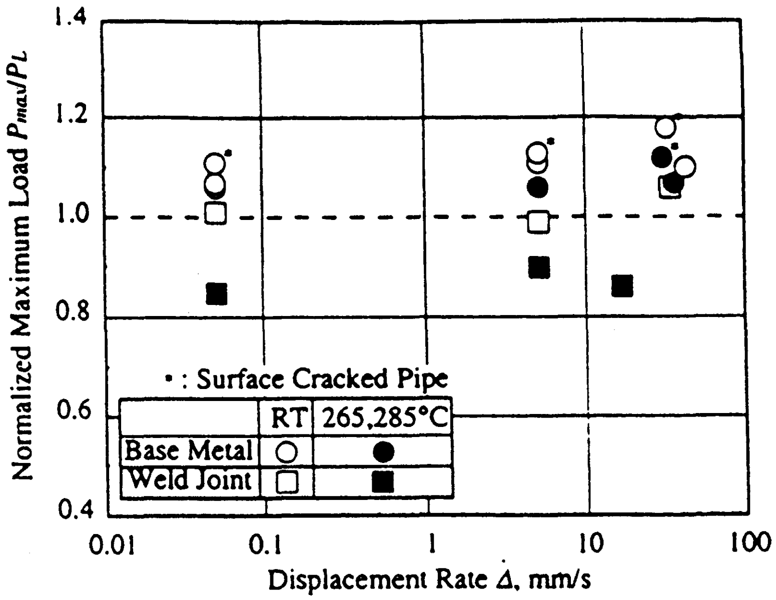

Figure 6 Relationship between normalized maximum load and displacement rate

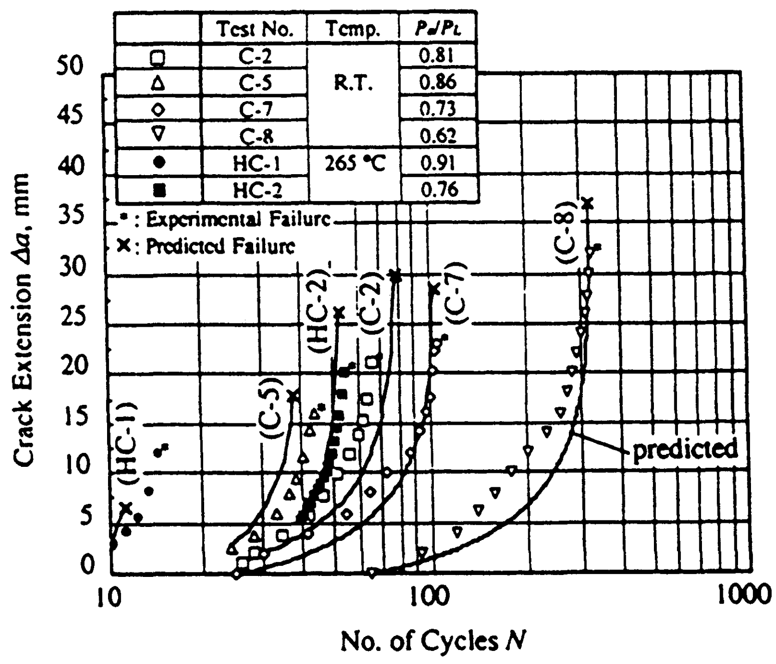

Figure 7 Relationship between crack extension and number of loading cycles

3 Effects of Dynamic Strain Aging on the Leak-Brefore-Break Analysis in SA 106 Gr.C Piping SteeI

I.S. Kim*, J.W. Kim (KAIST)

Effects of Dynamic Strain Aging on the Leak-Before-Break Analysis in SA106 Gr.C Piping Steel

Jin-Weon Kim and In-Sup Kim
Department of Nuclear Engineering
Korea Advanced Institute of Science and Technology

Abstract

The characteristics of dynamic strain aging (DSA) on material properties used in leak-before-break (LBB) analysis were discussed. Using these material data, the effect of DSA on the LBB analysis was estimated through the evaluation of leakage-size-crack and flaw stability in SA106 Gr.C piping steel. Also, the results were represented as a form of "LBB allowable load window". In the DSA temperature region, the leakage-size-crack length was smaller than that at other temperatures and it increased with increasing tensile strain rate. In the results of flaw stability analysis, the lowest instability load appeared at the temperature corresponding to minimum J-R curve which was caused by DSA. The instability load near the plant operating temperature depended on the loading rate of J-R data, and decreased with increasing tensile strain rate. These are due to the strain hardening characteristic and strain rate sensitivity of DSA. In the "LBB allowable load window", LBB allowable region was the narrowest at the temperature and loading conditions where DSA occurs.

1. Introduction

The leak-before-break (LBB) concept has been applied to design for high energy piping in nuclear power plant. The stress-strain curve and J-R curve of material are used for LBB analysis, and they have direct influence on the evaluation of LBB conditions [1]. Accordingly, it can be expected that the characteristics of dynamic strain aging (DSA) in material may influence the results of LBB analysis, since the occurrence of DSA depends on temperature and deformation rate and changes mechanical properties.

Although a number of studies on DSA related to LBB were reported [2,3,4], most of them focused on the crack jump at quasi-static loading rate and on the loss of fracture toughness under dynamic loading at the normal plant operating temperature. The effect of DSA on the results of LBB assessment has not been quantitatively estimated. In this study, therefore, the effect of DSA on the LBB analysis was estimated through the evaluations of leakage-size-crack and flaw stability for simple case using material properties obtained from systematic tensile and J-R tests.

2. Material Properties for LBB Analysis

The calculations of leakage-size-crack length and flaw stability in LBB analysis require the stress-strain curve and J-R curve [5]. The tensile and J-R tests were carried out under various temperature and loading conditions to illustrate the characteristics of DSA in SA106 Gr. C steel which has been used for main steam line piping in nuclear power plant. In the results, the effect of DSA on the material properties for LBB analysis was discussed.

2.1 Yield Stress

As shown in Fig. 1, the 0.2% σ_{ys} generally decreased with increase in temperature although there was a plateau at a certain range of temperature. The temperature at which a plateau appeared, shifted to higher temperatures with increasing strain rate and coincided with serrated flow region. The σ_{ys} at temperatures lower than 200°C showed the usual positive strain rate dependence. At temperature range of plateau associated with serrated flow, however, positive strain rate dependence of σ_{ys} disappeared and reappeared at 400°C.

It is noted that σ_{ys} is affected by static strain aging (SSA) rather than DSA [6]. However, many studies observed a plateau or a small peak of σ_{ys} [7], and a slight strain rate sensitivity [8] in the temperature range of DSA. Therefore, the decrease in σ_{ys} is due to high temperature softening, whereas the occurrence of plateau and disappearance of usual positive strain rate sensitivity reflect the effect of DSA over the high temperature softening.

2.2 Ramberg-Osgood Parameters

Ramberg-Osgood relation is usually used as power-law hardening relationship and it's parameters n and α are important input data in the LBB assessment. Generally, Ramberg-Osgood relation is represented as following equation.

$$\frac{\varepsilon}{\varepsilon_o} = \frac{\sigma}{\sigma_o} + \alpha\left(\frac{\sigma}{\sigma_o}\right)^n \qquad (1)$$

where σ and ε are true stress and true strain, σ_o is reference stress that is usually equal to yield stress, $\varepsilon_o=\sigma_o/E$, n is strain hardening exponent, and α is dimensionless constant. The Ramberg-Osgood parameters are strongly dependent on strain range of data fitted into Eq. (1) [1,9]. In the present study, stress-strain data between $1.05\sigma_o$ and 10% strain were selected to screen out points on the yield plateau.

The parameter n is plotted against testing temperatures at various strain rates in Fig. 2. In comparing dependence of n on temperature and strain rate with that of σ_{uts}, the temperature region where n is smaller than that at room temperature (RT), is consistent with σ_{uts} hardening region where DSA operates. In this temperature region, also, strain rate dependence of n showed inverse trend in comparison with other temperatures, in the same manner as the strain rate dependence of σ_{uts}. These suggest that the parameter n is directly affected by DSA, and the decrease in the value of n and positive strain rate dependence at the normal plant operating temperature range are caused by DSA.

The parameter α varied with temperature in the similar manner as the σ_{ys} as shown in Fig. 3, although the dependence of temperature and strain rate is less clear than that in σ_{ys}. The value of α decreased gradually with increase in temperature and showed positive strain rate dependence except the region of temperature in which the plateau appears. The dimensionless constant α is related to both σ_{ys} and strain hardening of material. In particular, α is sensitive to the value of σ_{ys} [10]. This is consistent with the present observation. From the characteristics of α, it can be concluded that the appearance of plateau and slight strain rate sensitivity near

300°C are attributable to DSA as discussed in σ_{ys}. However, the influence of DSA on this parameter is less obvious than that on the parameter n.

2.3 J-R Curves

Fig. 4 exhibits the J-R curves of material at different temperatures for load-line displacement rates of 0.4 and 4.0 mm/min. The dependence of the fracture resistance on temperature and loading rate was apparent. As shown in the Fig. 4, it was noted that as the temperature increased from ambient, the J-R curves exhibited lower values until a critical temperature reached and exhibited higher values at higher temperatures. The critical temperatures at which J-R curve attained a minimum, were shifted to higher temperature with faster loading rate and were observed at the temperature ranges 250°C and 296°C for load-line displacement rates of 0.4 and 4.0 mm/min, respectively. The J-R curves at load-line displacement rate of 0.4 mm/min were higher than those at 4.0 mm/min between RT and 250°C, whereas the J-R curves above 296°C showed negative loading rate dependence.

The variation of J_i with temperature for each load-line displacement rate is given in Fig. 5. The crack initiation toughness, J_i, was defined as value of J-integral at the crack initiation point obtained from DCPD method. The trend of variation in J_i with temperature and loading rate was similar to that of J-R curves. The minimum points of J_i appeared at temperatures of 200~250°C and 250~296°C for load-line displacement rates of 0.4 and 4.0 mm/min, respectively. At these temperatures the values of J_i were smaller, about 30%, than those at RT for each load-line displacement rate. Up to 200°C the J_i increased with increasing loading rate, but the trend was inversed, that is negative strain rate sensitivity, at the temperature of 296°C. It was observed that reduction of fracture toughness and negative loading rate dependence occur at the temperature region of DSA. Also, the lower fracture resistance region with loading rate is a important characteristic of DSA in fracture behavior.

3. Effect of DSA on LBB Analysis

3.1 LBB Analysis

The evaluation of leakage-size-crack and flaw stability was performed for simple piping system using material data discussed in the previous section. The sets of material properties to identify the characteristics of DSA were employed in the analysis as input data. The J-R curves were extrapolated using a following power-law relationship [11] in order to get the large amounts of crack growth needed for the analysis.

$$J = J_i + C\Delta a^m \tag{2}$$

where C and m are fitting parameters. The fitting parameters obtained from the regression of data points between 0.5 and 2.5 mm in crack extension, and listed in Table 1. It was assumed that pipe has a circumferencial through wall crack and a dimension of 670 mm outer diameter and 32 mm thickness. The piping system was operated under 7.3 MPa and 289°C steam, and was subjected to remote axial tension and bending moment as shown in Fig. 6.

The calculation of crack length for given leak rate was performed using PICEP code [12]. All calculations were based on the assumptions of a flaw surface roughness of 0.05 mm and an elliptical circumferential crack which plastic-zone was corrected. For a given load level, the crack length that produces the desired 37.85 *l*/min (10gpm) leak rate was determined.

J/T diagram method was employed for evaluation of flaw stability [1]. The elastic-plastic J-integral estimation formula from EPRI NP-6301-D [13], known as the EPRI/GE estimation method, was used in the J and T calculations. This method superposes solutions corresponding to elastic and fully plastic conditions to obtain the elastic-plastic results for through-wall crack in a pipe. For the case of a through-wall crack in a pipe under remote axial tension and bending moment loading, the following J-integral estimation equation is used for the elastic-plastic solution.

$$\begin{aligned} J &= J_e + J_p \\ &= f_t \cdot \frac{P^2}{4Rt^2E} + f_b \cdot \frac{M^2}{R^3t^2E} + \alpha\sigma_0\varepsilon_0 R(\pi-\theta)\cdot\left(\frac{\theta}{\pi}\right)\cdot h_1 \cdot \left(\frac{P}{P_0'}\right)^{n+1} \end{aligned} \tag{3}$$

The individual terms are as described in detail in Reference [13]. The instability point in the J/T method is found by plotting $J_{applied}$ against $T_{applied}$ and $J_{material}$ versus $T_{material}$ on a single figure as illustrated by a plot showing J versus T in Fig.7. The intersection of the two curves is the instability point and the corresponding J value is J_{inst}, from which the instability load can be determined.

3.2 Effect of DSA on the Leakage-Size-Crack

Fig. 8 shows the dependence of leakage-size-crack length on temperature and strain rate of material properties. The crack length at RT was the largest. The smallest crack length for same load level was observed at 296°C rather than at 400°C. The variation in crack length was not linear with temperature, particularly it was clear at 1.39×10^{-4}/s. The crack length increased with increasing σ_{ys} and n, and with decreasing α. The role of σ_{ys} and n is dominant. Accordingly, the largest value of σ_{ys} and n at RT is a cause of maximum crack length. Although the value of σ_{ys} at 296°C is larger than that at 400°C, the crack length at 296°C is smaller. This is owing to small n at 296°C associated with DSA in tensile properties.

In comparing the leakage-size-crack lengths at each temperature, the crack length for 6.95×10^{-2}/s at 296°C was larger than that for 1.39×10^{-4}/s, whereas crack length at 1.39×10^{-4}/s was larger than that at 6.95×10^{-2}/s for other temperatures. The variation in σ_{ys} and α with strain rate at same temperature is small compared with that in parameter n except for data at RT. Therefore, the inverse trend of crack length with strain rate at 296°C relates to the changing of dependence of n on strain rate in the DSA region. Consequently, the strain hardening characteristic of DSA results in a decreased leakage-size-crack length at 296°C, and the negative strain rate dependence in DSA region is a cause of increasing leakage-size-crack length with increasing strain rate.

3.3 Effect of DSA on the Flaw Stability

The effect of loading rate in material properties on the instability load for a given crack length, $2\theta_c/C=0.1$, was represented in Fig. 9 as a function of temperature. It showed that the variation of instability load with temperature was similar to that of J-R curve for each loading rate. The minimum load appeared at a certain range of temperature which depends on loading rate of J-R data. It shows that a decrease in J-R curve caused by DSA alters instability load significantly, although the crack driving force of J-applied decreases due to the enhanced tensile properties and balances out the decrease in J-material [14].

Also, the effect of strain rate of tensile data on the instability load was observed. In the temperature below 200°C, the instability load at 1.39×10^{-4}/s was smaller than that at 6.95×10^{-2}/s. Between 200 and 296°C, however, the trend of variation with strain rate was reversed. According to the results of parametric study, the instability load for a given crack length increased with increasing σ_{ys}, and with decreasing α and n. In the lower temperature region, therefore, an increase in instability load with strain rate is due to high value of σ_{ys}. However, the variation of σ_{ys} with strain rate is negligible between 200 and 296°C, while the value of n increases with increasing strain rate. Accordingly, a decrease in instability load with strain rate is caused by high value of n at high strain rate in this temperature region. The disappearance of strain rate sensitivity of σ_{ys} and positive strain rate sensitivity in n are characteristics of DSA in the tensile properties.

Because of the characteristics of DSA in the material properties, the minimum instability load occurs near the nuclear power plant operating temperature, and the temperature corresponding to minimum load depends on loading rate of J-R data. In addition, the DSA decreases instability load with increasing strain rate of tensile data in this temperature region.

3.4 LBB Allowable Load Window

Figs. 10 and 11 represent the effects of DSA on the LBB analysis as a form of "LBB allowable load window" [15]. The band between the minimum moment to produce desired leakage rate and the maximum-allowable-moment for a given crack length is LBB acceptable region. In these figures, the safety factor for leakage-size-crack length and applied load was not applied. Fig. 10 shows the LBB allowable region as a function of temperature of material properties at quasi-static loading condition. The LBB allowable region at 250 and 296°C were decreased by about 30% compared with that at RT or 350°C. It reflects that DSA reduces LBB allowable region significantly. Fig. 11 exhibits the LBB allowable region with various combinations of tensile data with J-R data at 296°C, near the plant operating temperature. The variation of LBB allowable region with loading rate of J-R data was considerable, whereas the influence of strain rate in tensile data was negligible. LBB allowable region at loading rate of

4.0mm/min in J-R data was smaller, about 15%, than that of 0.4mm/min for same strain rate of tensile data. As shown in Fig. 11, LBB allowable region depends on the loading rate of material data at plant operating temperature. However, it is very difficult to know loading rate for practical piping system with certainty. In order to obtain the conservative results in the LBB assessment, the effects of loading rate on the material behavior have to be investigated and then the loading condition corresponding to lower bound material properties should be used for material test.

4. Conclusions

Using material properties in SA106 Gr.C piping steel obtained from various testing conditions, the evaluations of leakage-size-crack and flaw stability for simple piping system was conducted to estimate the effect of dynamic strain aging (DSA) in material on the results of leak-before-break (LBB) analysis. The main conclusions are as follows:

1. The leakage-size-crack length in the dynamic strain aging (DSA) region was smaller than that at other temperatures. Also, DSA increased the crack length with increasing strain rate. These are due to the strain hardening characteristic and negative strain rate sensitivity of DSA in tensile properties.

2. The instability load reduced in the DSA region, and the temperature corresponded to a minimum load depended on loading rate of J-R data. In this region, the instability load decreased with increasing strain rate of tensile data. This is owing to a decrease in fracture toughness, a disappearance of strain rate sensitivity of σ_{ys}, and an enhancement of strain hardening caused by DSA.

3. LBB allowable region in the range of DSA was decreased by about 30% compared with that in other region of temperatures. Also, it varied with loading rate of material data at plant operating temperature.

References

[1] NUREG-1061, Vol.3, October 1984.
[2] B. Mukherjee, Nucl. Eng. & Des. 111, 1989, p63.
[3] C. W. Marschall, M. P. Landow and G. M. Wilkowski, NUREG/CR-6098, October 1993.
[4] C. W. Marschall, R. Mohan, P. Krishnaswamy and G. M. Wilkowski, NUREG/CR-6226, October 1994.
[5] B. F. Beaudoin, D. F. Quinones and T. C. Hardin, J. Pres. Ves. & Piping 43, 1990, p67.
[6] S. Lou and D. O. Northwood, J. Mater. Eng. & Perf. 3, 1994, p344.
[7] S. S. Kang and I. S. Kim, Nucl. Tech. 97, 1992, p336.
[8] C. C. Li and W. C. Leslie, Metall. Trans. 9A, 1978, p1765.
[9] M. L. Vanderglas, Int. J. Pres. Ves. & Piping 43, 1990, p241.
[10] NRCPIPES-*Computer Code and User's Guide*, Mar. 1995.
[11] G.M. Wilkowski, G. Karmer, P.Vieth, R. Francini, and P. Scott, *PVP-Vol.280*, ASME, 1994, p221.
[12] D.M. Norris and V. Chexal, *PICEP, EPRI NP-3596-SR*, Dec. 1987.
[13] A. Zahoor, *EPRI NP-6301-D*, Vol.1, June, 1989.
[14] O. E. Lepik, B. Mukherjee, Int. J. Pres. Ves. & Piping 43, 1990, p285.
[15] A.D. Nana and K.K.Yoon, *PVP-Vol.287/MD-Vol.47*, ASME, 1994, p35.

Table 1 Parameters of J-R curves obtained from power-law fitting(Δa = 0.5~2.5 mm).

Loading Rate	Temp. (°C)	J_i (kJ/m^2)	C	m
0.4 mm/min	RT	153.44	464.7	0.7899
	150	115.23	425.0	0.7626
	200	97.95	415.5	0.6841
	250	102.53	363.4	0.6403
	296	131.68	377.9	0.6910
	350	148.60	517.1	0.8302
4.0 mm/min	RT	175.74	483.2	0.7604
	150	146.42	484.4	0.6957
	200	118.85	438.1	0.7420
	250	108.96	393.3	0.6479
	296	109.55	352.5	0.6125
	350	210.28	352.5	0.6889

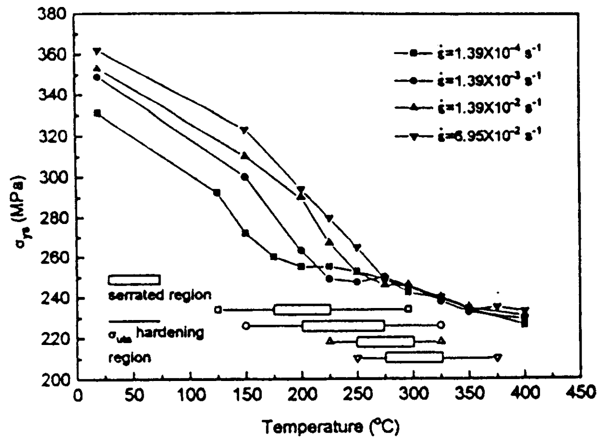

Fig. 1 Dependence of yield stress on temperature and strain rate.

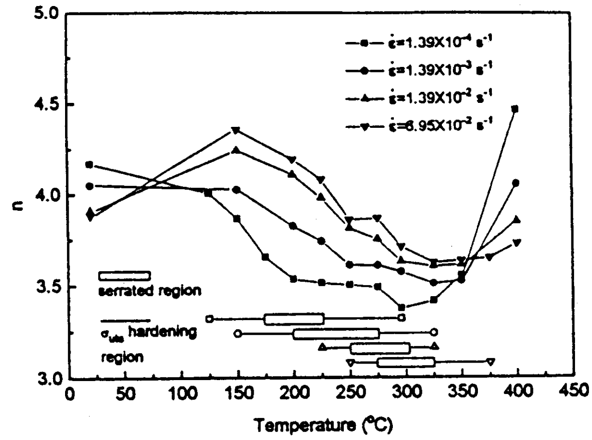

Fig. 2 Dependence of n parameter in Ramberg-Osgood relation on temperature and strain rate.

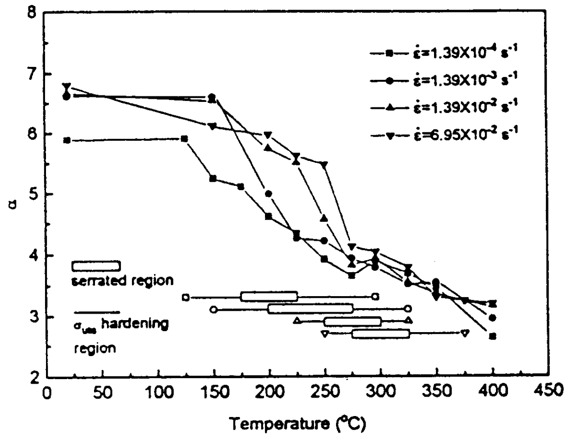

Fig. 3 Dependence of n parameter in Ramberg-Osgood relation on temperature and strain rate.

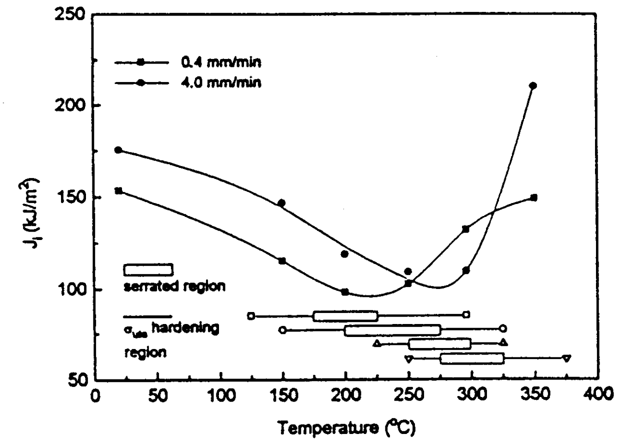

Fig. 5 Dependence of crack initiation fracture toughness, Ji, on temperature and loading rate.

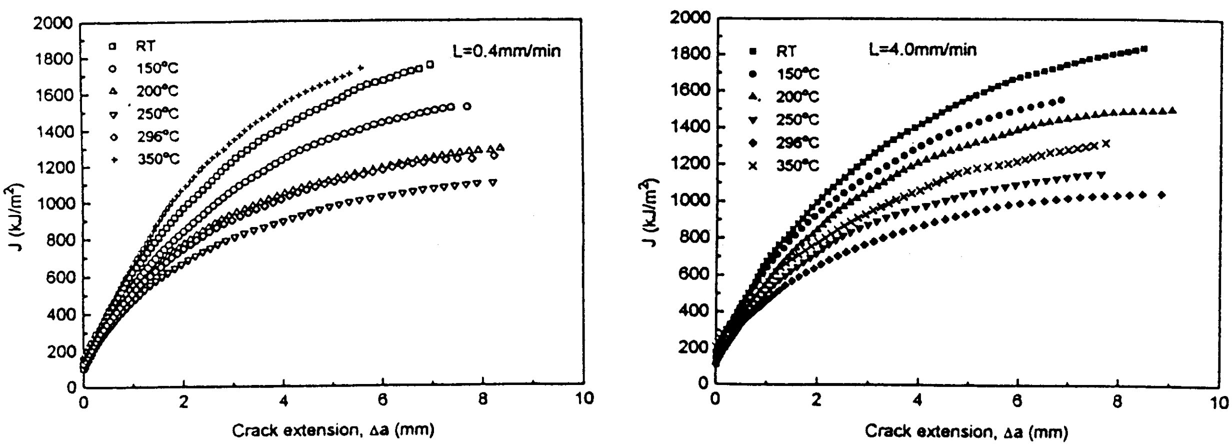

(a) (b)

Fig. 4 Dependence of J-R curve on temperature and loading rate of (a) 0.4mm/min and (b) 4.0mm/min.

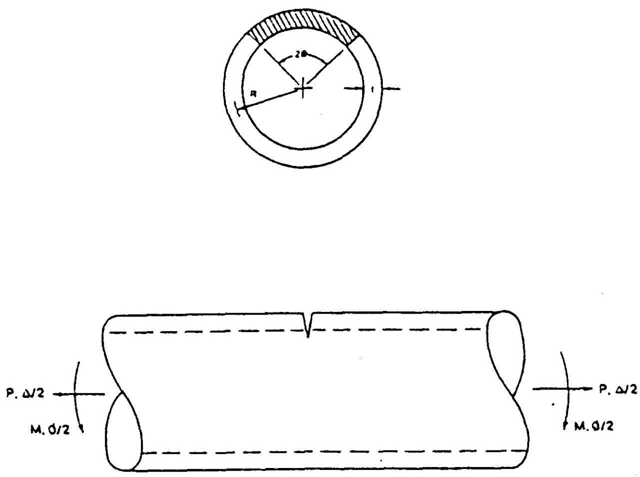

Fig. 6 Circumferential throughwall-cracked in a pipe and applied loads.

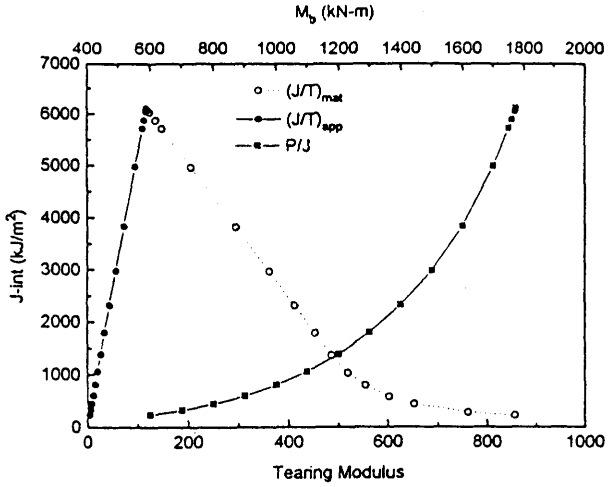

Fig. 7 Calculation of instability load by using typical J/T method.

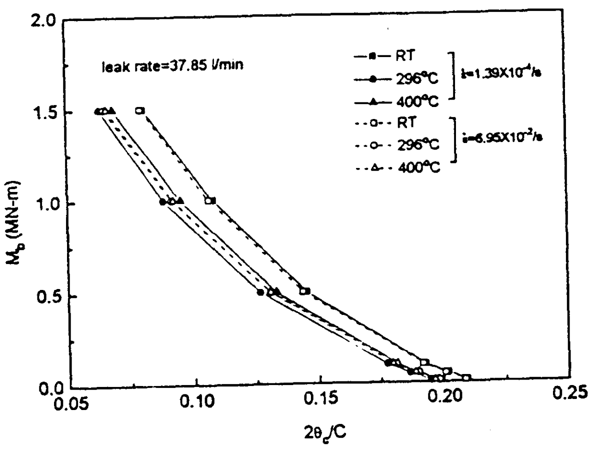

Fig.8 Minimum bending moment versus leakage-size-crack length calculated by PICEP code.

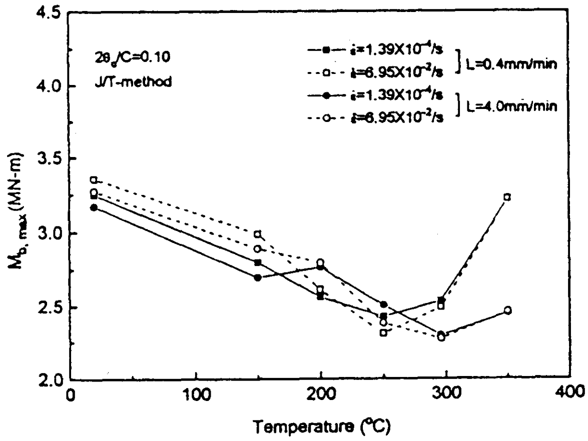

Fig. 9 Effect of temperature and loading rate of material data on the instability load for $2\theta_c/C=0.1$.

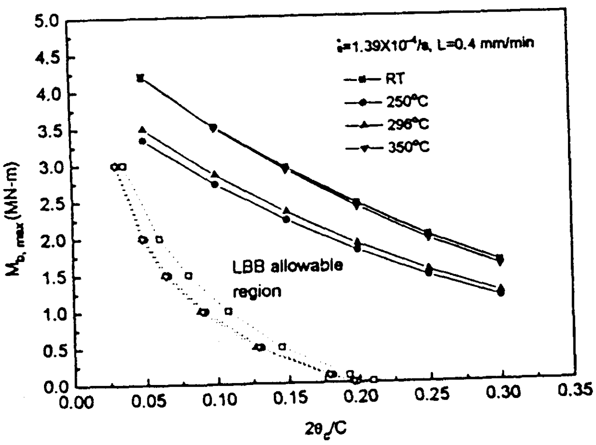

Fig. 10 Variation in LBB allowable region with temperature of tensile and J-R data at quasi -static loading rate.

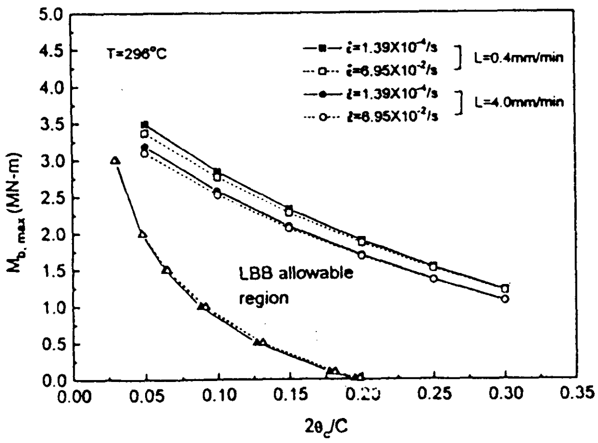

Fig. 11 Variation in LBB allowable region with loading rate of tensile and J-R data at 296°C.

4 Probabilistic Fracture Mechanics Analyses of Nuclear Pressure Vessels Under PTS Events

G. Yagawa* (Univ. of Tokyo), S. Yoshimura (CRIEPI),
M. Hirano (JAERI)

PROBABILISTIC FRACTURE MECHANICS ANALYSES OF NUCLEAR PRESSURE VESSELS UNDER PTS EVENTS

Genki YAGAWA and Shinobu YOSHIMURA
Department of Quantum Engineering and Systems Science,
The University of Tokyo,
7-3-1 Hongo, Bunkyo, Tokyo 113, Japan
Tel. : +81-3-3812-2111 Ext. 6993
Fax : +81-3-5684-3265
e-mail : yagawa@gen.u-tokyo.ac.jp

Naoki SONEDA
Central Research Institute of Electric Power Industry,
2-11-1 Iwado-kita, Komae, Tokyo 201, Japan

Masashi HIRANO
Japan Atomic Energy Research Institute,
2-4 Shirokata-shirane, Tokai-mura, Naka-gun, Ibaraki 319-11, Japan

Abstract

This paper describes some recent research activities on probabilistic fracture mechanics (PFM) for nuclear reactor pressure vessels (RPVs) performed by the RC111 research committee of the Japan Society of Mechanical Engineers (JSME) under a subcontract of the Japan Atomic Energy Research Institute (JAERI). To establish standard procedures for evaluating failure probabilities of nuclear RPVs, we have performed PFM analyses for aged RPV under pressurized thermal shock (PTS) events. The basic problems are chosen from some of US benchmark problems such as EPRI (Electric Power Research Institute) and US NRC (Nuclear Regulatory Commission) joint PTS benchmark problems and H. B. Robinson problems. Various sensitivity analyses are performed to quantify effects of uncertainty of data on failure probabilities. Employed in this study are four PFM computer codes developed in Japan and in USA.

1. INTRODUCTION

Studies on efficient utilization and life extension of operating nuclear power plants have become increasingly important since ages of the first-generation nuclear power plants are approaching their design lives [1]. It is easy to imagine that a practical life of plant might be usually longer than its design life by considering conservatism embedded in design practices. In order to predict a remaining life of plant, it is necessary to select those critical components that strongly influence the plant life, and to evaluate their remaining lives by considering aging effects of materials and other factors. However, when evaluating reliability of nuclear structural components, some problems are quite formidable because of lack of information regarding a past operating history, material property change and uncertainty in damage models. Accordingly, if structural integrity and safety are evaluated by deterministic fracture mechanics approaches, it is expected that the results obtained are too conservative to perform a rational evaluation of plant life and to make judgment of life extension because of accumulation of conservatism of all related factors.

In this regard, the Probabilistic Fracture Mechanics (PFM) has become an important tool [2-4]. The PFM approaches are regarded as appropriate methods to rationally evaluate plant life since it can consider various uncertainties such as sizes and distributions of cracks, degradation of material strength due to aging effects, accuracy and frequency of pre- and in-service inspections. For example, they can be used to improve maintenance or inspection schedule of structural components of nuclear power plants [5-7]. They are also expected as tools to derive input data for the probabilistic safety assessment (PSA) or the probabilistic risk assessment (PRA).

A number of PFM computer programs have been developed and applied in practical situations in the last two decades [8-22]. Some of the present authors have developed the three-dimensional (3D) J-integral database based on fully plastic solutions [23, 24] and a fully automated finite element system for calculating 3D stress intensity factors [25], and performed PFM analyses of nuclear piping using the database [26, 27]. They have also developed an efficient PFM computer program using a parallel Monte Carlo method [28, 29].

On the other hand, the PFM approaches have some weak points such that PFM analysis results are hardly verified through experiments. Thus it is key issues to verify the consistency and the validity of PFM computer programs through the comparison of calculation results of some well defined benchmark problems [30, 31].

In Japan, one research activity on PFM approaches to the integrity studies of nuclear pressure vessels and piping (PV&P) was initiated in 1987 by the LE-PFM subcommittee organized in the Japan Welding Engineering Society (JWES) under a subcontract of the Japan Atomic Energy Research Institute (JAERI), and had continued for three years [31, 32]. The activity was followed by the RC111 research committee organized in the Japan Society of Mechanical Engineers (JSME) in 1991, and finished in 1995 [33]. Many researchers from 4 universities, 3 research institutes, 3 utilities, 5 venders and 2 software companies participated the activity. The purpose of the activity was to establish standard procedures for evaluating failure probabilities of Japanese nuclear PV&P, combining the state-of-the art knowledge on structural integrity of nuclear PV&P and modern computer technology such as parallel processing. Within the activity, we have set up the following three kinds of PFM round-robin problems on (a) primary piping under normal operating conditions, (b) aged RPV under normal and upset operating conditions, and (c) aged RPV under pressurized thermal shock (PTS) conditions. The basic part of the last PTS problems is taken from some of US benchmark problems [30, 34]. For these round-robin problems, various sensitivity analyses were performed to quantify effects of uncertainty of data on failure probabilities. Some of the analysis results can be found in elsewhere [28, 31, 35-37].

This paper summarizes some sensitivity studies on aged RPVs under PTS events. Here two original Japanese PFM computer programs [17, 20] are utilized, together with two US ones such as OCA-P [12] and VISA-II [15].

2. PFM ANALYSIS PROCEDURE OF RPV FAILURE UNDER PTS EVENTS

A nuclear RPV is typically modeled as a thick cylinder, which is subjected to operating internal pressure and temperature. There are several scenarios in PTS events. For example, when a loss-of-coolant accident (LOCA) is occurred, the inner surface of the vessel is suddenly cooled down by lower temperature water provided from an emergency core cooling system (ECCS). If a LOCA is less severe, i.e. a small-break LOCA (SBLOCA), both thermal tensile stress and mechanical tensile stress due to the internal pressure are applied to the vessel simultaneously, and an postulated inner surface crack might start to grow under a certain condition [8, 34, 38, 39]. In the present PFM analyses, a conditional probability of vessel failure, i.e. crack initiation and vessel break, under one PTS event is calculated using the Monte Carlo method. The PFM analysis consists of the deterministic analysis part and the probabilistic analysis one. In the deterministic analysis part, we first calculate a transient temperature distribution, a transient stress distribution, and stress concentration, considering a specific transient. In a real situation, the beltline portion of the vessel is first cooled by the ECCS, and thus the vessel temperature distributes all in the thickness, axial and circumferential directions. In the typical PFM analyses of PTS events, only a temperature distribution in the thickness direction is taken into account for the purpose of simplicity. The thermal stress caused due to such a temperature distribution and the mechanical tensile stress caused due to the internal pressure are mainly considered. The peak stress caused due to mismatch between clad and base materials in thermal expansion coefficient is taken into account as well. If reliable data are available, residual stress could be included in the analysis.

The linear elastic fracture mechanics (LEFM) is basically employed in the present PFM analyses, so that the stress intensity factor K is calculated. Fracture toughnesses, i.e. crack initiation toughness K_{Ic} and crack arrest toughness K_{Ia}, are regarded as functions of neutron fluence and temperature of material. Thermal aging effects are not explicitly considered, but are already included in fracture toughness values together with irradiation embrittlement effects.

Random variables to be considered are initial crack depth and aspect ratio, fracture toughness, neutron fluence, RT_{NDT}, impurity content of vessel material, and so on. The normal distributions are assumed for all the random variables except the initial crack depth. If any reliable distributions are available, they should be employed in the analyses. Otherwise, well known open data found in literature are used. The number of cracks existing within the vessel could also be a random variable. To consider such a situation, the Poisson distribution is assumed.

In the present analyses, the probability of crack initiation exceeding a K_{Ic} value and that of vessel break, i.e. the K value of a growing crack exceeding a K_{Ia} value are calculated. As optional calculations, fracture at an upper shelf toughness area, plastic collapse of uncracked ligament and warm prestress effects are considered.

3. PFM CODES AND ANALYSIS PROBLEMS

Four PFM computer programs are employed in this study. The two of them, i.e. PROFMAC-II [17] and MHIPFM [20] are Japanese codes, and the others are US codes, i.e. OCA-P [12] and VISA-II [15]. PROFMAC-II is developed by Central Research Institute of Electric Power Industry (CRIEPI), while MHIPFM is developed by Mitsubishi Heavy Industries Ltd. (MHI). All the codes adopt the Monte Carlo method.

Two sets of round-robin problems are analyzed in the present study. The one is taken from the PTS benchmark study organized by both EPRI and US NRC in 1992 [30]. The other is taken from US H. B. Robinson problems [34], which were solved by Oak Ridge National Laboratory (ORNL) in 1985 using OCA-P. In the latter analyses, vessel failure probabilities were calculated for 28 postulated transients of the reactor.

The EPRI/NRC PTS benchmark problems originally include thirteen cases and some additional special cases, which were set up to clarify the difference of the existing US PFM codes. Main features of the basic cases named A1 and B1 can be summarized as follows :

(a) No cladding is assumed.
(b) Exponential decay of coolant temperature with time is assumed.
(c) Coolant-wall heat transfer coefficient and internal pressure are assumed to be time-independent.
(d) Axial (case A1) and circumferential (case B1) infinitely long cracks are assumed.
(e) Original OCTAVIA crack depth distribution [8] is assumed.
(f) RT_{NDT} shift and through-wall fluence attenuation in US Regulatory Guide 1.99 Rev.2 [40] are assumed.
(g) K_{Ic} and K_{Ia} criteria are employed as crack initiation and crack arrest criteria, respectively.
(h) Upper-shelf toughness of 220 $MPa\sqrt{m}$ is employed.
(i) No warm prestress (WPS) effect is considered.

Main features of the H.B. Robinson problem are as follows :

(a) Cladding is considered.
(b) Temperature, coolant-wall heat transfer coefficient and internal pressure are time-dependent, and specific to each of postulated transients.
(c) Axial infinitely long crack is assumed.
(d) Marshall distribution of crack depth and Marshall crack detection probability [41] are employed.
(e) RT_{NDT} shift of Guthrie equation [38] and through-wall fluence attenuation in US Regulatory Guide 1.99 Rev.2 [40] are assumed.
(f) K_{Ic} and K_{Ia} criteria are employed as crack initiation and crack arrest criteria, respectively.
(g) No WPS effect is considered.

One of the 28 postulated transients, called case "9.22B" assuming a main steamline break event, was adopted in the present study.

To evaluate K values for a crack subjected to arbitrarily distributed thermal loading, so called influence function methods are useful. Ref. [42] gives the influence functions for infinitely long axial cracks and those for fully circumferential cracks. Ref. [43] presents the influence functions for a semi-elliptical surface crack in the axial direction in cylinder. Ref. [15] presents the influence functions similar to those of Ref. [42], but taking into account cladding. In the present study, those functions are adopted.

4. COMPARISON STUDY OF FOUR PFM CODES

The EPRI/NRC PTS benchmarking problems were first analyzed using the following three PFM codes, i.e. PROFMAC-II [17], OCA-P [12] and VISA-II [15]. The analysis results of case B1, i.e. conditional break probability vs. neutron fluence, are shown in Figure 1. The figure show fairly good agreement.

Next the transient "9.22B" of H.B. Robinson PTS problem was calculated using OCA-P and MHIPFM [20]. The conditional break probability of an original ORNL analysis [34] was 3.61×10^{-4}, while those of the present analyses are 4.38×10^{-4} (OCA-P) and 4.87×10^{-4} (MHIPFM). Although the present analysis results are slightly higher than that of the ORNL analysis, they agree well among others in an engineering sense. This slight difference might be caused due to some error of input data. Coolant temperature, heat transfer coefficient and pressure are not given in any numeral forms in the original literature [34], and then we took these data from the figures.

These results clearly demonstrate that the Japanese and US PFM codes are reliable to perform the present study.

5. SENSITIVITY ANALYSES

Using the four PFM codes, various sensitivity analyses are performed on the two sets of PTS problems in order to quantitatively evaluate effects of input data on failure probabilities of RPV under PTS events. The input data studied are initial crack shape, the probabilistic distribution of initial crack depth, cladding, RT_{NDT} shift, impurity content, the through-wall distributions of material properties, preservice inspection (PSI) and warm prestressing.

5.1 Effects of Initial Crack Shape

Using VISA-II code, we examined effects of initial crack shape on failure probabilities, solving the EPRI/NRC PTS benchmarking problems. Figure 2 shows calculated break probabilities for axial crack cases. Here an infinitely long axial crack and semi-elliptical surface cracks with four different aspect ratios, i.e. 2, 6, 10 and 100, are assumed. The figure shows that as increasing the crack aspect ratio, break probability increases, and that assuming an infinitely long crack gives the largest break probability. When assuming an aspect ratio of 6, the results are very close to those of the infinitely long crack cases. We performed similar sensitivity analyses for circumferential crack cases, and found the same tendency. There are very few data on probabilistic distributions of crack aspect ratio in literature. Only a normal distribution and a log-normal one proposed by LLNL [13] are often utilized. These distributions suggest that the averaged aspect ratio ranges 2 to 3.

5.2 Effects of Initial Crack Depth

Several probabilistic distributions of initial crack depth have been proposed and used in PFM analyses. Figure 3 shows six kinds of typical distributions, i.e. (a) & (b) the upper and the lower limits of the Lorence Livermore National Laboratory (LLNL) distribution [9], (c) Marshall distribution [41], (d), (e) Weibull and log-normal distributions of Brueckner-Foit model [10] and (f) OCTAVIA distribution [8]. Figure 4 shows calculated break probabilities for axial crack cases, adopting the six distributions shown in Figure 4. Analyzed here are again the EPRI/NRC PTS benchmarking problems. VISA-II code is used. Figure 4 shows that the discrepancy among the six results ranges over two orders of magnitude. The upper limit of the LLNL distribution, the Marshall distribution and the lower limit of the LLNL distribution give almost the similar and highest results among the six distributions. Although there are some research activities to obtain plant-specific distributions of crack depth using pre-service / inservice inspection (PSI/ISI) data [44], it is still popular to use open data in literature. The Marshall distribution may be the most popular one. Figure 4 suggests that using the Marshall distribution gives us reasonably conservative results for PFM problems of PTS events. Further detailed discussions on effects of crack depth distributions on failure probabilities can be found elsewhere [35, 36].

5.3 Cladding Effects

Using the influence functions for K values in refs. [15, 42], we examined cladding effects on failure probabilities. PROFMAC-II is used here. Figure 5 shows calculated break probabilities. Here axial cracks are again assumed. Case A1 (without cladding) and case A11 (with cladding) of the EPRI/NRC benchmarking problems are solved. Figure 5 clearly shows that considering cladding raises break probabilities by about one order of magnitude. Since any influence functions for a circumferential crack with cladding have not been developed, cladding effects are still not clearly understood in such cases. As conclusions, cladding effects have to be taken into account.

5.4 Effects of RT_{NDT} Shift

VISA-II code employs the three kinds of RT_{NDT} shift equations, i.e. (a) the modified Gathrie equation [42], (b) Randall equation [12] and (c) the equation in US Regulatory Guide 1.99 Rev. 2 [40]. (d) One Japanese equation is also proposed in JEAC4206 [45]. In the original EPRI/NRC benchmarking problems, the equation of (c) was employed. In the present study, case A1 (infinitely long axial crack) is solved assuming the above four RT_{NDT} shift equations. VISA-II code is utilized. The analysis results show that equations of (b) and (c) give almost the same results, while (a) and (d) give almost the same results. The four results range within a few factors difference. In other words, any of the above four equations for RT_{NDT} shift can be used.

5.5 Effects of Impurity Content

Impurities such as Cu and Ni are known to have large influence to the estimation of neutron irradiation embrittlement of vessel materials. According to the RT_{NDT} shift equations mentioned previously, Cu content affects RT_{NDT} shift value more directly than Ni content. Then influences of Cu content were examined in detail, solving the EPRI/NRC benchmarking problems with OCA-P code.

Figure 6 shows calculated break probabilities plotted against wt. % of Cu content. The variation range of Cu content in the figure corresponds to the actual data for the base metals of US RPV materials. The figure clearly illustrates that the variation of Cu content significantly influences break probabilities, and that the break probability for Cu content of 2.2 wt.% is more than two orders greater than that of 1.2 wt.%.

5.6 Through-wall Distribution of Material Properties

As pointed out in the report of the EPRI/NRC PTS benchmarking study [30], one of the largest differences among various PFM codes for PTS problems was caused due to the difference in modeling the through-wall distribution of material properties such as K_{Ic}, K_{Ia} and RT_{NDT} shift. The question arisen was whether deviations of these properties from their mean values are resimulated at every steps of crack propagation or not. When this problem was solved at the first time, VISA-II resimulated all of the three material properties at every steps of crack propagation (Procedure 1), OCA-P resimulated only K_{Ic} and K_{Ia} values (Procedure 2), and WPFM [11] resimulated none of them (Procedure 3), i.e. fixed these material properties during crack propagation. Since WPFM estimated the highest failure probability, Procedure 3 was finally recommended as the standard procedure.

In the present study, the effects of the modeling of the through-wall distribution of the three material properties are again examined using OCA-P and VISA-II codes. Figure 7 shows calculated break probabilities for the three different procedures. The difference between the results of Procedures 1 and 3 is of more than one order of magnitude, and Procedure 3 gives the highest break probability. Conservatism embedded in Procedure 3 is a strong motivation to adopt this procedure as standard. However, further investigation is still required since there is not any physical basis for this procedure.

5.7 Effects of PSI

Recently, a new data on probability of non-detection of crack, i.e. Arakawa equation, which is for UT-based PSI, was proposed in Japan [46], based on a number of experimental data. The Marshall equation [41] is also popularly used. These data are shown in Figure 8. Here Arakawa (inner) means the data for embedded cracks, while Arakawa (surface) means the data for surface crack. The EPRI/NRC benchmarking problems of axial crack cases are solved, assuming the three different PSIs of Figure 8. PROFMAC-II is used here. Figure 9 shows the analysis results. For the purpose of comparison, the figure also shows the results without any PSI. Figure 9 shows that PSI with the accuracy of Arakawa equations reduces break probabilities significantly, i.e. two to three orders of magnitude. In Japan, UT-based PSI is applied to a whole volume of vessel, and X-ray based PSI is further applied to welded portions. Considering the fact that actual cracks are generally embedded, the Arakawa equation for embedded cracks seems a reasonable choice as standard in Japan.

5.8 WPS Effects

The warm prestressing (WPS) effect has been well verified through various experiments. Nevertheless, most of integrity assessments for PTS events are performed without considering this effect. Neither PFM problems employed in the present study originally take the WPS effect into account. The effects are here evaluated, assuming that a crack does not begin to propagate when the K value is in a decreasing process. Figure 10 shows break probability for the axial crack case of the EPRI/NRC benchmarking problem. Figure 11 shows that of the H. B. Robinson problem. In both problems, failure probability reduces by considering WPS effects. In the H. B. Robinson problem, such a reduction effect is not so significant, while failure probability reduces by nearly two orders of magnitude in a lower neutron fluence region in the EPRI/NRC benchmarking problem.

6. CONCLUSIONS

Benchmarking study using the four different PFM codes, i.e. two Japanese and two US's, were performed, and the consistency of the codes were verified. Using these codes, some sensitivity analyses were conducted to quantitatively evaluate the influences of the input data, i.e. (a) initial crack shape, (b) the probabilistic distribution of initial crack depth, (c) cladding, (d) RT_{NDT} shift, (e) impurity content, (f) the through-wall distributions of material properties, (g) pre-service inspection (PSI) and (h) warm prestressing. It is clearly shown that in most cases, these data affect failure probabilities significantly. Therefore, we should use in the PFM analyses as reliable input data as possible. However, if any reliable data are not available, the data resulting in most conservative results could be chosen, referring the analysis results presented in this paper. In order to establish standard procedures to evaluate best estimates of failure probabilities of nuclear PV&P components, we will continuously improve the round-robin problems and accumulate sensitivity analysis results.

ACKNOWLEDGMENTS

The authors wish to thank all the members of the RC111 committee in the Japan Society of Mechanical Engineers (JSME) for their efforts to perform this work, and also thank the Japan Atomic Energy Research Institute (JAERI) for financial support.

REFERENCES

[1] M. Akiyama et al., Technical challenge toward safe and long-lived nuclear power plant, Journal of Atomic Energy Society of Japan, 33 (1991) 205-242 (in Japanese).
[2] J. M. Broom, Probabilistic fracture mechanics - A state-of-the art review, Proceedings of 1984 ASME PVP Conference, Vol. PVP-92, pp.1-19, (1984).
[3] G. Yagawa, Structural integrity assessment of nuclear power plants using probabilistic fracture mechanics, Nuclear Engineering, 34 (1988) 19-30 (in Japanese).
[4] D. O. Harris and K. R. Balkey, Probabilistic considerations in life extension and aging, Technology for the '90s, ASME PVP Division, pp.243-269, (1993).
[5] Risk-based inspection development of guidelines, NUREG/GR-0005, (1992).
[6] F. A. Simonen and H. H. Woo, Analysis of the impact of inservice inspection using a piping reliability model, NUREG/CR-3869, (1984).
[7] D. O. Harris and D. Dedhia, Setting reinspection intervals for seam welded piping by use of probabilistic fracture mechanics and target reliability values, Proceedings of 1995 ASME/JSME Joint PVP Conference, Vol. PVP-304, pp.443-451, (1995).
[8] W. E. Vesely, E. K. Lynn, and F. F. Goldberg, The OCTAVIA computer code : PWR reactor pressure vessel failure probabilities due to operationally caused pressure transients, NUREG/CR-0258, (1978).
[9] D. O. Harris, E. Y. Lim and D. D. Dedhia, Probabilistic pipe fracture in the primary coolant loop of a PWR plant, NUREG/CR-2189, UCRL-18967, (1981).
[10] A. Brueckner-Foit et al., Curve fitting to defect size distributions for the calculation of failure probability, Nuclear Engineering and Design, 74 (1982) 75.
[11] F. J. Witt, WPFM-The Westinghouse probabilistic fracture mechanics computer program, NUREG/CP-0047, (1983).
[12] R. D. Cheverton and D. G. Ball, OCA-P - A deterministic and probabilistic fracture mechanics code for application to pressure vessels, NUREG/CR-3618, (1984).
[13] T. Y. Lo, et al., Probability of pipe failure of in the reactor coolant loop of Combustion Engineering PWR plants, NUREG/CR-3663, UCRL-53500, (1984).
[14] J. Dufresne, A. C. Lucia, J. Grandemange and A. Pellissier-Tanon, The COVASTOR program, Nuclear Engineering and Design, 86 (1985) 139-146.
[15] F. A. Simonen, K. I. Johnson, A. M. Liebetrau, D. W. Engel and E. P. Simonen, VISA-II - A computer code for predicting the probability of reactor pressure vessel failure, NUREG/CR-4486, PNL-5775 RF, R5, (1986).
[16] T. Fujioka and K. Kashima, A sensitivity study in probabilistic fracture analysis of light water reactor carbon steel pipe, Int. Journal of Pressure Vessels and Piping, 52 (1990) 403-416.
[17] N. Soneda, T. Onchi and T. Takao, Sensitivity analysis of PTS event by probabilistic fracture mechanics, Transactions of 11th SMiRT, Vol.G, pp.165-170, (1991).
[18] K. Watashi and I. Furuhashi, Probabilistic fracture mechanics analysis code CANIS-P, Transactions of 11th SMiRT, Vol. G2, pp.343-348, (1991).
[19] N. Handa and T. Uno, Application of the probabilistic fracture mechanics to the multiple crack problem and inelastic behavior problem, Trans. 11th SMiRT, Vol.G2, pp.349-353 (1991).
[20] K. Hojo, M. Takenaka, H. Kaguchi, G. Yagawa and S. Yoshimura, Applications of probabilistic fracture mechanics to FBR components, Nuclear Eng. and Design, 42 (1993) 43-49.
[21] T. L. Dickson, J. A. Keeney and J. W. Bryson, Validation of FAVOR code linear elastic fracture solutions for finite length flaw geometries, Proceedings of 1995 ASME/JSME PVP Conference, Vol.PVP-304, pp.51-58, (1995).
[22] S. Yoshimura, Some structural integrity studies of pressure vessels and piping in Japan - A Review, International Journal of Pressure Vessels and Piping, 65 (1995) 101-107.
[23] G. Yagawa, S. Yoshimura and H. Ueda, An estimation scheme for J- and C*- integrals of surface cracks, Proceedings of International Symposium on Pressure Vessel Technology and Nuclear Codes & Standards, Seoul, pp.8.15-8.22, (1989).

[24] G. Yagawa, Y. Kitajima and H. Ueda, Three-dimensional fully plastic solutions for semi-elliptical surface cracks, Int. Journal of Pressure Vessel and Piping, 53 (1993) 457-510.
[25] S. Yoshimura, J.-S. Lee and G. Yagawa, Automated system for analyzing stress intensity factors of 3D cracks : Its applications to analyses of two dissimilar semi-elliptical surface cracks in plate, Transactions of ASME, Journal of Pressure Vessel Technology, Submitted for Publication.
[26] G.-W. Ye, G. Yagawa and S. Yoshimura, Probabilistic fracture mechanics analysis based on three-dimensional J-integral database, Engineering Fracture Mechanics, 44 (1993) 887-893.
[27] G. Yagawa and G.-W. Ye, A probabilistic fracture mechanics analysis for cracked pipe using 3-D model, Reliability Engineering and System Safety, 41 (1993) 189-196.
[28] S. Yoshimura, M.-Y. Zhang and G. Yagawa, Life extension simulation of aged reactor pressure vessel material using probabilistic fracture mechanics analysis on a massively parallel computer, Nuclear Engineering and Design, 158 (1995) 341-350.
[29] S. Yoshimura, J.-S. Lee, G. Yagawa, K. Sugioka and T. Kawai, New probabilistic fracture mechanics approach with neural network-based crack modeling : Its application to multiple cracks problem, Proc. 1995 ASME/JSME PVP Conference, Vol.PVP-304, pp.437-442, (1995).
[30] B. A. Bishop, Benchmarking of probabilistic fracture mechanics analyses of reactor vessels subjected to pressurized thermal shock (PTS) loading, EPRI Research Project 2975-5, Final Report, (1993).
[31] G. Yagawa, S. Yoshimura, N. Handa, K. Watashi, T. Fujioka, H. Ueda, T. Uno, M. Uno, K. Hojo and S. Ueda, Study on life extension of aged RPV material based on probabilistic fracture mechanics - Japanese round robin -, Transactions of ASME, Journal of Pressure Vessel Technology, 117 (1995) 7-13.
[32] JWES, Report of Atomic Energy Research Committee, Japan Welding Engineering Society, JWES-AE-9003, (1990) (in Japanese).
[33] Final Report of RC111 Committee, Japan Society of Mechanical Engineers, (1995).
[34] D. L. Selby et al., Pressurized thermal shock evaluation of the H.B. Robinson Unit 2 nuclear power plant, NUREG/CR-4183, Vols.1, 2, (1985).
[35] S. Yoshimura, H. Akiba, Y. Otani and G. Yagawa, Probabilistic fracture mechanics analyses of LWR's pressure vessels and piping : Quantitative study on influences of distributions of initial crack sizes, Proceedings of 20th MPA Seminar, Vol.2, pp.44.1-10, (1994).
[36] N. Soneda, M. Hirano, Y. Otani, Y. Urabe, S. Yoshimura, and G.Yagawa, Japanese PTS benchmarking study using probabilistic fracture mechanics, Proceedings of ICONE-3, Vol.1, pp.405-410, (1995).
[37] Y. Kanto, S. Yoshimura, H. Ueda, N. Handa, M. Hirano, N. Soneda and G. Yagawa, Application of probabilistic fracture mechanics to pressure vessels and piping of nuclear power plants : JSME Activity, Proceedings of ICONE-3, Vol.1, pp.411-416, (1995).
[38] US NRC, NRC staff evaluation of pressurized thermal shock, Enclosure A to Commission Paper SECY-82-465, (1982).
[39] R. M. Gamble, Evaluation of limits on BWR pressure vessel hydrotest temperature and PWR low-temperature overpressurization protection system, EPRI TR-102850 (1993).
[40] US NRC, Regulatory Guide 1.99(Task ME 305-4), Radiation embrittlement of reactor vessel materials, Revision 2, (1988).
[41] W. Marshall, An assessment of the integrity of PWR pressure vessels. UKAEA, (1982).
[42] D. L. Stevens et al., VISA : A computer code for predicting the probability of reactor pressure vessel failure, NUREG/CR-3384, (1983).
[43] I. S. Raju and J. C. Newman, Stress intensity factors for internal and external surface cracks in cylindrical vessels, Trans. ASME, Journal of Pressure Vessel Technology, 104 (1982) 293-298.
[44] R. P. Menich, J. R. Foulds and D. D. Dedhia, SAVER : Statistical analysis of vessel examination results, Proc. 1995 ASME/JSME PVP Conf., Vol.PVP-304, pp.461-472 (1995).
[45] JEAC, Testing Methods for Verification of Fracture Toughness of Nuclear Power Plant Components, JEAC 4206, (1991).
[46] T. Arakawa, Japanese evaluation of the Japanese results, Ultrasonic Inspection of Heavy Section Steel Components, The PISC II Final Report Part-II, pp.409-427 (1988).

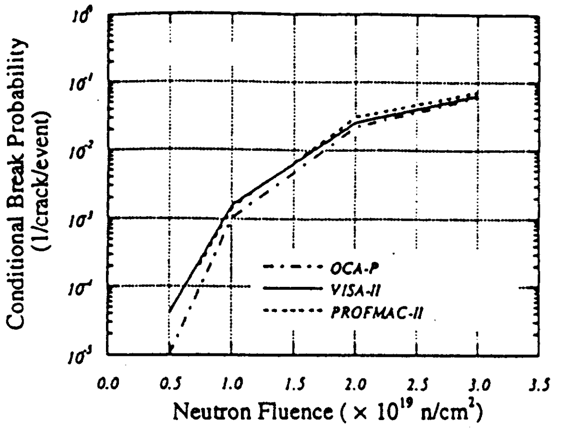

Fig.1 Break probabilities of circumferential crack cases calculated with three PFM codes

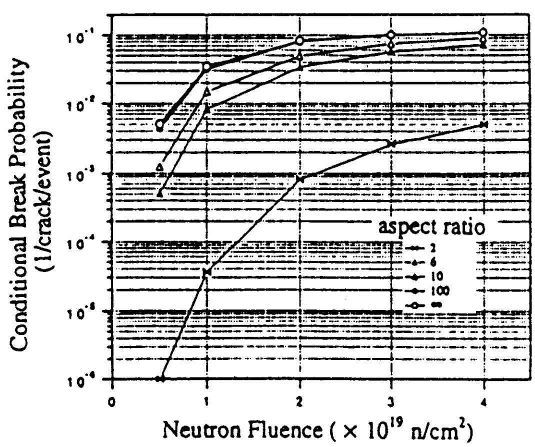

Fig.2 Break probabilities of axial crack cases for five different crack shapes

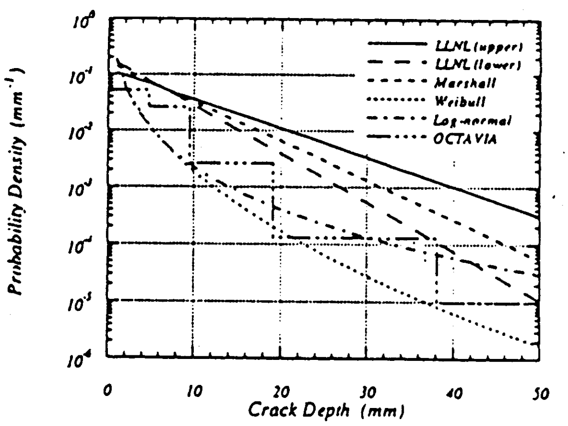

Fig.3 Probabilistic distributions of initial crack depth

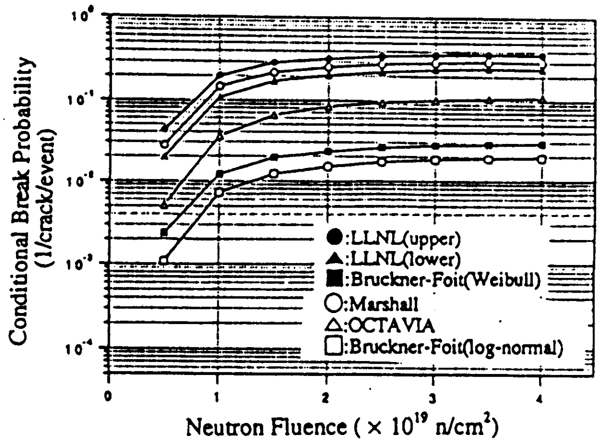

Fig.4 Break probabilities of axial crack cases for six different crack depth distributions

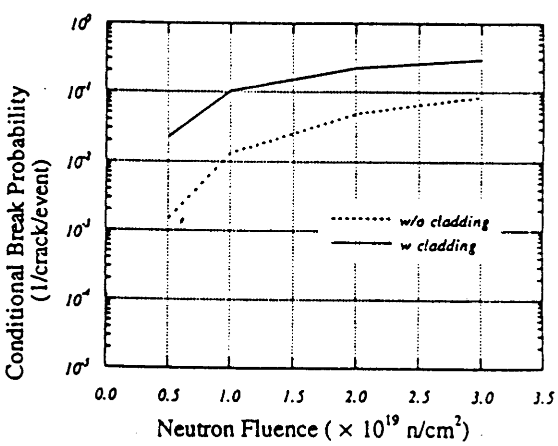

Fig.5 Break probabilities of axial crack cases with / without cladding

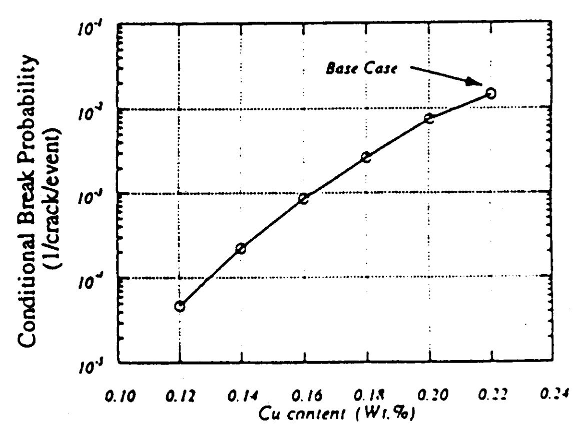

Fig.6 Break probabilities plotted against Cu content

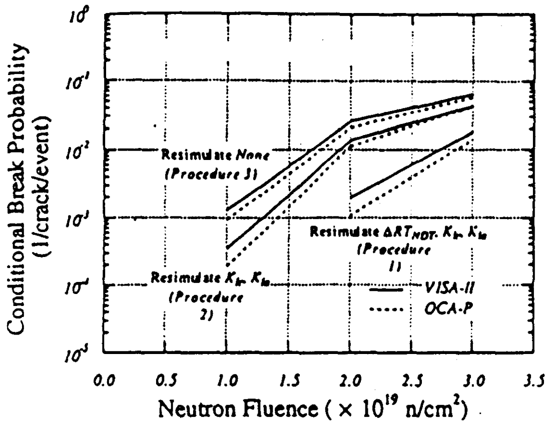

Fig.7 Break probabilities for three different procedures of considering through-wall distributions of material properties

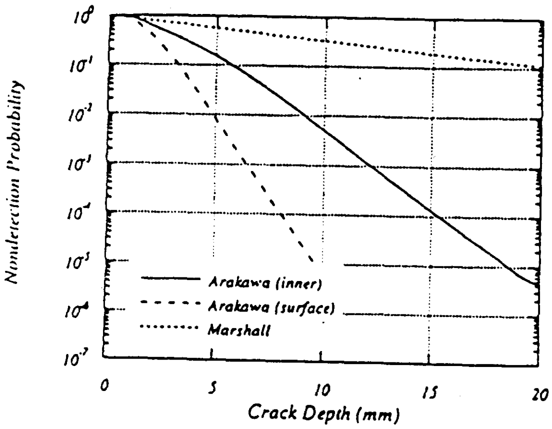

Fig.8 Probability distributions of nondetection of crack

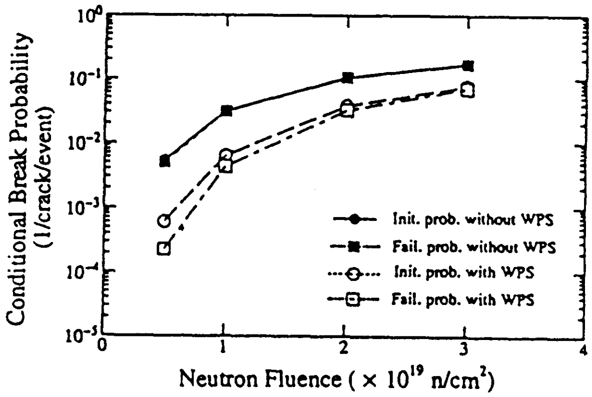

Fig.10 WPS effect on failure probability (EPRI/NRC problem)

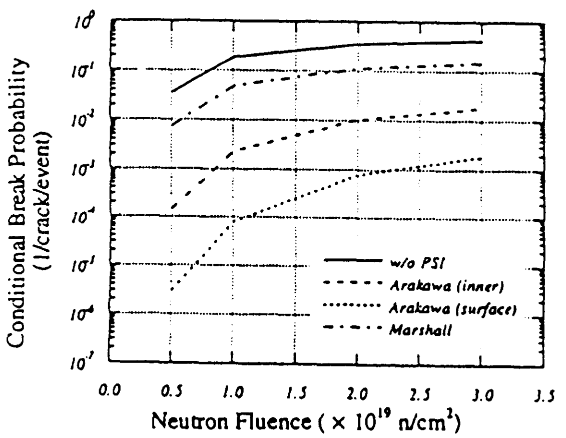

Fig.9 Break probabilities of axial crack cases for four different probabilities of nondetection of crack

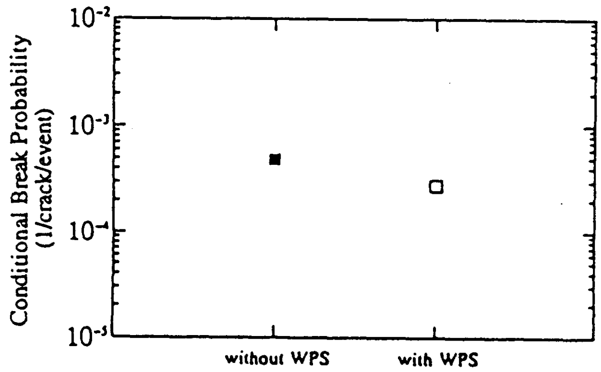

Fig.11 WPS effect on failure probability (H. B. Robinson problem)

5 Improved Toughness of the SA 508 Class 3 Steel for Nuclear Pressure Vessel Through the Steel-Making and Heat Treatment

J.T. Kim*, H.K. Kwon, H.S. Chang (HANJUNG)

Improved Toughness of the SA 508 Cl. 3 Steel for Nuclear Pressure Vessel Through the Steel-Making and Heat Treatment

J. T. Kim, H. K. Kwon, and H. S. Chang

R & D Center, HANJUNG, Changwon, Korea

Abstract

The compartive investigations of forgings by three steel-making procedures of SA 508 class 3 have proven that vacuum carbon deoxidation(VCD) offered low toghness properties, even though the toughness met the required values. The toghness properties of the steel by VCD were closely related with the cooling rate from the solution treating temperature. To obtain the secure toughness for the VCD steel, the recommendable minimum cooling rate from the austenitizing temperature is 15℃/min. The modified VCD steel by adding aluminium and silicon-killed steel were though obtained the secure toughness properties. The fracture toughness(K_{IC}) was significantly improved by the silicon-killing and the modified VCD. These were resulted from the fine austenitic grain size. It is observed that the grain size was below 20μm when using the modified VCD and silicon-killing, and that was 50μm when using VCD.

Introduction

The Reactor Pressure Vessel(RPV) of the pressurized water reactor nuclear power plants is manufactured using forgings and plates in manganese-nickel-molybdenum low alloy steel designated according to the ASME/ASTM standards SA 508 class 3 and SA 533 Type B class 3. This steel is manufactured by silicon-killing or VCD. However, since the influence of the steel-making practices on the toughness properties of the RPV steel has not been systematically investigated[1, 2], we have studied to improve the toughness properties of the forged steel for RPV through the steel-making procedures. It has been investigated the effects of cooling rate at austenitizing temperature on the Charpy impact resistance of the 2 1/4Cr-1Mo steel[3, 4], however, few report for the SA 508 class 3 steel has been found[5].

Therefore, the effects of the steel-making procedures on the toughness properties of the SA 508 class 3 steel were investigated by using several shell forgings, which were manufactured by three steel-making methods. The first is the VCD, the second is the modified VCD by adding aluminium, and the third is the silicon-killing method. The effects of cooling rate from the solution treating temperature on the toughness properties were also studied because the secure toughness properties in the VCD steel had not been obtained.

Experimental Procedures

Several shell forgings for RPV of 1000 MWe nuclear power plant were manufactured by using conventional hot pierced ingots. The applied steel-making procedures are VCD, modified VCD by adding aluminium, and silicon-killing. The chemical compositions of the examined steel are indicated in the Table 1. The forged shells were normalized at 900℃, quenched in water at 880~900℃ and then tempered at 650℃. The simulated post weld heat treatment for the test blocks was executed for 32h at 620~630℃. The cooling rates were measured at various locations of the shell with attached thermocouples during quenching. In order to examine the effects of cooling rate on the Charpy V-notch impact properties for the VCD steel, the cooling rates of the specimens were varied from 1℃/min to 150℃/min. The heat treating conditions of the specimen manufactured by VCD method are described in Table 2.

The influence of steel-making procedures on the Charphy V-notch impact properties of the SA 508 class 3 steel has been examined at through-thickness of the shell. The nil-ductile transition temperature(T_{NDT}) by the drop weight test and fracture toughness were examined at 1/4-thickness of the shell thickness. The fracture toughness(K_{IC}) values were converted from the J_{IC} tested at room temperature, that is, $K_{IC} = [\ E \cdot J_{IC}/(1 - \nu^2)\ ]^{1/2}$, where E is Young's modulus and ν is Poisson's ratio.

Results and Discussion

The tensile properties of the SA 508 class 3 steel manufactured by three steel-making methods were measured at 1/4-thickness of the shell. These results are described in Fig. 1. From the these results it seems that the tensile properties are not related with the steel-making procedures for this steel. However, the elongation was slightly improved by the silicon-killing, while the tensile and yield strength were almost same regardless of the steel-making methods.

The Charpy V-notch impact transition curves of the SA 508 class 3 steel with steel-making methods in the tangential and axial direction are shown in Fig. 2 and Fig. 3, respectively. These are the typical results obtained at 1/4-thickness of the shell for RPV. From these results the 68Joule(50ft-lb) energy transition temperature(vTr_{68}) and 50% shear fracture appearance transition temperature($FATT_{50}$) are summarized in Table 3. The vTr_{68} and the $FATT_{50}$ of the VCD steel were higher than those of the modified VCD and silicon-killed steels. Furthermore, the deviations of vTr_{68} and $FATT_{50}$ of the VCD steel were larger than those of the modified VCD and silicon-killed steels.

The life-time of the RPV is limited because of the core area embrittlement, so the resistance against fast fracture of the SA 508 class 3 steel shell is indexed by the means of the reference nil-ductile transition temperature(RT_{NDT}). Fig. 4 shows the variations of various transition temperatures of the SA 508 class 3 steel for RPV with steel-making processes. From this result silicon-killed steel has the best values.

The fracture toughness(K_{IC}) of the SA 508 class 3 steel was significantly improved by the silicon-killing and modified VCD. The K_{IC} values of forgins by the VCD, modified VCD and silicon-killing at room temperature are 426, 574 and 665MPa$\sqrt{}$m, respectively.

It is suggested that these were resulted from the reducing of sulphur content and the fining of the austenitic grain size. It was analyzed that the sulphur contents of the VCD, modified VCD and silicon-killed steel were 0.004, 0.0035 and 0.002%, respectively. Therefore, the contents of deliterious sulphidic non-metallic inclusion for the fracture toughness and Charpy impact resistance might be reduced by decreasing the contents of sulphur. It was observed that the grain size was 20μm when using the modified VCD and silicon-killing, and that was 50μm when using VCD.

Many investigators[1, 2] have been studied the effects of the steel-making methods on the mechanical and metallurgical properties of a steel. P. Bernabei et al[1] are recommended VCD process for the SA 508 class 3 steel, regardless of the deoxidation practice, for a given grain size, Charpy V-notch impact energy at 4.4℃ after welding is always higher than in quenched and tempered condition. Comparing the steel manufactured by the three steel-making methods, they observed that the VCD heat showed the best $FATT_{50}$ and absorbed energy values. However, when the heavy wall thick steel is manufactured by VCD, the grain size is coarsened and the secure toughness properties are not obtainable. Therefore, many a forgemasters have been preferred to add aluminium or deoxidize by silicon to manufacture the better forging shell for RPV.

Fig. 5 shows the variations of vTr_{68} and $FATT_{50}$ with cooling rate of the SA 508 class 3 steel by VCD. The cooling rates were measured between 800℃ and 500℃, which is the range of bainite trasformation temperature in this steel. From the results the transition temperatures of the vTr_{68} and $FATT_{50}$ were lowered as the cooling rate increased. The Charpy V-notch impact energy at 4.4℃($E_{4.4}$) were also improved as the cooling rate increased. The variations of $E_{4.4}$ with the cooling rates are shown in Fig. 6. When cooling rate at 880℃ was 1℃/min, the ferrite content of about 20% was observed. However, when the cooling rate is above the 10.1℃/min, it was not observed any ferrite phase as shown in Fig. 7. In case of 10.1℃/min in cooling rate, the Charpy impact resistance was though satisfied the required conditions, but its values were low margin states. From these results, in order to obtain the secure Charpy V-notch impact properties in the SA 508 class 3 steel for RPV, it is suggested that the recommendable minimum cooling rate from austenitizing temperature to bainite finish temperature is 15℃/min.

Moreover, the influences of the double heat treatment on the Charpy V-notch impact properties of this steel were also examined, and these effects were shown in Fig. 5 by open indicators(○, △). The double heat treatment means the repeated process of quenched and tempered treatment. When double heat treatment for this steel was performed, the transition temperatures and impact energy were improved. Fig. 8 shows the grain sizes of the single heat treated and double heat treated steel. The grain size of the double heat treated steel is finer than that of the single heat treated one. It may be resulted from the new grains formed at prior austenitic and bainitic lath colony boundaries via dissolution of the two phase(α + γ) duplex structure which had formed on heating.

Concluding Remarks

The tensile properties were almost same regardless of the steel-making for the SA 508 class 3 steel, though the elongation was slightly improved by the silicon-killing. Comparing the 68 Joule energy, 50% shear fracture appearance, and reference nil-ductile transition temperature(vTr_{68}, $FATT_{50}$ and RT_{NDT}) of the steels manufactured by the VCD, modified VCD and silicon-killing methods, the silicon-killed steel has the best properties. The fracture toughness(K_{IC}) was significantly improved by the modified VCD and silicon-killing. The are resulted from the fining of austenitic grain size. The toughness properties of the steel by VCD were closely related with the cooling rate from the solution treating temperature. To obtain the secure toughness for the VCD steel, the recommendable minimum cooling rate from the austenitizing temperature is 15℃/min.

References

1. P. Bernabei, L. Callegari, M. Scepi, and T. Salinetti, Steel Forgings, ASTM STP 903, E. G. Nisbett and A. S. Melilli, Eds., American Society for Testing and Materials, PA, 1986, p. 275
2. M. Erve, F. Papouschek, K. Fischer, and Ch. Maidorn, Nuclear Engineering and Design, vol. 108, (1988) p. 487
3. W. E. Erwin and J. G. Kerr, WRC 275, Feb., (1982)
4. Y. Murakami, T. Nomura, and J. Watanabe, Application of 2 1/4Cr-1Mo Steel for Thick-Wall Pressure Vessels, ASTM STP 755, G. S. Sangdahl and M. Semchyshen, Eds., American Society for Testing and Materials, PA, 1982, p. 383
5. T. Kodaira, Tetsu to Hagane, vol. 73, No. 14, (1987) p. 1656

Table 1. Chemical compositions of the SA 508 class 3 steel used in study.

Heat	Cemical composition (wt%)													
	C	Si	Mn	P	S	Ni	Cr	Mo	V	Cu	Al	As	Sn	Sb
VCD	0.18	0.075	1.35	0.0055	0.004	0.78	0.135	0.525	0.0055	0.055	0.0055	0.0032	0.0025	0.00095
Modified VCD	0.2	0.085	1.35	0.0075	0.0035	0.83	0.155	0.5	0.004	0.04	0.013	0.0044	0.0035	0.0009
Si-filled	0.21	0.24	1.36	0.007	0.002	0.92	0.21	0.49	0.005	0.03	0.022	0.0034	0.0025	0.0007

Table 2. Heat treatment of the SA 508 class 3 steel used in study.

		Cooling Rate (℃/min) (800 ~500℃)		Heat Treating Condition					
		1st	2nd	Austenizing		Tempering		PWHT	
				Tem.(℃)	Time(hr)	Tem.(℃)	Time(hr)	Tem.(℃)	Time(hr)
As Received				880	6.5	625	6.5		
				885	5.5	665	9	625	40
Simulation Heat Treatment	A	1		880	2	650	10	610	31
	B	10.2		880	2	650	10	610	31
	C	20.1		880	2	650	10	610	31
	D	27.8		880	2	650	10	610	31
	E	150		880	2	650	10	610	31
	B+B	10.1	11.4	880	2	650	10	610	31
	C+C	20	18.2	880	2	650	10	610	31
	D+C	25.6	20	880	2	650	10	610	31

Cooling Rate in the Real RPV Shell	Cooling Rate at Various Thickness			
	Out Surface 1/8t	Out Surface 1/4t	Out surface 1/2t	Inner Surface 1/4t
	100℃/min	39℃/min	22.5℃/min	26℃/min

Table 3. The nil-ductile transition temperature(T_{NDT}), 68 Joule transition temperature(vTr_{68}) with the steel-making practices of the SA 508 class 3 steel.

Steel-making Practices	Transition Temperature(℃)	
	T_{NDT}	vTr_{68}
VCD	-12 ~ -18	-4 ~ -15
Modified VCD	-23 ~ -35	-29 ~ -36
Silicon-killing	-23 ~ -29	-31 ~ -48

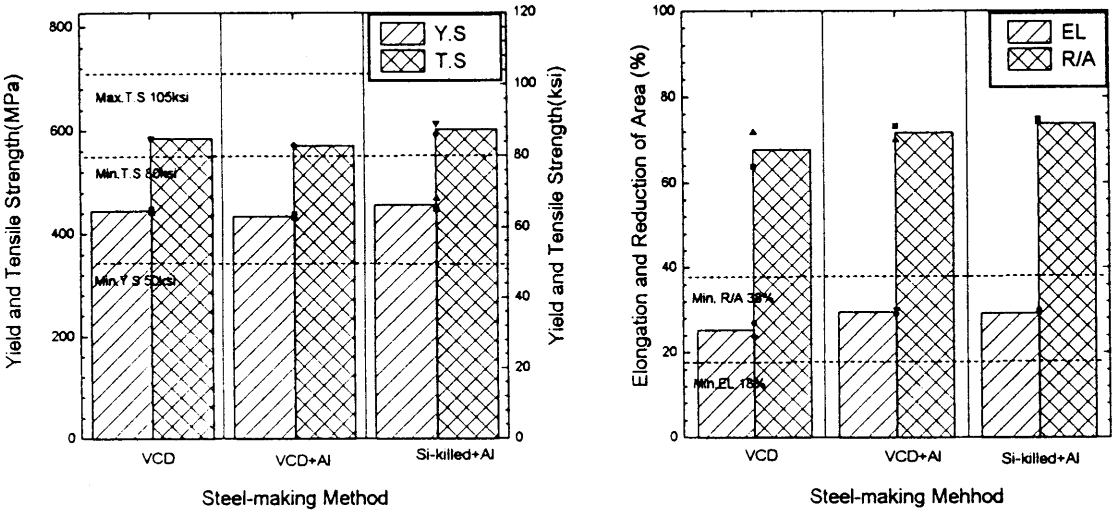

Fig. 1. Comparison of tensile properties of the forged SA 508 class 3 steel for the reactor pressure vessl with steel-making method.

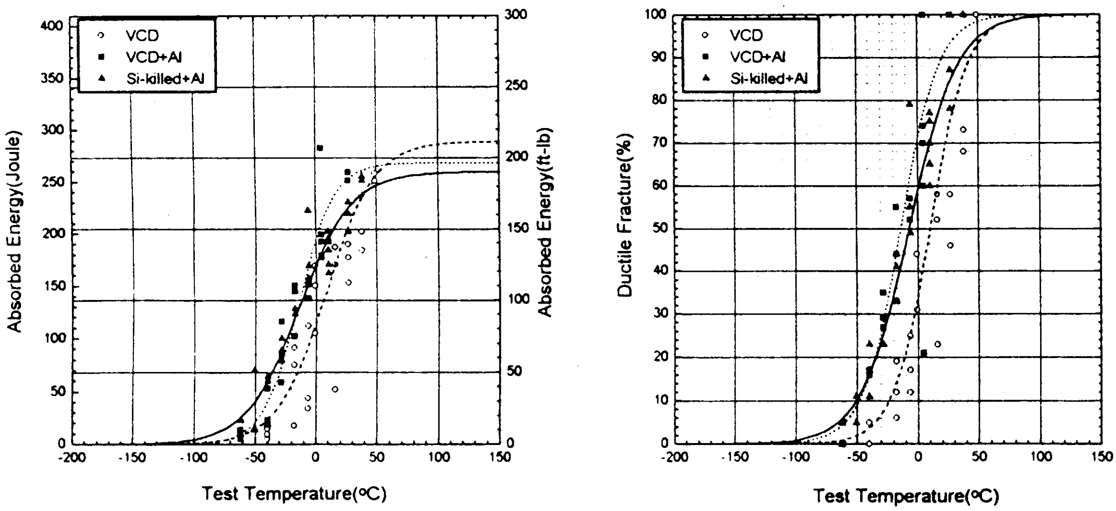

Fig. 2. Charpy V-notch impact transition curves of forged SA 508 class 3 steel for reactor pressure vessel with steel-making method. The specimens were taken in the tangential direction.

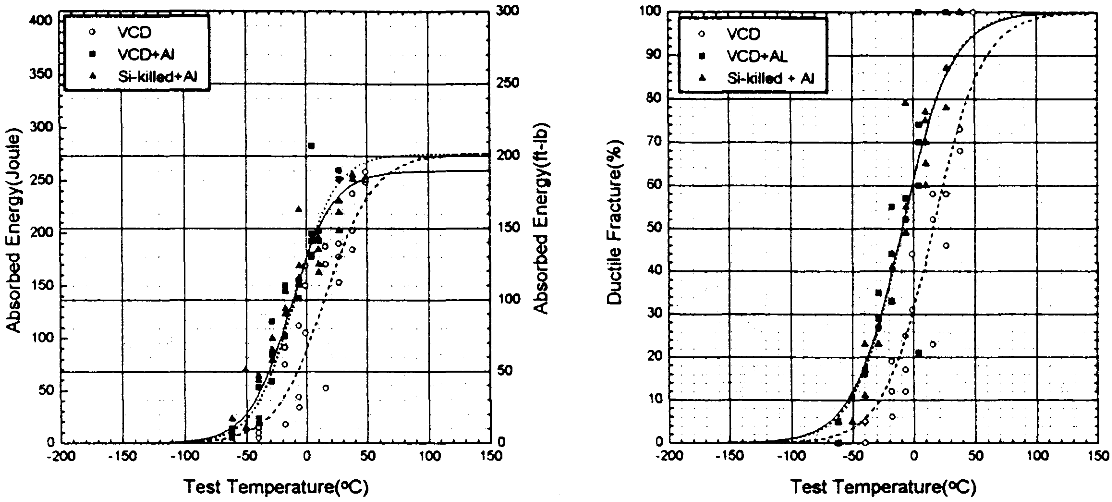

Fig. 3. Charpy V-notch impact transition curves of forged SA 508 class 3 steel for reactor pressure vessel with steel-making method. The specimens were taken in the axial direction.

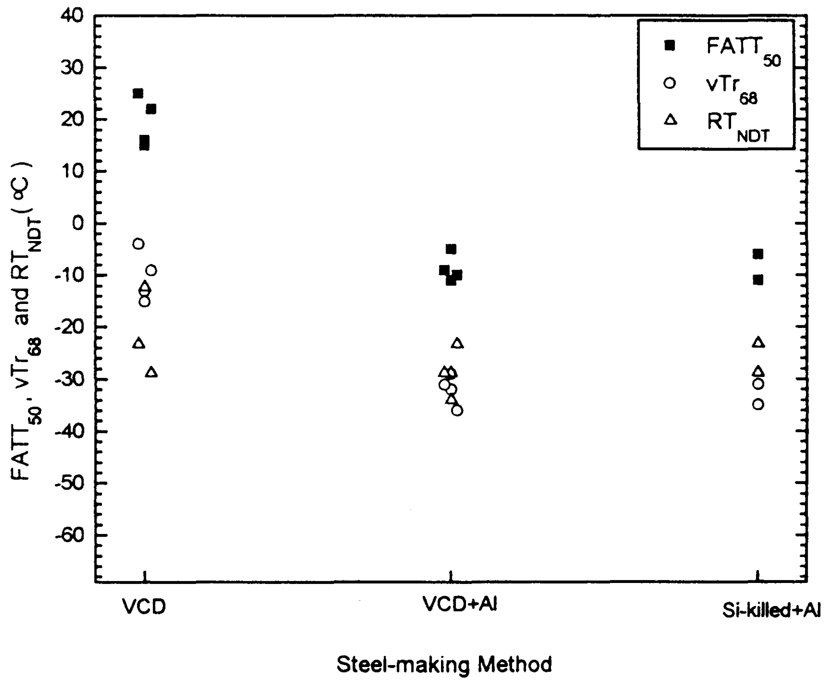

Fig. 4. Comparison of various transition temperatures of the forged SA 508 class 3 steel for reactor pressure vessel with steel-making method.

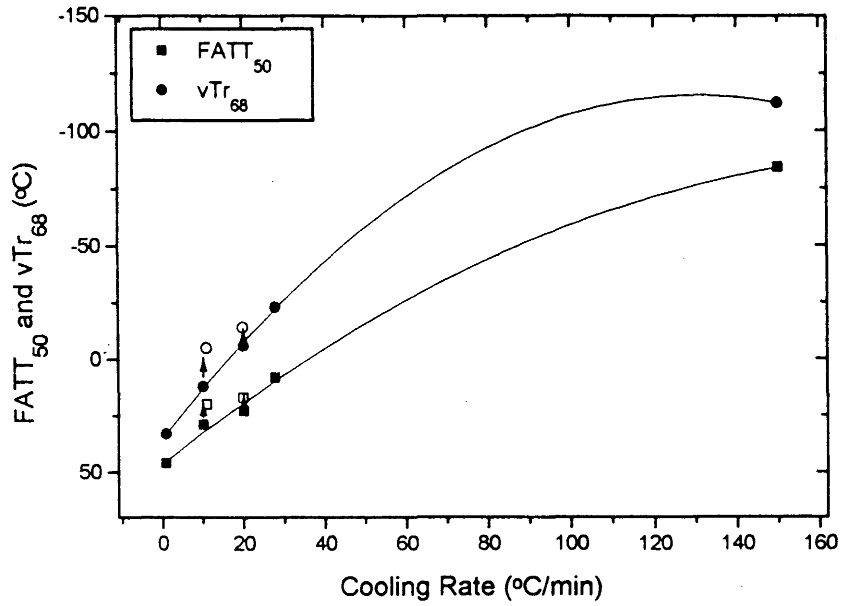

Fig. 5. The variations of 68 Joule(50ft-lb) energy and 50% shear fracture appearance transition temperature(vTr68 and FATT50) with cooling rate of the SA 508 class 3 steel by VCD.

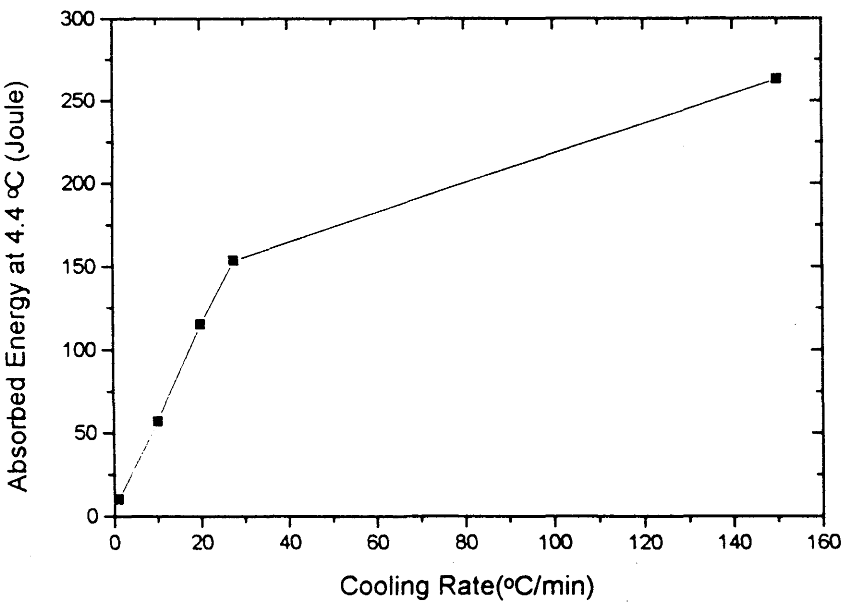

Fig. 6. The variations of charpy V-nocth impact energy at 4.4 °C with cooling rate of the SA 508 class 3 steel by VCD.

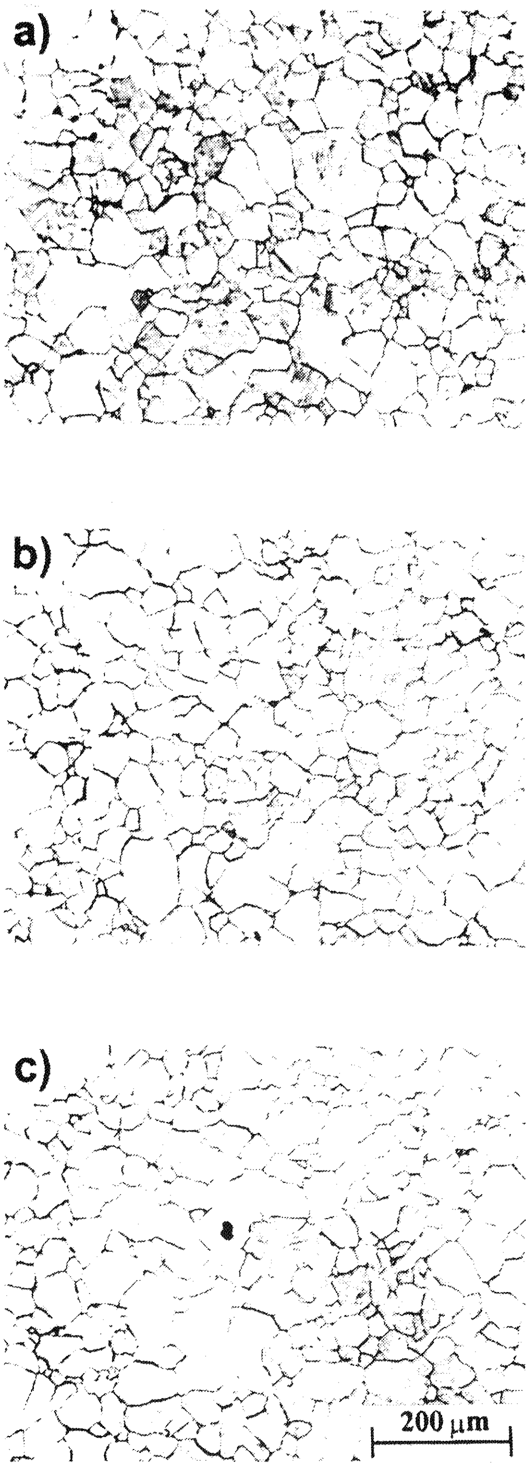

Fig. 8. Grain sizes of the SA 508 class 3 steel with cooling rate at 880℃. a) 1℃/min, b) 10.1℃/min, c) 10.1 + 11.4℃/min(double quenched and tempered treatment)

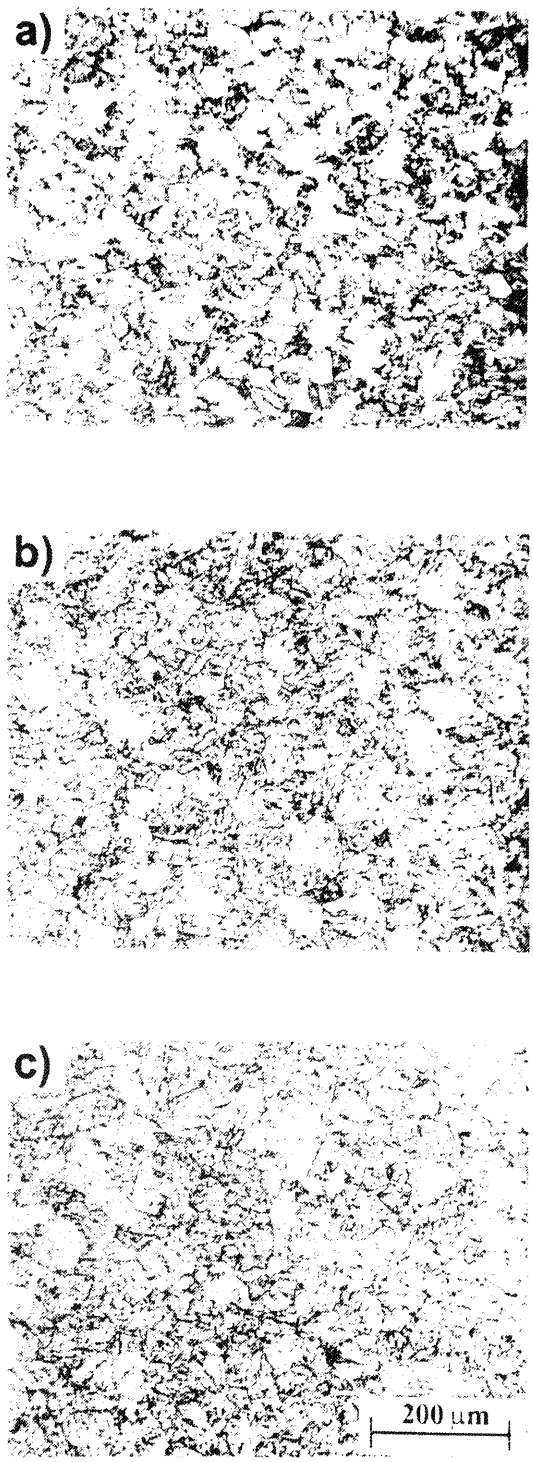

Fig. 7. Microstructures of the SA 508 class 3 steel with the cooling rate at 880℃. a) 1℃/min, b) 10.1℃/min, c) 10.1 + 11.4℃/min(double quenched and tempered treatment)

SESSION B

6 Crack Shape Evolution of Surface Flaws under Fatigue Loading of Austenitic Pipes

I.S. Hwang*, J.H. Kim (Seoul National Univ.)

Crack Shape Evolution of Surface Flaws under Fatigue Loading of Austenitic Pipes

I.S. Hwang and J.H. Kim

Department of Nuclear Engineering, Seoul National University
Shinlim-dong, Gwanak-ku, Seoul 151-742, Korea

From the results of fatigue crack growth and fracture tests of a Ni-Fe base superalloy (Incoloy 908), an improved fatigue life analysis model has been derived from the framework of Newman and Raju. For a plate geometry with an initial semi-elliptical surface crack in its thickness direction, the new model can predict the evolution of crack aspect ratio for a wide range of initial crack geometry for Incoloy 908 that has been considered as a primary candidate for the ITER central solenoid conduit. The improved model is applied to the ITER central solenoid magnet life prediction. The model predicted the conduit fatigue lives that are about two times the values obtained by assuming the constant aspect ratio during the crack growth, for both free-standing and bucked against central solenoid designs. Therefore the realistic modeling is recommended for the future magnet conduit designs.

1. Introduction

The fatigue crack growth behavior and fracture mechanics properties of a nickel-iron base superalloy (Incoloy 908) have been presented for a temperature range from 298 K to 4 K [1].

The material used for property measurement had a processing history that simulates the anticipated manufacturing schedule of a central solenoid magnet conduit for the International Thermonuclear Experimental Reactor (ITER) [2]. The Conceptual Design Activity (CDA) of the ITER has shown that the plasma pulse-cycle life was limited due to fatigue crack growth phenomenon in the superconductor conduit when a free-standing coil design was used for the central solenoid [3]. During the Engineering Design Activity (EDA), the BACS (Bucked Against Central Solenoid) design has been adopted in order to alleviate tensile load and hence the fatigue impact on the conduit. At the bottom and top ends of the central solenoid, however, the bucking is not accomplished due to the configuration of the toroidal field coils. Hence, the EDA design analysis must ensure that the fatigue crack growth in the conduit will not limit the ITER system life.

Fatigue analysis during CDA was based on the assumption that a semi-elliptical surface crack will grow in the conduit thickness direction with a constant aspect ratio (crack depth/crack half length) until the final fracture. The final fracture was predicted based on the linear elastic fracture mechnics (LEFM). The fracture mechanics measurements for Incoloy 908 showed two significant deviations from the CDA design models in that 1) the aspect ratio of a surface crack changes systematically with crack growth and 2) the plasticity involved in the final fracture is too extensive to apply the LEFM approach [1].

Since the accuracy in fatigue and fracture analysis of superconducting magnet structure impact directly on both reliability and economy of the future nuclear fusion system, the development of refined design models are desirable. In this paper, we present an improved design model for fatigue analysis of Incoloy 908 conduit based on the property measurement and data analysis. The model is then applied to the current central solenoid design and the implication of the improved prediction results on the ITER magnet R&D has been discussed.

2. Fatigue Crack Growth Model Development

The fastest fatigue crack growth is expected to take place in the conduit thickness direction from the initial surface flaw with a semi-elliptical geometry, as shown in Figure 1. Although the initial flaw is likely to be associated with welds, the model development is based on the currently available data of Incoloy 908 base metal. Newman and Raju showed that surface crack growth can be predicted by applying Paris Law to each of the transverse and thickness direction, as follows[4];

$$\frac{dc}{dN} = C_B(\Delta K)^m \tag{1}$$

$$\frac{da}{dN} = C_A(\Delta K)^m \tag{2}$$

where dc/dN and da/dN are the crack growth per stress cycle expressed in mm/cycle, and constant C_A, C_B and m are the material constants, and ΔK is the amplitude of stress intensity factor during a fatigue cycle. They also developed the stress intensity factor for the semi-elliptical surface crack in Ref. [4].

In the surface cracked tension test of Incoloy 908, crack length at surface was measured using an optical microscope. Table 2 shows the test data for two tension fatigue tests (#203 and #204) started from a semi-circular EDM notch which have more measurement data points than other tests. Using these data, dc/dN is computed after Eq. (1) where the exponent m is set to 3.0 for the temperature range from 298 K to 4 K, based on our earlier fatigue test results with compact tension specimens [1]. The calculation of stress intensity factor, K, after Newman and Raju equation [4] at $\phi = 90°$ (A) and $= 0°$((B) requires the crack aspect ratio value. Since these tests showed final aspect ratio values different from the initial of 1.0, the estimation of C_B is possible by assuming two diffrent values, i.e., the initial and the final values. Two different C_B-values are then geometrically averaged to determine the constant, as follows;

$$C_B = \sqrt{C_1 \cdot C_2} = 4.06 \times 10^{-9} \qquad ,(\text{mm / Cycle})(\text{MPa}\sqrt{\text{m}})^{-3}$$

Thus we obtained the Paris Law model for a surface crack growing in the transverse direction in Incoloy 908 plate, as follows;

$$\frac{dc}{dN} = 4.06 \times 10^{-9} \times (\Delta K)^{3.0} \qquad ,(\text{mm / Cycle}) \tag{3}$$

Figure 1 compares the surface crack data with Eq. (4) as well as Paris Law correlation of compact tension specimens obtained for Incoloy 908 at room temperature. The correlations for two specimen designs agree to each other within a factor of two.

For the development of da/dN, Newman-Raju suggested to apply a correction factor of 0.9 on the stress intensity factor calculated for the point B of Fig. 1 after Ref. [4], in order to better fit to experimental data such that the coefficient C_A can be determined from C_B by;

$$C_A = \frac{1}{0.9^m} C_B$$

Table 1 summarizes the surafce cracked tension test results for a wide range of aspect ratio. Low aspect ratio data were obtained by bending fatigue loading[1]. To derive the appropriate correction factor for Incoloy 908 from experimental data, the coefficient C_A is assumed to be;

$$C_A = \frac{1}{\alpha^m} C_B$$

By the least square fitting of the data set, α is determined to be 0.904. This value is almost the same as 0.9 used by Newman and Raju[4]. Finally Eq.(2) becomes ;

$$\frac{da}{dN} = 5.5 \times 10^{-9} \times (\Delta K)^{3.0} \qquad ,(\text{mm / Cycle}) \tag{4}$$

Using the final fatigue crack growth analysis model given by Eqs.(3) and (4), the entire surface cracked tension data set of Incoloy 908 that included both testion and bending tests are predicted reasonably well, as shown in Fig 3.

Using the model for Incoloy 908, the fatigue life of test specimens in Table 2 was calculated.

The measured and calculated fatigue life to reach the final measured crack depth is shown to agree to each other with the maximum error of about 50%, as shown in Figure 4. The fact that Incoloy 908 behavior agrees well with the model in Ref.[4] suggests that the base metal has fairly uniform mechanical properties in both a- and c- directions.

3. Application to Fusion Magnet Design Analysis

ITER CDA Central Solenoid Design

In the ITER CDA, the fatigue life in the central solenoid conductor conduit was calculated by assuming an initial surface flaw with an aspect ratio (a/c) of 0.2. The design requires a total of 40,000 plasma pulse cycles. During each plasma pulse cycle, two tensile loading cycles are involved ; one associated with the pre-bias and the other with the end of burn(EOB). The stress during each loading cycle ranges between a peak value and a minimum of zero. The geometric and material properties of central solenoid conductor conduit used for the CDA analysis are listed in Table 3.

In order to examine the effect of evolving aspect ratio during crack growth on fatigue life, the calculation is made by applying the new correlations of Eqs.(3) and (4) while assuming Incoloy 908 as the conduit material. Although Eqs. (3) and (4) were obtained from the fatigue test at room temperature, these are applied to the magnet operation temperature of 4 K. As the fatigue crack growth rate of Incoloy 908 is lowered by a factor of two at 4 K, the use of room temperature model would result in pessimistic predictions[1]. The EOB stress is assumed to be 0.8 times the pre-bias stress. The results of calculation are compared for the case of a fixed and changing aspect ratio in Table 5. From these results, it is shown that the new model allowing the evolution of aspect ratio with crack growth predicted about two times the cycle life of the case with the constant aspect ratio. Therefore the realistic treatment of surface crack growth leads to a significant gain in the design life compared with the constant aspect ratio model.

ITER EDA Central Solenoid Design

In the ITER EDA(Engineering Design Activity), Incoloy 908 is assumed as the central solenoid conduit material, and other design parameters are listed in Table 4. It is evident that the BACS design significantly reduces stress and fatigue burdens. The design requirement of operational cycle is a 100,000 stress cycles that corresponds to a 50,000 plasma pulse cycles with a safety factor of 2. This value of cycle correspond to a 200,000 stress cycles when pre-bias stress and EOB stress are considered. In this case, EOB stress is also assumed to be 0.8 times the pre-bias stress as in the previous CDA case. The results of predicted conduit lifetime is shown in Table 5. When the aspect ratio is assumed to remain constant during the crack growth, the predicted fatigue life is about 180,000 cycles. When the aspect ratio evolution is taken into account using Eqs. (3) and (4), the life is predicted to be about 395,000 cycles. The new prediction, thus, shows that the design requirement of ITER EDA is satisfied with a significant margin, with the BACS design.

5. Conclusion

Fatigue behavior of surface cracks in a superconductor conduit material, a Ni-Fe superalloy, is predicted based on an empirical model that takes account of the evolution of crack shape during the crack growth. The model predicts that the aspect ratio (a/c) of surface flaws asymptotes to 1.0, i.e., to a semi-circular geometry under the cyclic tension loading during plasma pulse cycling of fusion magnets. The measured fatigue lives of Incoloy 908 surface cracked tension specimen agree well with the model prediction within a factor of two. The results implicate that fatigue life can be predicted at the greater accuracy by taking into account of evolving aspect ratio with fatigue crack growth. The consideration of the aspect ratio evolution of surface crack during fatigue cycle results in an increase in the calculated cycle life of the conduit material by more than a factor of two, when applied to the central solenoid magnet design for the International Thermonuclear Experimental Reactor (ITER). Nevertheless the Bucked Against Central Solenoid(BACS) design is required to meet the

ITER design requirement on fatigue life.

Acknowledgement

Authors would like to express their deep gratitude to the Korea Science and Engineering Foundation for the financial support.

References

[1] R.L. Tobler, I.S. Hwang and M.M. Steeves, Fracture Mechanics Behavior of a Ni-Fe Superalloy Sheath for Superconducting Fusion Magnet, Part I : property measurement, submitted to Fusion Engineering and Design, 1995

[2] L.S. Toma, I.S. Hwang, M.M. Steeves, and R.N. Randall, Thermomechanical Process Effects on Hardness and Grain Size in Incoloy Alloy 908, Adv. Cryo. Eng. Maters., Vol. 40(1994) 1307-1314.

[3] IAEA, ITER Magnet System, ITER Document Series No.26 ,1990

[4] J.C. Newman, Jr. and I.S. Raju, An Empirical Stress-Intensity Factor Equation for the Surface Crack, Eng. Fract. Mechs., Vol. 15, 185-192, 1981.

[5] K. Nishioka, K. Hirakawa and I. Kitaura, Fatigue Crack Propagation Behaviors of Various Steels, Sumimoto Search No. 17, 39-55, 1977.

[6] D.L. Corn, A Study of Cracking Techniques for Obtaining Partial Thickness Cracks of Pre-selected Depths and Shapes, Eng. Fract. Mechs., Vol. 3, 45-52, 1971.

[7] J.G. Merkle, A Review of Some of the Existing Stress-Intensity Factor Solution for Part-through Surface Cracks, U.S.Atomic Energy Commision ORNL-TM-3983, 1973.

[8] A. Nyilas, Fatigue Charaterization of Jacket Materials at 4 K, KfK Report on NET Study Contract 89-201, 1990.

[9] T.W. Orange, Fractire Testing with Surface Crack Specimens, Journal of Testing and Evaluation, Vol 3, No. 5, 335-342, Sep. 1975

[10] N. Mitchell, Fatigue Assessment of the Structural Steel in Superconducting Coils for Tokamaks, Fus. Eng. Des., Vol.19(1992) 225-233.

[11] Z. Mei, C.R. Krenn, and J.W. Morris, Jr, Initiation and Growth of Small Fatigue Cracks in a Ni-Base Superalloy, Metall. Trans. A, vol 26A(1995) 2063-2073.

Table 1. Surface cracked tension test results for a wide range of aspect ratio.

Spec. NO.	Fatigue Loading Type	Initial a(mm)	Initial 2c(mm)	Final a(mm)	Final 2c(mm)	Thickness t(mm)	Width b(mm)	Fatigue Loading (kN)
#201	Tension	0.89	1.76	1.218	2.55	5.850	12.295	35.6
#202	Tension	0.864	1.778	1.396	3.15	5.80	12.725	26.7
#203	Tension	0.864	1.804	1.854	4.266	6.275	12.700	29.8
#204	Tension	0.864	1.778	2.996	6.552	6.250	12.700	26.7
#205	Tension	N/A	N/A	N/A	N/A	6.225	12.675	35.6
#206	Bending	0.127	2.54	1.320	4.038	6.350	12.700	3.0
#207	Bending	0.127	2.54	1.778	4.826	6.150	12.675	3.0
#208	Tension	0.127	2.49	0.864	2.972	5.925	12.675	35.6

Table 2. Test data for two tension fatigue test(specimen #203 and #204) conducted at 10 Hz and R=0.1 at room temperature.

Specimen #203			Specimen #204		
Point	Cycles,N (Number)	Crack Length 2c,(mm)	Point	Cycles,N (Number)	Crack Length 2c,(mm)
1.	16,000	not yet	1.	25,000	not yet
2.	21,000	1.84	2.	41,000	2.73
3.	26,000	2.64	3.	55,000	3.24
4.	30,000	2.80	4.	71,000	3.99[A]
5.	35,000	2.88	5.	82,000	4.10
6.	42,000	3.44	6.	92,000	4.41
7.	47,000	3.60	7.	100,000	5.38
8.	51,000	4.00	8.	105,000	5.66
9.	53,000	4.08	9.	111,0000	6.55
10.	55,000	4.27	ANOTE : load pin break/replaced here		

Table 3. Geometric and material properties of the Central Solenoid conduit used in the fatigue calculation for ITER CDA design.

Parameter	**Used data**
Material	Incoloy 908
Material Condition	Base metal, reaction heat treatment 650 °C/200h
Conduit Thickness	3 mm
Conduit External Width	30 mm
Fatigue Peak Load (R-ratio)	450 MPa (0)
Initial Crack Shape	Semielliptical surface flaw under pure Mode I loading
Initial Crack Size	a = 0.15 mm c = 0.75 mm
Fatigue analysis safety factor on lifetime	2

Table 4. Geometric and material properties of the Central Solenoid conduit used in fatigue calculation for the ITER EDA design.

Parameter	**Used data**
Material	Incoloy 908
Material Condition	Base metal, reaction heat treatment 650 °C/200 h
Conduit Thickness	5.5 mm
Conduit External Width	50.5 mm
Fatigue Peak Load (R-ratio)	238.3 MPa (0.188)
Initial Crack Shape	Semielliptical surface flaw under pure Mode I loading
Initial Crack Size	a = 0.275 mm c = 1.375 mm
Fatigue analysis safety factor on lifetime	2
Fracture analysis safety factor on K_{Ic}	1.5

Table 5. Results of calculated fatigue life of the Central Solenoid conduit for ITER CDA and EDA design.

Calculation Method	**CDA**		**EDA**	
	allowable plasma pulse cycle	allowable CS-pulse cycle	allowable plasma pulse cycle	allowable CS-pulse cycle
Design requirement (considering safety factor of 2)	80,000	160,000	100,000	200,000
constant aspect ratio model (a/c=0.1)	21,000	42,000	180,000	360,000
Present model ($(a/c)_i$=0.1)	45,000	90,000	395,000	790,000

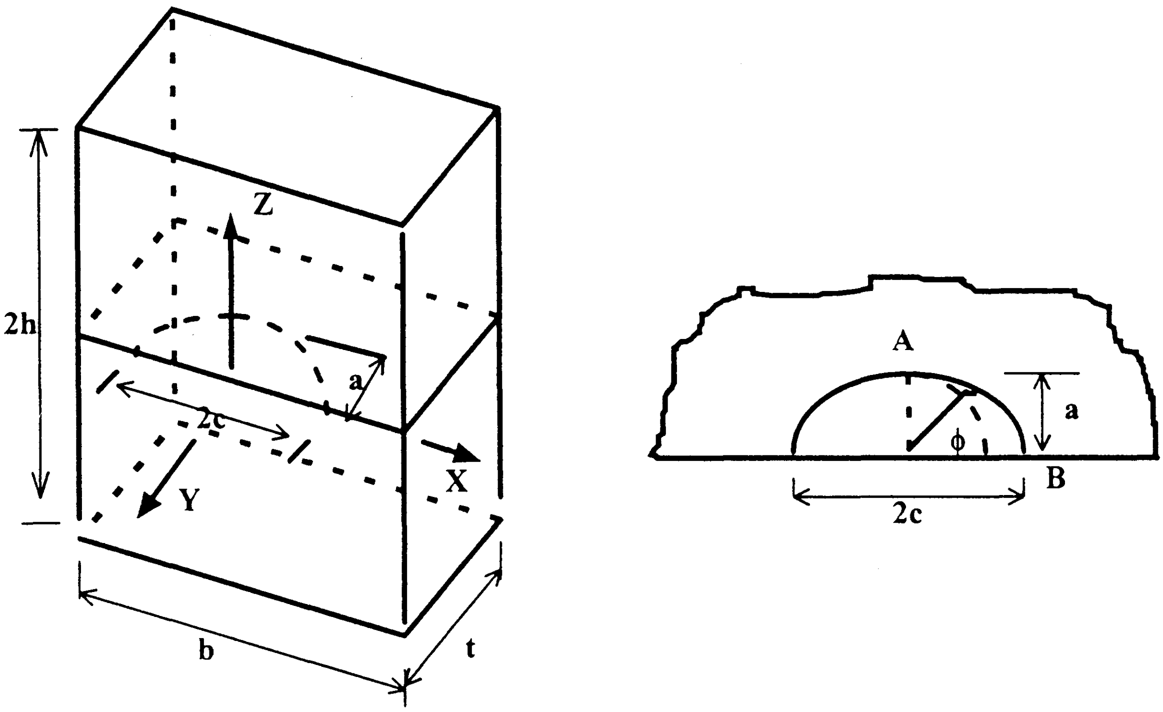

Fig. 1 Surface flaw with a semi-elliptical geometry in finite plane.

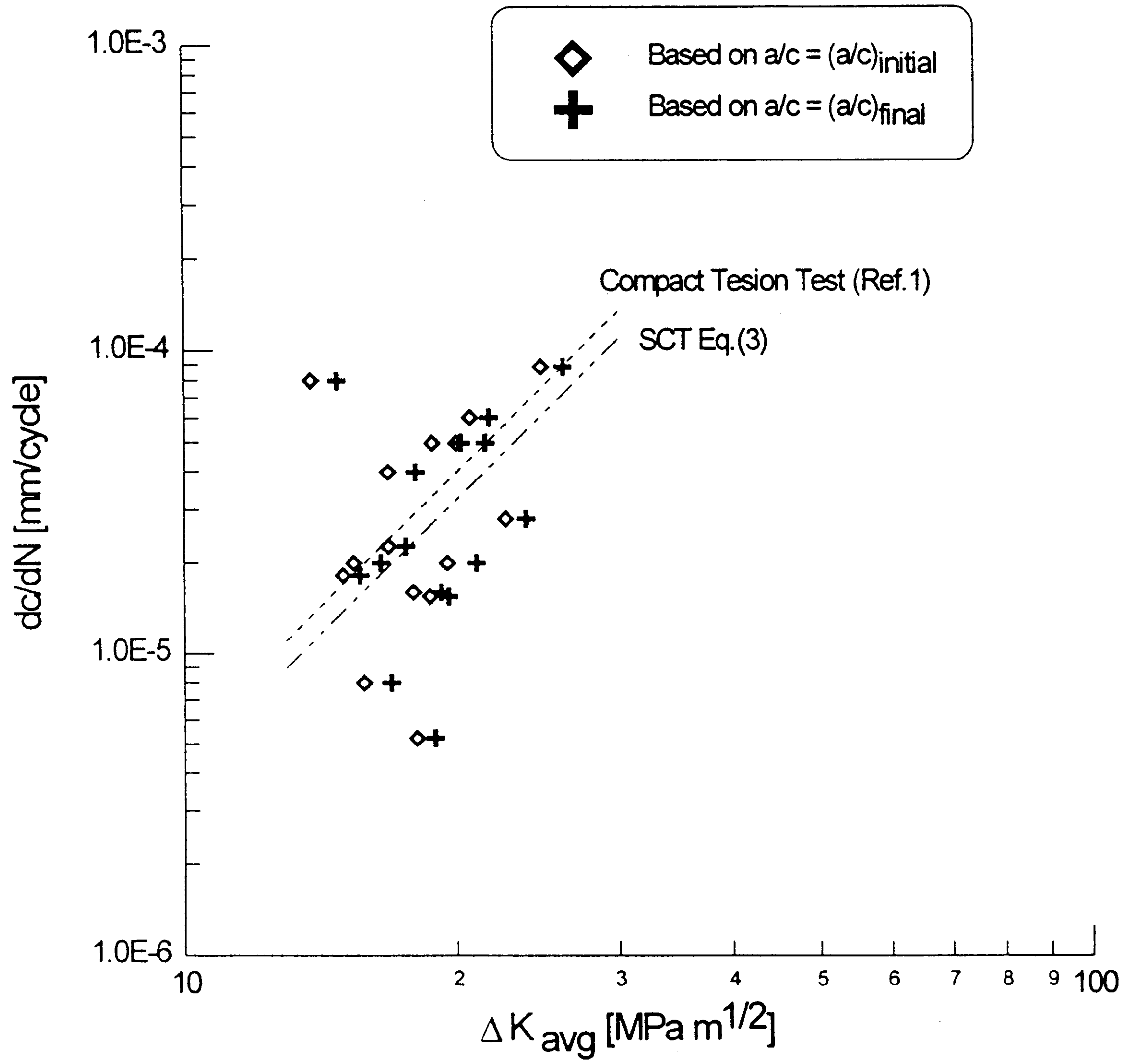

Fig. 2 Crack growth rate in transverse direction vs. Stress intensity factor and predicted power-law curve for SCT specimen #203 and #204 and Paris law correlation of compact specimens obtained for Incoloy 908 at room temperature.

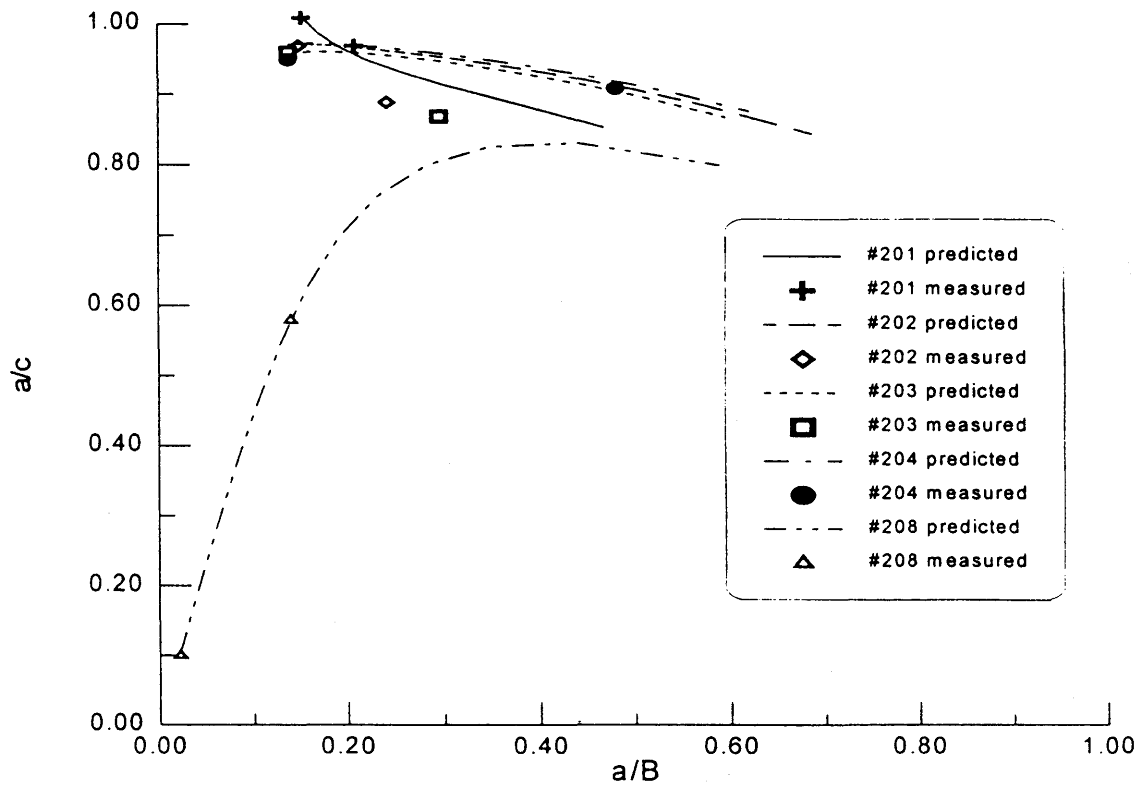

(a)

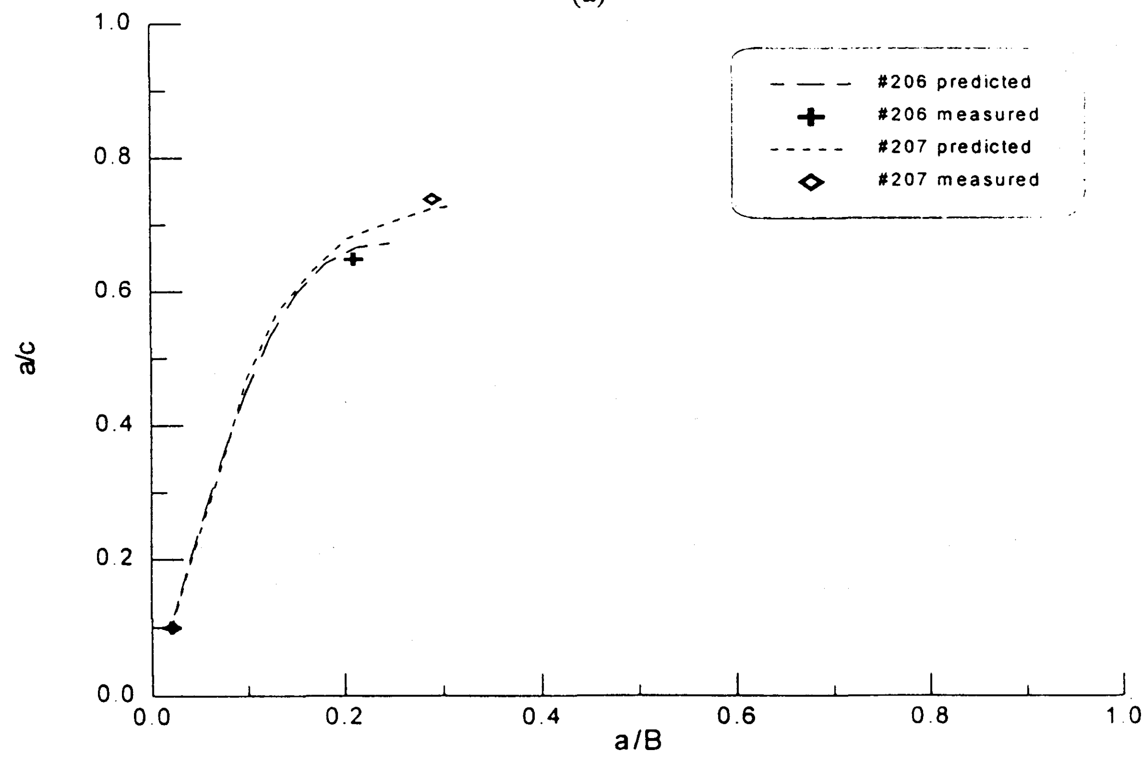

(b)

Fig. 3 Changes of aspect ratios with crack growth as predicted by the optimized α for specimens under (a) pure tension load and (b) pure bending load.

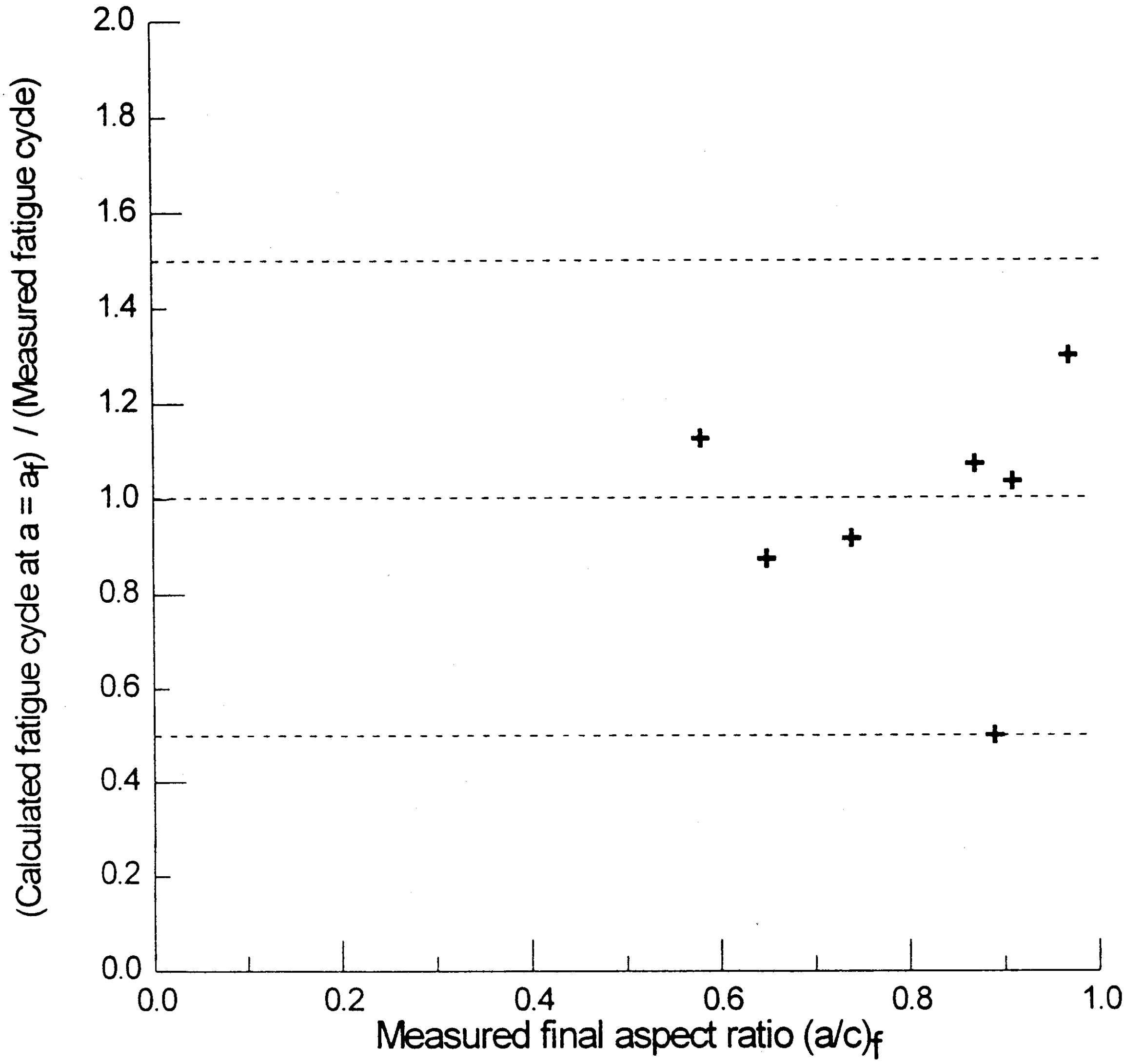

Fig. 4 The ratio of a calculated fatigue life to a measured fatigue life to the final crack depth, a_f for all specimens of Table 1.

7 Study on the Effect of the Crack Length on the J_{IC} Value

M. Kikuchi* (Science Univ. of Tokyo)

STUDY ON THE EFFECT OF THE CRACK LENGTH ON THE J_{IC} VALUE

Masanori Kikuchi
Science University of Tokyo, Noda, Chiba, 278, Japan

ABSTRACT

The ductile fracture tests are carried out using CT specimen, three point bend specimen and CCT specimens made of A533B steel and Aluminum alloy with different crack lengths. It is shown that the apparent J_{IC} value increases due to the decrease of the crack tip constraint. It is pointed out that the increase of the apparent J_{IC} value is partly due to the error of the conventional equation to estimate the J value. Based on the FEM analyses, these apparent J_{IC} values are corrected and are compared with the valid J_{IC} values. The good co-relation between apparent J_{IC} value and the Q factor, proposed by O'Dowd and Shih, is shown for every specimens.

1. Introduction

The J integral concept is one of the most important parameters in the elastic-plastic fracture mechanics. The HRR solution[1,2] gives the theoretical basis for the J integral fracture criterion. It means that when the crack tip stress fields agree with the HRR solution, the J integral is the dominant parameter which describes the stress, strain and displacement fields at the crack tip uniquely.

By the authors previous papers[3,4], it has been shown that the crack tip stress fields don't agree with HRR solutions well in many cracked plates. In such cases, the J integral is not a unique dominant parameter and the fracture criterion may become different. It is called the constraint effect. O'Dowd and Shih [5,6] proposed Q factor as the second term, which corresponds to the stress triaxiality at the crack tip. Anderson [7], Jun [8], and Nikishikov [9] also proposed other parameters which improves the estimation of the crack tip fields in the elastic-plastic fields, respectively.

In this paper, the fracture toughness tests of A533B steel and Aluminum alloy specimens are conducted using several kinds of specimen configurations and crack lengths. The effect of the initial crack length on the apparent fracture toughness is studied. Then the finite element analyses are conducted and the crack stress fields are compared with HRR solutions. The apparent fracture toughness values are corrected based on the numerical results, and the relation between Q factor and the corrected apparent fracture toughness is obtained.

2. Fracture toughness tests.

Figure 1 shows the shapes and sizes of the test specimens made of A533B steel. The three point bend specimen is made in three cases with different initial crack lengths. They are changed in a/W=0.1, 0.3 and 0.55. In the CCT specimen, the crack length is changes in two cases, as 2a/W=0.4 and 0.6. The same three point bend specimens are made by Aluminum alloy 2025-T6. The crack length is also changed in three cases as same as Fig.1. The CT specimens with a/W=0.3 and 0.6 are also made by the same aluminum alloy. The mechanical properties of these two materials are shown in Table 1. Both materials show ductile behaviors at fracture.

The fracture toughness tests are conducted based on the JSME testing standards[10]. As there is no testing standard for CCT specimen, the similar method as CT and three point bend specimens are applied to this specimen. The JIC value is defined as the J value at the initiation of the stable crack growth. The results of every specimens for both materials are shown in Table 2. As they don't show the constant value for each material, they are called the apparent J_{IC} value, J_{IC}^{ap}. The JSME standard states that the valid J_{IC} value should satisfy the following two conditions.

$$b \geq 25\frac{J_{IC}^{ap}}{\sigma_{fs}} \qquad (1)$$

$$B \geq 25\frac{J_{IC}^{ap}}{\sigma_{fs}} \qquad (2)$$

Where b is the ligament length and σ_{fs} is the flow stress. In the A533B specimens, the three point bend specimen with a/W=0.55 satisfies these conditions, and in aluminum alloy specimens, three point bend specimen with a/W=0.55 and CT specimen with a/W=0.6 satisfy these conditions. Then the valid J_{IC} values are determined as 135kN/m for A533B steel, and 6.5kN/m for aluminum alloy, respectively. It is noticed that other JICap values are much larger than the valid values for both materials. As the initial crack length becomes small, the apparent J_{IC} value becomes larger. In both CCT specimens, the J_{IC}^{ap} values of two specimens are nearly equal to each other, and both values are about 1.37 times larger that the valid one. The effect of the initial crack length is not recognized.

The increase of J_{IC}^{ap} values by the decrease of the initial crack length is important for the application of the fracture mechanics to the practical problems. In the real structure, almost all of the real cracks are shallow surface cracks. The crack length of them are comparatively smaller than the thickness of the plate. The constraint effect is inevitable. Then the method to estimate the apparent increase of the J_{IC} value is preferable.

3. Microscopic observation of dimple fracture of Aluminum alloy specimen.

In the 2025-T6 aluminum alloy specimen, the ductile fracture occurs due to the nucleation, growth and coalescence of voids. Clear dimple patterns are observed on the fracture surface, as shown in Figure 2. This is the fracture surface of CT specimen with a/W=0.1. The diameter of these dimples are measured. The results are shown in Table 3. In this table, number N means the number of dimples in $0.12mm^2$ area at the crack tip and at midpoint of the specimen. In every specimens, the number of dimples and average dimple diameters are nearly same values.

Then the diameters of preceding voids are also measured. Preceding voids are the void nucleated at the crack tip just before the dimple fracture, as shown in Figure 3. Crack growth occurs by the coalescence of these preceding voids. The diameter of a preceding void indicates the critical value of void coalescence, which is one of the important parameters for the dimple fracture. They are nucleated in front of the crack tip during stable crack growth. They are observed by introducing a fatigue cracking after stable crack growth test. Figure 4 shows the photo of preceding voids. They are observed independently on the fatigue crack surface. Their number and diameters in $0.12mm^2$ area at the crack tip are also measured. The results are shown in Table 4. Similar to Table 3, these values are nearly same for every specimens.

The results of Tables 3 and 4 show that these microscopic fracture process as void nucleation, growth and coalescence, are not affected by the change of the initial crack length. It means that the microscopic dimple fracture mechanism does not change due to the change of the constraint at the crack tip. The constraint effect appears only on the macroscopic parameters as J integral.

4. Numerical analyses by FEM.

The elastic-plastic FEM analyses are conducted for these three types of specimens. Figure 5 is an example of the numerical model of 3PB specimen. By the symmetry of the structure, a quarter part of the whole specimen is analyzed. As the pre-crack is introduced by the fatigue loading, the crack front configuration has some curvature. It's shape ia measured in the experiment and is used in the FEM modelling.

The stress-strain relations of these two metals are approximated by the following equation.

$$\varepsilon = \frac{\sigma}{E} \qquad for \;\; \sigma \le \sigma_0$$
$$\varepsilon = \frac{\sigma}{E} + \left\{ \left(\frac{\sigma}{E'}\right)^n - \left(\frac{\sigma_0}{E'}\right)^n \right\} \qquad for \;\; \sigma \ge \sigma_0 \qquad (3)$$

Where σ_0 is the yield stress, E' and n are constants. They are determined as E'=400Mpa, n=7 for aluminum alloy, and 1055Mpa and 7 for A533B steel, respectively. These relations are also approximated by the Ramberg-Osgood type equations.

$$\frac{\varepsilon}{\varepsilon_0} = \frac{\sigma}{\sigma_0} + \alpha\left(\frac{\sigma}{\sigma_0}\right)^n \qquad (4)$$

Where α and n are 1.48 and 8 for Aluminum alloy, and 4.1 and 8 for A533B steel, respectively. They are used to calculate HRR fields at the crack tip.

4.1 Crack tip stress field.

Figure 6 shows the crack tip stress fields of 3PB and CT specimens made of A533B steel. They are the results at the midplane of the specimen thickness when the J integral at this location is nearly 135 kN/m, the valid J_{IC} value. The solid line is the HRR solution. The stress field of 3PB specimen with a/W=0.55 agrees well with HRR solution. It is reasonable because this specimen gives the valid JIC value. As the a/W value decreases, the crack tip stress deviates from the HRR solution gradually. In the CCT specimens, the crack tip stresses of both specimens with different 2a/W values agree well, and both are largely different from HRR solution. Obviously, these deviations of the stress fields from HRR solution have relations with the apparent increase of JIC values in these specimens.

O'Dowd and Shih proposed Q factor as the second parameter for the crack tip stress field, which is defined by the next equation.

$$Q = \frac{\sigma_{\theta\theta} - (\sigma_{\theta\theta})_{HRR}}{\sigma_0} \qquad at \;\; r = \frac{2J}{\sigma_0}, \;\; \theta = 0^\circ \qquad (5)$$

Where $(\sigma_{\theta\theta})_{HRR}$ is the $\sigma_{\theta\theta}$ by the HRR solution, and r is the distance from the crack tip. Q factor is calculated and is shown in Figure 7. It shows the Q factor distribution along the crack front. In every specimens, the absolute value of Q is small in the center of the specimen and increases near the free surface. The largest Q value is given by CCT specimens.

4.2 Correction of J_{IC}^{ap} value.

The J value is evaluated using the conventional equation in the

experiment. They are:
for 3PB and CT specimens,

$$J = \frac{(1 - \nu^2)}{E}K^2 + \frac{\eta A_{pl}}{Bb} \tag{6}$$

and for CCT specimen,

$$J = \frac{(1 - \nu^2)}{E}K^2 + \frac{1}{Bb}\left(\int_0^{\Delta} P d\Delta - \frac{P\Delta}{2}\right) \tag{7}$$

where the first term is the elastic part, and the second term is the plastic part of the J integral, respectively. The first term is evaluated by the stress intensity factor by referring the Handbook[11], and the second term is obtained by the load-displacement record obtained experimentally. η in equation (6) is the constant defined by the specimen configuration. Originally, these equations are used for the deep cracked specimen. In this study, short cracked specimens are used. Then the numerical error of the J integral due to these conventional equations should be evaluated. The J integral is evaluated using eqs.(6) and (7) based on the load-displacement relation obtained by the numerical analyses, and they are compared with those by the contour integration. The results of A533B steel specimens are shown in Figure 8. The ordinate is the J by the contour integration and the abscissa is the J by the conventional equation. Both J values of deep cracked 3PB specimens agree very well. But the results of short cracked 3PB and CCT specimens show that both values are different from each other largely. It is considered that the contour integration gives the correct J value. It means that the J value is not correctly evaluated by the conventional equation for these specimens. Then the experimental J_{IC}^{ap} values are corrected using these results. The J_{IC}^{ap} value of 3PB specimen with a/W=0.1 is 339 kN/m, which corresponds to 222 kN/m by the contour integration. By the similar way, every J_{IC}^{ap} values are corrected and the results are shown in Table 5. The J_{IC}^{ap} values of aluminum alloy specimens are also corrected. As noticed by this Table, the valid J_{IC} value changes little by this correction, and other values change largely.

The relation between the corrected J_{IC}^{ap} value and the Q factor is shown in Figure 9. The J_{IC}^{ap} value is normalized by the valid J_{IC} value of each material. It is noticed that the relations of two metals are very similar to each other. Though some amount of data scatter exist, they are approximated by a single line. Of course, the number of data is not enough. But this result suggests that by obtaining enough data, we could estimate the J_{IC}^{ap} value from the Q value. The problem is that we should conduct FEM analyses for calculating Q factor. But recently, the computer capacity has developed rapidly, and it is not difficult now to conduct three dimensional elastic-plastic analysis using adequately fine mesh pattern. For this goal, the data of shallow surface crack problem are needed. This is our future target.

5. Concluding remarks.

The J dominant crack tip fields do not exists in many practical crack problems, and the J integral is not the unique fracture parameter in these problems. It seems the relation between J_{IC}^{ap} value and Q factor enables to estimate the J_{IC}^{ap} value for these cases. Other methods proposed by other authors[7-9] should also be studied from the practical viewpoint. So far, the new and reliable fracture criterion has not been proposed yet. For the establishment of new fracture criterion, the mechanisms of the dimple fracture should be studied more precisely. Then many researchers' corporation concerning experimental, theoretical and numerical studies may be needed.

References

[1] JW. Hutchinson, J. Mech. Phys. Solids, vol.16 (1968), pp.13-31
[2] J.R. Rice and G.F. Rosengren, Ibid, vol.16 (1968), pp.1-13
[3] M. Kikuchi, Int. J. Fracture, vol.58 (1992), pp.273-283
[4] M. Kikuchi, Int. J. Pressure Vessel and Piping, 63 (1995), PP.315-326
[5] N.P. O'Dowd and C.F. Shih, J. Mech. Phys. Solids, vol.39, No.8 (1991), pp.989-1015
[6] N.P. O'Dowd and C.F. Shih, Ibid, vol.40, (1992), pp.939-963
[7] T.L. Anderson, Int. J. Fracture, vol.41 (1989), pp.79-104
[8] S. Jun, Engineering Fracture Mechanics, vol.44 (1993), pp.789-806
[9] G.P. Nikishkov, A. Bruckner-Foit and D. Munz, Engineering Fracture Mechanics, vol.52, N.4 (1995), pp.685-701
[10] JSME S-001, Standard Method of Test for Elastic-Plastic Fracture Toughness J_{IC} (Supplement, 1st Edition), (1992)
[11] Y. Murakami et al., STRESS INTENSITY FACTORS HANDBOOK, Pergamon Press

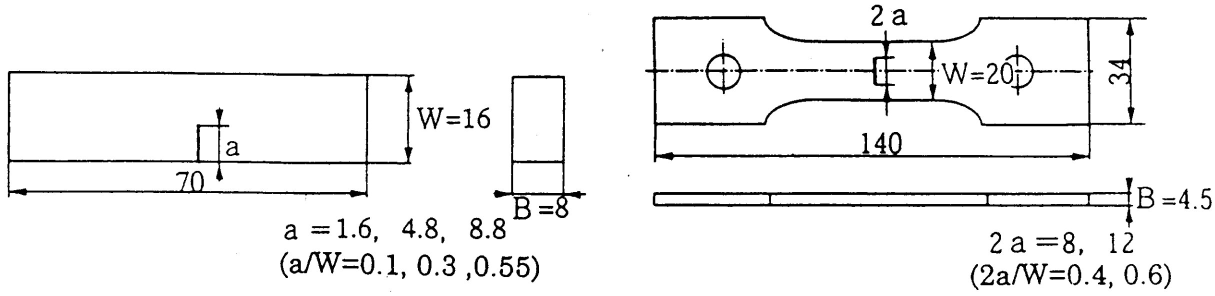

Three-point-bend (3PB) specimen

CCT specimen

Fig.1 Shapes and sizes of the test specimens made of A533B steel

Table 1 Mechanical properties

Material	Yield stress	Tensile Strength	Flow stress	Young's Modules
A533B	599MPa	720MPa	660MPa	206GPa
2025-T6	27.4MPa	387MPa	331MPa	27.4GPa

Table 2 Apparent Fracture Toughness values

	Three Point Bend			C T		CC T	
Crack length／Specimen Width	0.1	0.3	0.55	0.3	0.6	0.4	0.6
A533B J_{IC}^{ap} (kN/m)	339	239	135	------	------	185	186
2025-T6 J_{IC}^{ap} (kN/m)	16.7	8.6	6.4	7.5	6.5	------	-----

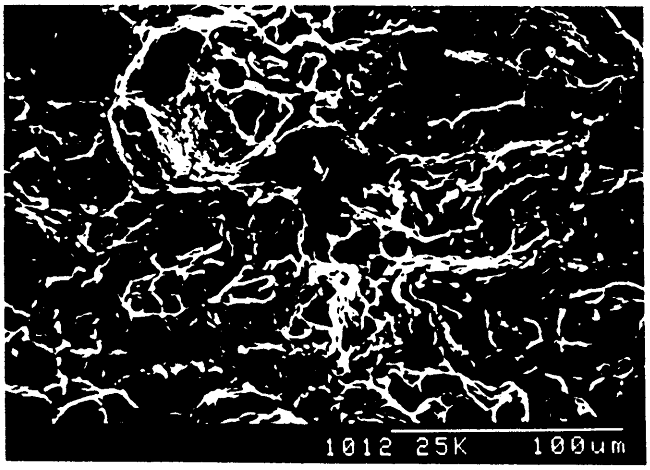

Fig.2 Dimple Fracture Surface (2025-T6)

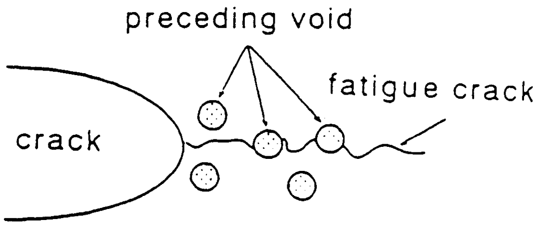

Fig. 3 Preceding Voids

Fig. 4 Photo of Preceding Voids (2025-T6)

Table 3 Number and Diameter of Dimples (2025-T6, 3PB)

a/W	N	D_0 (mm)
0.1	570	0.00724
0.3	555	0.00744
0.55	535	0.00749

Table 4 Number and Diameter of Preceding Voids (2025-T6,3PB)

a/W	N	D_0 (mm)
0.1	115	0.00462
0.3	128	0.00459
0.55	133	0.00452

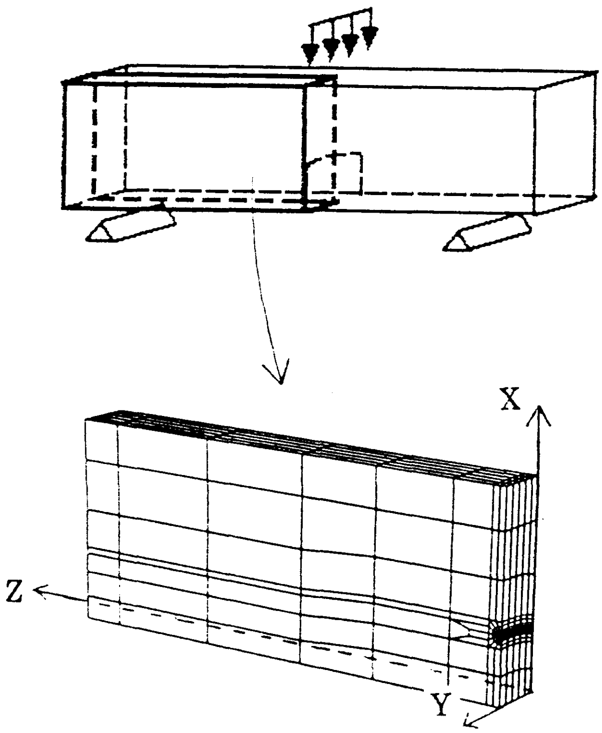

Fig. 5 Example of the Numerical Model of 3PB Specimen

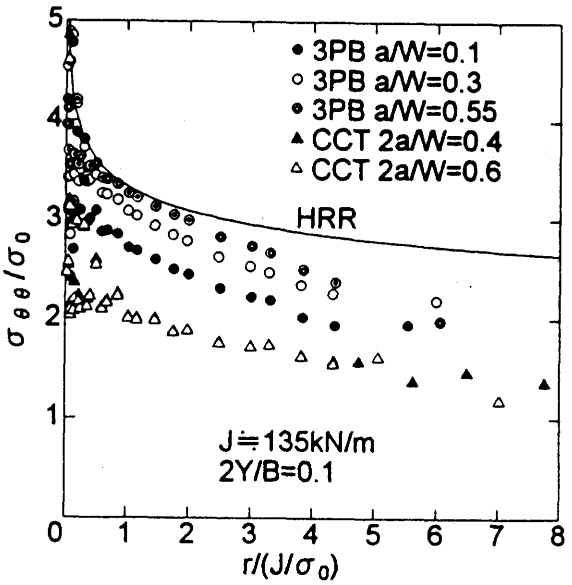

Fig. 6 Crack Tip Stress Fields of 3PB and CCT specimens made of A533B steel

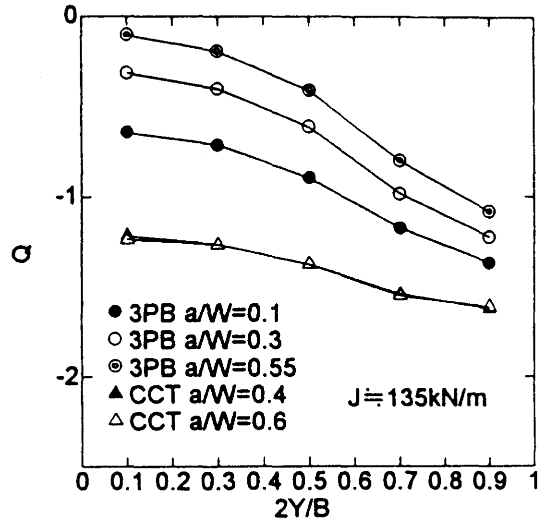

Fig. 7 Distributions of Q Factor at the Crack Tip (A533B steel)

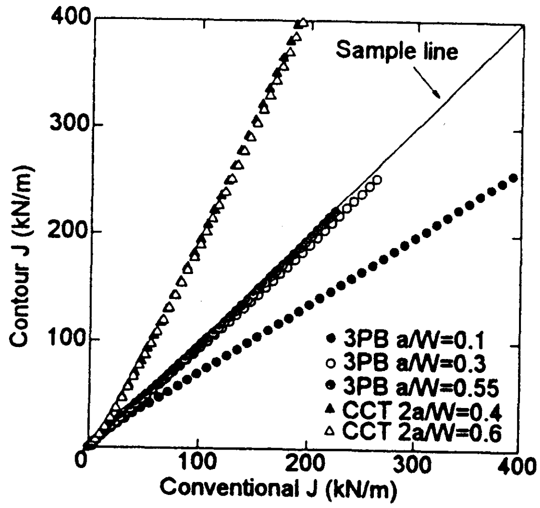

Fig. 8 Relation between J by the contour integration and J by the conventional equation

Table 5 Corrected Fracture Toughness values

	Three Point Bend			C T		CC T	
Crack length／Specimen Width	0.1	0.3	0.55	0.3	0.6	0.4	0.6
A533B J_{IC}^{ap} (kN/m)	222	228	130	------	------	392	387
2025-T6 J_{IC}^{ap} (kN/m)	8.2	8.0	6.3	7.8	6.6	------	-----

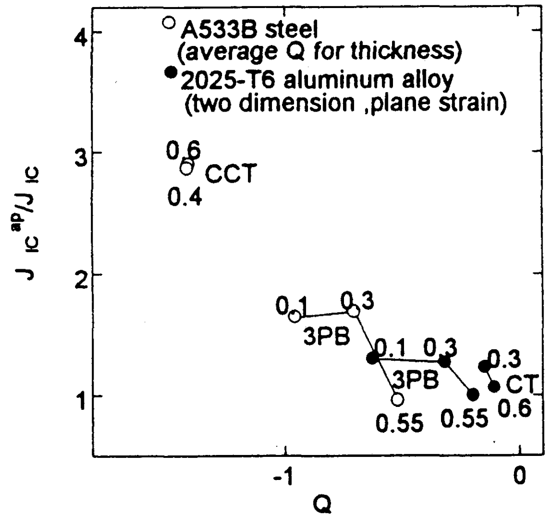

Fig. 9 Relation between Corrected J_{IC}^{ap} Value and Q Factor

8 Development of New Z-factors for the Evaluation of the Circumferencial Surface Crack in Nuclear Pipings

Y.H. Choi*, Y.K. Chung, Y.W. Park, J.B. Lee (KINS),
G. Wilkowski (Battelle Memorial Institute)

Development of New Z-Factors for the Evaluation of the Circumferential Surface Crack in Nuclear Pipings

Y. H. Choi*, Y. K. Chung*, Y. W. Park*, J. B. Lee* and G. Wilkowski**

(*) Korea Institute of Nuclear Safety, Korea
(*) Battelle Memorial Institute, USA

Abstract

The purpose of this study is to develop new Z-Factors to evaluate the behavior of a circumferential surface crack in nuclear pipings. Z-Factor is a load multiplier used in the Z-Factor method, which is one of the ASME Code Sec. XI's recommendations for the estimation of a surface crack in nuclear pipings. It has been reported that the load carrying capacities predicted from the current ASME Code Z-Factors, are not well in agreement with the experimental results for nuclear pipings with a surface crack. In this study, new Z-Factors for ferritic base metal, ferritic Submerged Arc Welding(SAW) weld metal, austenitic base metal, and austenitic SAW weld metal are obtained by use of SC.TNP method based on GE/EPRI method. The desirability of both the SC.TNP method and the new Z-Factors is examined using the results from 48 pipe fracture experiments for nuclear pipings with a circumferential surface crack. The results show that the SC.TNP method is good for describing the circumferential surface crack behavior and the new Z-Factors are well in agreement with the measured Z-Factors for both ferritic and austenitic pipings.

1. Introduction

In the design stage of pipings in nuclear power plants, it is assumed that there is no crack in the pipings.[1] There, however, are many micro-cracks in nuclear pipings because of material inhomogeneity and welding process problems. During plant operation, some micro-cracks may grow into surface cracks and/or through-wall cracks which give adverse effect on piping integrity.

ASME Boiler & Pressure Vessel Code Sec. XI "Rules for Inservice Inspection of Nuclear Power Plant Components" (hereafter we denote this code as ASME Code.) requires the safety evaluation of cracks which are detected during inservice inspection.[2-4] The Z-Factor method is one of the ASME Code's recommendations to evaluate the behavior of a circumferential surface crack in nuclear pipings. The Z-Factor is a load multiplier to compensate plastic load with elasto-plastic load. It has been reported that the load carrying capacities predicted from the ASME Code Z-Factor method are not well in agreement with the experimental results for nuclear pipings with a surface crack.[5-7] The reason for the disagreement is that the current ASME Code Z-Factors are not exact to predict the surface crack behavior in nuclear pipings.[7]

The purpose of this study is to develop new Z-Factors to evaluate the behavior of a circumferential surface crack in nuclear pipings. Many crack evaluation methods[5-17] such as J integral method including GE/EPRI method[5-7, 11-17], R6 method[8], and DPFAD method[9-10] have been proposed to describe the surface crack behavior in pipings. In this study, the SC.TNP method[14-16], which is based on the GE/EPRI method, is used to develop new Z-Factors for ferritic base metal, ferritic Submerged Arc Welding(SAW) weld metal, austenitic base metal, austenitic Gas Tungsten Arc Welding(GTAW) weld metal, austenitic Gas Metal Arc Welding(GMAW) weld metal, and austenitic SAW weld metal.

The desirability of both the SC.TNP method and the new Z-Factors is examined using the results from 48 pipe fracture experiments for nuclear pipings with a circumferential surface crack.[5-7]

2. ASME Code Z-Factor Method

In the ASME Code, the following criterion is specified for a circumferential surface crack in ferritic and austenitic pipings.

$$P_b \le S_c \,, \tag{1}$$

where P_b and S_c are the applied stress and the allowable stress respectively. The allowable stress, S_c, is determined by the ASME Code Z-Factor method as

$$S_c = \frac{1}{(SF)}\left(\frac{P'_b}{Z} - P_e\right) - P_m\left(1 - \frac{1}{Z(SF)}\right) , \tag{2}$$

where P'_b, P_e, P_m, and (SF) are the bending stress at incipient plastic collapse, the thermal stress (P_e = 0 for austenitic pipings), the membrane stress, and the safety factor. The above equation is basically similar to the equation of limit load method in the ASME Code. The Z-Factors in Eq. (2) for the ferritic and austenitic pipings are given in the ASME Code as follows : (Hereafter we denote Zasme for the Z-Factor given in the ASME Code.)

<u>Ferritic Base Metal</u>

$$Zasme\text{-}1 = 1.20\ [1 + 0.021 \cdot A \cdot (OD - 4)] \tag{3}$$

<u>Ferritic SAW Weld Metal</u>

$$Zasme\text{-}2 = 1.35\ [1 + 0.0184 \cdot A \cdot (OD - 4)] \tag{4}$$

<u>Austenitic Base Metal and GTAW/GMAW Weld Metals</u>

$$Zasme\text{-}3 = 1.0 \tag{5}$$

<u>Austenitic SAW Weld Metal</u>

$$Zasme\text{-}4 = 1.30\ [1 + 0.010 \cdot (OD - 4)] \,, \tag{6}$$

where OD is the pipe outside diameter(inches). The A in Eqs. (3) and (4) is a function of R_m/t, which is the ratio of the pipe mean radius(R_m) to the pipe wall thickness(t), given as (we denote Aasme for the A given in the ASME Code)

$$Aasme = [0.125\left(\frac{R_m}{t}\right) - 0.25]^{0.25} \qquad : \quad 5 \le \left(\frac{R_m}{t}\right) \le 10 \qquad (7)$$

$$= [0.4\left(\frac{R_m}{t}\right) - 3.0]^{0.25} \qquad : \quad 10 \le \left(\frac{R_m}{t}\right) \le 20 \quad . \qquad (8)$$

As seen in Eqs. (3)-(8), both Zasme-1 and Zasme-2 are functions of the pipe outside diameter and R_m/t, while Zasme-4 is a function of the pipe outside diameter only. The value of Zasme-3 is 1 because fully plastic behavior is assumed for the austenitic base metal and GTAW/GMAW weld metal.

3. Development of New Z-Factors

3.1 Definition of Z-Factor

The Z-Factor as a load multiplier is defined as

$$Z = \frac{M_L}{M_{EP-\max}} \quad , \qquad (9)$$

where M_L and $M_{EP\text{-}max}$ are the limit load under fully plastic condition and the maximum load under elasto-plastic condition respectively.

The limit load for a circumferential surface crack, M_L, under fully plastic condition is given as [2]

(1) $\theta + \beta \le \pi$

$$M_L = 2\,\sigma_f\,R_m^2\,t\left\{2\sin\beta - \left(\frac{a}{t}\right)\sin\theta\right\} \qquad (10)$$

$$\beta = \left\{\pi - \left(\frac{a}{t}\right)\theta - \pi\left(\frac{P_m}{\sigma_f}\right)\right\} \qquad (11)$$

(2) $\theta + \beta > \pi$

$$M_L = 2\,\sigma_f\,R_m^2\,t\left\{2 - \frac{a}{t}\right\}\sin\theta \qquad (12)$$

$$\beta = \frac{\pi}{2 - \frac{a}{t}}\left\{1 - \frac{a}{t} - \frac{P_m}{\sigma_f}\right\} \quad , \qquad (13)$$

where θ is the half crack length, β is the angle from (-)y-axis to neutral plane, σ_f is the flow stress, and a is the crack depth. The cross section geometry of piping with a circumferential surface crack is shown in Fig. 1. P_m in Eqs. (11) and (13) is the stress due to the pipe internal pressure (p), given by

$$P_m = p \frac{R_i^2}{(R_o^2 - R_i^2)} \quad , \tag{14}$$

where R_i and R_o are the pipe inside radius and the pipe outside radius respectively.

The maximum load under elasto-plastic condition, $M_{EP\text{-}max}$, is obtained from the SC.TNP method as following section.

3.2 Determination of $M_{EP\text{-}max}$ using SC.TNP Method

As mentioned above, many methods such as the J integral method including GE/EPRI method[5-7, 11-17], R6 method[8], and DPFAD method[9-10] have been proposed to describe the circumferential surface crack behavior in pipings under elasto-plastic condition. Based on the GE/EPRI method, Ahmad et al.[15-16] proposed SC.TNP method(Surface Crack for ThiN Pipe) to evaluate the circumferential surface crack behavior.

In the SC.TNP method based on the GE/EPRI method, J is divided into elastic component of J (J_e) and plastic component of J (J_p). For a circumferential surface crack in pipings, the J_p is expressed as[13]

$$J_p = \alpha \cdot \varepsilon_0 \cdot \sigma_0 \cdot (1 - \frac{a}{t}) \cdot a \cdot h_1 \cdot \left[\frac{\sqrt{3}}{2} \frac{t}{b} \frac{\sigma}{\sigma_0} \right]^{n+1} \tag{15}$$

where ε_0 and σ_0 are the reference strain and the reference stress respectively, h_1 is the GE/EPRI coefficient given in the GE/EPRI Handbook[13], b is the uncracked ligament, and α and n are the strain hardening coefficient and the strain hardening exponent respectively, which are determined from the following stress(σ) vs. strain(ε) relation.

$$\frac{\varepsilon}{\varepsilon_o} = \alpha \left(\frac{\sigma}{\sigma_o} \right)^n . \tag{16}$$

Under the applied moment, M, the stress σ in Eq. (15) can be expressed as[15-16]

$$\sigma = \left(\frac{M}{4 \cdot R_m^2 \cdot t \cdot H_n} \right) \left\{ \frac{\sin\rho + \cos\gamma}{1 + \left(\frac{a \cdot h_3}{2t} \right) \left(\frac{\sqrt{3}}{2} \frac{t}{b} \right)^n} \right\}^{\frac{1}{n}} , \tag{17}$$

where ρ is the angle from x-axis to neutral plane(i.e. $\rho=\pi-\beta$), γ is the angle from y-axis as shown in the Fig. 1, and H_n and h_3 are numerical coefficients given in the reference [15] and the GE/EPRI Handbook[13] respectively.

Using the Eqs. (15)-(17), and J-R curve of pipe material, the relation between moment and pipe rotation can be calculated by numeric iterations. The maximum load under elasto-plastic condition(M_{EP-max}) can be easily determined form the relation.

3.3 Reference Material Properties used in the Z-Factor Calculation

In order to calculate Z-Factor for nuclear pipings, the reference material properties of the related nuclear pipings has to be given first.

Table 1 represents the reference tensile properties for ferritic and austenitic pipings used in this study.[5-7, 17] These tensile properties were obtained from base metals of both the ferritic pipings and the austenitic pipings. The same tensile properties obtained from the base metals are also used for weld metals for the purpose of conservatism.

Fig. 2 shows the reference J-R curves for the ferritic base metal and the ferritic SAW weld metal, while Fig. 3 shows those for the austenitic base metal including austenitic GTAW/GMAW weld metals and the austenitic SAW weld metal.[5-7, 17]

3.4 New Z-Factors for Ferritic Pipings (Znew-1 and Znew-2)

For a given material, Z-Factors are functions of fracture parameters such as pipe outside diameter(OD), R_m/t, the crack depth, and crack length. In this study, Z-Factors for given materials are calculated for the above four fracture parameters. The pipe is unpressurized in all calculations.

The effects of pipe outside diameter and R_m/t on the new Z-Factor for the ferritic base metal (Znew-1) are investigated for 3 cases of pipe outside diameters (OD=4.5, 16, and 42 inches) with R_m/t=10. and 3 cases of R_m/t (R_m/t=5, 10, and 20) with OD=42 inches respectively.

For a given pipe outside diameter and R_m/t, Z-Factors for both 4 cases of crack depth (a/t=0.1, 0.3, 0.5, and 0.75) and 4 cases of crack length (θ/π=0.1, 0.25, 0.5, and 1) are calculated.

For OD=16 inches with Rm/t=10, the limit moments, the maximum moments obtained from the SC.TNP method, and the Z-Factors are shown in Figs. 4, 5, and 6 respectively. As shown in Fig. 6, the new Z-Factors are not sensitive to either the crack depth or the crack length.

We define the maximum Z value among 16 cases in Fig. 6 as the new Z-Factor corresponding to the given pipe outside diameter and R_m/t (i.e. OD=16 inches and R_m/t=10) for conservatism. The ASME Code Z-Factor in the figure shows a constant value because the ASME Code Z-Factor is not a function of crack depth or crack length.

The other Z-Factors corresponding to the other pipe outside diameters and/or the other R_m/t values can be determined by same method.

Fig. 7 shows the new Z-Factors for the ferritic base metal as a function of the pipe outside diameter with R_m/t=10. The new Z-Factors are lower than the ASME Code

Z-Factor by about 40%. The figure also shows that the increasing rate of the new Z-Factor decreases gradually as the pipe outside diameter increases, while the ASME Code Z-Factor increases linearly as the pipe outside diameter increases.

The new Z-Factor for ferritic base metal can be fitted up to OD=42 inches as (hereafter we denote Znew for the new Z-Factor)

$$Znew-1 = 1.2[0.744+0.0152 \cdot A_{new-1} \cdot (OD-4) - 0.0002 \cdot A_{new-1} \cdot (OD-4)^2], \quad (18)$$

where A_{new-1} is a new A value for ferritic base metal, which can be obtained from the relation between A_{new-1} and R_m/t as shown in Fig. 8. The A_{new-1} value decreases as the R_m/t value increases, while the Aasme values increases as the R_m/t value decreases. A_{new-1} can be fitted as

$$A_{new-1} = [0.0125\left(\frac{R_m}{t}\right) + 0.875]^{-2.791} \quad : \quad 5 \leq \frac{R_m}{t} \leq 20. \quad (19)$$

New Z-Factors for ferritic SAW weld metal (Znew-2) can be obtained through same method used in the determination of Znew-1. The effects of crack depth, crack length, pipe outside diameter, and R_m/t on Znew-2 are also investigated.

Znew-2 as a function of the pipe outside diameter is shown in Fig. 9. The Znew-2 also show similar tendency to Znew-1 The Z-Factor for ferritic SAW weld metal can be fitted up to OD=42 inches as

$$Znew-2 = 1.35[0.742+0.0134 \cdot A_{new-2} \cdot (OD-4) - 0.000176 \cdot A_{new-2} \cdot (OD-4)^2] \quad (20)$$

where A_{new-2} is new A value for the ferritic SAW weld metal given as

$$A_{new-2} = [0.1161\left(\frac{R_m}{t}\right) + 0.161]^{-0.383} \quad : \quad 5 \leq \frac{R_m}{t} \leq 20. \quad (21)$$

3.5 New Z-Factors for Austenitic Pipings(Znew-3 and Znew-4)

New Z-Factors for austenitic base metal and austenitic GTAW/GMAW weld metal(Znew-3), and austenitic SAW weld metal(Znew-4) are also obtained through similar methods used in the Z-Factor calculation of ferritic pipings.

The effects of crack depth(a/t=0.1, 0.3, 0.5, and 0.75), crack length (θ/π=0.1, 0.25, 0.5, and 1), pipe outside diameter(OD=4.5, 16, and 42 inches with R_m/t=10), and R_m/t(R_m/t=5, 10, and 20 with OD=42 inches) on Znew-3 and Znew-4 are also investigated.

Figs. 10 and 11 show Znew-3 and Znew-4 as a function of the pipe outside diameter with R_m/t=10, respectively. As shown in the figures, the values of Znew-3 are similar to Zasme-3 although Znew-3 under OD=20 inches is slightly lower than 1. The values of Znew-4 are slightly higher than Zasme-4. The difference between the new Z-Factors and the ASME Code Z-Factors in austenitic pipings is smaller than those in ferritic pipings because the austenitic pipings is more ductile than the ferritic pipings. The

Z-Factors can be fitted up to OD=42 inches as

$$Znew-3 = 1.00[0.729 + 0.0217 \cdot A_{new-3} \cdot (OD-4) - 0.000286 \cdot A_{new-3} \cdot (OD-4)^2] \quad (22)$$

$$Znew-4 = 1.30[1.048 + 0.0203 \cdot A_{new-4} \cdot (OD-4) - 0.000267 \cdot A_{new-4} \cdot (OD-4)^2] \quad (23)$$

where A_{new-3} and A_{new-4} are new A values for austenitic base metal and austenitic SAW weld metal respectively, given as

$$A_{new-3} = [0.0608\left(\frac{R_m}{t}\right) + 0.392]^{-0.512} \quad : \quad 5 \le \frac{R_m}{t} \le 20 \quad (24)$$

$$A_{new-4} = [0.0778\left(\frac{R_m}{t}\right) + 0.222]^{-0.369} \quad : \quad 5 \le \frac{R_m}{t} \le 20. \quad (25)$$

4. Results and Discussions

4.1. Pipe Fracture Experiments

In the last decade, a number of pipe fracture experiments have been performed for nuclear pipings with a surface crack and/or a through-wall crack as parts of piping research programs such as Degraded Piping Program[5], IPIRG(International Piping Integrity Research Group) Program[6], and Short Crack Program[7].

Table 2 is a summary of 48 pipe fracture experiments obtained from the above programs. Experiment number, material specification, pipe outside diameter(OD), pipe wall thickness(t), crack depth(a/t, %), crack length(θ/π, %), yield stress(S_y), ultimate tensile stress(S_u), reference strain(ε_0), strain hardening coefficient(α) and strain hardening exponent(n) given in Eq. (16), J-R curve coefficients(J_{IC}, C, m) from the relation of $J = J_{IC} + C(\Delta a)^m$, where the unit of Δa is [mm], design stress intensity(S_m) from the ASME Code Sec.III[1], pipe internal pressure(p), test temperature(T), and maximum moment measured from the pipe fracture experiments(M_{exp}) are given in the table.

Thirteen surface crack experiments for ferritic base metal, 2 for ferritic SAW weld metal, 25 for austenitic base metal, and 4 for austenitic GTAW weld metal, 4 for austenitic SAW weld metal were performed under four point bending load. The pipe outside diameter ranged from 114.3 mm(4.5 inches) to 711.2 mm(28 inches). Twenty experiments were performed with pipe internal pressure ranging from 1.55 MPa to 39.3 MPa. Test temperature ranged from room temperature(21 °C) to PWR operating temperature(288 °C). The potential drop method was used to determine the crack growth amount.

Detailed contents including experimental facilities, experimental methods, data processing, and crack evaluation methods are provided in the references [5-7].

4.2 Desirability of the SC.TNP method

Table 3 represents the maximum moment measured from the pipe fracture experiments and the maximum moments predicted from the SC.TNP method[14-16], the R6 method[8], and the DPFAD method[9-10]. In the table, fracture ratio is also shown to compare the results from the above three methods with the measured maximum moment. In order to consider the pipe internal pressure effect, the fracture ratio(FR) is defined as a stress term, given by

$$FR = \frac{(\sigma_{\exp} + \sigma_p)}{(\sigma_{pred} + \sigma_p)} \tag{26}$$

The $\sigma_{\exp}$ and σ_p are the measured stress from experiments and the calculated stress induced by pipe internal pressure respectively. The σ_{pred} is the predicted stress obtained from the SC.TNP method, the R6 method, or the DPFAD method. The $\sigma_{\exp}$, σ_{pred}, and σ_p are given as

$$\sigma_{\exp} = \frac{M_{\exp} R_m}{I} \tag{27}$$

$$\sigma_{pred} = \frac{M_{EP-\max} R_m}{I} \tag{28}$$

$$\sigma_p = p \frac{R_i^2}{(R_o^2 - R_i^2)} \tag{29}$$

The I is the moment of inertia given by

$$I = \left(\frac{\pi}{4}\right)\{R_o^4 - R_i^4\} \tag{30}$$

For the ferritic pipings, the average fracture ratios obtained from the SC.TNP method, the R6 method, and the DPFAD method are 0.99, 1.42, and 1.42 respectively. For the austenitic pipings, the average fracture ratios obtained from the SC.TNP method, the R6 method, and the DPFAD method are 1.10, 1.39, and 1.31 respectively. This results show that the SC.TNP method gives good results to predict the maximum load for both ferritic and austenitic pipings. The well known R6 and DPFAD method give conservative results by about 30-40%.

4.3 Desirability of new Z-Factors

The measured Z-Factors, Zmeas, from the experiments can be easily obtained from the pipe fracture experiments using the relation of

$$Zmeas = \frac{M_L}{M_{\exp}} \quad , \tag{31}$$

where M_L and M_{exp} are the limit moment calculated from Eqs. (10)-(13) and the maximum moment measured from the pipe fracture experiment respectively.

The measured Z-Factors(Zmeas), the ASME Z-Factors (Zasme) obtained from Eqs. (3)-(8), and new Z-Factors(Znew) obtained from Eqs. (18)-(25) for 48 pipe fracture experiments are also given in Table 3.

The average values of Znew/Zmeas are 0.974 and 0.966 for ferritic pipings and austenitic pipings respectively, while the total average values of Zasme/Zmeas are 1.350 and 1.133 for ferritic pipings and austenitic pipings respectively. This result shows that the new Z-Factors obtained from the SC.TNP method are well in agreement with the measured Z-Factors for both ferritic and austenitic pipings. However, it has to be pointed out that the new Z-Factors give slightly non-conservative results within about 4%. Fig. 12 shows the comparison of Zasme/Zmeas with Znew/Zmeas for the 48 pipe fracture experiments.

5. Conclusions

In this study, new Z-Factors to evaluate the behavior of a circumferential surface crack in nuclear pipings are developed by use of the SC.TNP method. The desirability of both the SC.TNP method and the new Z-Factors are examined using the results from 48 pipe fracture experiments for the nuclear pipings with a circumferential surface crack. The conclusions of this study are as follows :

(1) The SC.TNP method is good for describing the circumferential surface crack behavior in nuclear pipings.

(2) The new Z-Factors obtained from the SC.TNP method are well in agreement with the measured Z-Factors for both ferritic and austenitic pipings.

References

1. ASME, Rules for Construction of Nuclear Power Plant Components, ASME Boiler and Pressure Vessel Code, Section III, Division 1, 1992.
2. ASME, Rules for Inservice Inspection of Nuclear Power Plant Components, ASME Boiler and Pressure Vessel Code, Section XI, 1992.
3. D. M. Norris, et al., Evaluation of flaws in austenitic steel piping, EPRI Report, Electric Power Research Institute, NP-4690, 1986.
4. D. M. Norris, et al., Evaluation of flaws in ferritic piping, EPRI Report, Electric Power Research Institute, NP-6045, 1988.
5. G. M. Wilkowski, et al., Degraded piping program- Phase II, USNRC Report, US Nuclear Regulatory Commission, NUREG/CR-4082, 1989.
6. G. M. Wilkowski, et al., International piping integrity research group - final report, BMI Report, Battelle Memorial Institute, 1993.
7. G. M. Wilkowski, et al., Fracture behavior of short circumferentially surface-cracked

pipe, USNRC Report, US Nuclear Regulatory Commission, NUREG/CR-6298, 1995.
8. I. Milne, et al., Assessment of the integrity of structures containing defects, CEGB Report, CEGB, R/H/R6-Rev 3, 1986.
9. J. M. Bloom, Validation of the deformation plasticity failure assessment diagram (DPFAD) approach - the case of an axial flaw in a pressurized cylinder, Trans. ASME, Journal of Pressure Vessel Technology 112 (1990) 213-217.
10. J. M. Bloom, Extension of the failure assessment diagram approach semi-elliptical flaw in pressurized cylinder, ASME winter annual meeting, 1983.
11. P. C. Paris, H. Tada, A. Zahoor, and H. Ernst, The theory of instability of the tearing mode of elastic-plastic crack growth, ASTM STP 668, 1970, pp. 5-36.
12. J. W. Hutchinson and P. C. Paris, Stability analysis of J-controlled crack growth, ASTM STP 668, 1979, pp. 37-53.
13. V. Kumer, et al., An engineering approach for elastic-plastic fracture analysis, General Electric company corporate research and development, EPRI Report, Electric Power Research Institute, NP-1931, 1981.
14. J. M. Bloom and S. N. Malik, Procedure for the assessment of the integrity of nuclear pressure vessels and piping containing defects, EPRI Report, Electric Power Research Institute, NP-2431, 1982.
15. P. M. Scott and J. Ahmad, Experimental and analytical assessment of circumferentially surface-cracked pipes under bending, USNRC Report, US Nuclear Regulatory Commission, NUREG/CR-4872, 1987.
16. J. Ahmad, et al., A Predictive J-estimation method for circumferentially surface-cracked pipes of power-low hardening material in pure bending, in Advanced in Fracture and Fatigue For The 1990's - Load history effects of fracture resistance", Proceeding of ASME PVP Conference, Honolulu in Hawaii, 1989
17. S. Rahman, N. Ghadiali, D. Paul, and G. Wilkowski, Probabilistic pipe fracture evaluations for leak-rate-detection application, USNRC Report, US Nuclear Regulatory Commission, NUREG/CR-6004, 1995.

Table 1 Reference Tensile Properties of Ferritic and Austenitic Pipings

Material Type	Sy (MPa)	Su (MPa)	εo	α	n
Ferritic Pipings	186.84	411.62	0.0010423	2.51	4.2
Austenitic Pipings	131.00	448.85	0.000716	9.58	3.2

Table 2. Test Matrix of 48 Pipe Fracture Experiments for Ferritic and Austenitic Pipings

Exp.	Material Specification			OD	t	a/t	θ/π	Sy	Su	ε0	α	n	J1c	C	m	Sm	p	T	Mexp
Number				mm	mm	%	%	MPa	MPa				MN/m			MPa	MPa	C	MN-m
1	Ferritic	Base	A 106	169.3	7.44	50.8	63.1	212.4	467.5	0.00110	0.499	7.22	0.2590	0.1376	0.988	124.80	0	288	0.0380
2	Pipings	Metal		167.5	14.78	50.3	68.0	319.9	620.5	0.00152	1.970	5.37	0.1075	0.1171	0.814	124.80	0	288	0.0801
3				168.2	21.46	52.6	63.3	258.6	570.2	0.00134	0.171	8.26	0.1970	0.0821	0.788	124.80	0	288	0.1174
4				402.6	26.42	53.2	66.2	237.2	610.2	0.00124	2.189	3.73	0.1489	0.0925	0.470	124.80	0	288	0.7484
5				404.9	12.70	53.5	66.2	262.0	611.6	0.00138	2.972	4.00	0.1380	0.1098	0.602	124.80	0	288	0.3656
6				167.5	13.49	43.2	64.7	319.9	620.5	0.00152	1.970	5.37	0.1075	0.1171	0.814	124.80	15.51	288	0.0772
7				167.4	14.02	41.9	72.0	319.9	620.5	0.00152	1.970	5.37	0.1075	0.1171	0.814	124.80	15.51	288	0.0816
8			SA333	265.2	17.27	42.0	70.0	239.2	527.5	0.00124	2.134	5.58	0.1576	0.1364	0.492	124.80	0	288	0.2211
9				272.0	17.12	43.0	71.0	239.2	527.5	0.00124	2.134	5.58	0.1576	0.1364	0.492	124.80	0	288	0.2342
10				270.6	15.06	48.0	67.8	239.2	527.5	0.00124	2.134	5.58	0.1576	0.1364	0.492	124.80	0	288	0.1951
11				272.8	16.61	52.5	65.9	239.2	527.5	0.00124	2.134	5.58	0.1576	0.1364	0.492	124.80	18.27	288	0.1600
12				765.0	38.99	16.6	49.8	244.1	575.0	0.00131	2.109	3.97	0.3660	0.1721	0.759	135.14	9.10	288	7.2022
13			A 516	711.2	22.68	25.0	50.0	231.0	544.0	0.00119	1.382	5.64	0.2154	0.1219	0.727	124.80	9.56	288	2.1899
14		Weld	A 106	403.2	25.37	50.0	67.0	237.2	610.2	0.00124	2.189	3.73	0.0823	0.0789	0.630	124.80	15.49	288	0.5946
15		Metal	SAW	609.6	42.67	25.0	60.5	234.4	541.9	0.00114	3.206	3.41	0.0531	0.0859	0.698	124.80	15.51	288	2.5753
16	Austenitic	Base	TP316	405.1	9.80	51.1	65.8	166.9	470.2	0.00095	5.164	4.34	0.3818	0.2115	0.717	96.18	0	288	0.2303
17	Pipings	Metal		406.7	9.47	25.0	47.6	224.1	508.8	0.00108	5.012	4.95	0.5839	0.3375	0.725	137.90	1.55	99	0.3564
18			CF8M	325.1	31.12	50.0	65.3	173.1	501.3	0.00097	14.350	2.60	0.3597	0.1080	0.744	120.66	15.51	288	0.3858
19				399.6	26.34	50.0	55.0	231.0	610.2	0.00113	2.165	4.17	0.0877	0.1340	0.814	120.66	15.51	288	0.6723
20				321.7	29.64	58.0	66.0	173.1	501.3	0.00097	14.350	2.60	0.3597	0.1080	0.744	120.66	15.51	288	0.4096
21			TP304	167.4	7.01	50.2	63.4	146.9	448.9	0.00080	8.658	3.37	0.8730	0.1045	0.937	116.87	0	288	0.0295
22				168.6	13.61	51.8	65.9	138.6	449.5	0.00076	11.230	3.57	0.6457	0.2611	0.982	116.87	0	288	0.0596
23				168.3	22.48	44.2	65.3	150.3	477.1	0.00082	3.722	4.18	0.6949	0.4394	0.809	116.87	0	288	0.1009
24				168.3	14.91	52.0	49.0	138.6	449.5	0.00076	11.230	3.57	0.6457	0.2611	0.982	116.87	0	288	0.0714
25				168.1	14.99	41.5	60.0	138.6	449.5	0.00076	11.230	3.57	0.6457	0.2611	0.982	116.87	0	288	0.0650
26				168.0	13.94	100.0	64.7	138.6	449.5	0.00076	11.230	3.57	0.6457	0.2611	0.982	116.87	0	288	0.0652
27				167.9	14.05	100.0	62.6	138.6	449.5	0.00076	11.230	3.57	0.6457	0.2611	0.982	116.87	0	288	0.0603
28				168.4	14.00	100.0	65.5	138.6	449.5	0.00076	11.230	3.57	0.6457	0.2611	0.982	116.87	0	288	0.0635
29				158.9	14.30	53.5	69.0	138.6	449.5	0.00076	11.230	3.57	0.6457	0.2611	0.982	116.87	0	288	0.0553
30				413.5	28.32	47.5	66.0	299.2	739.1	0.00162	3.930	5.07	2.2767	1.2923	0.502	137.90	0	21	1.2606
31				114.3	8.89	50.0	38.0	246.8	629.5	0.00138	2.556	5.50	1.7688	0.3433	0.642	137.90	0	21	0.0411
32				114.3	9.02	50.0	59.4	246.8	629.5	0.00138	2.556	5.50	1.7688	0.3433	0.642	137.90	0	21	0.0330
33				114.3	8.53	25.0	38.7	246.8	629.5	0.00138	2.556	5.50	1.7688	0.3433	0.642	137.90	0	21	0.0377
34				114.3	8.81	25.0	60.8	246.8	629.5	0.00138	2.556	5.50	1.7688	0.3433	0.642	137.90	0	21	0.0336
35				114.3	8.79	75.0	41.3	246.8	629.5	0.00138	2.556	5.50	1.7688	0.3433	0.642	137.90	0	21	0.0375
36				114.3	8.51	75.0	64.5	246.8	629.5	0.00138	2.556	5.50	1.7688	0.3433	0.642	137.90	0	21	0.0303
37				114.3	9.27	50.0	57.5	246.8	629.5	0.00138	2.556	5.50	1.7688	0.3433	0.642	137.90	0	21	0.0323
38				166.6	20.88	21.8	50.0	150.3	477.1	0.00082	3.722	4.18	0.6949	0.4394	0.809	120.66	0	288	0.1542
39				168.3	7.06	25.0	50.0	146.9	448.9	0.00080	8.658	3.37	0.8730	0.3316	0.854	116.87	0	288	0.0430
40				168.3	13.44	52.1	70.9	138.6	449.5	0.00076	11.230	3.57	0.6457	0.2611	0.982	116.87	24.48	288	0.0341
41		Weld	TP 304	167.2	14.83	50.0	64.2	138.6	449.5	0.00076	11.230	3.57	0.0960	0.1022	0.823	116.87	15.17	288	0.0411
42		Metal	SAW	413.5	26.19	50.0	67.0	180.0	458.5	0.00096	7.191	4.90	0.0960	0.1022	0.823	116.87	11.03	288	0.5016
43				416.3	26.42	50.0	68.6	180.0	458.5	0.00096	7.191	4.90	0.1860	0.1601	0.802	116.87	11.03	288	0.4455
44			TP 304	168.3	22.33	50.0	65.2	138.6	449.5	0.00076	11.230	3.57	0.6457	0.2611	0.982	116.87	7.93	288	0.0932
45			GTAW	168.3	22.63	50.0	63.5	138.6	449.5	0.00076	11.230	3.57	0.6457	0.2611	0.982	116.87	32.75	288	0.0633
46				168.3	22.58	50.0	64.9	138.6	449.5	0.00076	11.230	3.57	0.6457	0.2611	0.982	116.87	39.30	288	0.0536
47				416.1	39.17	38.0	65.4	180.0	458.5	0.00096	5.547	4.23	0.6226	0.4598	0.795	116.87	22.41	288	0.9917
48			TP316 SAW	711.2	30.23	25.0	50.0	143.4	427.5	0.00081	9.456	3.28	0.0580	0.1482	0.793	96.18	10.14	288	2.0942

Table 3. Measured and Predicted Maximum Moments, Fracture Ratios, and Z-Factors for 48 Pipe Fracture Experiments

Exp. Number	Material Specification			Measured Max. Moment	Predicted Max. Moment			Fracture Ratio			Z-Factor		
				Mexp	SC.TN	R6	DPFAD	SC.TN	R6	DPFAD	Zmeas	Zasme	Znew
				MN-m	MN-m	MN-m	MN-m						
1	Ferritic Pipings	Base Metal	A 106	0.0380	0.0476	0.0312	0.0339	0.80	1.22	1.12	0.978	1.272	0.938
2				0.0801	0.0787	0.0577	0.0541	1.02	1.39	1.48	1.051	1.252	0.947
3				0.1174	0.1176	0.0716	0.0652	1.00	1.64	1.80	0.898	1.243	0.951
4				0.7484	0.7250	0.4840	0.4724	1.03	1.55	1.58	1.104	1.467	1.095
5				0.3656	0.4036	0.2943	0.2973	0.91	1.24	1.23	1.214	1.602	1.046
6				0.0772	0.0720	0.0514	0.0495	1.06	1.41	1.46	1.033	1.254	0.946
7				0.0616	0.0679	0.0473	0.0465	0.92	1.25	1.26	1.213	1.253	0.947
8			SA333	0.2211	0.2083	0.1534	0.1571	1.06	1.44	1.41	1.024	1.346	1.012
9				0.2342	0.2130	0.1567	0.1619	1.10	1.50	1.45	0.985	1.354	1.015
10				0.1951	0.1921	0.1403	0.1451	1.02	1.39	1.35	1.032	1.359	1.010
11				0.1600	0.1448	0.0773	0.1092	1.07	1.60	1.30	0.970	1.356	1.014
12				7.2022	7.3577	4.5184	4.0048	0.98	1.52	1.68	0.980	1.844	1.213
13			A 516	2.1899	2.6685	1.7065	1.7891	0.85	1.21	1.17	1.359	2.001	1.144
14		Weld Metal	A 106	0.5946	0.4797	0.2698	0.3010	1.18	1.75	1.63	1.089	1.618	1.209
15			SAW	2.5753	2.8616	1.9276	1.6256	0.92	1.26	1.43	1.449	1.784	1.324
16	Austenitic Pipings	Base Metal	TP316	0.2303	0.2630	0.2056	0.2429	0.88	1.12	0.95	1.134	1	0.900
17				0.3564	0.4654	0.4082	0.3670	0.77	0.88	0.97	1.229	1	0.898
18			CF8M	0.3858	0.2761	0.2214	0.2877	1.31	1.55	1.27	1.105	1	0.935
19				0.6723	0.6638	0.3985	0.5095	1.01	1.49	1.24	1.252	1	0.967
20				0.4096	0.2426	0.1768	0.2486	1.52	1.92	1.49	0.865	1	0.930
21			TP304	0.0295	0.0394	0.0297	0.0289	0.75	0.99	1.02	1.020	1	0.781
22				0.0596	0.0502	0.0416	0.0465	1.19	1.43	1.28	0.856	1	0.794
23				0.1009	0.0882	0.0643	0.0704	1.14	1.57	1.43	0.859	1	0.801
24				0.0714	0.0650	0.0579	0.0613	1.10	1.23	1.17	0.978	1	0.795
25				0.0650	0.0589	0.0518	0.0559	1.10	1.26	1.16	1.010	1	0.795
26				0.0652	0.0511	0.0405	0.0353	1.27	1.61	1.84	0.738	1	0.794
27				0.0603	0.0526	0.0425	0.0370	1.14	1.42	1.63	0.842	1	0.794
28				0.0635	0.0510	0.0401	0.0350	1.24	1.58	1.81	0.750	1	0.794
29				0.0553	0.0436	0.0352	0.0397	1.27	1.57	1.39	0.784	1	0.786
30				1.2606	1.2764	0.9807	1.1132	0.99	1.29	1.13	0.956	1	0.979
31				0.0411	0.0400	0.0366	0.0308	1.03	1.12	1.33	0.807	1	0.742
32				0.0330	0.0331	0.0268	0.0242	1.00	1.23	1.36	0.791	1	0.742
33				0.0377	0.0414	0.0392	0.0332	0.91	0.96	1.14	0.944	1	0.742
34				0.0336	0.0386	0.0318	0.0302	0.87	1.06	1.11	0.969	1	0.742
35				0.0375	0.0385	0.0339	0.0290	0.97	1.10	1.29	0.833	1	0.742
36				0.0303	0.0296	0.0217	0.0193	1.02	1.40	1.57	0.685	1	0.742
37				0.0323	0.0346	0.0281	0.0254	0.94	1.15	1.27	0.849	1	0.742
38				0.1542	0.1241	0.0908	0.0919	1.24	1.70	1.68	0.746	1	0.799
39				0.0430	0.0526	0.0436	0.0422	0.82	0.99	1.02	1.022	1	0.782
40				0.0341	0.0267	*	0.0185	1.17	*	1.43	0.757	1	0.793
41		Weld Metal	TP 304 SAW	0.0411	0.0276	0.0194	0.0288	1.35	1.72	1.31	1.134	1.334	1.440
42				0.5016	0.3445	0.2563	0.3804	1.33	1.64	1.24	1.074	1.460	1.658
43				0.4455	0.3847	0.2698	0.4236	1.12	1.44	1.04	1.190	1.461	1.660
44			TP 304 GTAW	0.0932	0.0644	0.0508	0.0521	1.42	1.76	1.72	0.781	1	0.801
45				0.0633	0.0532	0.0336	0.0475	1.14	1.55	1.23	0.999	1	0.801
46				0.0536	0.0477	0.0246	0.0421	1.08	1.59	1.17	1.067	1	0.801
47				0.9917	0.8979	0.5456	0.7697	1.08	1.57	1.22	0.930	1	1.002
48			TP316 SAW	2.0942	2.0335	1.2516	1.6823	1.02	1.45	1.18	1.354	1.612	1.781

* : not calculated

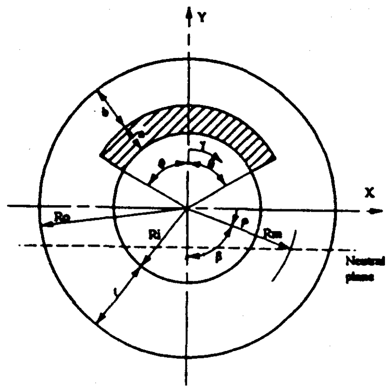

Fig. 1. Cross Section Geometry of Piping with Circumferential Surface Crack

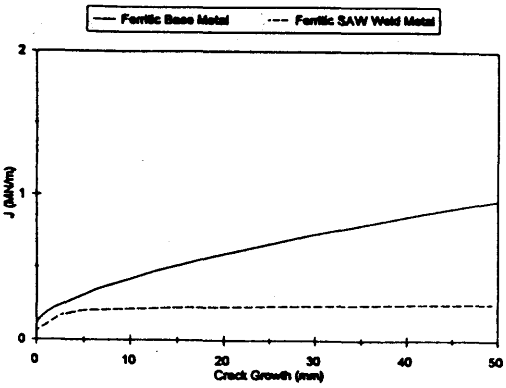

Fig. 2. Reference J-R Curves for Ferritic Base Metal and Ferritic SAW Weld Metal

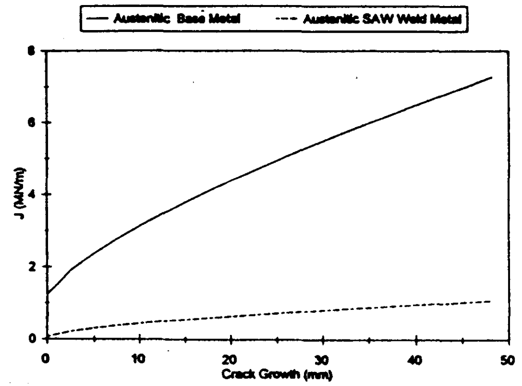

Fig. 3. Reference J-R Curves for Austenitic Base Metal and Austenitic SAW Weld Metal

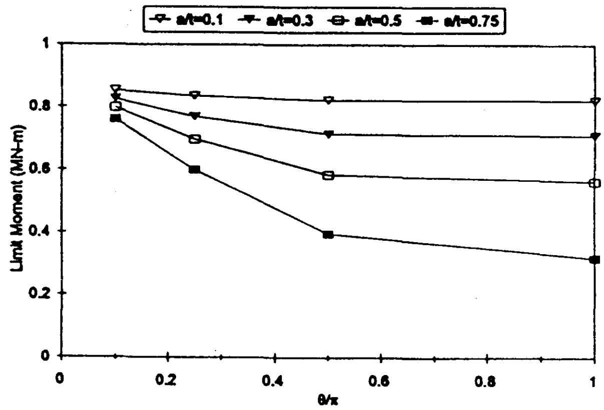

Fig. 4. Limit Moment for Ferritic Base Metal with OD=16 inches ($R_m/t=10$)

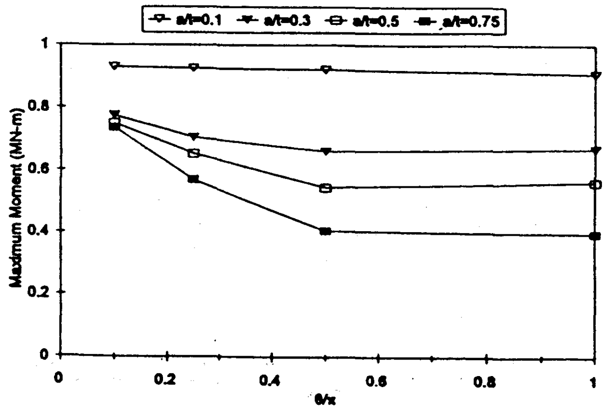

Fig. 5. Maximum Moment for Ferritic Base Metal with OD=16 inches ($R_m/t=10$)

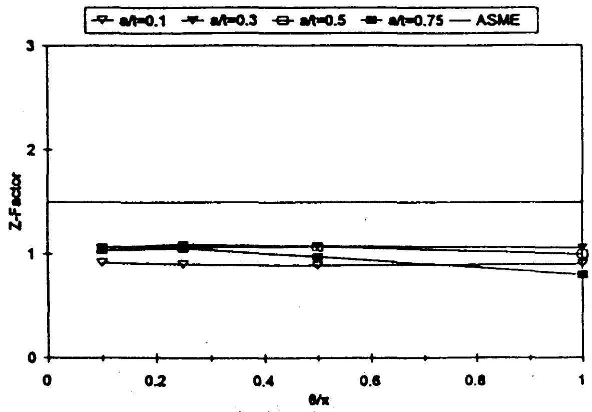

Fig. 6. Z-Factors for Ferritic Base Metal with OD=16 inches ($R_m/t=10$)

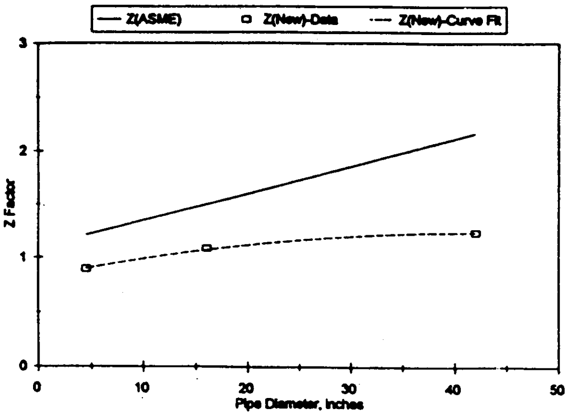

Fig. 7. Comparison of New Z-Factor (Znew-1) with ASME Z-Factor (Zasme-1) for Ferritic Base Metal

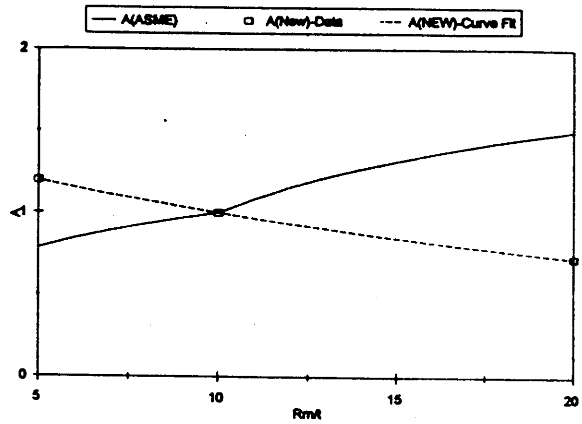

Fig. 8. Comparison of New A value(Anew-1) with ASME A value(Aasme) for Ferritic Base Metal

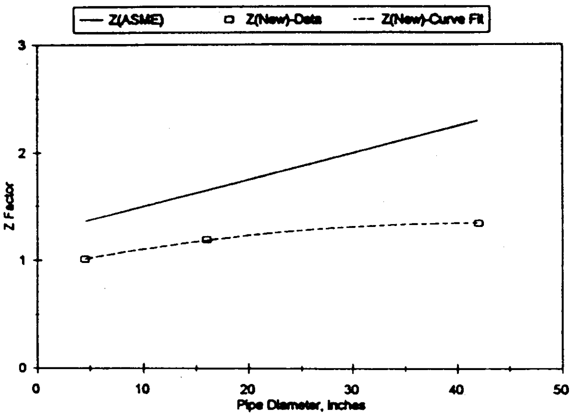

Fig. 9. Comparison of New Z-Factor (Znew-2) with ASME Z-Factor (Zasme-2) for Ferritic SAW Weld Metal

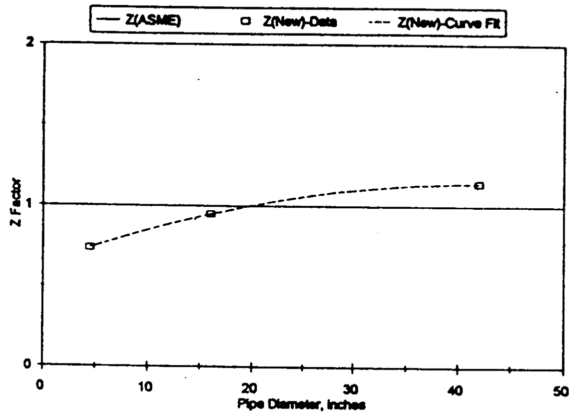

Fig. 10. Comparison of New Z-Factor (Znew-3) with ASME Z-Factor (Zasme-3) for Austenitic Base Metal

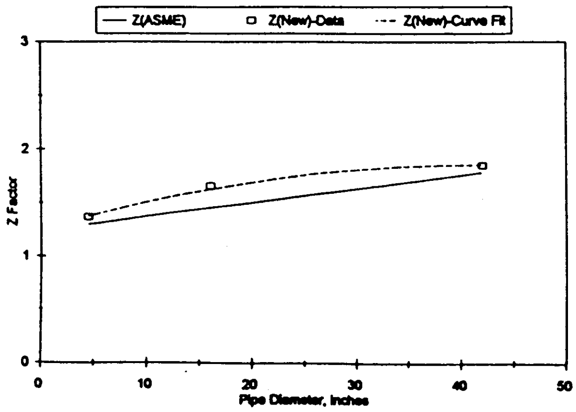

Fig. 11. Comparison of New Z-Factor (Znew-4) with ASME Z-Factor (Zasme-4) for Austenitic SAW Weld Metal

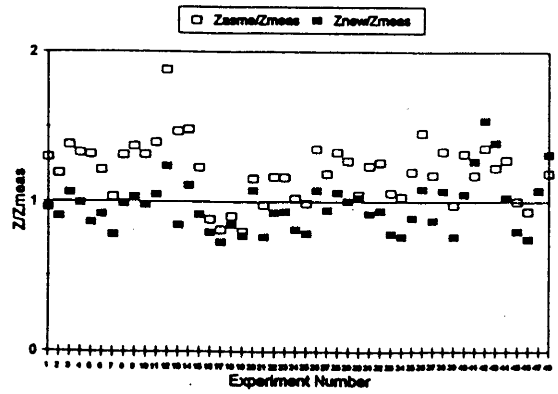

Fig. 12. Comparison of Zasme/Zmeas and Znew/Zmeas for 48 Pipe Fracture Experiments

9 Requirements for Pressure Boundary Integrity of Operating Nuclear Plant-Japanese Standards

H. Kobayashi* (Tokyo Institute of Technology)

Presented at International Workshop on the Integrity of Nuclear Components, May 7-9, 1996, Korea Institute of Nuclear Safety, Taejon, Korea

New Maintenance Code for Operating Nuclear Power Plants in Japan (Draft)

by

K. Iida (Japan Power Engineering and Inspection Corporation)

H. Kobayashi (Tokyo Institute of Technology)

Y. Imamura (Mitsubishi Heavy Industries, Ltd.)

K. Hasegawa (Hitachi, Ltd.)

Abstract

As of the beginning of 1995, forty-eight (48) light water reactors (LWRs) are operating in Japan, twenty-six (26) of which are boiling water reactors and twenty-two (22) pressurized water reactors, and more are under planning or construction phase. These LWRs constitute the main body of nuclear power generation units in Japan, although there are three other power reactors of different kinds; a gas-cooled reactor, an advanced thermal reactor and a fast breeder reactor. The oldest ones among the LWRs were commissioned in 1970, experiencing more than twenty years of operation. Consideration for the increasing aged plants brings up an important technological task to maintain and improve the reliability of operating nuclear plants, which would be essential, technically and socially, for nuclear power generation in Japan to keep growing.

With these backgrounds, the Japan Power Engineering and Inspection Corporation (JAPEIC), under entrustment from the Ministry of International Trade and Industry (MITI), constituted a technical committee, named the Committee on Nuclear Plant Operation and Maintenance Standards (POMS Committee) in the fall of 1993, to develop a maintenance code for operating nuclear power plants.

Since the Japanese law requires nuclear power plants to undergo an annual

inspection, the plants are shut down annually as scheduled for two or three month period during which refueling operation and inspection of the facility, systems and components are carried out. The inspection activities include in-service inspection (ISI) in which the integrity of pressure retaining components is examined by non-destructive examination techniques and in-service testing (IST) in which systems and active components are functionally examined. Some of the examinations are required and sometimes attended by the government authorities, while the others are autonomous ones based on the utility's judgement. The JAPEIC's POMS Committee is intended to comprehensively examine annual inspection requirements which should be provided by the government codes and/or private voluntary standards, and to construct a new application system for the requirements to be fitted in. Due to the restriction of the period given to the Committee for the first phase being until March, 1996, the Committee is concentrating its efforts on the area of ISI for the period. The facilities, systems and components to be examined by the Committee activities are those covered by MITI Notification No.501, the technical standard for nuclear power plants, which roughly correspond to Class 1, 2, 3 and MC Components specified in ASME Boiler and Pressure Vessel Code, Sections III and XI.

The new maintenance code (draft) comprises three parts, Non-Destructive Examination and Inspection (NDE) Rules, Flaw Evaluation Rules and Repair/Replacement Rules. This paper presents the summary of a draft of the NDE Rules and Flaw Evaluation Rules. Major differences between Japanese Code and ASME Code are emphasized.

Refferences

(1) Y. Imamura and K. Iida, Development of Nuclear Plant Operation and Maintenance Code in Japan, 1995 ASME/JSME Pressure Vessels and Piping Conference, Panel Session "A Look at Current Activities of ASME Section XI", July 23-27, 1995, Honolulu, Hawaii, USA.

(2) K. Iida and K. Hasegawa, Acceptance Standard for Pipes in New Maintenance Code (Draft) for LWR in Japan, Inquiry Number ISI-94-21, ASME Code Section XI SG Eval. Stand., March 6, 1996, Charlotte, NC, USA.

New Maintenance Code for Operating Nuclear Power Plants in Japan (Draft)

by

K. Iida (JAPEIC)

H. Kobayashi (TIT)

Y. Imamura (MHI)

K. Hasegawa (Hitachi)

New Maintenance Code in Japan

is developed by the Committee on

"Nuclear Plant Operation and Maintenance Standards in Japan"

(1994 ~ 1995, Chairman : Prof. K. Iida)

The committee is organized by

"The Japan Power Engineering and Inspection Corporation (JAPEIC)"

under the sponsorship of

"The Ministry of International Trade and Industry (MITI)"

Design/Manufacture and Maintenance/Inspection Codes for Nuclear Power Plants

	U.S.A. ASME B & PV Vode	Japan
D/M Code	Sec.Ⅲ, Div.1	MITI Notification No.501
M/I Code	Sec.XI, Div.1	Draft

ASME Boiler & Pressure Vessel Code
Sec. XI

Rules for Inservice Inspection

of Nuclear Power Plant Components

↓

Requirements for Pressure Boundary Integrity

of Operating Nuclear Plants

Maintenance Codes in Foreign and Domestic Countries

Code	Country	ISI Rule	NDE Rule	Evaluation Rule
ASME, Sec.XI	U.S.A.	○	○	○
R/H/R6 Document	U.K.	–	–	○
KTA	Germany	○	○	–
RSEM, RCCM	France	○	○	○
NE14	Switzerland	○	○	–
Handbook	Sweden	–	–	○
JEAC 4205 (old)	Japan	○	○	–
Draft (new)	Japan	○	○	○

ISI : In-Service Inspection

NDE : Non-Destructive Examination and Inspection

New Maintenance Code in Japan

① Non-Destructive Examination and Inspection Rules

② Flaw Evaluation Rules

③ Repair/Replacement Rules

Impact of Flaw Evaluation Rules

- ○ Design/Manufacture Code

  Flaw Detection → Repair/Replacement

- ○ Maintenance/Inspection Code

  Flaw Acceptance → Continued Operation

Maintenance Code for Operating Nuclear Power Plants in Japan (Draft)

- General Rules
  - Terminology
  - Inspection Rules
    - Article 1 General Requirements
    - Article 2 Requirements for Class 1 Components (JWA)
    - Article 3 Requirements for Class 2 Components (JWB)
    - Article 4 Requirements for Class 3 Components (JWC)
    - Article 5 Requirements for Class 4 Components (JWD)
    - Article 6 Requirements for Component Supports (JWF)
  - Evaluation Rules
  - Repair/Replacemet Rules

Inspection Intervals and Program

Japanese Code = ASME Code, Program B

Inspection Interval	Years	Min.Test(%)	Max.Test(%)
1st (10 years following initial start of plant commercial service)	3 7 10	16 50 100	34 67 100
2nd	13 17 20	16 50 100	34 67 100
3rd	23 27 30	16 50 100	34 67 100
4th	33 37	50 100	67 100
5th	43 47	50 100	67 100
↓	↓	↓	↓

Percentage of UT in ISI (per 10 years)

Japanese Code

	RPV		Vessel		Pipe
	DW/SD	GW	DW/SD	GW	DW/SD
Class 1 Component	100%	7.5%	25%	7.5%	25%
Class 3 Component	——		7.5%	—	7.5%

DW : Dissimilar Welds

SD : Structural Discontinuity

GW : General Welds

Percentage of UT in ISI (per 10 years)

ASME Code

	Vessel	Pipe
Class 1 Component	100%	25%
Class 2 Component	100%	7.5%

Flaw Evaluation Procedure

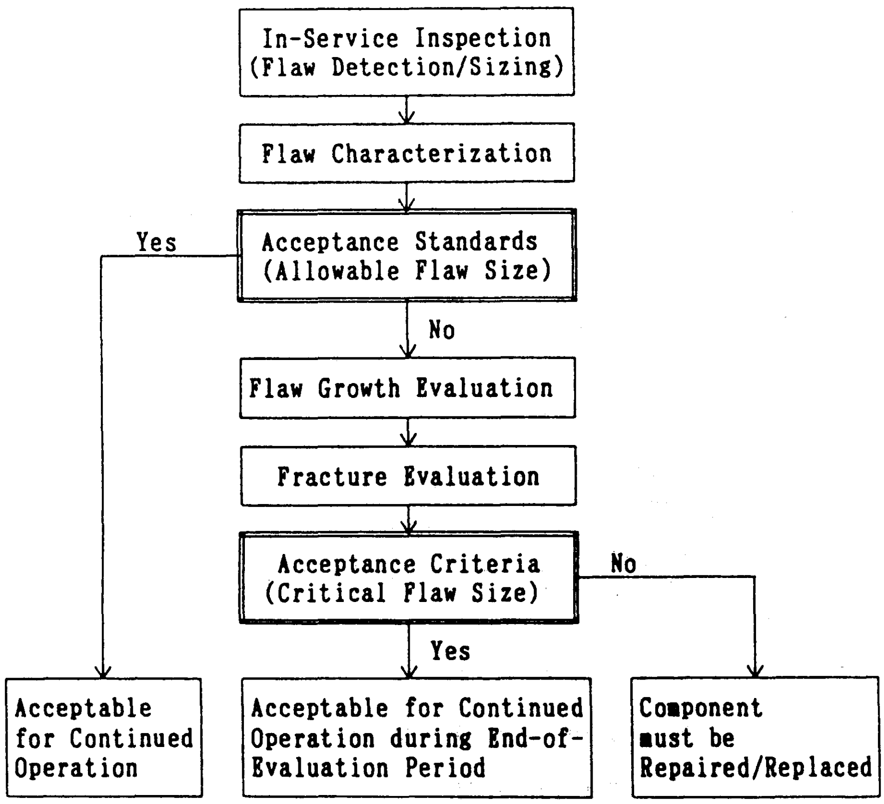

Flaw Detectability/Sizing Accuracy by Ultrasonic Examination

Reference : Proving Tests by Nuclear Power Engineering Co.

Object : Ferritic Vessel Steels (t=50～250mm, Clad & Unclad)

Ferritic Pipe Steels, Austenitic Pipe Steels (t=5～50mm)

Flaw : Surface Planar Flaws

Detectability

Thickness t(mm)	5	21.4	37.5	50	100	150	250
Depth a(mm)	1.5	1.5	1.5	2.0	4.0	6.0	10.0
a/t(%)	30	7.0	4.0	4.0	4.0	4.0	4.0
Length ℓ (mm)	6.0	6.0	15.0	16.5	18.5	19.0	19.0
a/ℓ (%)	25	25	10	12	22	32	53

Sizing Accuracy ($\pm 3\sigma$)

Depth a (mm)	± 3
Length ℓ (mm)	+21 −17

Acceptance Standards (Allowable Flaw Size)

- ○ Over Detectability by NDE
- ○ Validation by Fracture Mechanics Evaluation
- ○ Continuity between Ferritic Vessel and Pipe Standards
- ○ Combined Ferritic and Austenitic Pipe Standards
- ○ Minimum Allowable Flaw Depth a=1.5mm
- ○ Limit of Aspect Ratio a/ℓ >0.06
- ○ Subsurface Flaw a/t = Surface Flaw a/t×1.04Y

Technical Basis of Allowable Flaw Size for Pressure Vessels

○ ASME Code, Sec.III

Postulated Flaw Size, $a/t=25\%$ for $a/\ell=1/6$

○ ASME Code, Sec.XI

Allowable Flaw Size, $a/t=2.5\%$ for $a/\ell=1/6$, $t=100\sim300$mm

Constant K for Conbinations of a/t and a/ℓ

$$\text{Allowable Flaw Size} = \frac{1}{10} \times \text{Postulated Flaw Size}$$

○ Over Detectability by NDE → Bare Margin

○ Validation by Fracture Mechanics Evaluation → Sufficient Margin

Allowable Planar Flaws for Vessels

Wall Thickness t(mm)	Japanese Code	ASME Code
$t\leqq64$	$a\geqq1.5$mm Min.(Vessel, Pipe Standards)	Given a/t
$64<t<100$	Given a	Given a
$100\leqq t\leqq300$	Given a/t	
$300<t<400$	Given a	
$400\leqq t$		Given a/t
Aspect Ratio	$a/\ell\geqq0.06$	No Limitation
Clad Thickness	Consideration	No Consideration
Nozzle Corner	No Consideration	Consideration

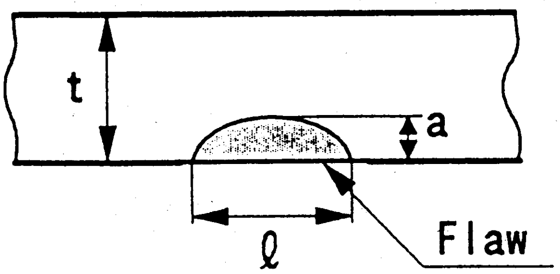

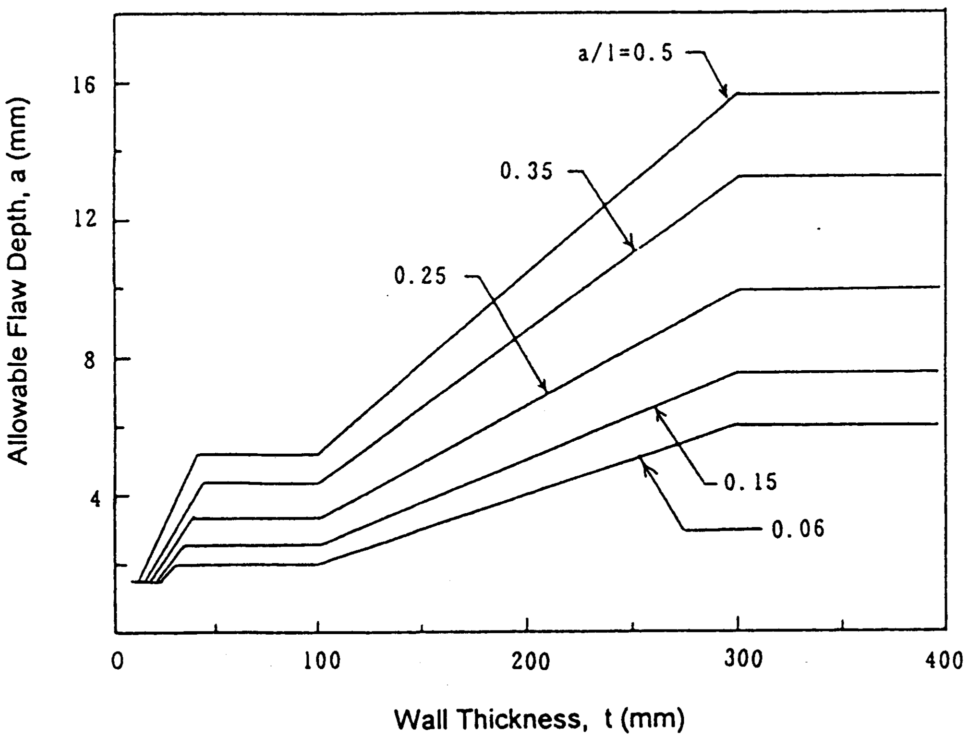

Allowable Planar Flaws for Vessels

Inconsistency of Allowable Flaw Sizes for Pipes in ASME Code

○ Inconsistency of Allowable Flaw Sizes for Ferritic Vessels(V) and Pipes(P)

$$a_P > a_V$$

○ Comparison of Allowable Flaw Sizes for Ferritic(F) and Austenitic(A) Pipes

	Large a/ℓ	Small a/ℓ
PSI	$a_F = a_A$	$a_F < a_A$
ISI	$a_F > a_A$	$a_F < a_A$

F : Low Toughness, A : High Toughness

Allowable Planar Flaws for Pipes

Combined Ferritic and Austenitic Pipe Standards

Pipe Thickness t(mm)	Allowable Flaw Size
$t \leqq 80$	Cut-off a=1.5mm Given a/t $a/t = 12(a/\ell) + 6$
$80 < t$	Given a

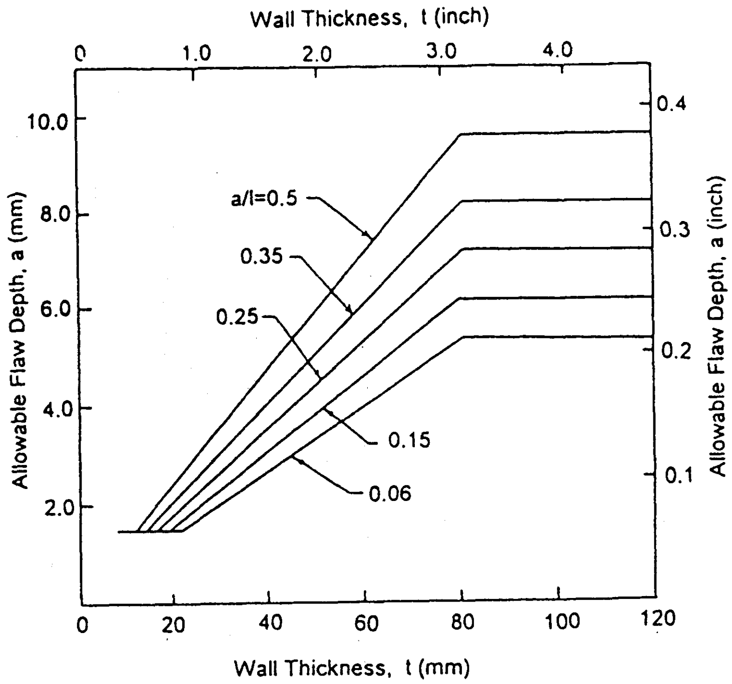

Allowable Planar Flaws for Ferritic and Austenitic Pipes

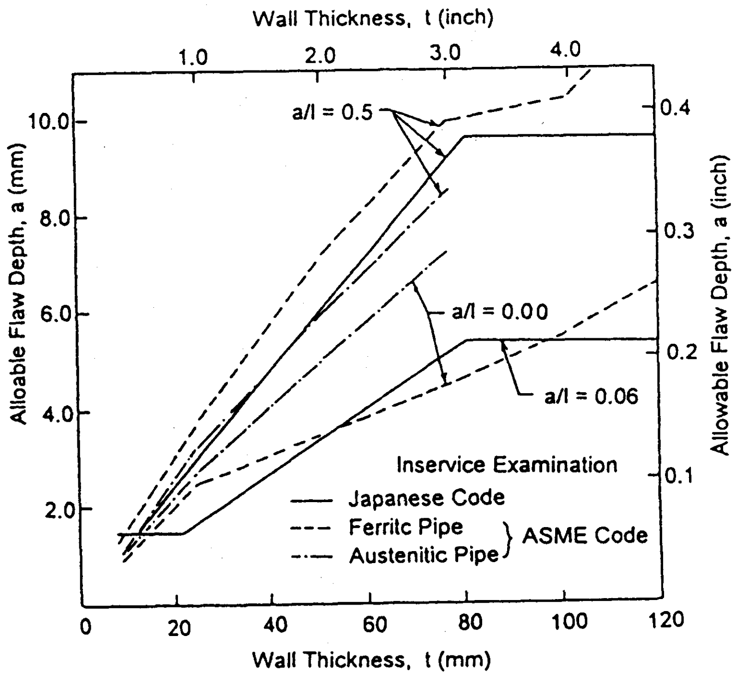

Comparison of Allowable Flaws between Japanese and ASME Codes

Whole Constitution of Evaluation Rules

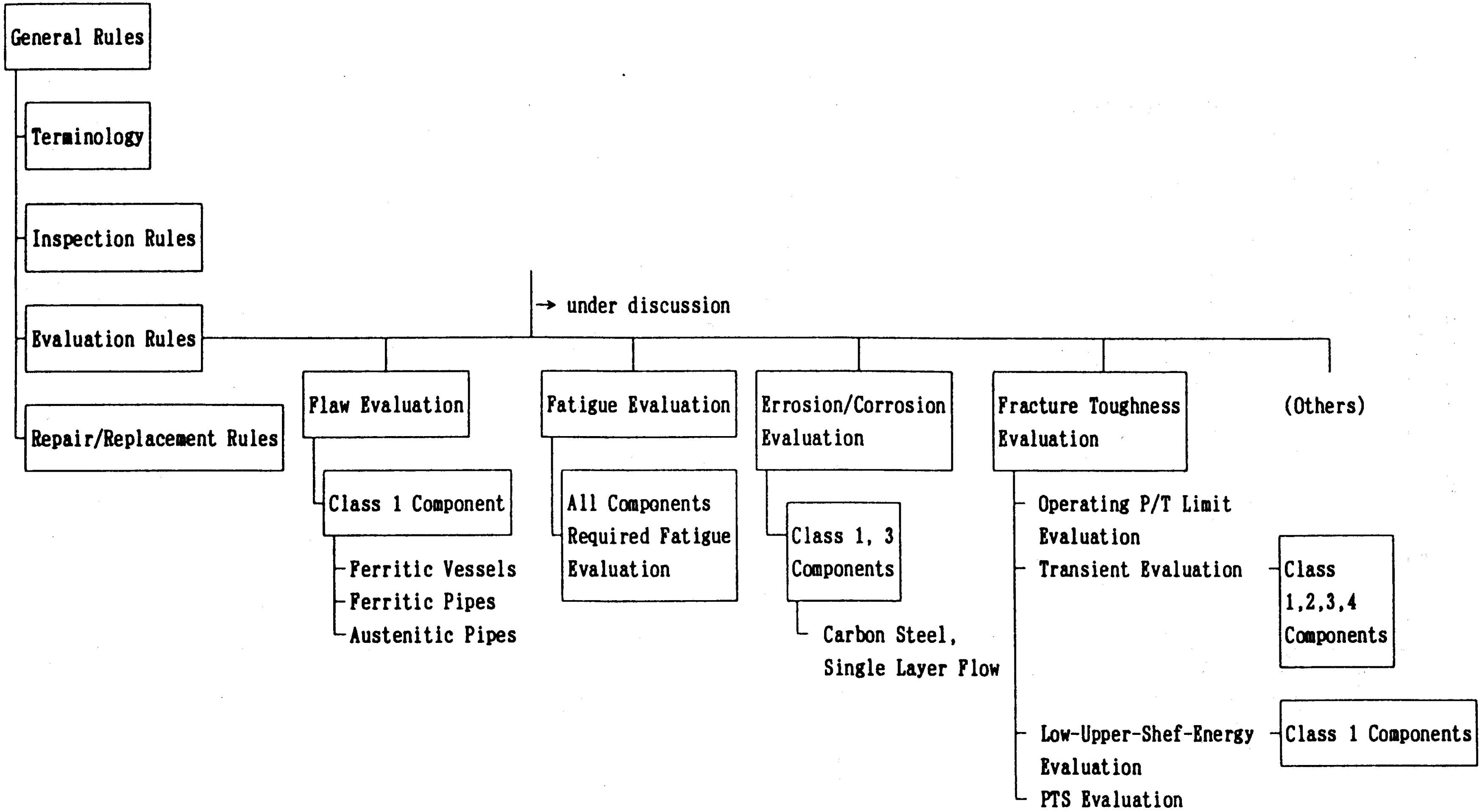

Acceptance Criteria

	Japanese Code	ASME Code
Vessel Wall Thickness	No Limitation	$t \geqq 4$ inch
Pipe Nom. Dia.	$D \geqq 2.5$ inch	$D \geqq 4$ inch
Austenitic Cast Steel Ferrite Content	No Limitation	Cont. < 20%

Flaw Growth Evaluation

	Japanese Code	ASME Code
Loading Conditions No. of Occurence	Operation Records	Design Conditions
Order of Transients	No Consideration	Consideration
Flaw Shape Change	Both a & ℓ Shape Change Consideration	Both a & ℓ
Coalescence of Adjacent Flaws	Consideration	No Consideration
Ferritic Piping SCC	No Consideration	Consideration

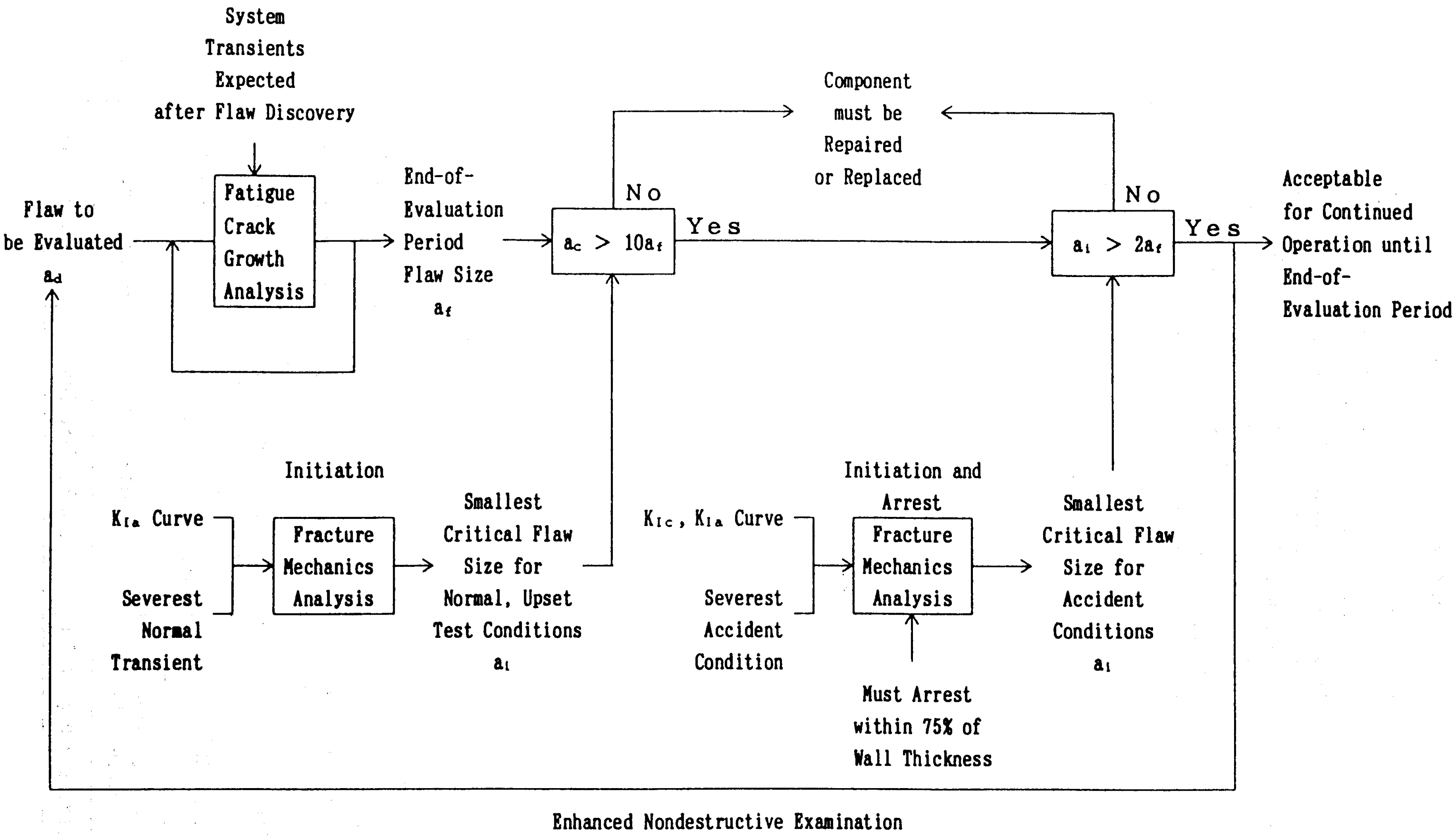

Flaw Evaluation Sequence of Pressure Vessels (ASME Code)

Fracture Toughness of Ferritic Vessels

Initiation and Arrest Toughness ($MPa\sqrt{m}$)

$$K_{Ic} = 36.49 + 22.79 \exp[0.036(T - RT_{NDT})]$$

$$K_{Ia} = 29.45 + 13.68 \exp[0.0261(T - RT_{NDT})]$$

Neutron Irradiation Embrittlement (℃)

$$RT_{NDT} = [RT_{NDT}]_o + \Delta RT_{NDT} + M$$

Parent Materials

$$\Delta RT_{NDT} = [CF] f^{0.29-0.04 \log f}$$

$$[CF] = -16 + 1210P + 215C_u + 77\sqrt{C_u \cdot N_i}$$

Welds

$$\Delta RT_{NDT} = [CF] f^{0.25-0.10 \log f}$$

$$[CF] = 29 - 24S_i - 61N_i + 301\sqrt{C_u \cdot N_i}$$

$$f(\times 10^{19}\ n/cm^2,\ E>1\ MeV) = f_o \exp(-0.24a/25.4)$$

$$M = 2\sigma[\Delta RT_{NDT}]$$

Fracture Evaluation for Pipes

	Japanese Code	ASME Code
Flaw Stress	2.7 S_m	Ferritic : 2.4 S_m Austenitic : 3.0 S_m
Critical Flaw Size	$a/t \leqq 75\%$ $\theta \leqq 60°$	$a/t \leqq 75\%$ $\theta \leqq 360°$
Thermal Expansion Stress	Consideration (SF=1)	No Consideration

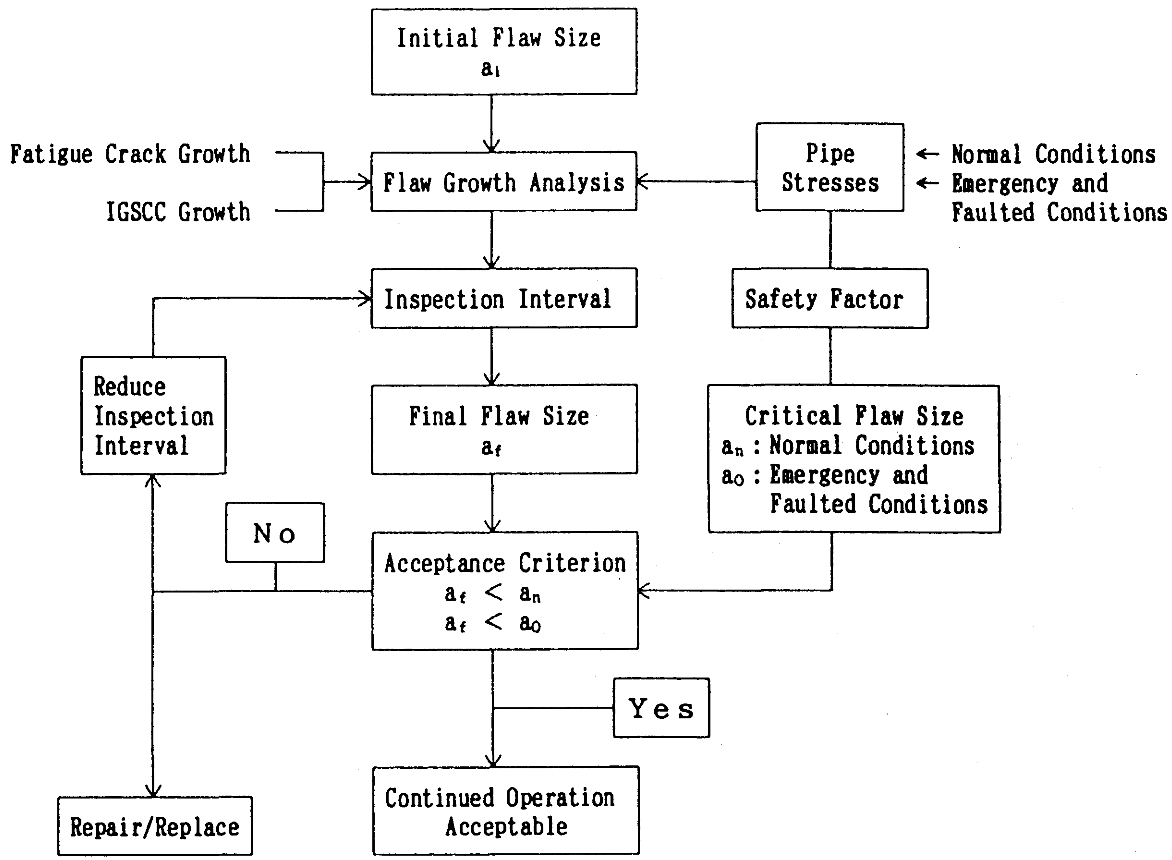

Flaw Evaluation Sequence of Pipes (ASME Code)

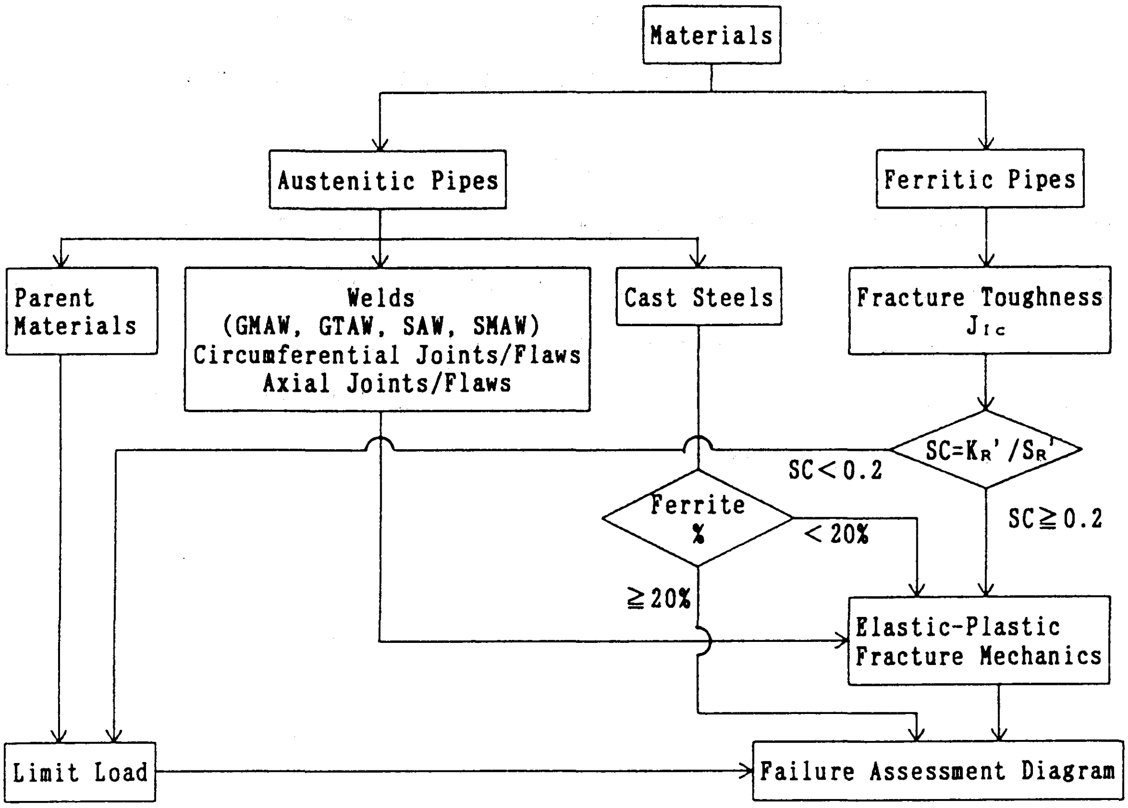

Fracture Criteria and

Fracture Evaluation of Pipes

Fracture Criteria for Austenitic Pipes

	Japanese Code	ASME Code
Limit Load	Parent Material Cast Steel(Ferrite<20%) Circumferential Joint/Axial Flaw Axial Joint/Circumferential Flaw	Circumferential Flaw : Parent Material Cast Steel(Ferrite<20%) GMAW, GAW Axial Flaw : All Materials
Elastic-Plastic Fracture Mechanics	Circumferential Joint/ Circumferential Flaw Axial Joint/Axial Flaw (GMAW, GTAW, SAW, SMAW)	Circumferential Flaw : SAW, SMAW
Failure Assessment Diagram	Cast Steel(Ferrite≧20%) All Materials and Flaws	

Limit Load Evaluation for Ferritic and Austenitic Pipes

Tables

Allowable End-of-Evaluation Period Flaw Depth to Thickness Ratio for

① Circumferential Flaws, Normal Operating (Including Upset and Test) Conditions

② Circumferential Flaws, Emergency and Faulted Conditions

③ Axial Flaws, Normal Operating (Including Upset and Test) Conditions

④ Axial Flaws, Emergency and Faulted Conditions

Screening Criteria for Ferritic Pipes

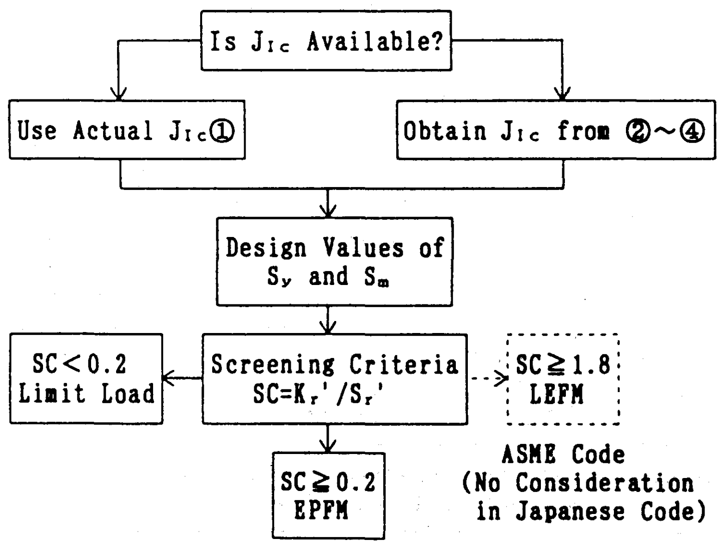

Elastic-Plastic Fracture Toughness of Ferritic Pipes

① Actual J_{Ic} by Tests

② Lower Bounds of J_{Ic} Data

③ J_{Ic} = 1.296 CVN

J_{Ic} : kJ/m^2, CVN : J(Lower Bounds), T≧20℃

④ Circumferential Flaws :

	T(℃)	$J_{Ic}(kJ/m^2)$
STS410, STS480, SFVC2B, SGV410, SGV480 TIG, SMAW, SAW UST≦20℃	20≦T	134
	10≦T<20	109
STPT480, Others	40≦T	114
	10≦T<40	63

$$\text{Axial Flaws : } J_{Ic}(A) = \frac{1}{2} J_{Ic}(C)$$

Elastic-Plastic Fracture Mechanics Evaluation for Ferritic and Austenitic Pipes

○ Circumferential Flaws

Tables of Limit Load Evaluation

$$\frac{P_m + P_b + P_e/SF}{S_m} \rightarrow \frac{Z[P_m + P_b + P_e/SF]}{S_m}$$

Ferritic Pipes

Z = 0.2885 log OD + 0.9573

Austenitic Pipes

TIG, SMAW : Z = 0.292 log OD + 0.986

SAW, Cast Steel (Ferrite<20%) : Z = 0.350 log OD + 1.215

○ Axial Flaws → Failure Assessment Diagram

Failure Assessment Diagrams for Ferritic and Austenitic Pipes

① Ferritic Pipes, Circumferential and Axial Flaws

② Austenitic Pipes, Circumferential Flaws

③ Austenitic Pipes, Axial Flaws

(Preparing)

④ Austenitic Cast Steel(Ferrite≧20%), Circumferential and Axial Flaws

(Preparing)

Future Problems

○ Official Codificaion of Draft

MITI Notification

Japan Electric Association Code/Guide

○ Construction of International Code

Unified Japanese and ASME Codes

Revised Edition of ASME Code

10 The Development Status of Mechanical Component Code for Nuclear Power Application in Korea

N.H. Kim*, J.S. Nah (KOPEC)

THE DEVELOPMENT STATUS OF MECHANICAL COMPONENT CODE FOR NUCLEAR POWER APPLICATION IN KOREA

NAM-HA KIM★, JIN-SOO NAH
Electric Power Industry Code Development Project
Korea Power Engineering Company, Inc.
Seoul, Korea

ABSTRACT

As of the present date, the majority of the mechanical components installed in Korea's Power Plants have been designed and manufactured in accordance with various foreign codes, even though many engineers are accustomed to the usage of the foreign codes, certain amount of problems occur because of foreign language, different units of measurement, terminology, and administrative requirements. Because of the difficulties experienced in applying differing codes, the Korean engineering community has been putting forth efforts in the development of the Korea Electric Power Industry Code, described KEPIC hereinafter, to resolve these problems.

This paper discusses the status of the present KEPIC-Mechanical Components Codes and discusses future development of KEPIC-Mechanical.

INTRODUCTION

In 1986, South Korea for the first time achieved a favorable balance-of-payments ratio in foreign trade, and the favorable balance has increased rapidly. This traditional agrarian country has transformed into a modernized, urban, industrial nation. This industrial growth and enhanced manufacturing/engineering ability has necessitated the development of the KEPIC.

Since early 1992, the engineering community has diligently pursued the development of the KEPIC to resolve numerous difficulties encountered in the implementation of foreign code requirements. As a result of these efforts, KEPIC for the areas of mechanical, electrical, structural, fire protection and quality assurance was published in November, 1995. The developed KEPIC-Mechanical embraces the general methodology and principles of ASME B&PV Code. This decision was based on our present and historical involvement with the ASME Code as being the Construction Code of Record on many of our projects. The KEPIC-Mechanical is divided into two Parts; namely, Level I is the adaptation of the ASME Code, Section III, Division 1 for steel components in the Nuclear Steam Supply System (NSSS). Level II contains the Balance of Plant (BOP) and Turbine/Generator systems. Table 1 provides the frame of these two levels. This paper introduces the developed KEPIC-Mechanical for nuclear and non-nuclear components and discusses the scope of future development for KEPIC- Mechanical.

TABLE 1. FRAME OF KEPIC-MECHANICAL

Level	Group	Item
I	Nuclear Components	General Requirements, Class 1,2,3 Components, Metal Containment, Component Supports, Core Support Structures
II	Non-Nuclear Components	General Requirements, Pressure Vessel, Heat Exchanger, Storage Tank, Piping, Pump, Valve, Condenser, Feedwater Heater
	Common Requirements to Components	Material Specifications, Non-Destructive Examination, Welding Qualification

NUCLEAR COMPONENTS

Nuclear Component Code covers design and construction rules for NSSS mechanical components for Pressurized Water Reactor (PWR) Plants. Safety-Related pressure retaining components, such as pressure vessels, piping, pumps, and valves fall within its jurisdiction. Nuclear Component Code is composed of the following three sections: 1) General Rules; 2) Component Code; and 3) Component Service Code.

The General Requirements, Subsection MNA of Nuclear Component Code follows the structural format and contents of the ASME Code, Section III, Division 1, Subsection NCA: with the exception of concrete components, which is part of KEPIC-Civil/Structural Code.

General Requirements

Classification of Components, MNA-2000, follows the guidelines of Subsection NCA-2000. Responsibilities and Duties, MNA-3000, is a simplified version of NCA-3000, such as owner, component manufacturers, material manufacturers, component installers, and authorized inspection agencies complies with the Korean Industrial System.

Quality Assurance, MNA-4000, meets the requirements of Subsection NCA-4000. The General Requirements differs from Subsection NCA by the addition of Documents, MNA-6000. This section delineates the appropriate documentation and records required by various organizations in the construction of nuclear components. Design Specification and Design Report shall be certified by Korean Mechanical Professional Engineer.

The Korea Electric Association will be responsible for the Certification of Authorization in accordance with MNA-8000.

Table 2 shows a comparison between the General Requirements of MNA and NCA.

TABLE 2. COMPARISON OF GENERAL REQUIREMENTS

Mechanical Component Code Subsection MNA		ASME Section III Subsection NCA	
MNA 1000	General	NCA 1000	Scope
MNA 2000	Classification of Components	NCA 2000	Classification of Components
MNA 3000	Responsibilities and Duties	NCA 3000	Responsibilities and Duties
MNA 4000	Quality Assurance	NCA 4000	Quality Assurance
MNA 5000	Authorized Inspection	NCA 5000	Authorized Inspection
MNA 6000	Documents		
MNA 8000	Certification, Nameplates and Data Reports	NCA 8000	Certificates of Authorization, Nameplates, Code Symbol Stamping, Data Reports
MNA 9000	Glossary	NCA 9000	Glossary

Component Code (Nuclear)

In the preparation of the Nuclear Component Code, an analogy was deliberately created between its structure and those of the ASME Code. This was done to alleviate confusion with engineering disciplines working between the two codes. As you see in Table 3 this was accomplished by the addition of "M" to each Subsection of the ASME Code, Section III, Division 1.

The structures are comparable to the ASME Code numbering system, of which the articles, paragraphs, and the same reference principles are used. The Subsections of Nuclear Component Codes are a direct correlation of the ASME Code, Section III, Division 1, 1992 Edition. However, there does exist some variances between the two, such as the use of American Standards versus the use of Korean Standards. One example, is the calibration of instruments and equipment, is performed in accordance with the Korea Standard Research Institute. ASME Code, Section II, V, and IX is directly applied without translation to support the Nuclear Component Codes. Table 3 shows the full listing of the applicable Nuclear Component Code in Korea.

Table 3. CONTENTS OF NUCLEAR COMPONENTS CODE

Administrative Rules	MNA, General Requirements
Component Codes	MNB, Class 1 Components MNC, Class 2 Components MND, Class 3 Components MNE, Metal Containments MNF, Core Support Structures MNG, Component Supports MNZ, Appendices
Service Codes	ASME Code Section II, Material Specifications ASME Code Section V, Nondestructive Examinations ASME Code Section IX, Welding and Brazing Qualification

NON-NUCLEAR COMPONENTS

The Non-Nuclear Component Code has evolved around the structure and contents of the Korean Standards. The Non-Nuclear Component Code presently focuses on the steam generating power facilities, but eventually will include components for petro-chemical plants and refineries.

The Non-Nuclear Component Code is composed of two sections. The primary section is the Component Code. Which delineates the general and technical requirements for materials, design, fabrication, examination, and testing for construction. The secondary section is the Service Code, which specifies the standards to be commonly used for manufacturing. Table 4 outlines the relationship of the Component Code and Service Code.

Table 4. Outline of Non-Nuclear Component Code

Component Code	Service Code		
General Components	Material Specification	Non-Destructive Examination	Welding Qualifications

Component Code (Non-Nuclear)

The Component Code is classified into General Requirements (MGA) and Technical Requirements (MGX). The format and contents follows the ASME Section Ⅲ Code.

General Requirements are in accordance with Korean Standard (KS) A 9000 Series. Quality System Standard, which were adapted from the ISO 9000 Series for the purpose of globalization. Table 5 shows the comparisons between ASME Code, Section Ⅲ, Subsection NCA and the General Requirements of MGA.

TABLE 5. COMPARISON OF GENERAL REQUIREMENTS

Mechanical Component Code Subsection MGA		ASME Section Ⅲ Subsection NCA	
MGA 1000	General	NCA 1000	Scope
MGA 2000	Classification of Components	NCA 2000	Classification of Components
MGA 3000	Responsibilities and Duties	NCA 3000	Responsibilities and Duties
MGA 4000	Quality Assurance	NCA 4000	Quality Assurance
MGA 5000	Authorized Inspection	NCA 5000	Authorized Inspection
MGA 6000	Documents	NCA 6000	
MGA 8000	Certification, Nameplates and Data Reports	NCA 8000	Certificates of Authorization, Nameplates, Code Symbol Stamping, Data Reports
MGA 9000	Glossary	NCA 9000	Glossary

The philosophy of ASME Section Ⅷ, Division 1, was used as a guideline for the development of Non-Nuclear Components. The contents of Non-Nuclear Components are limited to welded structures. The following is a summary of Non-Nuclear Components Code:

- o The Article of Contents follows ASME Section Ⅲ, Subsection ND.
- o Design requirements are expressed in SI units and the terminology of Korean Standards.
- o Material requirements for carbon steels, low alloy steels, and high alloy steels, which were used in Korean Plants.
- o Welding processes are selected for specific fabrication requirements.

The contents of the Component Code are made, as a rule, and shown in Table 6.

TABLE 6. CONTENTS OF THE NON-NUCLEAR COMPONENT CODE

Section Symbol	**Article**
MGX 1000	General
MGX 2000	Material
MGX 3000	Design
MGX 4000	Fabrication and Installation
MGX 5000	Examination
MGX 6000	Testing
MGX 7000	Overpressure Protection
MGX 8000	Marking

Service Code (Non-Nuclear)

The Service Codes contain material specifications, nondestructive examinations, and welding qualifications to pressure retaining parts as shown on Table 4.

Material Specifications are divided into four subsections, same as the ASME Code, Section Ⅱ, as follows:

o MDF - Ferrous Material Specifications

o MDN - Nonferrous Material Specifications

o MDW - Specifications for Welding Material

o MDP - Properties

Material Specifications consists of 25 ferrous material specifications, 18 nonferrous material specifications, and 19 welding material specifications, which were mainly utilized in the construction of nuclear and thermal power plants. The code will be supplemented to meet engineering needs and as technology develops within our industry. In the determination of allowable stress values for pressure parts, the maximum allowable stress values are established as the lowest value obtained from the criteria of ASME Code, Section II, Part D, Appendix 1, "Non Mandatory Basis for Establishing Stress Values."

Nondestructive examination (NDE) contains NDE methods and qualification requirements of NDE personnel. NDE requirements and methods have basically incorporated the ASME Code, Section V and the Korean Standards, which are applied to the construction of power plant components.

For the preparation of welding qualifications, ASME Section IX, Part QW, was used as a guideline. However, format and contents differ from the ASME Code. Welding qualification incorporated the welding data, specified in Part QW, into the applicable paragraphs of the welding procedure and welding performance qualification. This change was done to provide convenience for the end user. Qualification of welding materials follows the general requirements of AWS, A5.01, "Filler Metal Procurement Guidelines."

DISCUSSION

At present, there exist two component codes for Pressure retaining parts; one for nuclear and the other for non-nuclear. It is our future plan to merge the two into one major Pressure component code in which one Service Code will be applicable for both. This will be done with a conscientious effort by the Korean Mechanical Engineers. The main objective and reasoning for this consolidation is to bring within the engineering realm a more user friendly code while delineating the technical requirements of both. The KEPIC-Mechanical will evolve through our engineering community's experience and to be paced with the continuing technical betterments concerning design, construction, and operation of the mechanical components.

It is now being developed for other Mechanical Component Codes such as Turbine Generator, HVAC, Crane including addional Pressure Components Code. Table 7 shows outline of the Code in Preparation.

TABLE 7. OUTLINE OF KEPIC-MECHANICAL IN PREPARATION

	Title	**References**
Component Code	Power Boiler HVAC Crane Turbine Generator	ASME I ASME AG-1 ASME NOG-1, CMAA RRC-TA
Service Code	Brazing Qualification	ASME IX Part QB
Other Code	Operation and Maintenance of Mechanical Component Qualification of Mechanical Equipment	ASME OM Code, OM-S/G ASME QME-1

ATTACHMENT. LIST OF PRESENT KEPIC-MECHANICAL

Section	Sub-section	Title	Title
KEPIC-MN Nuclear Mechanical Components	MNA MNB MNC MND MNE MNF MNG MNZ	General Requirements Class 1 Components Class 2 Components Class 3 Components Class MC Components Component Supports Core Support Structures Appendices	ASME III NCA ASME III Div.1 NB ASME III Div.1 NC ASME III Div.1 ND ASME III Div.1 NE ASME III Div.1 NF ASME III Div.1 NG ASME III Div.1 Appendices
KEPIC-MG Non-Nuclear Mechanical Components	MGA MGB MGC MGD MGE MGF MGG MGH MGI	General Requirements Pressure Vessels Heat Exchangers Storage Tanks Power Piping Pumps Valves Surface Condensers Feedwater Heaters	ASME III NCA ASME VIII Div.1 TEMA, HEI API 650 ASME B31.1 API 610 ANSI B16.34 HEI HEI
KEPIC-MD Materials	MDF MDN MDW MDP	Ferrous Material Nonferrous Material Welding Material Properties	ASME II Part A ASME II Part B ASME II Part C ASME II Part D
KEPIC-ME Testing and Examination	MEN	Non-Destructive Examination	ASME V
KEPIC-MQ Welding	MQW	Welding Qualification	ASME IX Part QW
KEPIC-MI Inservice Inspection of Nuclear Power Plant Components	MIA MIB MIC MID MIE MIF MIL MIZ	General Requirements Class 1 Components Class 2 Components Class 3 Components Class MC and CC Components Class 1,2,3 and MC Component Supports Class CC Concrete Components Appendices	ASME XI Div.1 IWA ASME XI Div.1 IWB ASME XI Div.1 IWC ASME XI Div.1 IWD ASME XI Div.1 IWE ASME XI Div.1 IWF ASME XI Div.1 IWL ASME XI Div.1 Appendices

SESSION C

11 Progress of Component Aging and Structural Integrity Research Program at JAERI

K. Shibata* (JAERI)

Progress of Component Ageing and Structural Integrity Research Program at JAERI

Katsuyuki SHIBATA

Reactor Component Reliability Laboratory, Department of Reactor Safety Research, Japan Atomic Energy Research Institute, Tokai-mura, Naka-gun, Ibaraki-ken, 319-11 Japan

Abstract

At JAERI, the safety research of nuclear facilities is conducted in accordance with the Five-Year Safety Research Program of the Nuclear Safety Commission. Ageing and structural integrity research of JAERI has been conducted as one of the safety research prescribed in this Program. From the view points of plant safety and replacement technology, Reactor Pressure Vessel, Concrete structure and Electrical cables were identified as important key components to be investigated in the ageing research. This paper overviews the progress and results related to ageing and structural integrity research currently performed.

1. Piping Reliability Test program[1]

An extensive piping research program had been conducted to demonstrate the safety and reliability of LWR piping[1]. Three major tests, Pipe fatigue test, LBB test and pipe rupture test, were performed.

Pipe fatigue test was performed to prove the integrity of primary piping during the service period(Fig. 1). Flat plate specimens with one or two surface cracks were tested. From the test results a procedure to predict the multiple fatigue crack growth were proposed. To verify this procedure, straight and bend pipes with multiple cracks were tested. It was confirmed that the LWR pipings with a crack grown during service period have sufficient fracture resistance (Fig. 2).

LBB test, which involves the fracture test of circumferentially cracked piping under bending and the leak-rate test through fatigue cracked piping, was performed to examine the LBB of piping(Fig. 3~Fig. 6). It was shown that LBB of primary pipings can be jutified for pipes with 4-inch diameter or larger(Fig. 7, Table 1).

In addition, pipe rupture test was carried out to demonstrate the effectiveness of protective device against postulated pipe rupture.

2. Reserch Program on Integrity of Aged LWR components

In the Five-year Safety Research Program of NSC for the period ´96 ～´00. the research area related to the ageing is identified to be one of the important issue. JAERI has conducted the research on this area since late 1980´s. From the view points of plant safety and repare/replacement technology, Reactor Pressure Vessel (RPV), Concrete structure and Electrical cables were identified as key components to be investigated.

Objectives of the research is to improve and validate the prediction methodology, to evaluate the integrity of aged components and to utilize the results on regulatory issue. Subjects under investigation are described below. Most activities are concerned with the ageing issue of RPV.

1) Ageing mechanism and prediction methodology

(1) Irradiation embrittlement of RPV

- Irradiation tests using JMTR(Japan Material Testing Reactor) (Table 2. Fig. 8, Fig. 9)
  Fluence, Flux, Temperature Chemical compositions[2]
- Evaluation of fracture toughness of irradiated PV steels
  Correlation between mechanical properties[3]
- Investigation of embrittlement of decommissioned JPDR(Japan Power Demonstration Reactor) RPV[4] (Fig. 10, Fig. 11)
  Mechanical and metallurgical tests of trepans cut from JPDR RPV is underway under the cooperation with ORNL.

(2) Environmentally assisted cracking of RPV

- Investigation of JPDR RPV cracking
- Corrosion fatigue test in high temperature water environment[5]
  Influence of temperature, flow velocity, DO, crack branchinng phenomena

(3) Ageing of concrete structures

- Investigation of ageing of the biological shield wall of JPDR[6]
- Investigation of ageing of the JPDR containment vessel

2) Inspection and evaluation of ageing

- Improved crack detection technique by detecting the distorted component of magnetic flux of ECT [7](Fig. 12 ～Fig. 14)
- Detection of material degradation by MIM(Magnetic Interlogation Method)[8]
- Reconstitution technique on irradiated Charpy impact specimen using the SAJ (Surface Activated Joinig) (Cooperation with IHI)[9] (Fig. 15～Fig. 17)

3) Evaluation methodology for component integrity

- Integrity evaluation of an aged RPV based on EPFM
- Reliability analysia of an aged RPV based on probabilistic FM.

References

[1] K. Shibata, T. Isozaki et al.: Results of reliability test program on light water reactor piping, Nucl. Eng. Des., 153, 1994

[2] M. Suzuki and Y. Idei: Effects of neutron flux and irradiation temperatureon irradiation embrittlement of A533B steels, Presented at ASTM Symposium on Effects of Radiation on Materials, 1994, Sun Valley (to be published in ASTM STP1271)

[3] K. Onizawa and M. Suzuki: Fracture toughness evaluation in the Transition Region of reactor pressure vessel steel, IAEA specialists meeting on irradiation embrittlement and mitigation, Oct. 1995, Espoo, Finland

[4] M. Suzuki. Y. Idei, K. Onizawa: Investigation on irradiation embrittlement of reactor pressure vessel steel using decommissioned JPDR, IAEA Specialists meeting on Technology for Lifetime Management of NPP, Nov. 1994, Tokyo

[5] N. Nakajima and N. Ebine: Effect of local environmental condition on crack growth behavior in RPV steels of elevated temperature water environment, IAEA Specialists meeting on Technology for Lifetime Management of NPP, Nov. 1994

[6] Y. Idei et al.: Mechanical properties of JPDR biological shield concrete, JAERI-M 90-205, 1990

[7] N. Ebine, S. Takeuchi and K. Ara: Eddy current testing using a parallelogram probe of the distorted magnetic flux detection type, J. Magnetics Society of Japan, Vol. 20, No. 2, 1996

[8] K. Ara, N. Nakajima and N, Ebine: A new method of nondestractive measurement for assessment of material degradation of aged reactor pressure vessels, Presented at Japan-Central Europ Joint Workshop on Advanced Compiting in Engioneering, 1994, Poland

[9] K. Onizawa, K. Fukaya, Y. Nishiyama, et al.: Development of reconstitution technique of Charpy impact specimens by surface-activated joining for reactor pressure vessel surveillance, IAEA Specialists meeting on Technology for Lifetime Management of NPP, Nov. 1994, Tokyo

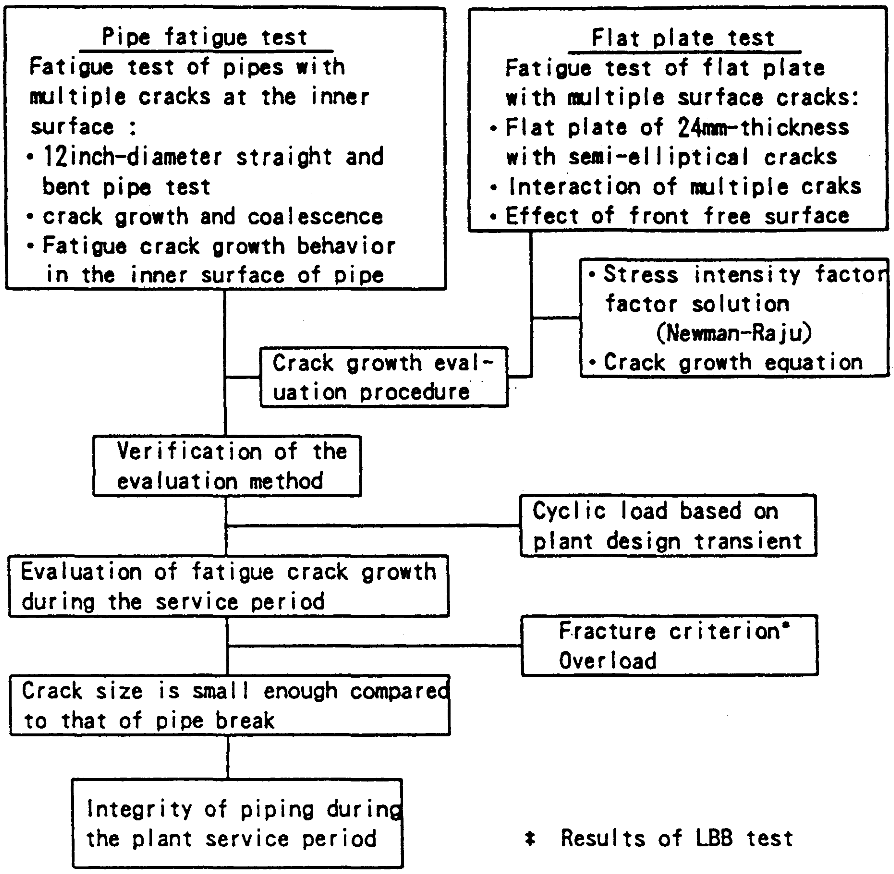

Fig. 1 Flow of the pipe fatigue test

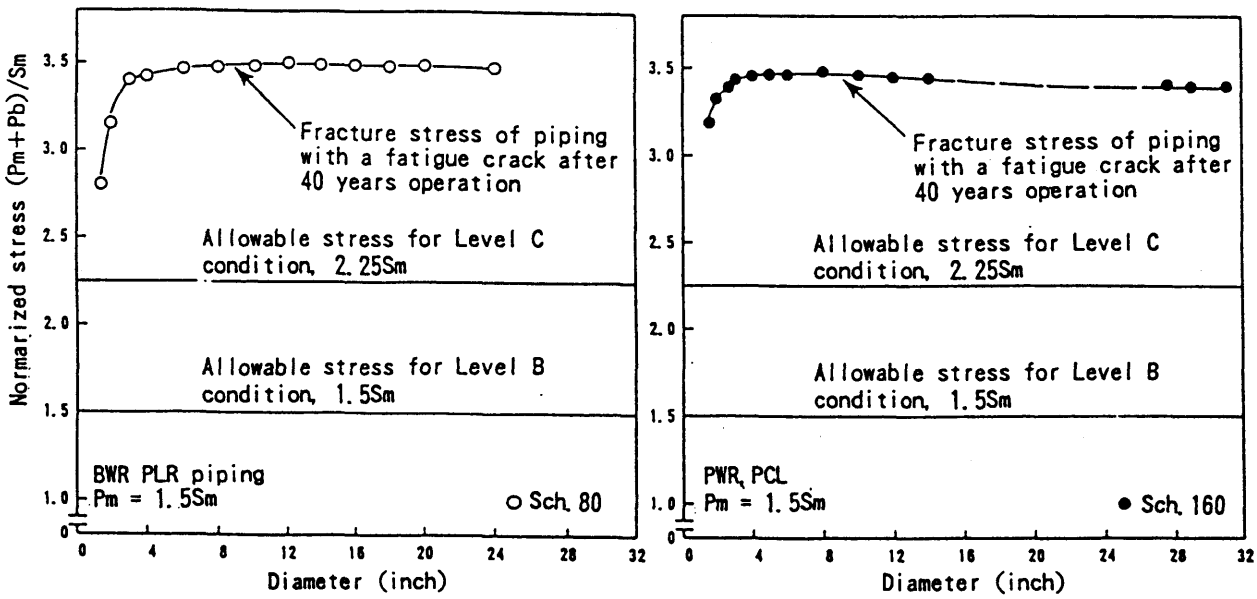

Fig. 2 Fracture stress of piping with a fatigue crack after 40 years operation
(BWR Primary Loop Recirculation Line and PWR Primary Coolant Line)

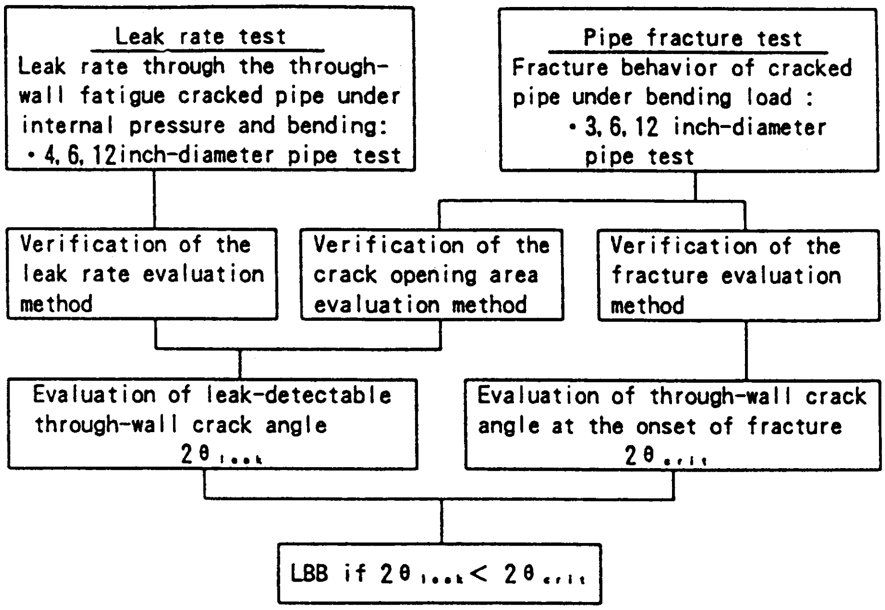

Fig. 3 Flow of LBB verification test

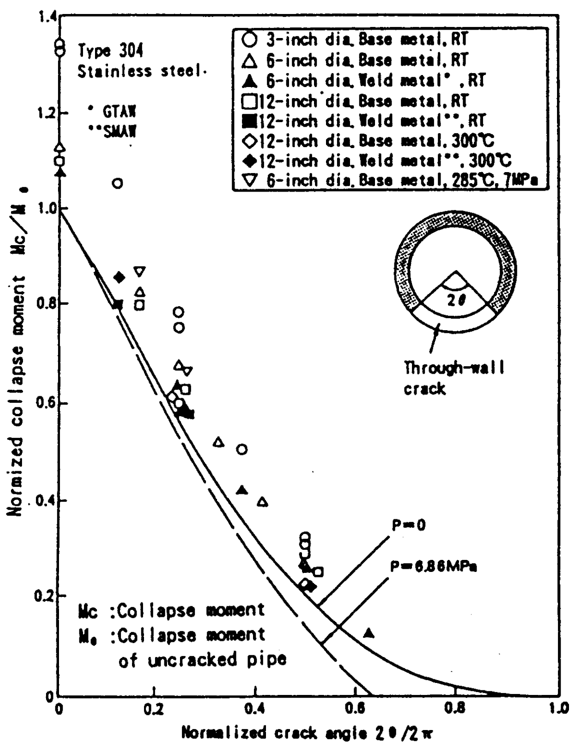

Fig. 4 Comparison between net-section collapse criterion and test results of through-wall cracked stainless steel pipes

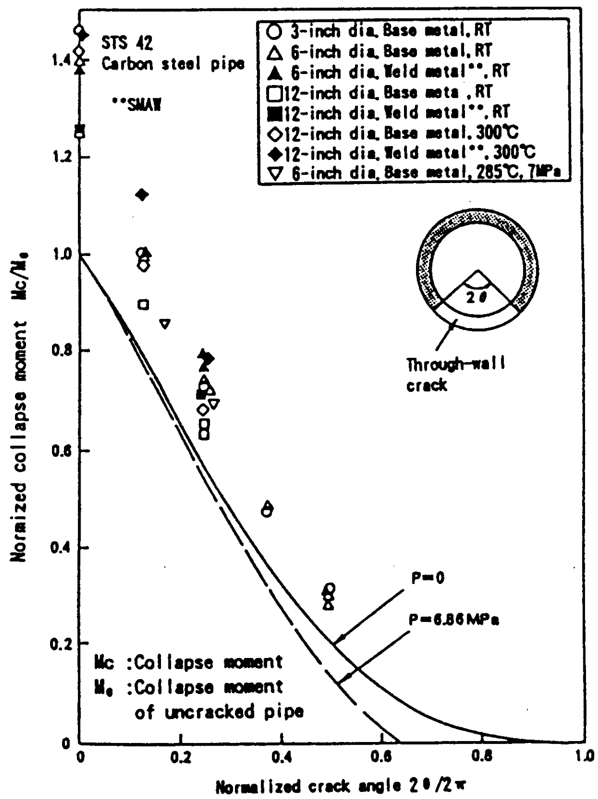

Fig. 5 Comparison between net-section collapse criterion and test results of through-wall cracked carbon steel pipes

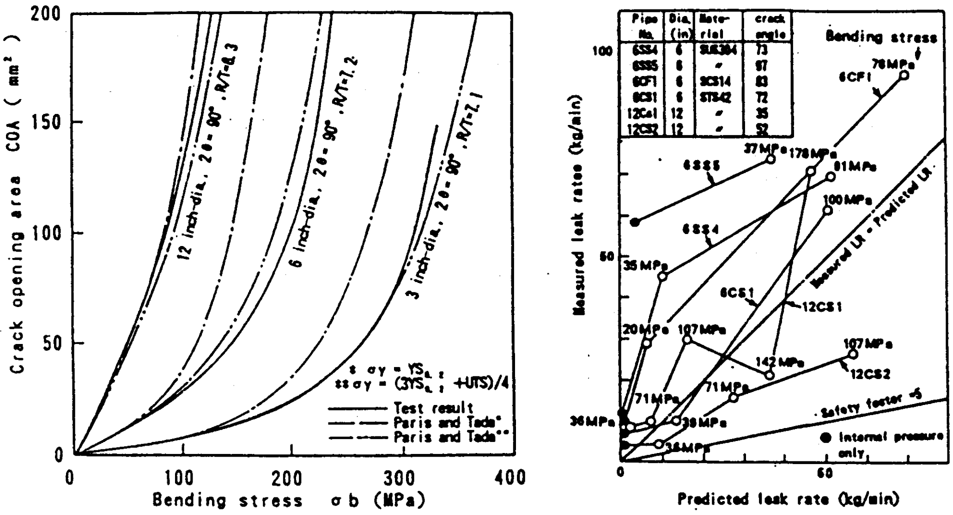

Fig. 6 Prediction of COA and leak rate

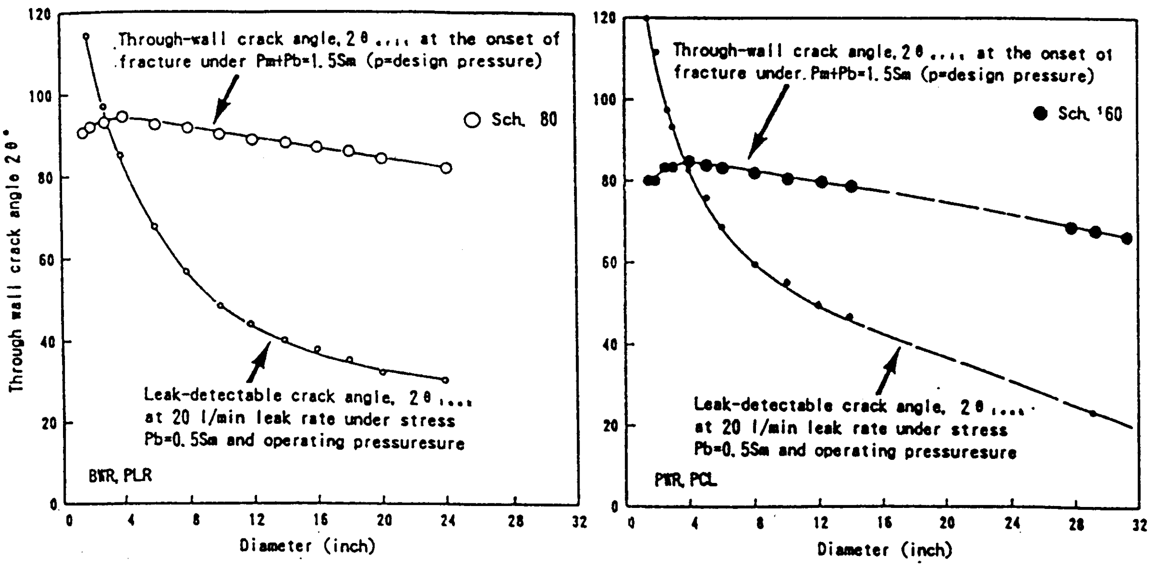

(a)Primary Loop Recirculation Line

(b)Primary Coolant Line

Fig. 7 Case studies of LBB in pressure boundary pipings of BWR and PWR

Table 1 Summary results of piping reliability test

Objectives	Test item	Results
Integrity of piping (Pipe fatigue test)	• Flat plate·test • Straight pipe test • Bent pipe test	• Empirical formula for the correction of front free surface effect in the part-through crack growth and interaction of multiple crack growth • Evaluation procedure of multiple crack growth • Evaluation of integrity of the primary piping in LWRs
Leak before break in piping (LBB test)	• Pipe fracture test • Vibration test • Leak rate test	• Fracture criterion of cracked pipe under static load • Fracture criterion of cracked pipe under cyclic load • COA evaluation procedure of through-wall cracked pipe • Leak rate evaluation procedure • Evaluation of LBB in the primary piping of LWRs

Table 2 Chemical composition of the materials used. (wt%)

Alloy	C	Si	Mn	P	S	Ni	Cr	Cu	Co	Mo	V	N
L	0.17	0.24	1.39	0.003	0.003	0.60	0.07	0.02	0.009	0.46	<0.01	0.0082
M	0.21	0.29	1.44	0.006	0.014	0.65	0.03	0.03	0.009	0.51	<0.01	0.0096

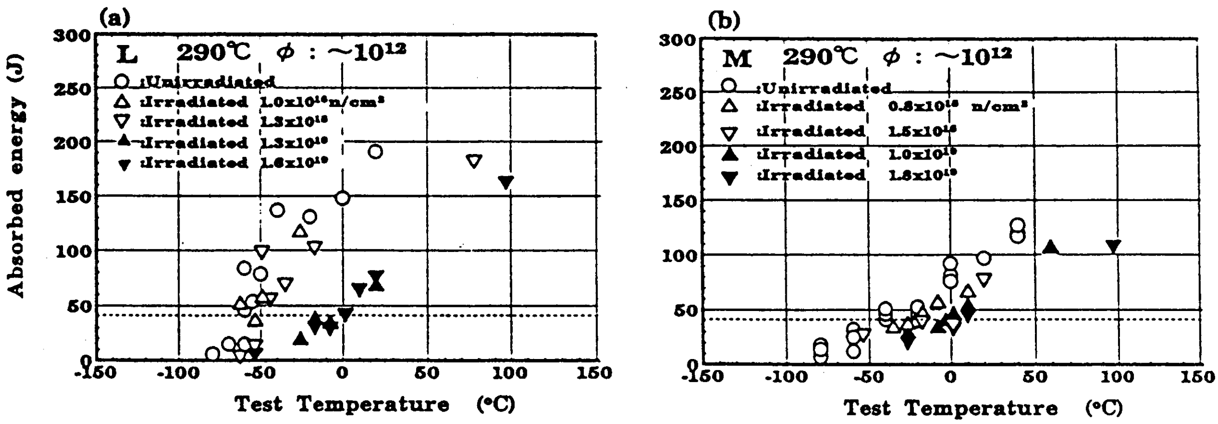

Fig. 8 Absorbed energy transition curves before and after irradiation to $1x10^{18}$ and $2x10^{19}$n/cm^2 (E>1MeV) at 290°C for (a) alloy L and (b) alloy M. All data are of dose rate of $\sim10^{12}$n/cm^2/s.

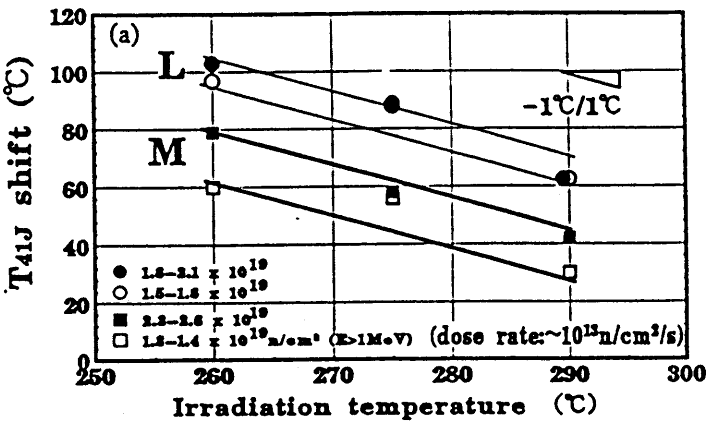

Fig. 9 Effects of irradiation temperature on (a) transition temperature shift after irradiation to $\sim2x10^{19}$ n/cm^2

[M. Suzuki et al.:Effect of neutron flux and irradiation temperature on irradiation embrittlement of A533B steels, Presented at ASTM symposium, 1994, Sun Valley (to be published in ASTM STP 1271)]

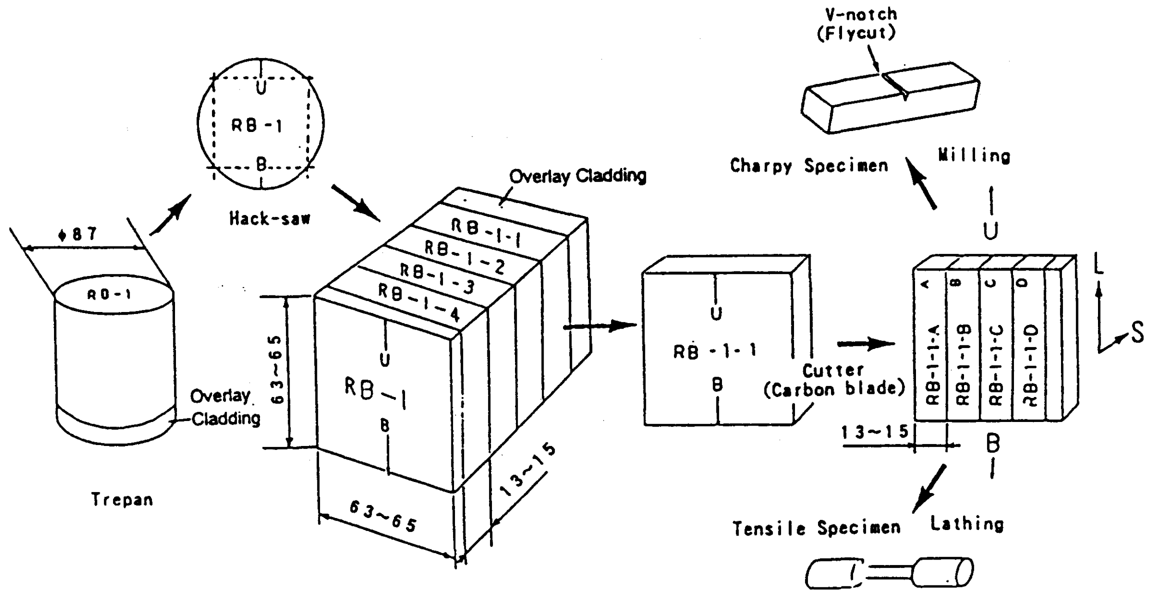

Fig. 10 Specimen machining procedure from Trepan cut from JPDR RPV

Experimental results expected from JPDR RPV investigation

1) Flux effects on Radiation Embrittlement-Verifivcation of Trend Curves
2) Through-thickness Attenuation of Irradiation Embrittlement
3) thermal Ageing-Irradiation Embrittlement Interaction
4) Annealing Characteristics of Real RPV material

[M. Suzuki and Y. Idei: Study on Through-thichness Attenuation of Irradiation Embrittlement using JPDR Pressure Vessel, JAERI-Res, 94-038, 1994]

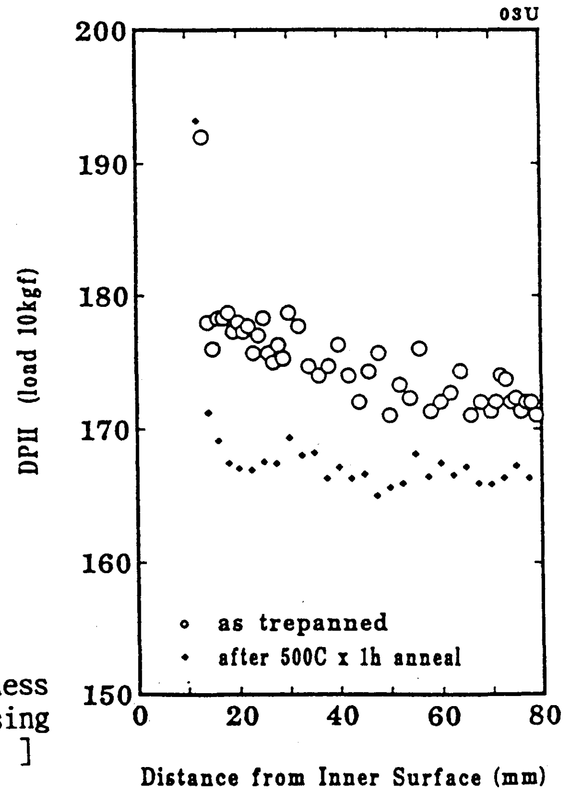

Fig. 11 Through-thickness measurement of hardness before and after Annealing

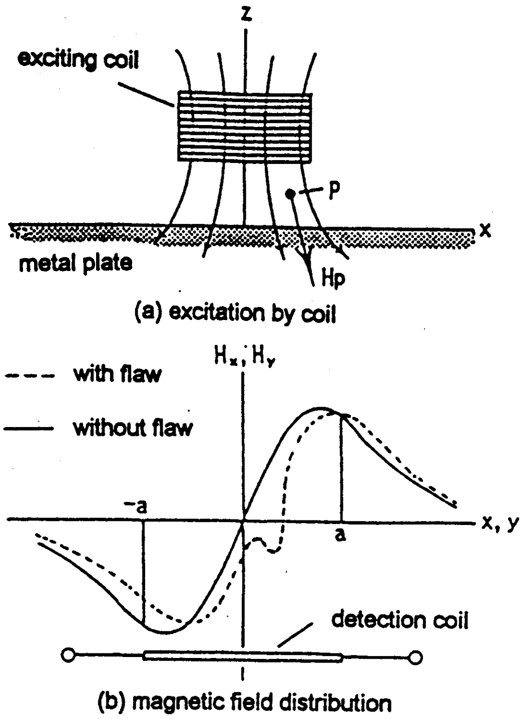

Fig. 12 Principle of eddy current probe detecting distorted magnetic flux

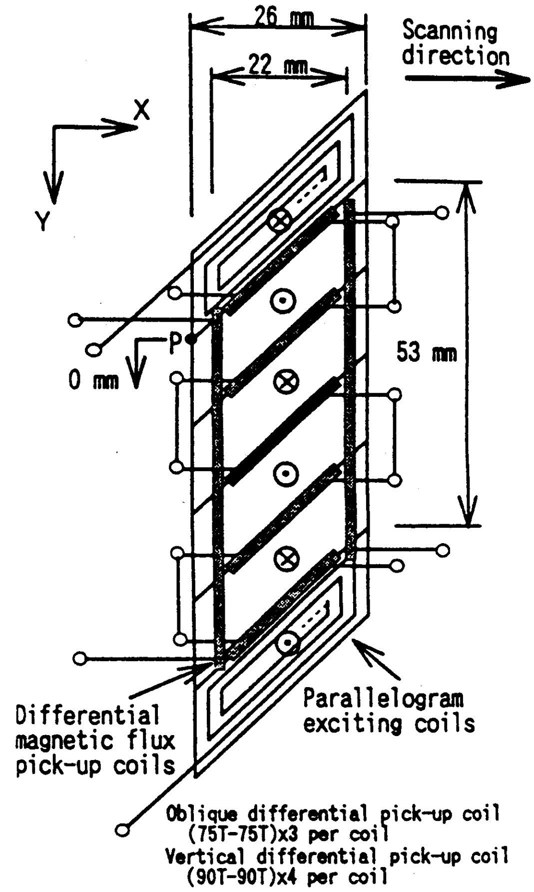

Fig. 13 Geometry of parallelogram eddy current probe

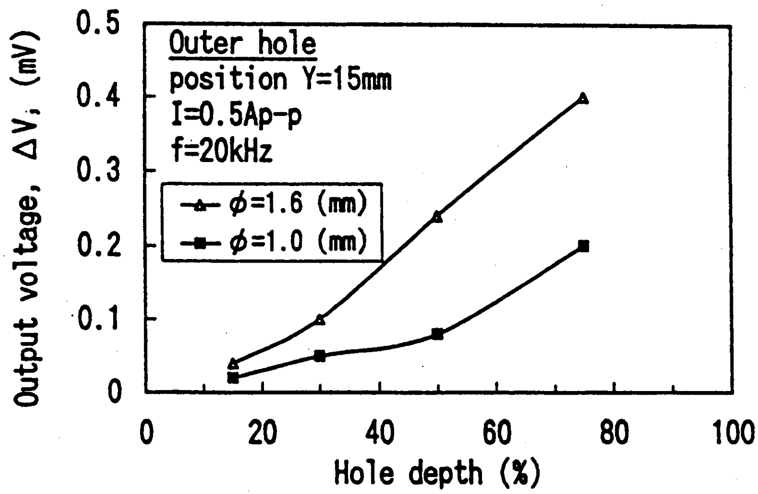

Fig. 14 Relation between detected voltage and depth of outer surface flaw

[N. Ebine, et al. :Eddy current testing using a parallelogram probe of the distorted magnetic flux detection type, J. Magnetics Society of Japan, Vol. 20, 1996]

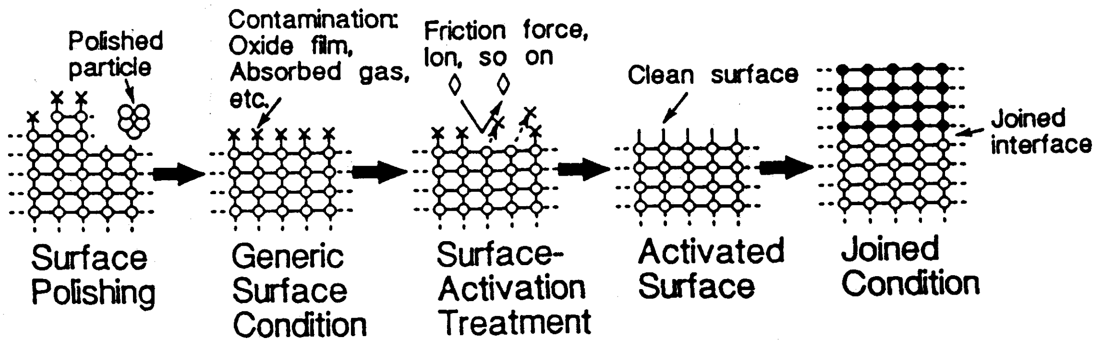

Fig. 15 Principle of SAJ(Surface Activated Joining)

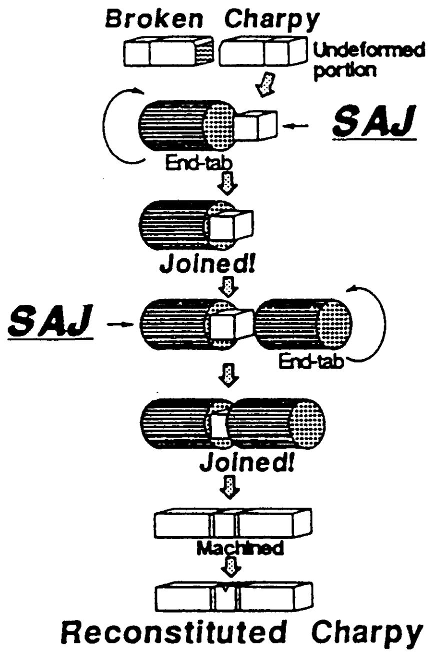

Reconstitution Procedure
Fig. 16

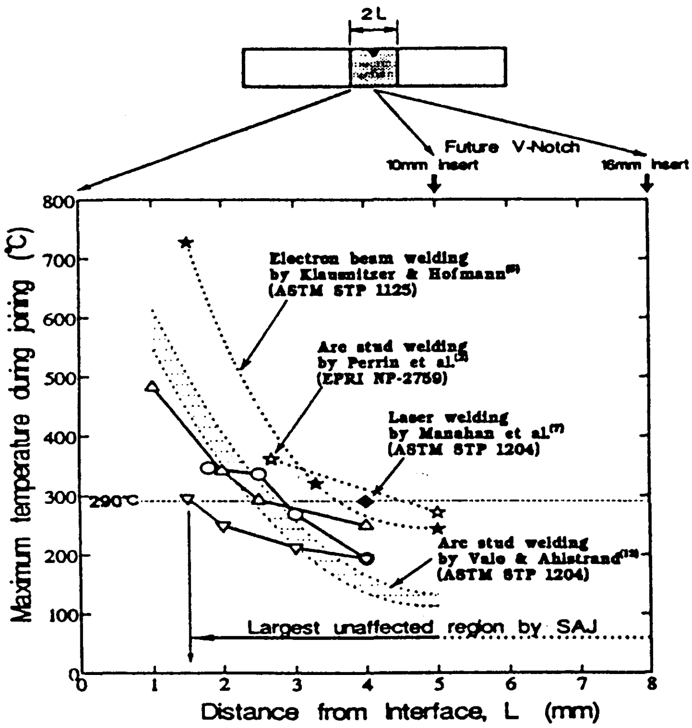

Fig. 17 Comparison with other method
-large unaffected zone by SAJ

[K. Onizawa, et. al. : Development of Reconstitution Technique of Charpy Impact Specimens, IAEA specialists meeting, Nov. 1994, Tokyo]

12 Development of Expert System for Nuclear Piping Integrity

Y.J. Kim*, M.W. Suh, C.S. Seok, H.K. Jun
(SungKyunKwan Univ.) Y.W. Park, Y.H. Choi, J.B. Lee (KINS)

DEVELOPMENT OF EXPERT SYSTEM FOR NUCLEAR PIPING INTEGRITY

Young-Jin Kim*, Myung-Won Suh, Chang-Sung Seok, Hyun-Kyu Jun
Dept. of Mechanical Engineering
Sung Kyun Kwan University
Suwon, Korea

Youn-Won Park, Young-Hwan Choi, Jeong-Bae Lee
Korea Institute of Nuclear Safety
Daejon, Korea

ABSTRACT

The objective of this paper is to develop the expert system called NPiES for nuclear piping integrity. This paper describes the structure and the development strategy of NPiES system. NPiES system consists of 5 parts; user interface, database, knowledge base, expert and integrity evaluation part. The user interface part is developed to connect the user and NPiES system effectively. In the database part, nuclear piping material properties are stored and the unknown material properties are provided through inferring the known material properties. Various rules for inferring material properties are stored in the knowledge-base part. The most appropriate evaluation method for given input condition is recommended in the expert part. Finally, the integrity evaluation part is developed for the evaluation of piping integrity effectively.

INTRODUCTION

The expert system, as a part of artificial intelligence (AI), is being applied for the purpose of design and diagnostic analysis in a variety of engineering fields. In nuclear industry, applications of AI technology to the integrity assessment of power plant facilities have progressed from early 80's and several softwares such as DIAS (Okamodo et al, 1987), ESR (Jovanovic et al 1991) and RAMINO (Lucia and Volta, 1991) have been developed.

Potential loss of structural integrity due to aging of nuclear piping may have a significant effect on the safety of nuclear power plants. Currently nuclear piping integrity evaluation is performed for defects found during in-service inspection. The integrity evaluation requires not only engineering knowledge but also comprehensive judgement based on the field experience.

In a majority of integrity evaluation softwares currently being used in nuclear industry, the integrity evaluation is usually performed after the material properties and the evaluation method are provided by the user. However the material properties such as fracture resistance curves and full stress-strain curves are not always available for early-built nuclear power plants. Therefore it is useful to the user if unknown material properties can be inferred from known material properties. In addition, although the selection of the integrity evaluation method has a significant effect on the accuracy of analysis results, it is not easy for non-expert users to choose the appropriate method for given information.

The objective of this paper is to develop the expert system called NPiES (Nuclear Piping Integrity Expert System) for nuclear piping integrity. This paper describes the structure and development strategies of NPiES system.

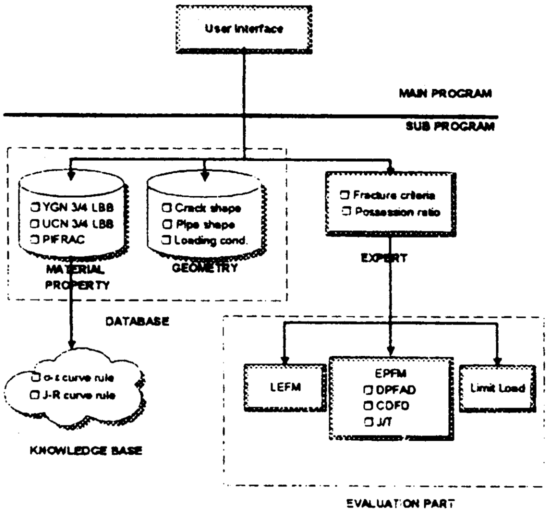

FIGURE 1. STRUCTURE OF NPiES SYSTEM

STRUCTURE OF NPiES SYSTEM

Figure 1 shows the structure of NPiES system. NPiES system is developed for PC (personal computer) and consists of 5 parts; user interface, database, knowledge base, expert and integrity evaluation part. Those are illustrated as followings.

User interface

The user interface part is developed under Windows 3.1 operating system environment to connect the user and NPiES system effectively. Pull-down menu driven method is adopted and frequently used menu is developed as toolbar for user's convenience.

Database

NPiES system has material property (tensile and fracture toughness) database for nuclear grade steels such as SA312 TP304, SA312 TP316, SA106 Gr.C etc. A majority of test data was obtained from domestic material test program such as Yonggwang 3&4 (Kim et al, 1993) with additional information obtained from literature survey. Various material constants such as Ramberg-Osgood parameters are directly provided, or can be obtained by curve-fitting the raw data for proper range. An effective database management system was constructed by utilizing DBase III+ and Microsoft ODBC (open database connectivity).

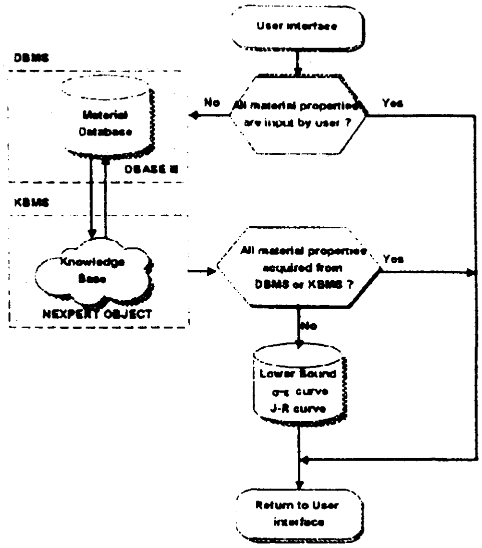

FIGURE 2. STRUCTURE OF HYBRID DATABASE

Figure 2 shows the structure of the database which is developed using the hybrid database format. An effective search for material property is possible by using the hybrid database which is connected with DBMS (database management system) and KBMS (knowledge base management system).

DBMS is utilized to search necessary material property from the stored material property. If necessary material property is not found in the database, KBMS is utilized to predict unknown material property from the knowledge which is stored in the knowledge base. In addition, the lower bound tensile and fracture toughness values which are provided in the EPRI report (Norris et al, 1988) are stored to compare with the predicted material property.

Knowledge base

In the knowledge base, the following levels of knowledge are stored.

Level 1 : Knowledge for inferring σ-ε curve from yield strength.

Level 2 : Knowledge for inferring σ-ε curve from yield strength and tensile strength.

Level 3 : Knowledge for inferring J-R curve from fracture strain.

Details of the knowledge base will be explained in the following chapter.

Expert part

In the expert part, proper integrity evaluation method for given input conditions is recommended based on either the possession ratio of material property or the criteria given in Appendix C and Appendix H of ASME Sec. XI (ASME, 1992). Details will be explained in the following chapter.

Integrity evaluation part

In the evaluation part, four evaluation modules such as LEFM (Linear Elastic Fracture Mechanics), EPFM (Elastic Plastic Fracture Mechanics), limit load method and fatigue analysis are provided for the purpose of piping integrity evaluation. And the EPFM module consists of three parts such as CDFD (Crack Driving Force Diagram), J/T and DPFAD (Deformation Plasticity Failure Assessment Diagram).

NPiES system is programmed by using the C++ language which supports OOP (Object Oriented Programming) and is modulized for the sake of easy expansion of the system.

The following analysis models are currently available in NPiES system.

- Axial surface crack under internal pressure
- Circumferential surface crack under tension
- Circumferential through-wall crack under tension
- Circumferential through-wall crack under bending moment
- Circumferential through-wall crack under bending moment and tension
- Circumferential surface crack under bending moment
- Circumferential surface crack under tension and bending moment
- Long axial surface crack under internal pressure
- Axial through-wall crack under internal pressure

INFERRING UNKNOWN MATERIAL PROPERTIES

Although the tensile properties of nuclear grade steels are easily found in open literature, the material constants C_1, C_2 of J-R curve are seldom found. The following empirical equation was obtained by statistically correlating the tensile data and the J-R data of SA312 TP304 and SA106 Gr.C (Kim et al, 1995).

$$C_1 = 1.687\, E\, k \left(S'_u \sqrt{\varepsilon_c}\right)^{1.66} \qquad (1)$$

$$C_2 = \begin{cases} 0.38 \text{ for carbon steel} \\ 0.61 \text{ for stainless steel} \end{cases} \qquad (2)$$

where E is Young's modulus, k is non-dimensional constant, S'_u is defined as S_u/E and ε_c is fracture strain.

In this research, the prediction of J-R curve from tensile data (Sy, E, ε_c) was performed, and the accuracy of above equations is obtained as 70 %. Accordingly, we define the certainty factor of rule (CF_{RULE}) as 0.7 to calculate the possession ratio of material property. The procedure for calculating the possession ratio will be explained later.

When the σ-ε curve is unknown, Ramberg-Osgood constant n value is obtained as (Bloom and Malik, 1982):

$$\frac{Su}{Sy}\frac{2.7183^{1/n}}{1.002+Sy/E}=\left\{\frac{1/n}{\ln(1.002+Sy/E)}\right\}^{1/n} \tag{3}$$

$$\frac{Sy}{Su}(1.002+\varepsilon_0)=\{n/2.7183\ln(1.002+\varepsilon_0)\}^{1/n} \tag{4}$$

and the α value is obtained as

$$\alpha=\frac{1}{(Sy/E)}\Big/\left\{\frac{\{\ln(1.002+Sy/E)\}^{(1/n)}}{(1.002+Sy/E)}\right\}^{n} \tag{5}$$

$$\alpha=\frac{E}{2.7183\,n\,Sy}\left(\frac{Sy}{Su}\right)^{n} \tag{6}$$

$$\alpha=\frac{\frac{1}{\varepsilon_0}\ln(1.002+\varepsilon_0)-1.002-\varepsilon_0}{(1.002+\varepsilon_0)^{n}} \tag{7}$$

The prediction of σ-ε curve from tensile data (Sy, Su, E) was performed, and the accuracy of above equations is obtained as 90 %. Accordingly, we define the CF_{RULE} as 0.9.
In addition, various rules for inferring J_{IC} and K_{IC} values from tensile data are also stored in the knowledge base.

SELECTION OF EVALUATION METHOD

An appropriate piping integrity evaluation method is usually selected based on the criteria given in Appendix C and Appendix H of ASME Sec. XI depending on piping material, applied load and material property. This criteria can only be used when all informations are available. In this paper the "possession ratio (PR) of material property" is proposed as a new criteria for selecting the most appropriate integrity evaluation method and the weight factor which is quantitatively determined through the sensitivity analysis is adopted to evaluate the effect of material property on fracture behavior.

Evaluation method based on the PR

In order to determine the most appropriate evaluation method for given input information, new method based on the PR which is defined as a ratio of given material property and required material property. The procedure for obtaining the PR can be explained as following.

Step 1 : Determine the scatter band of the material property from the database.

Step 2 : Perform integrity evaluation for a long axial surface crack in a pipe (Figure 3) with $\pm$20, $\pm$40% variation in material property.

Step 3 : Determine the weight factor for respective material property from the integrity evaluation results.

Step 4 : Determine the PR from the summation of weight factors for given material property.

Sensitivity Analysis

Limit load method. The limit load for a long axial surface crack in a pipe, as shown in Figure 3, is expressed as following (Zahoor, 1989).

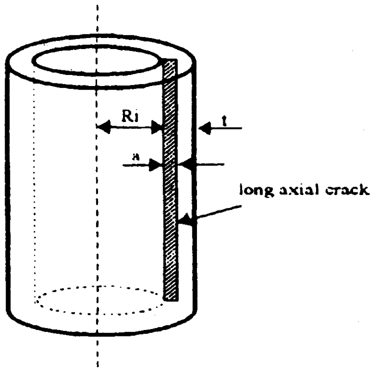

FIGURE 3. GEOMETRY OF A LONG AXIAL CRACK

$$P_L = S_f\{(1-x)/(1-x/M_2)\} \tag{8}$$

where

$M_2 = \sqrt{1+(1.61/4Rt)\,\ell^2}$

$x = a/t$

S_f = flow stress

Governing material property in the limit load method is flow stress which is defined as average value of yield strength (S_y) and ultimate tensile strength (S_u). Figure 4 shows the variation of limit load as a function of material sensitivity in the limit load method. Here P_{max} is the maximum load carrying capacity of pipe with certain variation of material property while P_{max0} is that with no variation of material property.

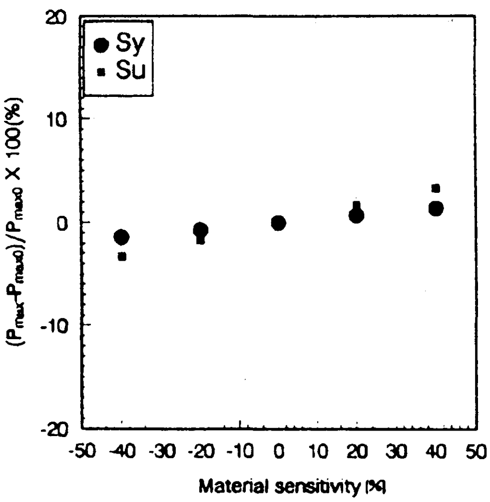

FIGURE 4. SENSITIVITY ANALYSIS RESULTS OF LIMIT LOAD METHOD

As shown in the figure, the sensitivity due to the variation of S_u value is higher than that due to the variation of S_y value. The weight factor (WF) for respective material property is defined from Figure 4 as following.

$$WF = \frac{SL_i}{\sum_{i=1}^{n} SL_i} \tag{9}$$

where n is the total number of material property and SL_i means the slope of i th material sensitivity vs load.

Accordingly the weight factors for respective material property are defined as given in Table 1.

TABLE 1. WEIGHT FACTOR FOR LIMIT LOAD METHOD

Material Property	S_y	S_u
Weight Factor	0.3	0.7

J/T and CDFD method. The J-integral for a long axial surface crack in a pipe is expressed as (Zahoor, 1989)

$$J = \pi t f S_h^2 / E + \alpha S_y (S_y / E) t h_1 (S_h / S_y)^{n+1} \tag{10}$$

where

$S_h = 2pR_0^2 / (R_0^2 - R_i^2)$

f = geometry factor

h_1 = shape function

and the J-R curve is expressed as following.

$$J_R = C_1 (\Delta a)^{C_2} \tag{11}$$

Governing material properties in the J/T and CDFD analyses are;

- Ramberg-Osgood constants ; α, n
- Yield strength ; S_y
- Material constants of J-R curve ; C_1, C_2

Figure 5 shows the variation of maximum load as a function of material sensitivity in the J/T method. As shown in the figure, the S_y value is the dominant factor and the weight factors for respective material property are defined as given in Table 2.

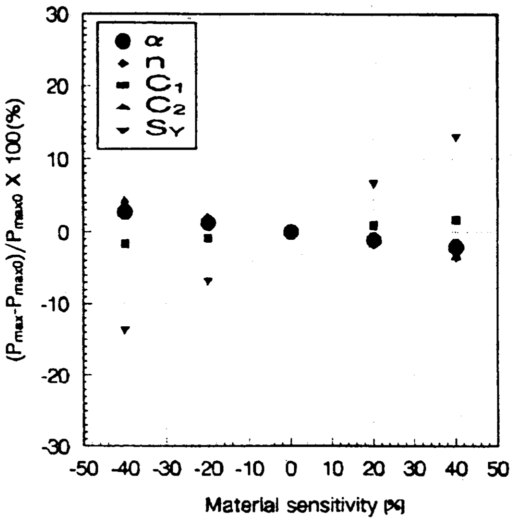

FIGURE 5. SENSITIVITY ANALYSIS RESULTS OF J/T METHOD

TABLE 2. WEIGHT FACTOR FOR J/T METHOD

Material Property	α	n	S_Y	C_1	C_2
Weight Factor	0.09	0.14	0.56	0.07	0.14

DPFAD method. In general, the equation for DPFAD curve is expressed as

$$
\begin{aligned}
J/J^{e}(a,P) &= 1/K_r^2 \\
&= \frac{J^{e}(a_{eff},P)}{J^{e}(a,P)} + \frac{J^{p}(a,P,n)}{J^{e}(a,P)}
\end{aligned}
\tag{12}
$$

Therefore, the governing material properties in the DPFAD analysis are same as those of J/T method. Figure 6 shows the variation of maximum load as a function of material sensitivity in the DPFAD method.

As shown in the figure, the S_Y value is the dominant factor as well. The weight factors for respective material property is defined as given in Table 3.

PR of material property

The PR of material property is computed based on the previously obtained weight factor and certainty factor of rule. Figure 7 shows an example for computing the PR.

Assume that α, n, S_Y, C_1, C_2 values are required for the analysis, and only α, n, S_Y values are given. If the inference for obtaining unknown material property is

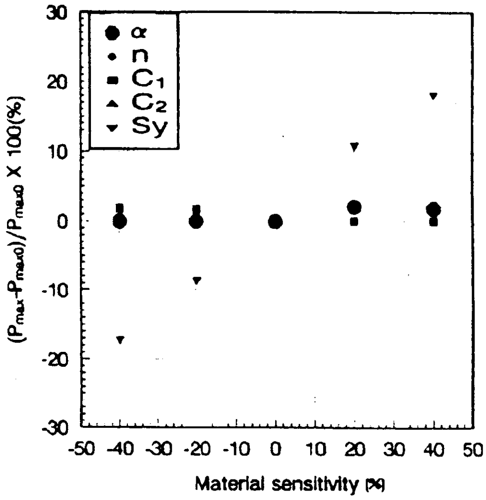

FIGURE 6. SENSITIVITY ANALYSIS RESULTS OF DPFAD METHOD

TABLE 3 WEIGHT FACTOR FOR DPFAD METHOD

Material Property	α	n	Sy	C_1	C_2
Weight Factor	[illegible]	0.06	0.65	0.10	0.07

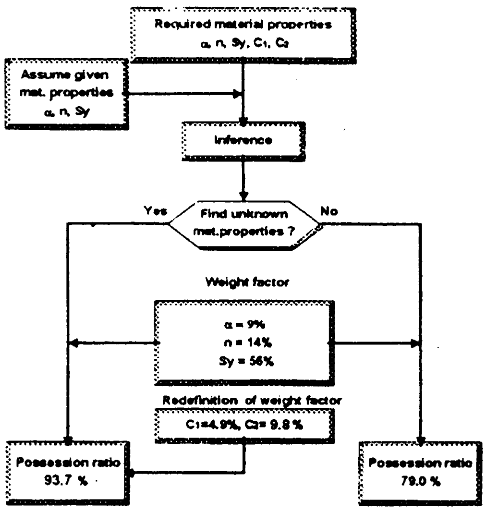

FIGURE 7. FLOW CHART FOR COMPUTING PR

failed due to insufficient input information, the current PR is computed as following.

PR = α (9%)+n (14%)+Sy (56%) =79%

If the inference is successful, the weight factor is redefined as following:

$$WF_R = CF_{RULE} \times WF_S \tag{13}$$

where,

WF_R = redefined weight factor

WF_S = weight factor defined by sensitivity analysis

CF_{RULE} = certainty factor of the rule which is used to infer unknown material properties

In the next phase, the PR is recomputed as following:

Step 1 : Redefinition of weight factor

$C_1 = 0.7 \times 7\% = 4.9\%$

$C_2 = 0.7 \times 14\% = 9.8\%$

Step 2 : Calculation of PR

$PR = \sigma\ (9\%) + n\ (14\%) + S_y\ (56\%) + C_1\ (4.9\%) + C_2\ (9.8\%)$

$= 93.7\%$

After obtaining the possession ratio of material property for respective integrity evaluation methods. the method which has the highest possession ratio is recommended as the most appropriate integrity evaluation method.

Evaluation method based on ASME Sec. XI criteria

In Appendix C and Appendix H of ASME Sec. XI, the evaluation procedures for austenitic and ferritic piping materials are given. The austenitic piping material is distinguished between austenitic materials with high fracture toughness and certain flux welds that have lower toughness. The base metal and non flux weld (GTAW, GMAW) evaluation is based on a plastic collapse failure mechanism and the allowable flaw sizes are generated from the limit load analysis. The flux weld evaluation is based on an unstable crack tearing failure mechanism and the allowable flaw sizes are determined using EPFM analysis methods.

The ferritic piping material is distinguished by high toughness materials (base metal) and certain lower toughness flux welds, which include shielded metal arc welds (SMAW) and submerged arc welds (SAW). Since the predicted failure mechanism for the flux welds was unstable, The flaw extension may occur at loads lower than the plastic collapse analyses. The applicable failure mode is defined depending on material toughness, load type and magnitude, and flaw size, shape and orientation. Finally, an appropriate evaluation method is recommended.

CASE STUDIES

To illustrate the usefulness of NPiES system, case studies were performed.

Figure 8 shows the analysis model of a pipe (mean radius R = 2160 mm, thickness t = 216 mm), (a) with an axial semi-elliptical crack (depth a = 54 mm, crack length 2c = 162 mm), (b) with a long axial crack (depth a = 54 mm). The pipe is under internal pressure of 17 MPa.

The material properties of the pipe are following.

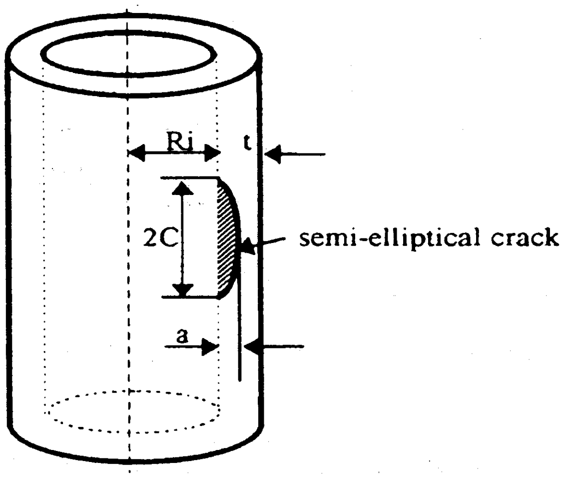

FIGURE 8. GEOMETRY OF AXIAL SEMI-ELLIPTICAL CRACK

S_y = 594 MPa
S_u = 703 MPa
E = 203 GPa

$$\left(\frac{\varepsilon}{\varepsilon_0}\right) = \left(\frac{\sigma}{\sigma_0}\right) + 2.0\left(\frac{\sigma}{\sigma_0}\right)^{8.6} \quad (14)$$

$$J_R = 132(\Delta a)^{[illegible]} \quad (kN/m) \quad (15)$$

Assuming that full material properties are not given, the following three case studies were performed.

Case I : Inferring σ-ε curve from S_y value.
Case II : Inferring σ-ε curve from S_y and S_u values.
Case III: Inferring J-R curve from ε_c value.

<u>Case I : Inferring σ-ε curve from S_y value.</u>

This case study is when the yield strength (S_y) is given instead of full σ-ε curve. Figure 9 shows the screen of database before inference and Figure 10 shows the screen after inference; Su = 891 MPa, α = 1.64, n = 6.09 and E = 197 GPa.

EPFM analyses were performed based on 4 different integrity evaluation methods (CDFD, J/T, DPFAD, limit load) and the results are summarized in Table 4. Here the safety factor is defined as ratio of operating pressure P against maximum load P_{max}. As shown in the table, the maximum difference between the Case I and reference case (when material properties are fully given) is within 25 %.

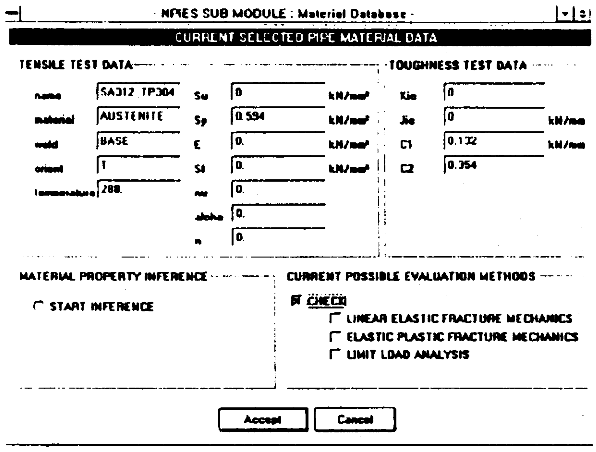

FIGURE 9. DATABASE SCREEN BEFORE INFERENCE FOR CASE I

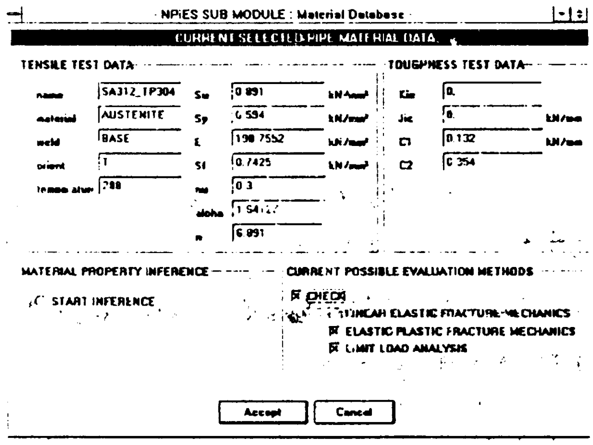

FIGURE 10. DATABASE SCREEN AFTER INFERENCE FOR CASE I

TABLE 4. ANALYSIS RESULTS OF CASE I

Crack Shape	Method	SF*	SF**	Diff.*** (%)
Axial Semi-Elliptical	CDFD	2.76	2.55	8
	J/T	-	-	-
	DPFAD	2.96	2.46	20
	Limit Load	4.12	3.29	25
Long Axial	CDFD	1.74	1.69	3
	J/T	1.91	1.62	8
	DPFAD	1.98	1.66	19
	Limit Load	3.82	3.06	24

SF* :Safety factor when inferring σ-ε curve from S_y value.

SF** :Safety factor when all material properties are fully given.

$$\text{Diff.}^{***} = \frac{SF^{*} - SF^{**}}{SF^{*}} \times 100$$

Case II : Inferring σ-ε curve from S_y and S_u values

This case study is when the yield strength (S_y) and the ultimate strength (S_u) are given instead of full σ-ε curve. After the inference, unknown material properties are obtained as; $\alpha = 10.99$, $n = 1.68$ and $E = 197$ GPa.

EPFM analyses were performed and the results are summarized in Table 5. As shown in the table, the maximum difference between the Case II and the reference case is within 15%.

TABLE 5. ANALYSIS RESULTS OF CASE II

Crack Shape	Method	SF*	SF**	Diff. (%)
Axial Semi-Elliptical	CDFD	2.86	2.55	12
	J/T	-	-	
	DPFAD	2.65	2.46	8
	Limit Load	3.59	3.29	9
Long Axial	CDFD	1.77	1.69	5
	J/T	1.85	1.62	14
	DPFAD	1.68	1.66	1
	Limit Load	3.53	3.06	15

SF* : Safety factor when inferring σ-ε curve from S_y and S_u values
SF** :Safety factor when all material properties are fully given.

This case study shows that the additional knowledge of S_u improves the analysis accuracy in the DPFAD method and the limit load method.

Case III : Inferring J-R curve from ε_c value

This case study is when the J-R curve of the pipe is not given. From tensile property, the J-R curve is obtained as; C_1 = 321 (kN/m), C_2 = 0.38.

EPFM analyses were performed and the results are summarized in Table 6. Since the limit load analysis is not affected by the J-R curve, it is not considered here. As shown in the table, the maximum difference between the Case III and the reference case is within 33%

TABLE 6. ANALYSIS RESULTS OF CASE III

Crack Shape	Method	SF*	SF**	Diff. (%)
Axial Semi-Elliptical	CDFD	2.97	2.55	16
	J/T	-	-	-
	DPFAD	3.00	2.46	22
Long Axial	CDFD	2.08	1.69	23
	J/T	1.47	1.62	9
	DPFAD	2.21	1.66	33

SF* : Safety factor when inferring J-R curve from ε_c value.
SF**: Safety factor when all material properties are fully given.

EPFM analyses cannot be processed without material's J-R curve in a majority of software. However, this case study shows that NPiES system still provides analysis results with reasonable accuracy even though J-R curve is not given.

CONCLUSION

NPiES system has been developed to evaluate the nuclear piping integrity. The system is designed such that the most appropriate integrity evaluation method for given information is selected based on the possession ratio of material property and the unknown material property is obtained through inferring the known material property. Several case studies were performed and the usefulness of NPiES system was demonstrated.

REFERENCE

ASME, 1992, "ASME Boiler and pressure vessel code, Section XI

Bloom, J.M. and Malik, S.N., 1982, "Procedure for the assessment of the integrity of nuclear pressure vessels and piping containing defects", EPRI NP-2431.

Chexal, V.K., Norrs, D.M. and Server, W.L., 1988, "Leak-Before-Break : An integrated approach for high energy piping", Int. J. Pres. Ves. & Piping, Vol.34, pp.237-254.

Kim, Y.J., Choy, Y.S., Seok, C.S., Yang, K.M., Ra, I.S. and Ahn, H.Y., 1993, "Fracture properties evaluation of BOP piping system for the Yonggwang 3&4 nuclear generating station" Trans. of the 12th SMiRT Conference, Vol.G., pp.435-440.

Kim, Y.J., Seok, C.S., Choy, Y.S. and Chang, Y.S., 1995, "Prediction of fracture resistance curve from tensile data", ASME-PVP Conference, Vol.304, pp. 277-284.

Kussmaul, K., Jovanovic, A. and Maile, K., 1991, "Expert system based life assessment of high temperature components", Trans. of the 11th SMiRT Conference, Vol.SD1, pp.73-84.

Lucia, A.C. and Volta, G., 1991, "A knowledge based system for structural reliability assessment", Trans. of the 11th SMiRT Conference, Vol.SD1, pp.91-96.

Okamodo, A., Kataoka, S. and Watanabe, M., 1987, "The development of expert system for defect identification and its assessment", Trans. of the 9th SMiRT Conference, Vol.B, pp.247-252.

13 Recent Progress in Korean Nuclear PLIM Progeam

T.E. Jin*, H.J. Choi (KOPEC), I.S. Jeong, S.Y. Hong (KEPCO)

Recent Progress in Korean Nuclear PLIM Program

Tae Eun Jin, Hyung Jip Choi, Korea Power Engineering Company
Ill-Seok Jeong, Sung-Yull Hong, Korea Electric Power Corporation

---

Summary

The recent developments in Korean nuclear power plant lifetime management program which has been performed for the last three years is introduced, together with the descriptions of maintenance activities. This leading Korean PLIM project has been focused on such areas as plant data survey, transient history, screening and prioritization of systems, structures and components (SSC), aging evaluation of major components and other supporting activities. The current status is outlined in terms of major tasks including aging evaluation of thirteen major components. The future long-term plan which eventually aims at maximizing the economic benefit for both the utility and its customers is presented. Also described is, from the viewpoint of plant life extension, the technical development.

1 INTRODUCTION

Nuclear power plant (NPP) technologies in Korea have been remarkably evolved since the commercial operation of Kori Unit 1 in 1978. As shown in Table 1, ten nuclear power plants are under commercial operation, while six nuclear plants are under construction and another seven nuclear plants are scheduled to be constructed.

In the early era of NPP industry, a vast amount of efforts had been devoted in Korea to accumulate the technology and experiences related to the plant construction. As time passes, plant aging and maintenance problems became a matter of concern in the NPP industry. Under these circumstances, Plant Lifetime Management(PLIM) of nuclear power plant attracts attention and is considered as an effective way to address this issue. This is because the PLIM has a strong possibility not only to solve the plant aging and maintenance problems but also to provide the vision of extended plant operation beyond the design lifetime.

As part of the long term nuclear technology development program by Korea Electric Power Corporation(KEPCO), the plant lifetime management project named "Nuclear Plant Lifetime Improvement and Management(I)" was started in November 1993 to cope with the aging and obsolescence of Kori Unit 1. At this stage of PLIM phase I, the project aims at a feasibility study of lifetime management of Kori Unit 1 together with the aging evaluation of the thirteen major components. The results of the PLIM(I) are expected to influence the decision making of long-term Kori Unit 1 lifetime improvement. Subsequently, the PLIM Phase II (Detail Lifetime Evaluation and Engineering) will be performed, in which the workscope and schedule are subjected to the outcomes of the feasibility study.

Table 1. Status of Nuclear Power Plants in Korea

Plant	Capacity (MW)	Operation	Type	Supplier		Construction	Remarks
				Reactor	T/G		
Kori #1	578	1978.4	PWR	W	GEC	Turn Key	
Kori #2	650	1983.7	PWR	W	GEC	〃	
Wolsong #1	700	1983.4	PHWR	AECL	Parsons	〃	
Kori #3	950	1985.9	PWR	W	GEC	Non-Turn Key	
Kori #4	950	1986.4	PWR	W	GEC	〃	
Yongwang #1	950	1986.8	PWR	W	W	〃	
Yongwang #2	950	1987.6	PWR	W	W	〃	
Ulchin #1	950	1988.9	PWR	Framatome	Alstome	〃	
Ulchin #2	950	1989.9	PWR	〃	〃	〃	
Yongwang #3	1000	1995.3	PWR	KHIC/KAERI	KHIC/KAERI	Localized	Korean Standard
Yongwang #4	1000	1996.4	PWR	KHIC/KAERI	KHIC/KAERI	Localized	Korean Standard
Wolsong #2	700	1997.6	PHWR	AECL	〃	〃	
Ulchin #3	1000	1998.6	PWR	KHIC/KAERI	〃	〃	Korean Standard
Wolsong #3	700	1998.6	PHWR	AECL	〃	〃	
Ulchin #4	1000	1999.6	PWR	KHIC/KAERI	〃	〃	Korean Standard
Wolsong #4	700	1999.6	PHWR	AECL	〃	〃	
New PWR #1	1000	2001.6	PWR	Not Decided	Not Decided	Localized	Korean Standard
New PWR #2	1000	2002.6	PWR	〃	〃	〃	Korean Standard
New PWR #3	1000	2003.6	PWR	〃	〃	〃	Korean Standard
New PWR #4	1000	2004.6	PWR	〃	〃	〃	Korean Standard
New PWR #5	1000	2005.6	PWR	〃	〃	〃	Korean Standard
New PHWR#1	700	2006.6	PHWR	〃	〃	〃	
New PWR #6	1000	2006.6	PWR	〃	〃	〃	Korean Standard

This paper thus introduces KEPCO's basic PLIM strategy, some recent developments in the on-going PLIM(I) and other works related to the lifetime management of Kori Unit 1. To date, field data survey, system/structures screening, components prioritization, fracture mechanics test of Kori Unit 1 reactor pressure vessel surveillance coupons and component aging evaluation of major components have been done. Other activities such as the economic analysis, regulatory considerations and key technology reviews remain to bo completed by the end of 1996.

2 KEPCO PLIM PROGRAM

The primary goal of KEPCO PLIM is to operate a plant safely and economically up to the plant specific design life. If the first goal is possible, then the operation of the nuclear power plant beyond the design life to the optimum life will be pursued as the second goal. Furthermore in parallel with the PLIM project, key technologies required for supporting the lifetime management are being developed. A specific feasibility study evaluates each plant's optimum lifetime which then becomes the target life of the PLIM efforts. The second goal of the PLIM program is to operate a plant up to the optimum lifetime. If such an optimum lifetime is longer than the design life, additional activities to operate the plant beyond the design life shall be incorporated in the long term preventive or predictive maintenance program.

The master plan for PLIM including the lifetime extension of Kori Unit 1 and other NPPs in Korea is composed of three phases with Kori Unit 1 being regarded as a leading model plant of technology development. Such categorization generically stems from the level of details and refinement that are to be accomplished during each phase of the project. In Phase I, feasibility of extending the lifetime of Kori Unit 1 in terms of technical, regulatory, economic aspects is established including aging evaluations of the prioritized thirteen major components. Phase II program will perform the detailed lifetime evaluation of the major components and other critical components screened in Phase I. The PLIM implementation plan for Phase III will be recommended based on the results obtained in the preceding Phases. For reference, overall descriptions for the phased PLIM programs are outlined in Table 2. This long term plan subjected to changes in accordance with the outcomes of the PLIM(I) feasibility study.

Table 2. Three Phases of the PLIM Program

Phases	Period	Contents
Phase I	1993 ~ 1996	Feasibility Study o Feasibility evaluation method and techniques o Kori Unit 1 PLIM feasibility o Phase II planning
Phase II	1997 ~ 2001	Detail Evaluation and Engineering o Kori Unit 1 detailed inspection and residual life evaluation o Documentations for license renewal o Planning for life extension
Phase III	2001 ~ 2008	Refurbish, Replace and Maintenance o Implementation o Advanced technology development

3 KORI UNIT 1 PLIM PROGRAM

3.1 PHASE I

The phase I workscope consists of the following ten tasks and is described in the sequence.

- o Task 1 : PLIM project plan and design life review
- o Task 2 : Screening major SSC's
- o Task 3 : Data survey and review
- o Task 4 : Evaluation of reactor pressure vessel
- o Task 5 : Evaluation of major SSC's
- o Task 6 : Monitoring systems for PLIM
- o Task 7 : Survey and review of PLIM regulation

- o Task 8 : Economic evaluation
- o Task 9 : PLIM technology development
- o Task 10: Feasibility study reports

3.1.1 Design life review

The major workscope of this task involves overall project planning and establishment of design life for the Kori Unit 1. Especially, the basis for 30-year design life of the Kori Unit 1 is reexamined, together with the provision of feasible amendments of its design life from 30 to 40 years. According to the archival documents survey, the design life of major components in Kori Unit 1 including the reactor pressure vessel is confirmed to be 40 years.

3.1.2 Screening and Prioritization

Critical component identifications for aging evaluation are an important part of the PLIM Phase I efforts, because to identify which components are crucial to the plant lifetime is necessary to ensure the proper focus of Phase I efforts at the beginning of the PLIM program. These critical components were identified though the application of Westinghouse Owner's Group (WOG) screening and prioritization criteria to the Kori Unit 1 system, structures and components.

The screening process applies safety-related criteria which are based upon the US NRC's license renewal rule (LR) and maintenance rule (MR) which are 10CFR54 and 10CFR50.65 respectively. Additionally, the screening process applies power production(PP) related criteria which are based on plant availability.

After screening the Kori Unit 1 systems and structures, critical components and structures were identified and prioritizes to determine their relative importance. Prioritization of Kori Unit 1 critical components applies ten attributes which were selected to assess the impact that either the replacement or refurbishment of these critical components would have on the decision to improve design life. For example, these attributes are cost to replace or refurbish, impact on plant availability and radiation dose, etc.

Prioritization result shows a similar result to the previous experiences.

3.1.3 Data Survey

As a prerequisite to the evaluation of the plant aging status, a huge amount of design and field data of Kori Unit 1 accumulated since commercial operation should be surveyed and reviewed. Even though tremendous man-power to re-produce useful data from the raw materials is required, data survey is the most important job that has to be done in the process of compiling operating transient numbers. Such data required for the PLIM (I) can be classified as follows.

- o General methodology and technical references
- o Operating transient history
- o Component design specification and manufacturing data
- o Maintenance and inservice inspection data

3.1.4 Major Components Life evaluation

In order to evaluate the aging status of Kori Unit 1, the following major components were selected at the beginning of the PLIM (I). All major components were ranked within top twenties of the component prioritization results.

- o Reactor pressure vessel
- o Reactor vessel internals
- o Control rod drive mechanisms
- o Reactor coolant system piping
- o Reactor coolant system charging and safety injection nozzles
- o Pressurizer
- o Pressurizer surge and spray lines nozzles
- o Reactor coolant pump
- o Reactor pressure vessel supports
- o Turbine
- o Generator
- o Containment
- o Cables

Subsequently, the stressors and the degradation sites and mechanisms in conjunction with the resulting failure modes and their operating history are identified through the appropriate tests and technical evaluations. In consequence, the task ends up with quantitative evaluations of the plausible age-related degradation mechanisms, with the aid of proven technical papers collected by literature survey and the generic technical procedures published by the off-shore organizations who performed life management study previously. Table 4 shows a life evaluation methodology with the reactor pressure vessel as an example.

Special attention is paid to the reactor pressure vessel for its significant importance in the nuclear PLIM program. Fracture toughness test of the WOL specimens from the Kori Unit 1 surveillance capsule irradiated for 34 EFPY showed that the fracture toughness of Kori Unit 1 beltline weld material is almost identical to that of other Linde 80 flux weld metals and better than the criteria of the fracture resistance curve proposed by the US. NRC draft regulatory guide DG-1023. For the comprehensive integrity assessment of the reactor pressure vessel, the pressurized thermal shock criteria of 10CFR50.61 is being applied to the Kori Unit 1.

In some cases where the design data are difficult to obtain, full engineering calculations

Table 4 - Summary of Evaluation Procedure for Reactor Pressure Vessel

sub-components	Specific ISI	Degradation Evaluation	Recommendations
Beltline Region	o No crack found o Pressure Vessel : SA508 Cl.2 low alloy steel o Weld Material: Linde 80 Flux Mn-Mo-Ni filler wire o Beltline Welding : B&W WF-233 (Cu 0.29 wt%)	**Radiation Embrittlement** o Verify with surveillance Coupon Test Result :2 criteria - Revise P-T Limit Curve with the Test Result o RT_{NDT} Transition - RT_{NDT} = initial RT_{NDT} + Margin - below 300 F during plant operation o Upper Shelf Energy(USE) - Unless satisfy 50 ft-lb, perform low fracture toughness test o Low fracture toughness test & elastic/plastic analysis - Verified safety up to 34EFPY **Fatigue** : simple method o Analyze cumulative usage Factor (CUF) using S_{ALT}, N_f design transient n_i of design stress report(DRS) & actual operating transient count n_k	o If RT_{pts} ≥ 300°F during lifetime, perform Plant Specific PTS o Rescreen PTS with revised PTS rule & additional surveill. test result o Flux reduction o Archive material test plan o Survey RPV thermal annealing trend o Environmental fatigue analysis trend review o Under clad cracking review
Outlet/Inlet Nozzle	o PSI found a crack at welding point at Outlet Nozzle to Shell o Verified it as no significant indication by the 2nd & 5th ISI o Confirm it as geometric by the 8th ISI	**Fatigue** : simple method o Analyze CUF using S_{ALT}, N_f, Design transient n_i of DSR and actual operating transient counts n_k	o For the point where U_{CNEW}≥ 0.67, detail fatigue analysis o Fatigue transient monitoring o Advanced ultrasonic technique
Instrumentation Nozzles and CRDM Housing Nozzles	o No crack found	**Fatigue** : Negligible CUF of 0.02 & 0.00 in DSR, no fatigue analysis required **PWSCC** : No PWSCC reported yet	o Detail inspection & analysis for life improvement
Flange Closure Studs	o No crack found	**Fatigue** : Analyze CUF using S_{ALT}, N_f, design transient n_i of DSR & actual operating transient counts n_k	o Replace for life improvement

are performed to establish the necessary data set. The PLIM (I), for instance, conducted fatigue lifetime evaluation of the Kori Unit 1 pressurizer surge line nozzle with the commercial finite element package, NISA, in order to provide an evaluation procedure of stress analysis and residual fatigue life. The result of this study demonstrated a very good agreement with that of the vendor design stress report which did not show the calculating procedure like a black box. In the end, the residual fatigue life of the nozzle operated for 15 years was sufficient to meet the first goal of Kori Unit 1 PLIM, that is 40 years.

3.1.5 PLIM Regulation Review

Regulatory rules are intended to guide the nuclear PLIM in a proper way. The preliminary survey about overseas license renewal trend and rule development is necessary to direct a domestic policy of rule making in the near future. The government body, the Ministry of Science and Technology, and its agency, Korea Institute of Nuclear Safety, are currently in charge of nuclear power plant licensing and other license-related issues in Korea. KEPCO provides such regulatory bodies with information and interim results of the PLIM study to help pro-actively the rule making.

3.1.6 Monitoring Systems for the PLIM

Prior to and in parallel with the further detailed evaluation of major components, the development and utilization of monitoring systems deserve due considerations. In this task, the currently available monitoring systems for the PLIM are thus be studied, together with the identification of degradation sites to be monitored.

3.2 RESEARCH ACTIVITIES

In addition to the feasibility study, five R&D items are under way in the areas of radiation embrittlement, corrosion and cracking, water chemistry, non-destructive examination, and aging of cable and I&C. Namely,

o Utilization of small or reconstituted specimens of reactor pressure vessel materials
o Pb stress corrosion cracking of steam generator tubes
o Evaluation of hideout return and steam generator crevice conditions
o Natural cracked small pipe specimen and defect signal analysis
o Destructive test of thermal and radiation exposed cable

3.3 COMPONENT REPLACEMENT

Kori Unit 1 steam generators, Westinghouse model WH-51, one of which has 3,388 Inconell 600MA tubes, have gone through a lot of maintenance works such as plugging, sleeving and chemical cleaning due to tube pitting/denting and primary water stress corrosion cracking.

The feasibility study for the steam generator replacement at Kori Unit 1 has already been completed on a separate basis from the PLIM project currently under consideration. Taking the plausible plant lifetime extension into account, both the deterministic and probabilistic economic evaluations of the related issues indicated that near-term replacement of steam generators with some plant rerating provides the most economically favorable option. The other optional scenario aimed at avoiding or postponing steam generator replacement by sleeving/plugging maintenance strategy turned out to be less cost-effective strategy. The necessary ensuing actions will then be taken regarding the steam generator replacement. KEPCO plans to replace it with Inconell 690TT tubes and stainless steel broached support plate by 1998.

According to the field inspection of Kori Unit 1 low pressure turbine rotor disc, many cracks were found at disc, dowel hole, and disc head due to moisture induced intergranular stress corrosion cracking. To verify the safe operation of the turbine with the fracture mechanics analysis, KEPCO provided a mitigation to re-inspect and repair the cracks during the next outage and then, however, determined to replace the rotor and diaphragm of the low pressure turbines with welding or mono-block type rotor.

4 SUMMARY

Nuclear PLIM is at present one of the most important tasks in Korean nuclear industry as Kori Unit 1, the first commercial nuclear unit, is being aged. This paper introduces

KEPCO's basic PLIM strategy, long-term plan, current interim results of Kori Unit 1 PLIM feasibility study and other related programs.

The feasibility study includes field data survey, screening and prioritization of the SSC's, component aging evaluation, and stress and fatigue analysis of pressurizer surge line nozzle. Fracture mechanics test of Kori Unit 1 reactor pressure vessel surveillance coupon was completed and the pressurized thermal shock study is recommended. In the remaining period of PLIM (I) project, further evaluation of major component aging, review of regulatory issues, and economical evaluation of Kori Unit 1 PLIM program, are expected to be done for the PLIM from the viewpoint of economic aspects.

Other projects that have to be considered for PLIM, such as process computer and I&C upgrade, plant uprating, probabilistic safety analysis and reliability centered maintenance are going to be undertaken separatedly It is anticipated that PLIM will provide a good way of long term life management of nuclear power plants in the cost-effective manner in Korea.

References

1. Korea Electric Power Corporation. 1994 White Paper of Korean Nuclear Power Plants, 1995
2. US. Nuclear Regulatory Commission. 10CFR Part 54, Requirements for Renewal of Operating Licenses for Nuclear Power Plants
3. US. Nuclear Regulatory Commission. 10CFR Part 50.65, Requirements for Monitoring the Effectiveness of Maintenance at Nuclear Power Plants
4. U.S. Nuclear Regulatory Commission. raft Regulatory Guide DG-1023, Evaluation of Reactor Pressure Vessels with Charpy Upper-Shelf Energy Less than 50 ft-lb, September 1993.
5. U.S. Nuclear Regulatory Commission. 10CFR Part 50.61, Fracture Toughness Requirements for Protection Against Pressurized Thermal Shock

CONTENTS

1. Historical Evolution of Korean Regulatory System

Korea has one of the most dynamic nuclear power programs in the world. During the last couple of decades, Korea has carried out a very ambitious nuclear power program as part of the national energy policy aimed at reducing the external vulnerability and insuring against the global fossil fuel shortage. The first Nuclear Power Plant (NPP) began its commercial operation in 1978. Now 11 units are in operation providing almost 50% of electricity in Korea. Seven units are under construction at the moment and 4 more units will be built by 2006. The current status of NPPs in Korea is summarized in Tablel 1.

Back in the beginning period of NPP operations from 1971 to 1978, the first commercial nuclear power program was implemented on a turnkey base. Kori Units 1 and 2 were ordered from Westinghouse, U.S.A. in 1969 and 1974, respectively and Wolsong Unit 1, the first CANDU plant, was ordered from the AECL, Canada in 1973. Contractors assumed overall responsibility for the construction schedule, inspection, startup and performance of the plants. During this period, domestic laws and regulations applicable to the licensing of NPP were not yet fully developed. Therefore the vendor countries' laws and regulations such as 10 CFR, Reg. Guide and Standard Review Plan (SRP) of USNRC were applied to the licensing review of Westinghouse PWRs. As for the CANDU plant, Canadian laws and regulatory requirements were applied as mandatory requirement. Construction permit (CP) and operating license (OL) were applied simultaneously in March 1976, as can be seen in the Canadian combined licensing approach and CP/OL was issued in 1978.

From the early 1980s, six NPPs (Kori Unit 3&4, Yonggwang Units 1&2, Ulchin1&2) were constructed by employing a component approach with foreign contractors. Contracts were awarded separately for major components of plants, thus enabling more domestic industries to participate as subcontractors in the projects. While on the regulatory and licensing side, the Nuclear Safety Center (NSC) was established in December 1981 as a regulatory expert organization, which was the predecessor of today's Korea Institute of Nuclear Safety (KINS). Two step licensing system, construction permit (CP) and operating license (OL), was formally incorporated into the law. However, the majority of important codes and standards applicable in the vendor countries (U.S. and France) were still applied to the licensing of these six plants only with some appropriate modifications. As for CANDU plant, the Final Safety Analysis Report (FSAR) was submitted by Korea Electric Power Co.(KEPCO) in 1982 according to the newly amended law and the

FSAR was reviewed once again at the NSC in order to confirm the design safety.

Starting from Yonggwang Units 3 & 4 contracts in 1987, Korea Power Co. (KEPCO) had assumed the overall management and responsibility for construction projects. The overriding priority for selecting suppliers was the condition of transferring higher nuclear technology to Korea. The prime contractors were domestic companies instead of foreign companies and several foreign companies were selected as subcontractors. The same approach applied to the contracts for Ulchin Units 3 & 4, and it will apply to the units that follow in the future.

In the licensing of Yonggwang Units 3 & 4 for construction, some regulatory difficulties emerged due to the scaled-down design from the reference plants of Combustion Engineering Co. (CE) designed Palo Verde's System-80. With intensive audit calculations and the third party verification in the area of safety analysis together with the technical support of the USNRC and the IAEA, the CP was issued to Yonggwang Units 3 & 4. Ulchin Units 3 & 4, which are the first standard units with substantially the same design features as Yonggwang Units 3 & 4, were licensed for construction with some conditions for implementing safety enhancement regarding mid-loop operation, safety depressurization system and hydrogen ignitors as part of severe accident mitigation, and ALARA. Recently, the licensing review for CP of Yonggwang Units 5 & 6 has been performing and several items has been investigated to enhance the safety such as, level control in CVCS, digitalization and duplication of the process control system, human factors in the remote shutdown system, PSA for low power and shutdown, the filtered vent system, etc.

Safety review for the construction permit(CP) of Wolsong units 2, and 3&4 had been conducted since 1991, and the CPs were issued in August 1992 for Wolsong 2, and in February 1994 for Wolsong 3&4. Operating licensing review for Wolsong 2 has been performing since May 1995 and the OL is scheduled in August 1996. Regulatory efforts during the CP stage have been focused on the following aspects; First, intensive review on the design changes/improvements compared with Wolsong 1. Second, applicability of the PWR safety issues to the units within a practical manner for the safety enhancement equal to or above international level. Third, design suitability and environmental effect arising from the construction and operation of multiple, 4, units at Wolsong site. Several domestic and foreign experts were invited to participate in the special review areas where high technology and accumulated experience were required.

A significant progress has been made so far in the development of Korean regulatory criteria, guides and procedures which are applicable to the standardized nuclear power plants, too. Industrial codes and standards are under development and will be completed in several years. Since the operating nuclear power plants are subject to deterioration due to ageing, appropriate aging management program such as periodic safety review (PSR) with the emphasis on probabilistic safety assessment (PSA) has been actively proposed and studied at the KINS. This will lead to the establishment of regulatory requirements for license renewal. In this regard too, Korea will keep collaborating, with the advanced countries, particularly with the vendor countries such as U.S.A, France and Canada.

During the safety review of foreign designed nuclear power plants, the licensing difficulties have been encountered mainly from diversified reactor types and vendor countries. The lessons have been learned from taking appropriate measures for the trouble-shooting of these problems such as difference Codes and Standards and differences in Regulatory Procedures and Practices

In this regard, Korea's long-term nuclear research and development program calls for a progressive design improvement for existing PWRs and PHWRs as well as for those to be built up to 2006. After that, next generation reactors will be developed and introduced in Korea.

Therefore, pertinent regulatory positions will be established step by step, keeping pace with the aforementioned nuclear R&D program, in terms of safety regulatory and licensing system, procedures, design requirements, codes and standards, etc.

Table 1. Nuclear Power Plants in Korea

Plant	Reactor Type	Capacity (MWe)	Reactor Manufacturer	T/G Manufacturer	Commercial Operation (Expected)
Kori					
Unit 1*	PWR	587	Westinghouse	GEC	1978.4
Unit 2*		650			1983.7
Unit 3*		950			1985.9
Unit 4*		950			1986.4
Wolsong					
Unit 1*	PHWR	678.7	AECL	Parson	1983.4
Unit 2**		700		KHIC/GE	(1997.6)
Unit 3**		700		KHIC/GE	(1998.8)
Unit 4**		700		KHIC/GE	(1999.8)
Yonggwang					
Unit 1*	PWR	950	Westinghouse	Westinghouse	1986.8
Unit 2*		950	Westinghouse	Westinghouse	1987.6
Unit 3*		1,000	KHIC/GE	KHIC/GE	1995.3
Unit 4*		1,000	KHIC/GE	KHIC/GE	1996.1
Unit 5**		1,000	KHIC	KHIC	(2001)
Unit 6**		1,000	KHIC	KHIC	(2002)
Ulchin					
Unit 1*	PWR	950	Framatome	Alsthom	1988.9
Unit 2*		950	Framatome	Alsthom	1989.9
Unit 3**		1,000	KHIC	KHIC	(1998.6)
Unit 4**		1,000	KHIC	KHIC	(1999.6)
Unit 5***		1,000	KHIC	KHIC	(2003)
Unit 6***		1,000	KHIC	KHIC	(2004)
New Entry	+	1,000	-	-	(2005)
	+	1,000	-	-	(2006)

* In Operation : 11 Units

** Under Construction :7 Units

*** Planned : 2 Units

\+ Reactor type will be determined by Nov. 1996.

2. Nuclear Regulatory Structure in Korea

In order to carry out the nation's nuclear power projects successfully, nuclear safety has to be assured through all stages of project development, including site selection, design, manufacturing, construction, operation and decommissioning.

The basic concept of nuclear safety in Korea, as in other countries, is not only to protect the plant crew and neighboring inhabitants from radiation hazards but also to minimize the subsequent from radiation and keep the radiation effects as low as reasonably achievable. This concept is basically underlined in the Atomic Energy Act of Korea, which provides the legal foundation for nuclear activities. Regulation and licensing of nuclear facilities in Korea are based on the provisions of the Atomic Energy Act, Enforcement Decree and Enforcement Regulation, Notice of the Minister of the MOST and Technical Specifications which are parts of the safety analysis reports (refer to Table 2).

The ultimate responsibility for the safety of a nuclear power plant (NPP) rests with the operating organization. The government, the Ministry of Science and Technology (MOST), has in nature a general responsibility for ensuring the protection of public health and safety by the regulatory control and safety inspection on a government level. The Korea Institute of Nuclear Safety (KINS), entrusted with the regulatory works by the government, performs a detailed assessment of the technical submissions and an inspection of nuclear facilities as a technical expert group.

In conformity with the atomic energy laws, the licensee should submit to the MOST various documents demonstrating the adequacy of the proposed design. It is then the task of KINS, to review the licensing documents and to determine whether the design complies with the specified safety requirements for siting, construction and operation of the proposed nuclear installations. The result of the technical review and assessment is reported to the government and then the MOST issues a permit or license to the utility based on the KINS' assessment report.

Nuclear safety inspection and enforcement are of vital importance to ensure that all activities at nuclear installations are in conformity with the regulatory requirements and licensee commitments. The MOST, the KINS and their regional offices at each nuclear power plant site have the responsibility to assign inspectors to manufacturing facilities, construction sites and operating nuclear installations in order to conduct nuclear safety inspections.

The fundamental regulatory structure in Korea is schematically described in Figure 1.

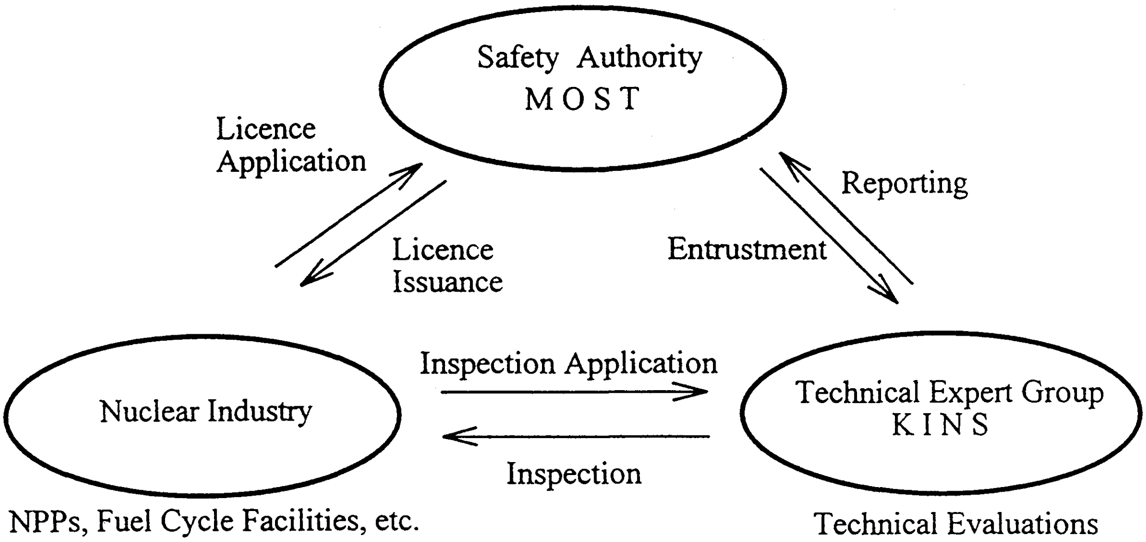

Fig.1 Fundamental Framework

Table 2. Legislative System of Atomic Energy Laws

Classification	Major Characteristics	Matters Concerning Technical Standards
Atomic Energy Act (Law)	Provides the basis for development and safety regulations of atomic energy (enacted March 1958, amended April 1982, amended May 1986)	- Provisions of requirements for construction permits and operating licenses for reactors - Provisions of requirements for permits for manufacturing enterprises of reactors and main components - Provisions of requirements for permit or designation for nuclear fuel cycle enterprises - Provisions of requirements for permits to use radioisotope and radioactive materials
Enforcement Decree of Atomic Energy Act (Presidential Decree)	Provides administrative and technical guidelines necessary for enforcement of Atomic Energy Act. (enacted September 1982)	- Standards for location, structure, facility, performance and operation of reactor facilities - Standards for location, structure, facility, physical security, and operation of nuclear fuel cycle facilities - Standards for radioisotope and radiation generating devices - Standards for transport, package and disposal of radioactive materials
Enforcement Regulation of Atomic Energy Act (Prime Ministerial Ordinance)	Provides the means for enforcement of Atomic Energy Act and Enforcement Decree of Act. (enacted April 1983)	- Standards for preparation of safety analysis report, environmental impact statement report, and notification of design and construction methods - Standards for security regulations - Standards for installation of radiation area and measurement of radiation dose
Notice of the Minister of Science and Technology	Provides in detail the administrative procedure and technical standards guides based on the atomic energy laws	- Detailed standards for radiation dose, *etc.* - Standard for preparation of operational technical specifications - Standards for technical capability and quality assurance program relevant to manufacturing permit - Guide for preparation of environmental impact statement report - Regulation of periodic inspection of reactor facilities - Technical standards for location, structure and equipment of reactor facilities

3. The Activities of the Korean Regulatory Organizations

The nuclear regulatory organizations in Korea are composed of three parts, namely, a national level decision-making body represented by the Atomic Energy Commission (AEC), a regulatory authority with enforcement power represented by the Ministry of Science and Technology (MOST) of the Korean Government and a technical expert group established to support the MOST with its technical expertise in the development of nuclear regulatory policy and also in the enforcement of nuclear safety laws and regulations, which is represented by the Korea Institute of Nuclear Safety (KINS).

The nuclear regulatory system is described schematically as follows :

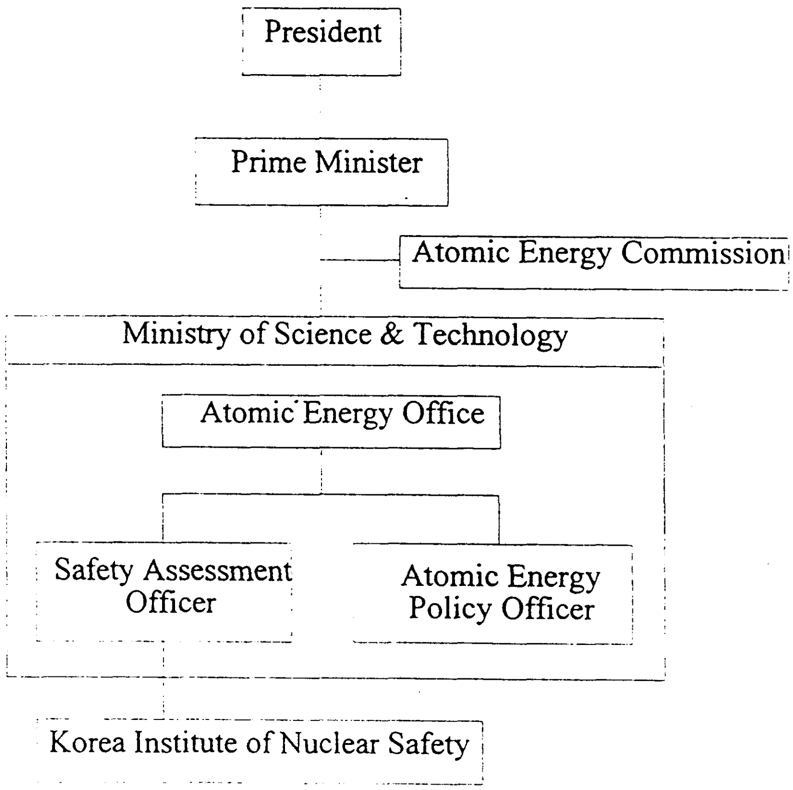

Fig. 2 Nuclear Regulatory Organization in Korea

The activities of AEC, the MOST and the KINS in the area of safety of NPPs can be summarized as follows:

- Atomic Energy Commission (AEC)

The Atomic Energy Commission (AEC) is chaired by the Deputy Prime Minister. The principal function of the Commission is decision-making on major nuclear policy issues such as R & D on a national level, industrial projects, and safety regulations.

The Special Committee on Nuclear Safety (SCNS) was established under the Commission in November 1989. The SCNS performs deliberations on the outstanding safety issues identified or developed in the licensing review process or various inspections by the KINS. Based on the deliberation by the SCNS, the AEC rules on the safety issues contained in the license application documents, then a license is issued by the Ministry of Science and Technology (MOST).

- Ministry of Science of Technology (MOST)

The MOST is the governmental organization responsible for establishing and implementing nuclear regulatory policies for the regulation of nuclear activities related to power and research reactors and radiation applications. It is also responsible for making nuclear research and development policies for peaceful uses of nuclear energy.

The MOST has the Atomic Energy Office under its framework, headed by the Assistant Minister who is supported by the Atomic Energy Policy Officer and the Nuclear Safety Officer. The MOST operates the Resident Inspectors Office at each plant site for the daily routine inspection of the plant.

- Korea Institute of Nuclear Safety (KINS)

The Korea Institute of Nuclear Safety was established in February 1990 through special legislation by the National Assembly. .The KINS is a technical expert group established to support the MOST with its technical expertise in the development of nuclear regulatory policy and also in the enforcement of nuclear safety laws and regulations. Entrusted by the government (Ministry of Science and Technology) in accordance with the Atomic Energy Act, KINS is responsible for :

. Safety review and evaluation to assure the safety of nuclear installations;
. Safety inspection for nuclear installations;
. Technical standards development;
. Radioisotopes and Radiation Generators Regulation ; and,
. Development of regulatory policy.

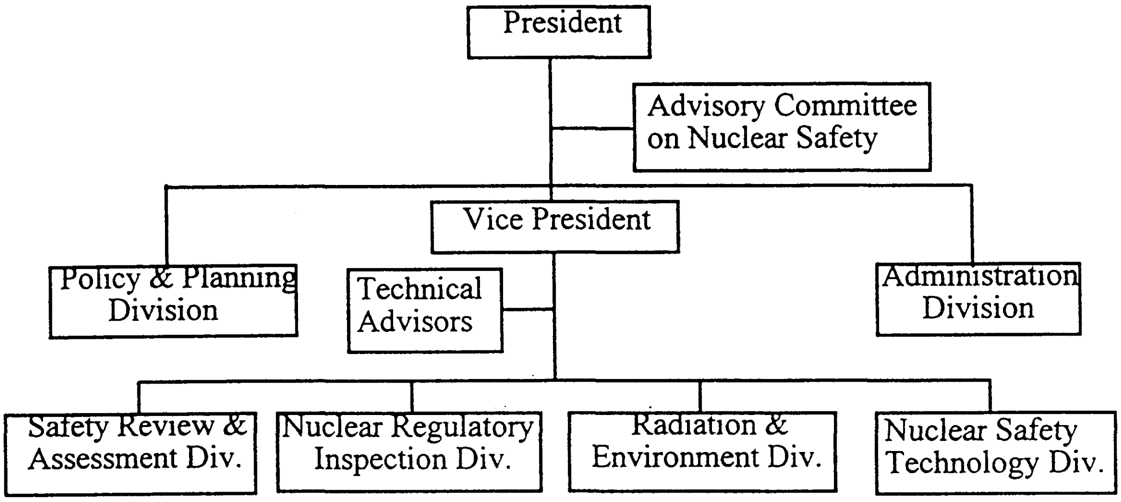

Figure 3 Korea Institute of Nuclear Safety Organization

4. Licensing Procedure for NPPs

The licensing procedure for NPP in Korea consists of two steps, in general, i.e., Construction Permit (CP) and Operating License (OL). The detailed licensing procedure for NPP is summarized in Figure 4

The basic philosophy behind licensing reviews in Korea is to lead the industry towards the achievement of higher safety levels for the proposed nuclear power plant, compare to the previous ones by progressively incorporating the design improvements. To achieve this goal, special attention should be paid to the following items during the licensing reviews :

- Feedback of domestic and foreign operating experiences.
- Application of new regulatory requirements.
- Incorporation of the improved design features of the evolutionary LWR's
- Evaluation of safety features against the severe accident.
- Establishment of well-defined Quality Assurance Program for major equipment and components.
- Independent assessment of computer codes and methodology used in safety analysis.

● Construction Permit (CP)

The review objectives of CP are to confirm the safety of the proposed NPP design, which should meet the related regulatory codes and standards, and to review the safety of the preliminary designs which include the principles and concepts of the plant's design and the implementation of the regulatory criteria, and also to evaluate the environmental impact and the strategy for minimizing its effects.

The main documents required for the application of CP consist of Preliminary Safety Analysis Report (PSAR) and Environmental Report (ER). Site Survey Report and Detailed Geological Survey Report are also required for the application of Early Site Approval and Limited Work Authorization before the construction permit.

● Operating License (OL)

For the OL, the safety of NPP operation is evaluated by confirming that the final design meets the acceptance criteria. The main documents required of the OL application are Final Safety Analysis Report (FSAR), Technical Specifications, Radiological Emergency Plan.

When changes or modifications are to be made on the nuclear facilities by the utility, a relevant Safety Analysis Report should be submitted, in accordance with the Atomic Energy Act, to the KINS through the MOST. The KINS performs a technical review and reports to the MOST on the results. Then the MOST issues a permit to the applicant based on the KINS' report.

- CANDU Licensing

Korean regulatory system employs two-step licensing approach based on the prescriptive regulation similar to that of the U.S. However, the Canadian regulatory system employs a one-step licensing approach based on the skills and technical consultations between the regulatory organization and the nuclear industry. Particularly, for CANDU reactors, the safety of plant design is reviewed continuously even after the issuance of license in Canada. In Korea, however, a two-step licensing approach is now official, even for CANDU reactors starting from Wolsong Unit 2 and the formats and contents of Safety Analysis Report are required to follow the specifics prescribed in the U.S. Regulatory Guide 1.70.

5. Regulatory Inspection

The regulatory inspection on the performance of a reactor facility is stipulated in Article 16 of the Atomic Energy Act. The regulatory inspection embraces the pre-operational inspection, the periodical inspection, the daily inspection conducted by resident inspectors, the special inspection, and QA inspection, which are explained in more detail as follows :

- Pre-operational Inspection

The applicant shall be subject to the pre-operational inspection to prove that the performance of the reactor facility meets the safety requirements specified in the relevant technical standards. If the utility, the licensee for construction and operation, passes all the pre-operational inspections, then the Operating License is officially issued by the MOST.

If the functional test results are unsatisfactory and the inspectors decide that proper corrections should certainly be made to improve the performance of the equipment and components, official findings or recommendations are issued, which are followed up with and resolved in order for the utility to pass the pre-operation inspection.

- Regulatory Periodical Inspection (RPI)

In accordance with the provision of the Enforcement Decree of the Atomic Energy Act, the licensee shall be subject to the regulatory periodical inspection, which is usually conducted on an annual basis. This inspection should show that the performance of the reactor facility, designed to withstand the pressure, radiation and other operating environments, is actually maintained in the state in which the reactor facility passed the pre-operational inspection. The Government then issues a license for operation.

The RPI consists of standard periodical inspection items (usually 50 - 60 items) which are established for each reactor type (refer to Table 3 & 4) and included are some special inspection items that are strategically selected based on the operating history and also on the experiences gained from the previous operating cycles. The inspection items are developed to cover all the technical areas and operational aspects of a plant. In the course of RPI, the inspectors also review the necessary utility documents, observe the utility activities and evaluate the maintenance and test records.

- Daily Inspection by Resident Inspectors

Operational safety of an NPP is continuously monitored through daily inspections at the plant site by the resident inspectors. The Resident Inspectors Office at each plant site consists of several government officers and KINS personnel. They monitor the safety parameters and review the station logs everyday to confirm whether the plant is operated in compliance with the technical specifications. They also routinely witness the safety-related functional tests such as start-up tests for emergency diesel generators, etc. If an event occurs, the resident inspectors investigate the event and report it immediately to the MOST. If the KINS and the MOST decide that the event is safety-significant then an in-depth investigation is necessary, and a joint special inspection team will be organized and assigned to the site.

- Quality Assurance (QA) Inspection

This QA Inspection is performed on an annual basis by the KINS staff to check whether the quality assurance activities of the utility are carried out in accordance with the QA program submitted to the regulatory authority.

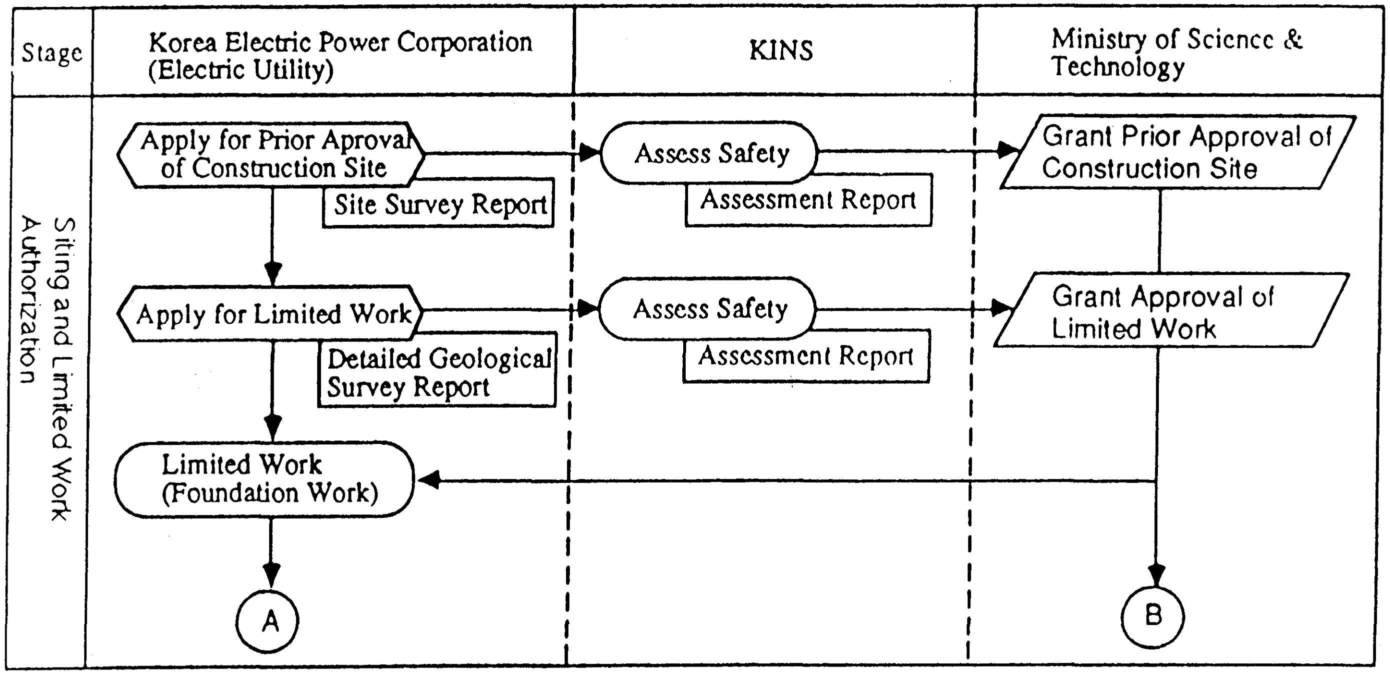

Fig. 4 Licensing Procedure for Nuclear Power Plants in Korea

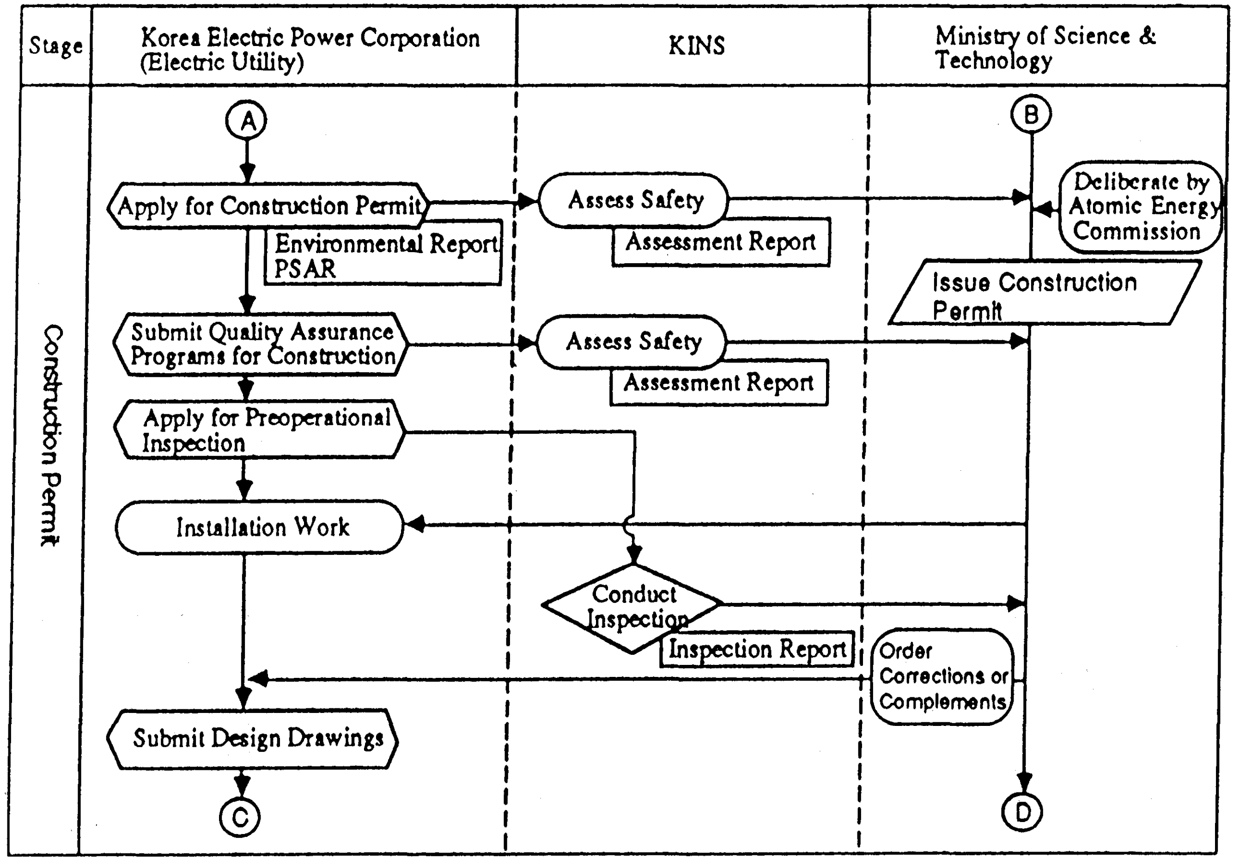

Fig. 4 Licensing Procedure for Nuclear Power Plants in Korea (continued)

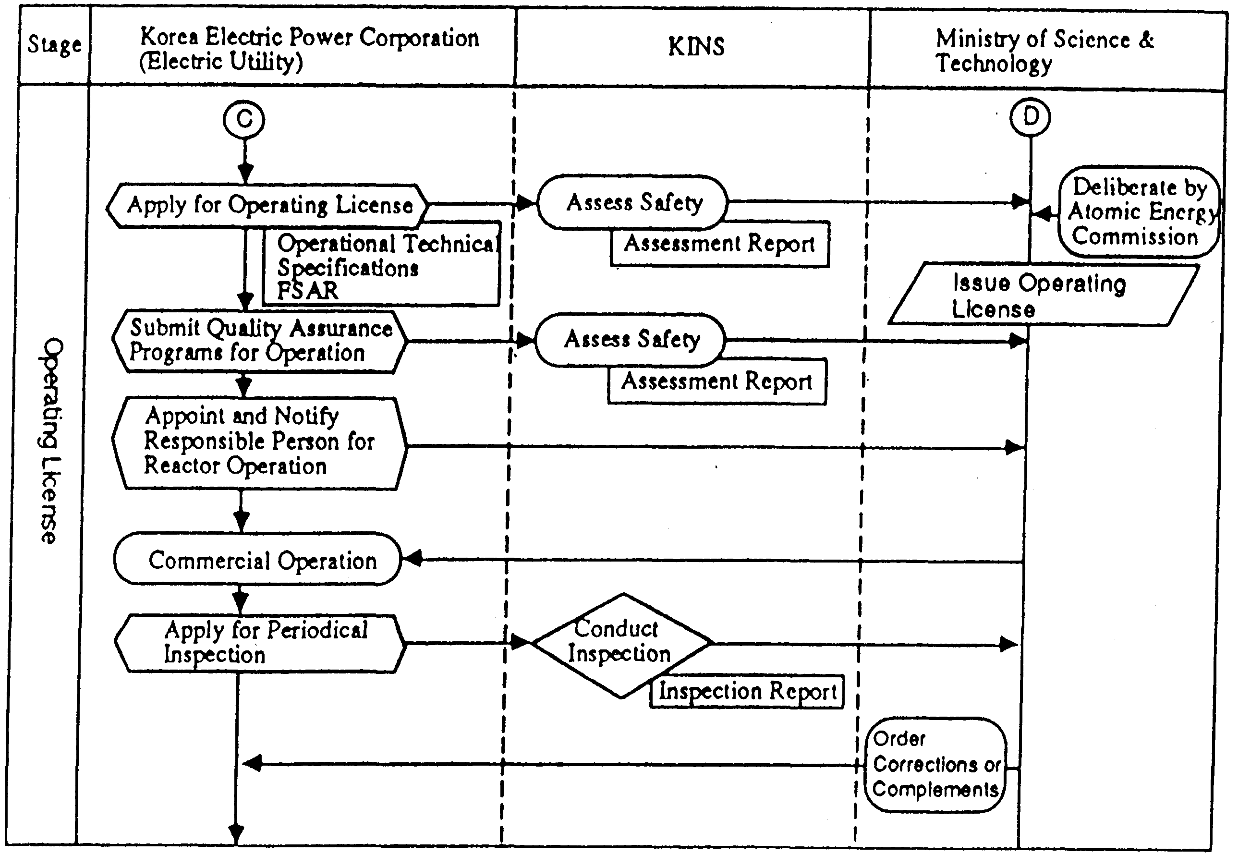

Fig. 4 Licensing Procedure for Nuclear Power Plants in Korea (continued)

Table 3 Standard Periodical Inspection Items (900 MWe PWR)

A: Witness, B: Test Result Review

System	Inspection Item	Method
Reactor	- Fuel Assembly Visual Inspection - Fuel Assembly Ultrasonic Inspection - Reactor Physics Test - Fuel Assembly Refueling Inspection	A A A A
Reactor Coolant System	- In-service Inspection - Pressure Boundary Check Valve and Pressure Isolation Valve Leakage Check - Pressurizer Power Operated Relief Valve Operation Test - Reactor Coolant Pump Inspection - Reactor Coolant Flow Rate Measurement - Digital Metal Impact Monitoring System and Acoustic Leakage Monitoring System Inspection	B B A A B B
Containment System	- Containment Building Penetration Isolation Status Check - Containment Spray System Operation Test - Containment Sump and Screen Visual Inspection - Containment Cooling Fan Operation Test - Hydrogen Recombiner Operation Test - Containment Local Leak Rate Test - Containment Integrated Leak Rate Test - Containment Isolation Valve Operation Test and Closing Time Measurement	B A A A A A A A
Engineered Safety Feature	- Boration System Automatic Valve Operation Test and Flow Rate Measurement - Residual Heat Removal System Pump Suction Isolation Valve Check - Emergency Core Cooling System Operation Test - Emergency Core Cooling System Throttling Valve Position Check - Accumulator Isolation Valve Operation Test - Auxiliary Feed Water System Throttling Valve Position Check - Accumulator Isolation Valve Operation Test - Auxiliary Feed Water System Operation Test - Charging Pump Inspection - Residual Heat Removal System Pump Inspection - Containment Spray Pump Inspection	B B A A A A A A A A A

System	Inspection Item	Method
Fuel Handling System	- Refueling Machine and Auxiliary Crane Check	A
	- Spent Fuel Pit Crane Interlock Check	A
	- Fuel Transfer System Inspection	B
Miscellaneous Safety Related System	- Main Steam Safety Valve Test	B
	- Main Steam Isolation Valve Closing Time Measurement	B
	- Hydraulic and/or Mechanical Snubber Inspection	B
	- Component Cooling Water System and Essential Sea Water System Operation Test	B
	- Fire Protection System Inspection	A
	- Primary System Safety Valve and Pressure Relief Valve Opening Pressure Set Point Check	A
	- Main Control Room Emergency Purification System Operation Test	A
Instrument and Control System	- Reactor Protection System Response Time Measurement	A
	- ESF Response Time Measurement	A
	- Control Rod Drop Time Measurement	A
	- Digital Rod Position Indicator Functional Test	B
	- ESF Slave Relay Operation Test	B
	- Steam Generator Narrow Range Level Monitoring System Calibration	B
	- Main Steam Pressure Monitoring System Calibration	B
	- Seismic Monitoring System Calibration	A
Emergency Electrical System	- Diesel Generator Functional Test	A
	- 125V Battery and Charger Capacity Test	B
	- Reactor Trip Breaker Functional Test	A
Plant Computer	- Computer Functional Test	B
Radiation Protection	- Radiation Monitor Test	A
	- Filter Functional Test	A
	- Radioactive Waste Treatment System Inspection	A
	- Radioactive Dosage Control	B
	- Radioactive Contamination and Work Control	A
	- Health Physics Planning	B
	- Radioactive Waste Management	A
	- Environment Monitoring System Management	A
Chemistry System	- Water Chemistry of primary and Secondary Coolant	B

Table 4 Standard Periodical Inspection Items (CANDU PHWR)

A: Witness, B: Test Result Review

System	Inspection Item	Method
Calandria	- Measurement for Fuel Channel Elongation	A
	- Check for Annulus Gas System	A
	- Check for Fuel Channel Flow	A
Fuel Handling & Storage Facility	- Fueling Machine	B
	- Spent Fuel Discharge and Emergency Cooling System	B
Safety System	- Emergency Core Cooling System	B
	- Emergency Water System	B
	- Main Steam Safety Valve	A
Primary Heat Transport System	- HT LRV Stroking Time Test	A
	- Primary Heat Transfer Pump	B
	- DN Monitoring System Sampling Line	B
	- Feeder Grayloc	B
	- Moderator Cover Gas System	B
Containment	- Containment Isolation Valve and Air Supply System	A
	- Airlock	A
	- Capacity Test for Compressed Air Storage Tank for Dousing System and Pressure Test for Instrument Air System	A
	- Dousing Water Air Supply NRV Leak Test	A
Safety Related Facilities	- Safety Class Pump Test	B
	- Safety Valve Test	A
	- Fail Safe Valve Check	B
	- Stand-by Diesel Generator	A
	- RSW System and RCW System	B
	- Chilled Water System	B
	- Fire Protection System	A
	- Earthquake Monitoring System	B
	- Dust Catcher	B
	- Water Chemistry	B
	- Heavy Water Management	B
Instrumentation & Control	- All Rod Drop Test for SDS #1	A
	- Pressurizer Heater Trip Test	A
	- Degasser Condenser Outlet High Temperature and Heavy Water Storage Tank High Level Valve Isolation Function Test	A
	- HT Purification Temperature Control & Override Test	A

System	Inspection Item	Method
Emergency Power Supply System	- Continuous Load Operation Test for EPS #1,2	A
	- Periodic Test of EPS (LOCA signal, Loss of Class IV Power, Design Load and Load of Class IV Power, Design Load and Load Trip Test)	A
	- Charge and Discharge Test for UPS Battery	B
Radiation Control	- Health Physics Program	B
	- Radiation Exposure Control	B
	- On-Site Radiation Monitoring System	A
Radioactive Wastes Management and Environment Management	- Radioactive Waste Management	B
	- Environmental Radiation Management	B
	- Meteorological Observation and Facility Management	B

6. Future Perspectives and Concluding Remarks

In Korea, " Continued Improvement of the Safety of Nuclear Power Plants" has been set as national policy for the construction and operation of NPPs. Safety related regulatory requirements under the Korea's atomic energy laws are strictly observed in the design, fabrication, construction, and operation of NPPs. The regulatory objective for nuclear safety can simply be termed into how to maintain and improve, where appropriate, the safety level of nuclear power plants and how to prepare for emergency situations. In order to achieve this objective, the regulatory authority of Korean government has established a set of safety requirements in terms of laws and regulations, policies, guidelines and programs.

Safety regulations will be improved further through the improvement of regulatory systems, introduction of new regulatory concepts, efficient management of regulatory organizations, and rationalization of technical standards. In particular, the following improvements are mainly considered :

(a) Strengthening of Q/A program in preparation of extensive localization of component design and manufacturing.
(b) Improvement of licensing system incorporating one-step licensing, which allows certification for standard designs and comprehensive site approval.
(c) Severe accident rule making and criteria established for next-generation reactors.
(d) Introduction of risk based regulation and license renewal.
(e) Development of safety assessment code systems.

Nuclear safety research will be conducted in the areas of NPP safety, environmental radioactivity, and the treatment and disposal of radioactive wastes, in order to maintain and further improve the safety levels. The safety of NPPs can be further improved by upgrading the qualification of operating personnel through training and education, and by strengthening the nuclear safety culture.

Korea has carried out a very ambitious nuclear power program since the early 1970s with a strong commitment to nuclear power development as an integral part of the national energy policy. However, the diversification of reactor types and vendors has caused some difficulties in regulating and licensing these nuclear power plants in Korea. These difficulties have been coped with through a continued effort to establish domestic regulatory positions and guidelines as well as forming a close cooperation with vendor country's regulatory organizations, vendors themselves, and particularly with the IAEA.

As the standardization of nuclear power plants and the development of next generation reactors, and the establishment of industrial codes and standards applicable to Korean nuclear power plants are making progress, the licensing system in Korea is expected to be stabilized. All these efforts will be continued in the future with an aim to make the nuclear power safer and more reliable.

KINS ORGANIZATION CHART